Exploring Genomic, Phenotypic, and Epigenetic Characteristics of Clinical Isolates of Streptococcus pneumoniae

Hannah Naomi Agnew

B. Sc. (adv)

A thesis submitted in fulfilment of the

Degree of Doctor of Philosophy

School of Biological Sciences

The University of Adelaide

Adelaide, South Australia, Australia

November 2023

Table of Contents

Abbreviations

α	Alpha
ABC	ATP Binding cassette
Adr	Attenuator of drug resistance
Aga	Alpha galactosidase
AGRF	Australian Genomics Research Facility
AI	Autoinducer
AI-2	Autoinducer 2
AI-2-P	Phosphorylated AI-2
AIP	Autoinducer signalling peptide
Ala	Alanine
APC	Antigen Presenting Cell
ATP	Adenosine tri-phosphate
β	Beta
BA	Blood agar
BBB	Blood Brain Barrier
BF	Bright field
BFI	Biofilm forming index
BgaA	β-galactosidase
BIR	Bacteriocin immunity region
Bp	Basepair/s
°C	Degrees Celsius
CbpA	Choline binding protein A
CbpD	Choline binding protein D
CbpE	Choline binding protein E
CcpA	Catabolite control protein A
CCR	Carbon catabolite repression
CDM	Chemically defined medium
CFU	Colony forming units
ChoP	Phosphorylcholine
CO_2	Carbon dioxide
COM	Chronic otitis media
ConA	Mannose/glucose-binding lectin from Canavalia ensiformis seeds

COVID-19	Coronavirus disease 2019
CpG	5'-C-phosphate-G-3'
CPS	Capsular polysaccharide
cre	Catabolite-responsive elements
CRM197	Non-toxic variant of diphtheria toxin used in pneumococcal conjugate vaccines
CSF	Cerebrospinal fluid
CSP	Competence-stimulating peptide
Δ	Delta or deletion of gene
DNA	Deoxyribonucleic acid
eDNA	Extracellular DNA
ssDNA	Single-stranded DNA
DMEM	Dulbecco's Modified Eagle's Medium
DOC	Deoxycholate
DPD	4,5-dihydroxy-2,3-pentanedione
EDTA	Ethylenediaminetetraacetic acid
Eno	Enolase
FCS	Foetal calf serum
FITC	Fluorescein isothiocyanate
Fe	Iron
Fru	Fructose
FruA	Fructose specific transport system, EIIBC or EIIC component
Gal	Galactose
GAPDH	Glyceraldehyde-3-phosphate dehydrogenase
gDNA	Genomic DNA
Gki	Glucokinase, house-keeping gene
Glc	Glucose
GlpO	Alpha-glycerophosphate oxidase
GM	Geometric mean
GS II	Griffonia simplicifolia lectin II
h	Hour/s
HCl	Hydrochloric acid
HEPES	N-2-hydroxyethylpipeazine-N'-2-ethanesulfonic acid His Histidine
HIV	Human immunodeficiency virus
HPr	Histidine-containing phosphocarrier protein

Hy1	Hyaluronate lyase
H_2O_2	Hydrogen peroxide
iC3b	Inactivated C3b
ICE	Integrative and conjugative element
IFN	Interferon
IgA	Immunoglobulin A
IgG	Immunoglobulin G
IL	Interleukin
I.N.	Intranasal
Indels	Insertions or deletions
IPD	Invasive pneumococcal disease
IR	Inverted repeat
LuxS	S-ribosylhomocysteine lyase
LytA	Autolysin
LPXTG	Sortase-anchored surface protein motif
MHC	Major histocompatibility complex
µ	Micro
µg	microgram/s
µl	microlitre/s
µM	micromolar
MAIT	mucosal-associated invariant T cell
MARCO	Macrophage receptor with a collagenous structure
mg	Milligram/s
ml	Millilitre/s
MLST	Multilocus sequence type
mM	Millimolar
min	Minutes
NADH	Reduced form of nicotinamide adenine dinucleotide molecules
NanA	Neuraminidase
NCBI	National Centre for Biotechnology Information
NCSP	Non-classical surface protein lacking secretion signals or anchorage motifs
NK	Natural killer
NLR	Nucleotide-binding oligomerisation domain-like receptor
NLRP3	NLR protein 3

nM	Nanomolar
NOD	Nucleotide domain-containing protein
NVT	Non-vaccine type
OD	Optical density
OM	Otitis media
PAF	Platelet-activating factor
PAFR	Platelet-activating factor receptor
PAMP	Pathogen-Associated Molecular Pattern
PavA	Adherence and virulence protein A
PavB	Pneumococcal adherence and virulence factor B
PBS	Phosphate-buffered solution
Pce	Phosphorylcholine esterase
PCR	Polymerase chain reaction
PCV7	7-valent CPS conjugate vaccine
PCV10	10-valent CPS conjugate vaccine
PCV13	13-valent CPS conjugate vaccine
PCV15	15-valent CPS conjugate vaccine
PCV20	20-valent CPS conjugate vaccine
PECAM1	Platelet endothelial cell adhesion molecule 1
PgdA	Peptidoglycan-N-acetylglucosamine deacetylase
PhtD	Polyhistidine triad protein D
PiaA	Pneumococcal iron acquisition protein A
PIGR	Polymeric immunoglobulin receptor
PiuA	Pneumococcal iron uptake protein A
Ply	Pneumolysin
PMA	Phorobol Myristate Acetate
PNA	Peanut agglutinin
PPSV23	23-valent CPS vaccine
PRCI	Phage-related chromosomal island
PRR	Pattern Recognition Receptor
PsaA	Pneumococcal surface antigen A
PspA	Pneumococcal surface protein A
PspC	Pneumococcal surface protein C
PsrP	Pneumococcal serine-rich repeat protein, pathogenicity island

PTS	Phosphoenolpyruvate phosphotransferase system
qRT-PCR	One-step relative quantitative real-time reverse transcription PCR
QS	Quorum sensing
Raf	Raffinose
RM	Restriction/modification
RNA	Ribonucleic acid
Rrg	Structural subunit proteins of the pilus
rRNA	Ribosomal RNA
RPMI	Roswell Park Memorial Institute
rpsL1	Small ribosomal subunit with an S12L mutation
SARS-CoV-2	Severe acute respiratory syndrome coronavirus 2
SB	Serum broth
SBA	Soybean agglutinin
SD	Standard deviation
SEM	Standard error mean
sec	Second/s
SNP	Single nucleotide polymorphism
SrtA	Pneumococcal sortase transpeptidase
SPD	Streptococcus pneumoniae database
SpsA	Secretory pneumococcal surface protein A (also known as PspC)
SpxB	Pyruvate oxidase
SsbB	Single-stranded DNA binding protein
ST	Sequence type
StrH	N-acetylglucosaminidase
T6P	Tagatose-6-phosphate
TCSTS	Two-component signal transduction system
Th	T helper cell
TLR	Toll-like receptor
TMD	Transmembrane domain
TRD	Target recognition domain
URT	Upper respiratory tract
WGA	Wheat germ agglutinin
WCV	Whole cell vaccine
WT	Wildtype

Zn	Zinc

Declaration

I certify that this work contains no material which has been accepted for the award of any other degree or diploma in my name, in any university or other tertiary institution and, to the best of my knowledge and belief, contains no material previously published or written by another person, except where due reference has been made in the text. In addition, I certify that no part of this work will, in the future, be used in a submission in my name, for any other degree or diploma in any university or other tertiary institution without the prior approval of the University of Adelaide and where applicable, any partner institution responsible for the joint award of this degree.

The author acknowledges that copyright of published works contained within the thesis resides with the copyright holder(s) of those works.

I give permission for the digital version of my thesis to be made available on the web, via the University's digital research repository, the Library Search and also through web search engines, unless permission has been granted by the University to restrict access for a period of time.

I acknowledge the support I have received for my research through the provision of an Australian Government Research Training Program Scholarship.

Signed

Hannah Naomi Agnew

Date 23/11/2023

Acknowledgements

The successful completion of my PhD journey would not have been possible without the unwavering support and invaluable guidance of many people, to whom I extend my deepest gratitude.

Foremost, I wish to express my heartfelt appreciation to everyone in the Research Centre for Infectious Diseases and Molecular Life Sciences building that have aided and supported me throughout my PhD. In particular, I would like to acknowledge all members, past and present, of the Paton, Wilson, Alsharifi labs and GPN group who made Level 4 a thriving, supportive, and enjoyable work environment.

Special thanks must be given to Cathy, the true powerhouse of the Paton lab. Your unwavering support and assistance have been a guiding light throughout my journey, and I can't thank you enough. Without your invaluable contributions, we would all be adrift.

To my fellow current postgraduate students, Chloe, Kate and Rachel, sharing this PhD journey alongside you has been a delightful and enriching experience. Our lab discussions and shared moments of commiseration over failed experiments and long hours have fostered an entertaining and supportive community. It's been a pleasure to have you as companions on this academic adventure.

I extend my deepest thanks to my past Paton lab members and friends, Alex, Layla and Kim. Alex, your unwavering assistance in the lab, no matter how many questions I posed, was truly appreciated. Sharing an office with you and getting coffee together were highlights of my first year. Layla, working with you this last year has been very enlightening and enjoyable. I very much appreciated your guidance in the lab, as well as all the entertaining conversations we had in the office or in our project meetings. Kim, I cannot begin to express my thanks for your invaluable support in the lab and mentorship during my undergraduate summer placement – it was a profoundly positive experience for me that played a pivotal role in shaping my aspiration to pursue a PhD. I would also be remiss not to mention how appreciative I was that you always made time for me to come chat with you mid-afternoon while you were busy working on your thesis; I hope you enjoyed the breaks!

Turning my attention to the Waters siblings, Jack and Sophie, I am extremely grateful for your presence in my academic journey. Jack, I am very grateful that you got to infiltrate our lab from Flinders University and work on your PhD with us. Sharing an office with you and Claudia had its

memorable moments, from the weekly debates with Claudia over the "guest Wi-Fi password" to the unforgettable sight of that towering wall of coffee cups.
Sophie, you have my deepest gratitude for your unwavering support and assistance over the past two years. Your vibrant personality and infectious positivity have significantly brightened my outlook and instilled hope in the success of our experiments. I must offer my sincere apologies again for scaring you so much in the first month – at least you will never forget to “pop the bubbles” and plug laptops in to charge. The days you were in the lab were highlights of my week, with being able to goof around together in the lab whilst still working like a well-oiled machine. Our daily coffee breaks provided the perfect opportunity to catch up on the latest developments, and, though I find your fascination with mice a tad unnerving, it added a unique and entertaining touch to our interactions. Thank you all for being instrumental in my academic journey, and I am truly appreciative of the camaraderie and support that you've provided.

I must also extend my heartfelt appreciation to Dr Erin Brazel, one of my co-supervisors, for all of your help and guidance you've provided during my PhD journey. I am aware that I was among your first students to supervise, and I genuinely hope that the experience has been as rewarding for you as it has been for me.
My sincere gratitude goes out to Professor James Paton for the privilege of working in your lab and having you as one of my supervisors. Your mentorship has been an indispensable asset during my PhD, and I take pride in having completed this journey under your guidance. Your immense reservoir of knowledge and experience serves as a constant source of inspiration for me, and I am immensely grateful for the opportunity you provided me three years ago when I undertook a summer placement.
Last but not least, undertaking my PhD would not have been possible without my principal supervisor Dr Claudia Trappetti. Words cannot adequately express how deeply grateful I am to you for the guidance and support you've offered, not only throughout my PhD but in life in general, especially over the last six months. I deeply cherish the friendship we have, and I hope we will be able to keep working together in years to come. Regardless of the path we follow, I eagerly anticipate the prospect of visiting you in Italy soon. Grazie mille cara!

Completing this PhD was only made possible with the unwavering love and support of my friends and family, but I would especially like to acknowledge the profound impact of those who are no longer with us. I want to offer special recognition to the memory of two individuals, my dear friend Salvador and my beloved grandma, RR, who played significant roles in shaping the person I am

today. The absence of their presence leaves an indescribable void, and I hold the cherished memories of our time together close to my heart. Thank you and know that I love you.

I would like to extend my deepest gratitude to my closest friends whose unwavering support has been a cornerstone of my journey through the challenges of my PhD.

To Tanisha, your constant support throughout my university journey, even when I'd go to your house and ignore you in favour of studying, has been a lifeline. Hearing your words of pride in my accomplishments has boosted my confidence and reinforced my belief in the path I've chosen with my PhD. Our friendship means so much to me, and I am profoundly grateful that you have stuck with me throughout the years – here's to many more years of friendship!

Now as for Emily, I must offer my heartfelt thanks for not only being a friend but for living with me while I navigated the challenges of my PhD. I am well aware of the difficulties of sharing space with me during my intense study periods, so I extend my sincere apologies along with my deepest appreciation for your unwavering support. Having a friend like you by my side is a true blessing, and I'm grateful that we've both completed our university journeys together.

Going to university would not have been possible without the unwavering support of my family. To each of you, I extend my deepest gratitude for your pivotal roles in my life.

To my grandparents, Pappy and RR, I thank you for always believing in me and celebrating my successes. Your influence has shaped the person I am today, and I am profoundly grateful for the love you have showered upon me.

To my brother-in-law, Tom, I very much appreciate your willingness to understand to engage with my research and challenge me to explain it better. Debating with you over not just my PhD, but many other topics, always made for an interesting time.

Lara, my sister, I am exceptionally thankful for your constant love and unwavering support, not only during this PhD journey but throughout my entire life. Your enduring belief in me and your willingness to lend a helping hand when I needed it have been invaluable. I consider myself incredibly blessed to have you as my sister, and I want you to know how deeply I love you.

I cannot begin to express the depth of my gratitude to my parents. None of this would have been possible without your unwavering support and guidance.

Dad, your steady and calm presence has been a grounding force in my life. We both share a stoic demeanour and a wicked sense of humour, and our quieter moments have been a source of comfort throughout my PhD.

Mum, we have basically been each other's therapist for the last few years – I am so grateful for your constant support and willingness to listen to me talk about my every day in the lab. Being able

to travel with you for my first international conference was a blessing and I will always remember that trip fondly.

Both of you have nurtured and guided me to become the best version of myself throughout my entire life. You've always encouraged me to follow my dreams, and for that, I couldn't be more thankful. I love you both deeply.

Lastly, to my nephew, Oscar, I am thankful that I was able to lull you to sleep by discussing my research and practicing my presentations while I was babysitting you. While I'm a bit disappointed that your first words weren't "*Streptococcus pneumoniae*," I'm confident you'll learn them in due time. I hope one day that you will find something to be as passionate about as I am about bacteria.

Publications and Conference Presentations

Publications	
Thesis Chapter	**Title**
Chapter 2	Agnew, H. N., Brazel, E. B., Tikhomirova, A., van der Linden, M., McLean, K. T., Paton, J. C., & Trappetti, C. (2022). *Streptococcus pneumoniae* strains isolated from a single pediatric patient display distinct phenotypes. *Frontiers in Cellular and Infection Microbiology*, 12, 866259-866259. doi:10.3389/fcimb.2022.866259
Chapter 3	Agnew, H. N., Atack, J. M., Fernando, A. R. D., Waters, S. N., van der Linden, M., Smith, E., Abell, A. D., Brazel, E. B., Paton, J. C., & Trappetti, C. (2023). Uncovering the link between the SpnIII restriction modification system and LuxS in *Streptococcus pneumoniae* meningitis isolates. *Frontiers in Cellular and Infection Microbiology*, 13. doi:10.3389/fcimb.2023.1177857
Appendix A	Tikhomirova, A., Brazel, E. B., McLean, K. T., Agnew, H. N., Paton, J. C., & Trappetti, C. (2022). The role of luxS in the middle ear Streptococcus pneumoniae isolate 947. Pathogens, 11(2), 216. doi:10.3390/pathogens11020216

Presentations		
Type	**Title**	**Conference**
Oral presentation	Streptococcus pneumoniae strains isolated from a single paediatric patient display distinct phenotypes.	Australian Society for Microbiology (ASM) SA/NT Branch Student Awards Event, Adelaide, South Australia, March 2022
Oral presentation	Streptococcus pneumoniae strains isolated from a single paediatric patient display distinct phenotypes.	The Molecular Biology of Bacterial Pathogens (BacPath 16), Brisbane, Queensland, September 2022

Poster presentation	Streptococcus pneumoniae strains isolated from a single paediatric patient display distinct phenotypes.	Adelaide Protein Group Awards Event, Adelaide, South Australia, November 2022
Oral presentation	Contribution of the LuxS/AI-2 quorum sensing system in Streptococcus pneumoniae meningitis isolates.	Australian Society for Microbiology (ASM) SA/NT Branch Student Awards Event, Adelaide, South Australia, March 2023
Oral presentation	Clinical Streptococcus pneumoniae strains recovered from mice show evidence of distinct disease progression, frequent switching and diverse carbohydrate metabolism.	European Meeting on the Molecular Biology of the Pneumococcus (Europneumo 16), Rethymno, Crete, Greece, May 2023
Poster presentation	Contribution of the LuxS/AI-2 quorum sensing system in Streptococcus pneumoniae meningitis isolates.	European Meeting on the Molecular Biology of the Pneumococcus (Europneumo 16), Rethymno, Crete, Greece, May 2023

Abstract

Streptococcus pneumoniae (the pneumococcus) is a prevalent nasopharyngeal commensal in humans that can transition from a harmless coloniser to a dangerous pathogen, contributing significantly to global bacterial infections and associated morbidity and mortality. Unfortunately, the intricate mechanisms influencing individual strain capabilities to cause localized or invasive pneumococcal diseases remain enigmatic, primarily due to the extensive genetic diversity between pneumococcal strains, with over 100 capsular serotypes superimposed on more than 12,000 clonal sequence types (STs).

This study builds upon prior research that used closely related strains, of the same serotype and ST, isolated from the blood and ears of patients to investigate factors influencing disease progression and outcome. Specifically, it was found in serotype 14 ST15 and serotype 3 ST180 blood and ear isolates pairs, that the ability to metabolise the carbohydrate raffinose, influenced by a single nucleotide polymorphism (SNP), resulted in distinct disease progression within an intranasal murine infection model (Minhas et al., 2019). This emphasises the importance of investigating minor disparities between closely related clinical isolates, whilst bypassing the significant genetic diversity inherent in *S. pneumoniae*.

In this project, a collection of clinical isolates was screened for carbohydrate metabolism. Among these, a pair of closely related pneumococcal isolates (serotype 15C, ST 8711) from the blood and cerebrospinal fluid (CSF) of a single paediatric meningitis patient exhibited significant differences in raffinose metabolism. The blood-derived isolate (60B) displayed defective raffinose metabolism, reduced gene transcription in the raffinose utilisation pathway and inability to use raffinose as a carbon source. In a murine intranasal infection model, 60B displayed higher bacterial counts in nasal tissue, compared to those infected with 60CSF, but couldn't survive in the ears of infected mice. Genome sequencing revealed a premature stop codon in the *aga* gene within the raffinose locus of both strains, suggesting the presence of impaired alpha-galactosidase activity in both strains. Moreover, genome analyses revealed no SNPs between these closely related strains, implying other factors were involved.

As genome sequencing did not provide a molecular basis for the observed differences, the *spnIII* type I restriction-modification system, known for its role in methylation and subsequent gene

regulation, was explored. Recombination of the *spnIII* locus leads to six different variants (A-F) of a methyltransferase, each with a distinct methylation pattern, resulting in unique bacterial subpopulations with varying phenotypic characteristics. Notably, *spnIIIB* has been associated with increased nasopharyngeal carriage and downregulation of the LuxS/AI-2 Quorum Sensing (QS) system (Manso et al., 2014), a universal communication channel among bacteria linked to virulence and biofilm formation in pneumococci (Trappetti et al., 2017; Trappetti, Potter, et al., 2011; Yadav et al., 2018).

The analysis of *spnIII* alleles in both strains showed a higher proportion of *spnIIIB* in 60B, correlating with reduced *luxS* expression. Deletion of *luxS* in both strains showed altered metabolic profiles and *in vivo* behaviour. Furthermore, this study revealed, for the first time, that *spnIII* not only influences LuxS production but also that LuxS, through an unknown mechanism, affects the proportion of *spnIII* alleles, potentially influencing disease progression in mice.

Collectively, these discoveries indicate that closely related *Streptococcus pneumoniae* isolates from a paediatric meningitis patient's blood and CSF demonstrate divergent raffinose metabolism, which correlates with disease outcomes in a murine model. Furthermore, it highlights the importance of the regulatory interplay between *luxS* and the *spnIII* type I restriction-modification system in shaping disease progression and outcomes.

Chapter 1: Introduction

1.1. Streptococcus pneumoniae (the pneumococcus)

Streptococcus pneumoniae (the pneumococcus) is a Gram-positive, alpha-haemolytic, diplococcal shaped bacterium that causes significant global morbidity and mortality each year. These bacteria commonly colonise the human nasopharynx asymptomatically and can be transmitted to other uninfected hosts via secretory droplets. After colonisation of the nasopharynx, pneumococci can move to other sites of the body and cause disease through relatively poorly understood mechanisms. Pneumococci are responsible for localised disease such as otitis media and sinusitis, or invasive diseases such as pneumonia, bacteraemia and meningitis. In spite of many years of research, with the development of multiple vaccines and antibiotics, *Streptococcus pneumoniae* continues to place a major burden on healthcare systems around the world.

1.1.1. Burden of disease

The extensive spectrum of both localised and invasive diseases caused by *S. pneumoniae* contributes to over 190 million infections worldwide each year, with a staggering 1.2 million deaths, solidifying its status as one of the most pathogenic bacterial species (Lavelle & Ward, 2022).
Pneumococcal infections are most commonly observed in individuals with weakened or not fully developed immune systems, such as the immunocompromised, children under five years of age, and the elderly. Although *S. pneumoniae* may asymptomatically colonise the nasopharynx of up to 95% of children (under 2 years) and 25% of adults (Trimble et al., 2020), in a proportion of cases, the organism spreads beyond the nasopharyngeal niche and establishes infections in deeper sites within the body including sterile sites such as the lungs, blood, and brain, leading to invasive pneumococcal diseases (IPDs) causing pneumonia, bacteraemia, and meningitis, respectively (Weiser et al., 2018).

IPD is a severe condition, causing approximately 1 million deaths annually, with a significant proportion occurring in children under the age of five in developing countries (Kadioglu et al., 2008; Iroh Tam et al., 2017). Furthermore, there were an estimated 120 million pneumonia episodes in 2010 – 2011, out of which 14 million progressed to severe disease (Walker et al., 2013). Of the IPDs, meningitis has a high case fatality rate; in higher-income countries, approximately 30% of meningitis cases result in fatality, while in lower-income countries, the case fatality rate rises to 50% (Brouwer et al., 2010). Importantly, in developing countries, the IPD mortality rate for children under five can range from 10% to 40%, potentially influenced by limited access to treatments,

relatively poor healthcare systems, and co-morbidities such as malnutrition and Human Immunodeficiency Virus (HIV) infections (Bogaert et al., 2004; Harboe et al., 2009; Madeddu et al., 2010).

In Australia, the mortality rate from IPD is less than 5% for both children under five years old and individuals over 65 years old (Australian Institute of Health and Welfare, 2019). However, IPD rates are higher in Indigenous populations compared to non-Indigenous populations (Forrest et al., 2000; Welfare, 2018).

There are various risk factors that contribute to pneumococcal carriage, such as malnutrition, poverty, limited access to healthcare, and exposure to crowded environments such as childcare centres (Lynch & Zhanel, 2010). In adults, additional risk factors including smoking, asthma, immunosuppression, age, and a history of respiratory infections increase the likelihood of carriage (Lynch & Zhanel, 2010).

Pneumococcal infections may also be exacerbated by other respiratory pathogens, such as Influenza virus, leading to increased morbidity and mortality. A notable historical example is the 1918-19 Spanish influenza pandemic, where a significant proportion of deaths (approximately 50 million) were attributed to secondary bacterial infections, primarily pneumococcal infections (Morens et al., 2008). Furthermore, during the H1N1 swine flu pandemic in 2009, a study revealed that 33% of all cases involved secondary bacterial coinfections, with 62% of those cases being caused by *S. pneumoniae* (Cillóniz et al., 2012).

Coronavirus disease 2019 (COVID-19) and *S. pneumoniae*

In the time since December of 2019, when the initial cases of Coronavirus disease 2019 (COVID-19) were recorded in Wuhan, China, there has been over 370 million infections worldwide, including more than 5 million deaths associated with the disease. COVID-19 is caused by severe acute respiratory syndrome coronavirus 2 (SARS-COV-2) and normally manifests as a respiratory tract infection, with many diverse symptoms. As with other respiratory tract infections, COVID-19 may go on to cause severe pneumonia, organ failure and death, particularly in the elderly and those who are immunocompromised. Interestingly, bacterial coinfection does not appear to frequently occur in those infected with COVID-19 (Amin-Chowdhury et al., 2020).

Early investigations of the relationship between COVID-19 and *S. pneumoniae* found that only a small proportion of COVID-19 patients had a bacterial co-infection and there was a low risk for the development of a secondary bacterial infection (Langford et al., 2020). However, it is important to

note that the validity of these studies may have been compromised due to several limitations. Firstly, the choice of pneumococcal detection methods employed in these studies may have introduced biases or inaccuracies in the results. Additionally, during the early stages of the pandemic, prevalent antibiotic prescribing for patients with COVID-19 might have influenced the outcomes of the studies. The widespread use of antibiotics in COVID-19 patients could have potentially affected the incidence and severity of pneumococcal infections (Langford et al., 2020; Stahlfeld et al., 2022).

Another potential factor impacting the frequency of recorded pneumococcal coinfection or secondary infection was the introduction of the COVID-19 containment policies and public information campaigns (Brueggemann et al., 2021). Following COVID-19 lockdown, large declines in IPD were observed. In the few cases where IPD and COVID-19 coinfections occurred, there was a higher chance of fatality, predominantly in the elderly (Amin-Chowdhury et al., 2020).

Although incidences of IPD and COVID-19 coinfection are rare, COVID-19 infections have been associated with a 3-fold higher likelihood of having pneumococcal carriage; in turn carriers were found to have diminished immune responses to COVID-19 (Mitsi et al., 2022).

Further studies into the association between COVID-19 and *S. pneumoniae* suggest that there is a synergistic relationship occurring between these pathogens in the upper airway. The association between the pathogens was found to be stronger in those patients with acute symptoms, but it remains unclear how pneumococci contribute to the symptoms of those infected with COVID-19 (Parker et al., 2022).

Taken together, these studies suggest that *S. pneumoniae* and COVID-19 have a synergistic relationship in the upper airway and colonisation of pneumococci can impair the immune response to COVID-19 infection through unknown mechanisms. Although incidence of coinfection of IPD and COVID-19 has been reported to be rare, likely due to the stringent lockdown measures early in the pandemic, in the observed incidences the case fatality rate was high.

1.2. Pneumococcal pathogenesis

1.2.1. Carriage and transmission

In spite of the substantial morbidity and mortality linked to pneumococcal disease, *S. pneumoniae* more frequently exists asymptomatically as a commensal within the human nasopharynx. This commensal colonisation, commonly referred to as carriage, is an essential preliminary step for the onset of pneumococcal disease. Importantly, carriage often transpires without apparent symptoms and occurs naturally within the first few months of life (Gray et al., 1980; Gray et al., 1982). The

prevalence of asymptomatic carriage displays significant variations based on age and geographical location, ranging from 18% to over 50% among healthy children and between 4% to 10% among adults, with peak rates observed at the ages of 2-3 years (Bogaert et al., 2004; Regev-Yochay et al., 2004; Hosseini et al., 2015; Wang et al., 2017). The human nasopharynx can concurrently house other potentially pathogenic bacterial species, including *Moraxella catarrhalis* and *Haemophilus influenzae*, alongside multiple serotypes or strains of pneumococci, which can manifest as either competitive or cooperative relationships (Shak et al., 2013; Shiri et al., 2013; Xu & Pichichero, 2014). Even the interactions between different strains of pneumococci can lead to intraspecies competition, influencing nasopharyngeal colonisation (Dawid et al., 2009). This competition has been highlighted in a study using murine models, which demonstrated that pre-existing pneumococcal colonisation can impede the establishment of a new strain (Li et al., 2013; Kono et al., 2016). Strikingly, human colonisation studies have demonstrated that pneumococcal acquisition following intranasal challenge correlates with increased diversity in the microbiota (Cremers et al., 2014). Of particular interest it has been reported that an increase of inflammation in the upper respiratory tract (URT), triggered by co-infection with upper respiratory viruses is most favourable for *S. pneumoniae* carriage (Nakamura et al., 2011). Viruses like Influenza induce the expression of pro-inflammatory cytokines, which in turn elevate the expression of epithelial receptors used by the pneumococcus for adherence (McCullers & Rehg, 2002). This compromise in the nasopharyngeal epithelium enhances the nutrient availability within the immediate environment, thereby fostering colonisation (Avadhanula et al., 2006).

S. pneumoniae primarily spreads from person to person through the inhalation of contaminated secretory aerosol droplets. Environments with high population density, such as day care centres and hospitals, contribute to the ease of transmission (Mandigers et al., 1994; Pessoa et al., 2013). The transmission is further facilitated during colder months when viral infections of the URT are prevalent, leading to an upsurge in the shedding of respiratory secretions and creating a conductive environment for transmission (Gwaltney et al., 1975; Musher, 2003; Numminen et al., 2015). The pneumococcus predominantly resides within the mucous layer overlaying the epithelium of the URT. Here, the release of pneumolysin (Ply) induces pore formation in host membranes (Boulnois et al., 1991), triggering heightened inflammation at the site (Parker et al., 2011; Karmakar et al., 2015), prompting increased shedding of pneumococci and facilitating transmission to new hosts (Zafar et al., 2017). Similarly, coinfection with the Influenza A Virus has demonstrated that in mouse pups, it heightens inflammatory conditions, intensifying pneumococcal shedding and subsequently amplifying transmission rates (Nakamura et al., 2011; Richard et al., 2014; Zafar et al., 2017).

Pneumococcal transmission is also affected by factors such as mucosal flow and secretion, which have been shown to correlate with increased transmission (Rodrigues et al., 2013).

Contact-dependent transmission of *S. pneumoniae* occurs through secretions from infected hosts, involving both direct person-to-person contact and contact with contaminated surfaces. In the aforementioned infant mouse study, transmission occurred amongst littermates through secretions containing pneumococci directly making contact with uninfected littermates' nasal mucosa or via the surface of the uncolonised mother mouse, which was shown to have a substantial number of pneumococci present on her teats (Zafar et al., 2017). Following dispersion from the host index, the *S. pneumoniae* must persist in the external environment to guarantee transmission to a new carrier. The survival of pneumococci on objects like soft toys handled by colonised children has also been characterised (Marks et al., 2014). The bacteria can persist for days under conditions rich in nutrients, such as human saliva (Verhagen et al., 2014). Furthermore, pneumococci demonstrate the ability to endure desiccation for several days, with biofilm colonies displaying greater viability compared to planktonic colonies. From this dormant state, the bacteria can revert to its original phenotype when conditions turn favourable (Walsh & Camilli, 2011; Marks et al., 2014).

Upon entering the nasopharynx of a new host, *S. pneumoniae* must overcome the initial hurdle in the URT of bypassing mucous entrapment (Feldman et al., 1992). The mucus consists of gel-like mucin glycoproteins, which form an overlay on the URT's epithelium, fortified with immunoglobulins and antimicrobial peptides (Rose & Voynow, 2006). Functioning as a formidable barrier, this mucus layer limits microorganisms from accessing the surface epithelium. These epithelial cells, in turn, serve as a protective shield for the underlying tissues and organs (Brooks & Mias, 2018). The orchestration between epithelial cells and mucus is vital for the process of mucociliary clearance. The negatively charged mucus ensnares potential invaders, while the cilia on epithelial cells engage in synchronised movement, propelling the trapped pathogens and mucus towards the oral cavity for expulsion (Antunes & Cohen, 2007; Nelson et al., 2007). Whilst this mucin layer serves to protect the epithelial layer of the URT from interactions with resident pathogens, it provides abundant nutrients for an environment conductive to bacterial residence (Yesilkaya et al., 2008).

For a successful establishment of pneumococcal colonisation, adherence to the epithelial cells lining the URT is imperative. This adherence hinges on the specific binding of pneumococcal adhesins to ligands on host receptors. *S. pneumoniae* are endowed with an array of adhesins that

bolster its binding capacity to the host epithelium, with their expression potentially amplified in response to inflammation for heightened adherence (Kc et al., 2017). Choline binding proteins, namely choline binding protein A (CbpA), present on pneumococci can bind to host cell glycoconjugates (Rosenow et al., 1997), and non-specific physiochemical interactions, including hydrophobic interactions, further contribute to this adherence process (Swiatlo et al., 2002). Some other adhesins present include surface-bound proteins like pneumococcal adherence and virulence protein A (PavA) and PavB, which bind to fibronectin and plasminogen, elements of the extracellular matrix (Holmes et al., 2001; Jensch et al., 2010). Phosphorylcholine (ChoP) present on cell wall teichoic acid has an affinity for the platelet-activating factor receptor (PAFR) on host cells, whilst CbpA, also known as PspC, binds polymeric IgG receptors (PIGR) as well as host factor H and vitronectin (Cundell et al., 1995; Zhang et al., 2000; Voss et al., 2013). Additionally, *S. pneumoniae* encodes at least 10 extracellular glycosidases, including neuraminidase A (NanA), β-galactosidase (BgaA) and N-acetylglucosaminidase (StrH), which act by cleaving terminal sugars from host cell surface glycoconjugates, producing carbohydrates for import and metabolism, whilst simultaneously exposing receptors for adherence to host epithelial cells (Kadioglu et al., 2008; King, 2010).

In the context of clearance of *S. pneumoniae* from the mucosal surfaces of the URT, both host IgA1 and passive immunisation play critical roles. However, pneumococci have developed mechanisms to elude immune defences, such as the secretion of an IgA1 protease that targets and disrupts the antibody hinge region. This action prevents the aggregation of pneumococci and counters the host's immune response (Janoff et al., 2014; Roche et al., 2015). Furthermore, to combat the lytic action of the host lysozyme, *S. pneumoniae* employs two essential enzymes: peptidoglycan-N-acetylglucosamine deacetylase (PgdA) and attenuator of drug resistance (Adr) (Davis et al., 2008). These mechanisms allow the bacterium to thwart the harmful effects of host lysozymes. When pneumococci are engulfed by host phagosomes upon successful immune system detection and action, a release of Ply occurs, inducing pore formation and initiating a pro-inflammatory immune response (Parker et al., 2011; Karmakar et al., 2015). The escalation of inflammation and respiratory secretions establishes inhospitable conditions for pneumococci, consequently prompting transmission to a new, more suitable host (Weiser et al., 2018).

1.2.2. Otitis media

S. pneumoniae is also a leading cause of localised diseases such as otitis media (OM) and sinusitis, with the primary causative agent of OM being the pneumococcus itself (Brook, 2013;

Danishyar & Ashurst, 2023). Although OM is not typically life-threatening, it has significant socioeconomic impact, as it is the most frequently diagnosed paediatric disease in developed countries affecting nearly all children during the first four years of life. Recurrent infections occur in approximately 20-30% of children, resulting in substantial treatment costs that amount to $4-5 billion per year in the USA alone (Brixner, 2005). Moreover, OM can lead to permanent hearing impairment, which has adverse effects on speech development and learning (Teele et al., 1990). The incidence and impact of chronic OM (COM) is particularly distressing in disadvantaged populations, such as Australian Indigenous children. The World Health Organisation (WHO) classifies it as a “massive public health problem” requiring urgent attention (Morris et al., 2005). In some indigenous communities, up to 61% of Aboriginal children experience COM, and up to 80% of them suffer from hearing loss due to tympanic membrane perforation (O’Connor et al., 2009).

This infection is facilitated by two neuraminidases, NanA and NanB, which possess the ability to cleave N-acetylneuraminic acid from glycoproteins, glycolipids on host cell surfaces and mucins (Loughran et al., 2019). This enzymatic action results in a reduction in overall viscosity, thereby enhancing access to the epithelial surfaces. Subsequently, NanA and NanB cleave oligosaccharides on these surfaces, revealing receptors that the pneumococcus can utilise for adherence (Stahl & O'Toole, 1972; Berry et al., 1996). The essential role of these neuraminidases in the development of OM is evident (Long et al., 2004; Wren et al., 2017), as demonstrated by a chinchilla infection model, where a neuraminidase-deficient mutant was eliminated from middle ear twice as rapidly as the wild-type pneumococci (Tong et al., 2000). Once resident within the middle ear, the pneumococcus triggers inflammation through cell surface proteins and Ply, which contributes to detrimental effects such as hearing loss and cochlear damage (Comis et al., 1993; Winter et al., 1997; Tuomanen, 2000).

Severe cases of OM can also lead to intracranial complications, with tympanogenic meningitis being a common occurrence. Bacteria from the middle ear can spread to the inner ear and subsequently reach the meninges. If left untreated, the resulting inflammation in the brain and spinal cord can lead to brain damage or even death (Schachern et al., 1992; Mook-Kanamori et al., 2011).

1.2.3. Invasive pneumococcal disease

The optimal lifestyle for *S. pneumoniae* involves stable colonisation of the nasopharynx, a strategic position that offers extended survival and facilitates its transmission to new hosts. However, instances of viral infection can elicit a pro-inflammatory cytokine response that adversely affects

the respiratory epithelium. Under such conditions, bacterial loads within the upper respiratory tract can surge. An increase in pneumococcal loads in the nasopharynx coupled with compromised epithelial barrier integrity enhances the likelihood of invading other host tissues, resulting in either localised of invasive diseases. Invasive pneumococcal disease (IPD) takes place when the pneumococci transverse into the lungs or infiltrates the protective layers of epithelial and/or endothelial cells encompassing the blood vessels or cerebrospinal fluid (CSF) compartments (Weiser et al., 2018).

Similar to nasopharyngeal colonisation, the pneumococci must skilfully evade mucus entrapment and mucociliary clearance. The entrapment avoidance is facilitated by the negatively charged capsule and the action of the zinc metalloprotease ZmpA, also known as the IgA1 protease, which degrades IgA1 and mitigates such entrapment (Fasching et al., 2007; Janoff et al., 2014). Subsequently, glycosidases like NanA, BgaA and StrH uncover glycan targets situated on the host epithelial surface by cleaving the terminal sugars from the host cell surface glyconjugates. These sites act as docking points for pneumococcal adhesins, a process that coincides with Ply-mediated suppression of ciliary beating, aiding in establishing infection (Kadioglu et al., 2008).

Upon contact with lung epithelial cells, adherence to the apical surface is facilitated by several factors including ChoP, choline-binding protein A (CbpA), the ancillary pilus subunit (RrgA), adherence and virulence protein A (PavA), and large surface-exposed glycoprotein (PsrP). This adherence is mediated by the interaction between ChoP and the Platelet-Activating Receptor (PAFR), as well as between CbpA and the polymeric immunoglobulin receptor (PIGR) (Zhang et al., 2000). Upon this binding, pneumococci manipulate host receptor recycling pathways, inducing endocytosis into lung epithelial cells, and ultimately facilitating the subsequent exocytosis onto the basolateral surface (Cundell et al., 1995). An alternative mode of passage to the interstitial spaces through the lung epithelium involves a paracellular route. Here, Ply and hydrogen peroxide (H_2O_2) damage the epithelium, while hyaluronate lyase (Hy1) and plasmin, which are bound to the bacterial surface vie enolase (Eno), glyceraldehyde-3-phosphate dehydrogenase (GAPDH), or choline binding protein E (CbpE), also known as Pce (phosphorylcholine esterase), contribute to the degradation of the extracellular matrix. These combined actions result in penetration of the lung epithelium. Importantly, interactions involving ChoP-PAFR and CbpA-PIGR also play a pivotal role in enabling pneumococci to transverse the endothelial barrier, allowing the bacteria to infiltrate the bloodstream and initiate haematogenous spread (Cundell et al., 1995; Zhang et al., 2000; Kadioglu et al., 2008; Hergott et al., 2015).

To breach the blood-brain barrier (BBB), pneumococci employ a strategic approach involving interactions with various receptors on the brain microvascular endothelium. Notably, *S. pneumoniae* once again harnesses the binding capabilities of ChoP-PAFR and CbpA-PIGR, alongside CbpA's interaction with the laminin receptor on the brain microvascular endothelium (Orihuela et al., 2009; Brown et al., 2014). Furthermore, in instances where pili are expressed, strains utilise the tip adhesin RrgA from pneumococcal pilus 1 to engage with PIGR and platelet endothelial cell adhesion molecule 1 (PECAM1) on the brain microvascular endothelium. Strikingly, experimental inhibition of these receptors yielded a reduction in brain invasion rates, as evidenced by a murine meningitis model study (Iovino et al., 2017).

Analogous to the tactics employed during invasion of the respiratory tract, a combination of Ply, α-glycerophosphate oxidase (GlpO)-generated H_2O_2, and activated plasmin – bound to pneumococcal surface proteins Eno, GAPDH and CbpE – can undermine the integrity of the BBB (Rayner et al., 1995; Attali et al., 2008; Mahdi et al., 2012). Another avenue for potential meningitis occurrence involves localised infections or retrograde axonal transport. In the latter scenario, pneumococci adhere to gangliosides on olfactory neurons located on the nasopharyngeal mucosa, leading to retrograde movement and potential access to the brain (van Ginkel et al., 2003). Furthermore, the introduction of exogenous sialic acid has been observed to stimulate this non-haematogenous spread across the BBB (Hatcher et al., 2016).

Strikingly, studies in mice have shown that pneumococci exhibit the ability to swiftly translocate from the nasopharynx to the dorsal meninges, within minutes. This implies the potential existence of an inward flowing fluidic connection that links the nasopharynx to the meninges, as opposed to being solely driven by receptor-mediated mechanisms. Furthermore, this process operates in a size-dependent manner as microspheres of the same size as pneumococci were able to translocate to the meninges, whilst larger microspheres were unable to, suggesting a size-restricted mechanism is at play (Audshasai et al., 2022).

1.3. Pneumococcal virulence determinants

1.3.1. The capsular polysaccharide

The capsular polysaccharide (CPS) forms the outermost layer of encapsulated pneumococci; it is considered the most important virulence factor, with a role in both protection and virulence. Currently there have been more than 100 structurally and serologically distinct capsular serotypes identified, with each serotype having different propensities to cause localised or invasive disease (Ganaie et al., 2021). The capsule ranges from 200 to 400 nm thick (Sørensen et al., 1988),

however nutrient availability can affect the thickness in some serotypes (Hathaway et al., 2012). In the majority of capsular serotypes CPS is covalently attached to the cell wall peptidoglycan (Sørensen et al., 1990), with the exception of serotypes 3 and 37, which attach through interactions with cell membrane phosphatidylglycerol (Cartee et al., 2005). Conversely to the other serotypes, biosynthesis of serotype 3 and 37 CPS utilises a synthase dependent mechanism, resulting in the capsule for serotype 37 only being composed of one sugar (glucose) and serotype 3 capsule being composed of two sugars (glucose and glucuronic acid). Serotypes 3 and 37 display the largest capsules of the known serotypes, predominantly appearing as mucoid colonies, however serotype 3 pneumococci are amongst the most virulent whilst serotype 37 pneumococci are less virulent (Austrian, 1981).
The CPS can exist in simple forms as linear polymers composed of repeating units of two or more monosaccharides, while more complex structures involve branched polysaccharides with repeat units comprising of up to six monosaccharides and additional side chains (Geno et al., 2015).

In the context of disease, CPS contributes to pneumococcal pathogenesis through various mechanisms. Within a given strain and serotype, capsular thickness has been found to directly correlate with virulence (MacLeod & Kraus, 1950). In turn, this correlates with the differences observed between pneumococcal serotypes in their capacity to cause IPD. Non-encapsulated pneumococci can colonize the upper respiratory tract and cause superficial eye infections; however, they rarely cause IPD (Keller et al., 2016).

The distinct CPS serotypes differ in their ability to inhibit opsonophagocytosis *in vitro* and their ability to elicit a humoral immune response. CPS is capable of interfering with both the classical and alternative complement pathways, acting as a physical barrier to inhibit the binding of immunoglobulins, C-reactive protein, and complement components to deeper surface structures. The CPS reduces the opsonisation with C3b/iC3b components of the complement pathway, consequently preventing the interaction between bound C3b/iC3b or Fc regions of immunoglobulins with their respective receptors on phagocytic cells (Abeyta et al., 2003; Hyams et al., 2010).

Although the CPS plays an important role in preventing immune clearance, the CPS impedes the adherence and invasion of host cells by sterically hindering the interactions between cell wall surface proteins and host receptors, preventing successful colonisation (Talbot et al., 1996; Hammerschmidt et al., 2005; Zafar et al., 2017). Therefore, the capacity to regulate capsule

expression at different times in the course of colonisation and infection is critical. Importantly, it has been found that during the infection progression from colonisation to invasion the pneumococci can greatly reduce the CPS thickness during invasion of host cells (Hammerschmidt et al., 2005), with significant changes in the expression of various virulence determinants to adapt to different host environments (Orihuela et al., 2004; Ogunniyi et al., 2012).

1.3.2. Other virulence factors

Streptococcus pneumoniae possesses an extensive repertoire of factors that play crucial roles in its virulence, including several surface and non-surface proteins that enhance its pathogenicity. Although there are numerous proteins that have been implicated in virulence, there are several notable examples that may have promise as potential vaccine candidates, including Pneumolysin (Ply), Choline-binding proteins (PspA, PspC/CbpA and LytA), transporters such as PsaA, PiaA and PiuA, as well as various LPXTG-anchored proteins. Importantly, it has been found that the expression of capsular polysaccharide (CPS) and Ply have been shown to enhance pneumococcal survival ex vivo for less nutrient-rich environments like airway surfaces (Zafar et al., 2017; Hamaguchi et al., 2018).

Pneumolysin (Ply), a potent and broad-acting virulence factor, is a soluble protein weighing 52 kDa (van Pee et al., 2017). Cholesterol-dependant cytolysins, such as Ply, are produced by Gram-positive bacteria, with Ply itself being present in nearly all pneumococcal isolates, with a highly conserved amino acid sequence and only a few variants (Mitchell et al., 1990; Lock et al., 1996; Kirkham et al., 2006; Yun et al., 2015). Within the membranes of target cells, Ply forms oligomers that are made up of approximately 40 monomer subunits. These oligomers create large ring-shaped pores that transverse the cell membrane and are approximately 260 Å in diameter (Tilley et al., 2005; Vögele et al., 2019). It is the pore-forming oligomers that are believed to be responsible for the various cytolytic and cell-modulatory activities exhibited by Ply (Badjugar et al. 2020). These cell-modulatory activities are exhibited at sub-lytic concentrations and include inhibiting ciliary beating on the respiratory and brain epithelia, suppressing phagocyte respiratory burst, inducing cytokine synthesis, and the subsequent activation and chemotaxis of CD4+ T-cells (Paton & Ferrante, 1983; Hirst et al., 2004; Kadioglu et al., 2004). Furthermore, it has been demonstrated, through site-directed mutagenesis, that Ply can activate the classical complement pathway even in the absence of antibodies and independently of its cell-modulatory activities, hence reducing serum opsonic activity (Paton et al., 1984; Mitchell et al., 1991).

Numerous *in vivo* studies, using mutagenesis of the *ply* gene, have unequivocally demonstrated that Ply significantly contributes to the virulence of pneumococci in mice, providing clear evidence for its role in pathogenesis (Berry et al., 1989; Berry et al., 1995; Feldman et al., 1991; Canvin et al., 1995; Rubins et al., 1996; Alexander et al., 1998; Jounblat et al., 2003; McNeela et al., 2010). Specifically, studies have investigated the impact of both complement activation and cell-modulatory functions of Ply on pneumococcal virulence *in vivo* (Canvin et al., 1995; Rubins et al., 1996; Alexander et al., 1998; Jounblat et al., 2003). However, certain isolates of pneumococci that produce a non-haemolytic variant of Ply have been found to be equally or even more virulent than isolates with strains with fully functional Ply, implying the presence of additional unknown functions of this virulence factor (Alexander et al., 1998; Kirkham et al., 2006), with non-haemolytic isolates provoking TLR4 or IFN- responses (Baba et al., 2002; Malley et al., 2003). Further indirect evidence supporting Ply's importance in pathogenesis comes from immunisation studies with native pneumolysin (Paton et al., 1983) or non-toxic recombinant Ply derivatives (Paton et al., 1991; Alexander et al., 1994), which conferred significant protection against multiple serotypes of pneumococci.

The Choline-binding proteins PspA, PspC/CbpA and LytA are pivotal pneumococcal virulence factors extensively characterised for their roles in pathogenesis. These proteins are attached to the cell wall through phosphorylcholine (ChoP) moieties present in the cell wall teichoic acid and lipoteichoic acid. Choline-binding proteins typically contain 20 amino acid repeat sequences that facilitate their attachment to the cell surface via ChoP, with significant variability in their N-terminal sequences (Jedrzejas, 2001a; Maestro & Sanz, 2016).

PspA consists of three structural domains, with an N-terminal region composed of repeated alpha-helices that protrude from the surface of pneumococci (Jedrzejas et al., 2001b). Notably, due to the high variability exhibited by PspA among different pneumococcal strains, the N-terminal sequence is used to classify it into three families, which are further divided into 6 clades (Hollingshead et al., 2000). Its mechanism of action involves inhibiting complement component C3 from binding to the pneumococcal cell surface, potentially due to its highly electronegative properties, effectively inhibiting opsonisation (Jedrzejas et al., 2001b; Kadioglu et al., 2008). Moreover, it acts as a lactoferrin binding protein, conferring protection against the bactericidal activity of apolactoferrin (Shaper et al., 2004). Whilst the contributions of PspA to these processes have been well-established, its *in vivo* role has been more challenging to decipher. Studies on serotype 3 and serotype 4 pneumococci have shown that PspA is essential for *in vivo* growth, but

this was not consistently observed in serotype 2 strains (Berry & Paton, 2000; Abeyta et al., 2003; Orihuela et al., 2004).

PspC, also known as choline binding protein A (CbpA) and secretory pneumococcal surface protein A (SpsA), is a multifunctional cell-surface protein with diverse roles (Kadioglu et al., 2008). It plays a vital role in pneumococcal adherence and colonisation, with *pspC* knockout mutants showing decreased binding to epithelial cells and sialic acid, resulting in diminished nasopharyngeal colonisation compared to wildtype strains and reduced virulence in murine pneumonia and sepsis models (Rosenow et al., 1997; Jounblat et al., 2003; Iannelli & Pozzi, 2004; Quin et al., 2005). PspC can also bind to the polymeric immunoglobulin receptor, a crucial step in facilitating the translocation of secretory IgA across the respiratory epithelium (Hammerschmidt et al., 2000; Zhang et al., 2000; Asmat et al., 2014). Furthermore, PspC can bind to factor H (Janulczyk et al., 2000; Dave et al., 2004) to prevent C3b formation via the alternative pathway of the complement system, thereby interfering with opsonisation and complement-mediated clearance (Quin et al., 2005).

LytA is a pivotal amidase that plays a critical role in pneumococcal cell autolysis by cleaving peptidoglycan N-acetylmuramoyl-L-alanine bonds (Howard & Gooder, 1974), particularly evident during pneumococcal growth in batch culture (Svendsen et al., 1979). Beyond its autolytic function, LytA is implicated in essential processes such as cell-wall biosynthesis and turnover. The importance of LytA in pneumococcal virulence is well-established, with strong evidence indicating its association with pathogenicity. Deletion of *lytA* has resulted in mutants that consistently displayed reduced virulence in both pneumonia and sepsis murine models of infection (Berry et al., 1989; Canvin et al., 1995; Berry & Paton, 2000; Orihuela et al., 2004). The contribution of LytA to virulence is likely due, in part, to the release of Ply, lipoteichoic acids and inflammatory peptidoglycan fragments upon pneumococcal lysis (Kadioglu et al., 2008; Mellroth et al., 2012).

Streptococcus pneumoniae possess 45 pneumococcal cell-surface lipoproteins (Bergmann & Hammerschmidt, 2006), with several playing a critical role in pneumococcal virulence. Among these, key contributions come from the metal-binding lipoproteins, pneumococcal surface antigen A (PsaA), pneumococcal iron acquisition A (PiaA) and pneumococcal iron uptake A (PiuA) (Kadioglu et al., 2008).

PsaA functions as the divalent metal-ion-binding lipoprotein component of the ATP-binding cassette (ABC) transport system with a primary role in the uptake of manganese ions (Dintilhac et al., 1997; Lawrence et al., 1998; McAllister et al., 2004). PsaA knockout mutants exhibit impaired growth in the absence of manganese (Dintilhac et al., 1997), reduced adherence to mammalian cells *in vitro* (Berry and Paton, 1996; Briles et al., 2000), and are avirulent in murine sepsis, pneumonia and colonisation models (Berry & Paton, 1996; Johnson et al., 2002; Marra et al., 2002; McAllister et al., 2004). Notably, studies on *psaA* mutants have suggested that manganese uptake is critical for resistance of pneumococci to oxidative stress. This is due to the importance of manganese for the function of the SodA enzyme, which aids in the detoxification of hydrogen peroxide produced during pneumococcal metabolism and reactive oxygen species generated during host innate immune responses (Yesilkaya et al., 2000; Tseng et al., 2002; McAllister et al., 2004).

PiaA and PiuA are lipoprotein metal-binding proteins associated with two ABC iron and iron-carrier uptake transporters (Whalan et al., 2005; Cheng et al., 2013; Kohler et al., 2016). The transporters demonstrate some redundancy, as deletion of either one results in a minor reduction in growth in iron-deficient medium, with deletion of both piu and pia resulting in significantly attenuated growth. Nevertheless, mutations in either of these transporters lead to decreased virulence in murine models of pneumoniae and sepsis, with the double mutant displaying the most significant reduction in virulence (Brown et al., 2002). Interestingly, it has also been noted that deletion of *luxS*, encoding a S-ribosylhomocysteine lyase, from the pneumococcal D39 strain results in a reduction of *piuA* expression and consequently leading to less iron being present in the *luxS* deletion mutant (Trappetti et al., 2013).

Gram-positive bacteria, including *S. pneumoniae*, employ sortase transpeptidases to covalently anchor certain surface proteins to their peptidoglycan. The pneumococcal sortase transpeptidase (SrtA) is responsible for recognising the LPXTG amino acid motif in certain surface proteins and anchoring them covalently to the peptidoglycan. The recognition of the LPXTG amino acid sequence, where “X” represents any amino acid, within the surface proteins is crucial for this anchorage. Whilst some pneumococci strains contain a single sortase gene, others encode multiple sortase-like genes (Bergmann & Hammerschmidt, 2006). In strains with multiple sortase-like genes, SrtA is primarily responsible for anchoring most LPXTG-containing protein, while other sortase proteins mediate the anchorage of specific subsets of surface proteins (Hava & Camilli, 2002). Studies utilising murine, chinchilla and *in vitro* adhesion models have demonstrated the SrtA

plays pivotal roles in pneumococcal colonisation, pneumonia and septicaemia (Kharat & Tomasz, 2003; Chen et al., 2005; Paterson & Mitchell, 2006b). Up to 20 pneumococcal proteins, including neuraminidases and Hic in some serotypes, are believed to be anchored by an LPXTG motif (Iannelli et al., 2002; Bergmann & Hammerschmidt, 2006).

Neuraminidases, also known as sialidases, play a vital role in cleaving terminal sialic acid residues off of various glycoproteins, glycolipids, cell surface oligosaccharides, and even soluble proteins such as lactoferrin and IgA2 (King et al., 2004; Yesilkaya et al., 2008). Pneumococci typically produce at least three neuraminidases: NanA, NanB and NanC. Of these, NanA is present in all strains, NanB is found in most and NanC is only present in approximately 50% of strains (Pettigrew et al., 2006). Whilst all neuraminidases can be secreted from the pneumococcal cell, only NanA contains an LPXTG motif, suggesting differing functions. This is further supported by NanB having a drastically lower optimum pH than NanA (Berry et al., 1996). Studies utilising loss-of-function neuraminidase mutants in acute pneumonia murine models have demonstrated the importance of both NanA and NanB in pneumococcal persistence in the respiratory tract and bloodstream (Manco et al., 2006). Furthermore, this study also found that the NanA mutant was rapidly cleared from the respiratory tract, whilst the NanB mutant was able to persist without any increase in bacterial load, indicating different roles for these enzymes (Manco et al., 2006). Whilst experimental evidence for the significance of NanC is lacking, sequence analysis of *nanC* across pneumococcal isolates suggested that any role it plays may be tissue-specific, with *nanC* being more common in isolates from cerebrospinal fluid (CSF) compared to carriage isolates (Pettigrew et al., 2006).

1.4. Vaccines and therapeutic strategies

1.4.1. Antibiotics and emerging resistance

Following the introduction of penicillin, a beta-lactam antibiotic, in the 1940s antibiotics have been widely used for the treatment of pneumococcal infections. However, the emergence of penicillin-resistant strains, first reported in a paediatric patient in 1967 (Hansman & Bullen, 1967), ushered in a dramatic increase in antibiotic resistance rates (Lynch & Zhanel, 2009; Cherazard et al., 2017). The inappropriate administration and overuse of beta-lactam antibiotics played a substantial role in the development and perpetuation of this resistance (Cherazard et al., 2017). This resistance primarily arises due to mutations in penicillin-binding proteins, rendering penicillin ineffective in inhibiting peptidoglycan production (van der Poll & Opal, 2009). The rates of pneumococcal penicillin resistance vary greatly across regions. Non-susceptibility rates exceed 50% in East Asia

and the Middle East, and 30% in Spain. In contrast, rates remain below 5% in Finland, Germany, and Sweden (Bruinsma et al., 2004; Lynch & Zhanel, 2009; Mamishi et al., 2014; Cherazard et al., 2017; El Moujaber et al., 2017).

In addition to beta-lactams, macrolide antibiotics like erythromycin, azithromycin, and clarithromycin have become standard in the treatment of pneumococcal infections (Cherazard et al., 2017). Macrolides are characterised by a large lactone ring ranging from 12 to 16 atoms in size (Zhanel et al., 2001). They function by binding to the 23S rRNA, consequently inhibiting RNA-dependent protein biosynthesis and leading to cell death (Cherazard et al., 2017). However, studies have shown a correlation between penicillin resistances and resistance to macrolide antibiotics, fluoroquinolones, and tetracycline (Lynch & Zhanel, 2009; Cherazard et al., 2017). The current global resistance rates to macrolides, ranging from 10 to 70%, continue to rise due to the persistent overuse of antibiotics (Zhanel et al., 2014). Furthermore, the SENTRY Antimicrobial Surveillance Program has reported a steady increase in resistance rates against erythromycin and clindamycin in pneumococcal isolates in the United States since 1998 (Jones et al., 2013). The high genetic transformability of pneumococci facilitates the rapid spread of antibiotic resistance through lateral transfer of resistance genes and cassettes. Moreover, the misuse of antibiotics exerts strong selective pressure that is driving the escalating rates of resistance and resulting in reliance on new and more costly treatment regimens. Consequently, there is a growing need for improved prevention and treatment strategies to combat pneumococcal disease and reduce the reliance on antibiotics.

1.4.2. Vaccines and serotype replacement

Pneumococcal disease poses a significant health challenge, and vaccination has been a vital strategy to prevent invasive diseases. The CPS of *S. pneumoniae* plays a crucial role in the colonisation and virulence of the bacterium and is highly immunogenic in adults. As a result, it has become the primary antigen target in current vaccine formulations (Bogaert et al., 2004). Early efforts by Robert Austrian and his team in the United States led to the licensure and release of a 14-valent purified CPS vaccine in 1977, offering protection against 14 of the most common invasive pneumococcal serotypes (Austrian et al., 1976; Smit et al., 1977). This vaccine effectively reduced morbidity and mortality in the healthy adult population. However, it had limited impact on overall pneumonia rates (Riley et al., 1977) and was very poorly immunogenic in young children (Douglas et al., 1983).

In 1983, an expanded coverage 23-valent polysaccharide vaccine (PPSV23) that provided coverage against 80-90% of the virulent pneumococcal serotypes was introduced. PPSV23 successfully reduced the incidence of IPD within the target population (older adults) and remains in use today. However, similar to the 14-valent purified CPS vaccine it did not have the same impact on carriage and pneumonia rates (Fine et al., 1994; Stanek et al., 2016). Notably, a major limitation of PPSV23 is its relatively low levels of immunogenicity in vulnerable populations, such as young children, the elderly and immunocompromised individuals. This diminished response is due to the CPS being a T-cell independent antigen, resulting in the majority of antibody response arising from the expansion of cognate B cells (Daniels et al., 2016). Therefore, whilst PPSV23 can induce an immune response, these vulnerable populations cannot mount an effective T-cell independent immune response, resulting in compromised vaccine efficacy (Heilmann, 1990; Shapiro et al., 1991).

To address these limitations, the development of polysaccharide-protein conjugate vaccines (PCVs), was undertaken, in which each of the included polysaccharide serotypes is conjugated to a protein carrier, promoting a T-cell dependent immune response, antibody maturation and the generation of memory cells. Initially, a 7-valent CPS conjugate vaccine (PCV7) was developed, covering serotypes 4, 6B, 9V, 14, 18C, 19F and 23F, with the CPS conjugated to CRM197, a non-toxic variant of diphtheria toxin. This vaccine was licensed in 1999 and elicited a T-cell dependent antibody response, even in children under 2 years old. It was highly protective against IPD caused by included serotypes, whilst providing additional herd immunity benefits in associated adult populations. However, despite its success against IPD, it provided very little protection against incidences of OM (Whitney et al., 2003; Hammitt et al., 2006; von Gottberg et al., 2014).

The effectiveness of CPS conjugate vaccines against the included serotypes is undeniable; however, their overall serotype coverage is limited. This has led to a concerning phenomenon known as “serotype replacement”, in which the rates of carriage and disease caused by non-vaccine serotypes has increased. This occurrence happens when the non-vaccine serotypes take advantage of the unoccupied nasopharyngeal niche and subsequently cause disease. Since the introduction of PCVs, this phenomenon has been reported, with the overall reductions in morbidity and mortality due to PCV introduction being offset by serotype replacement (Ghaffar et al., 2004; Lipsitch et al., 2007; Grivea et al., 2008; Dagan, 2009; van Gils et al., 2009; Gladstone et al., 2017; Corcoran et al., 2019; Kandasamy et al., 2020).

In 2010, due to this increase in the incidence of disease caused by non-vaccine serotypes, the serotype coverage of PCV7 was expanded to include six additional serotypes (1, 3, 5, 6A, 7F and 19A) in addition to the original seven serotypes, resulting in a 13-valent conjugate vaccine (PCV13). Notably, the inclusion of types 6A and 19A aimed to address the lower-than-anticipated cross-protection elicited by the 6B and 19F antigens present in PCV7 (Bryant et al., 2010).
In 2021, a 15-valent conjugate vaccine (PCV15) was approved for use in adults over the age of 18 years, following safety and immunogenicity trials in adults over the age of 50 (Peterson et al., 2018; Stacey et al., 2019). PCV15 contains two serotypes, 22F and 33F, in addition to those in the PCV13 formulation, following an increase in the diseases caused by these serotypes. PCV15 has also recently been approved in the US for use in persons under the age of 19 years, following a study in which PCV15 elicited similar immunogenicity and displayed similar safety and tolerability in children under 2 years (Platt et al., 2020). Following the development of PCV15, an additional five serotypes (8, 10A, 11A, 12F and 15B) were added to the formulation to create the 20-valent conjugate vaccine, PCV20, further protecting against more virulent serotypes. In October 2021, the PCV20 was approved for use in all adults over 65 years of age or in adults between the ages of 19 to 64 with underlying medical conditions following safety trials (Essink et al., 2021; Hurley et al., 2021).

The improvements in pneumococcal vaccines by the development of PCVs has significantly improved the protection against pneumococcal diseases, especially in vulnerable populations. The promotion of a more effective immune response, with greater serotype coverage, has resulted in these vaccines contributing to the reduction of pneumococcal disease burden, whilst simultaneously enhancing global public health efforts.

However, in light of the concerning trends of serotype replacement observed in pneumococcal carriage and IPD, coupled with the rising antibiotic resistance rates, the need for broader preventative strategies is becoming increasingly urgent.
Colonisation is known to trigger natural immunisation events by elevating anti-capsular and anti-protein antibody levels (McCool et al., 2002; Richards et al., 2010; Ferreira et al., 2013), with recent studies emphasising the pivotal roles of anti-protein antibodies in conferring natural immunity to pneumococci (Wilson et al., 2017; Ramos-Sevillano et al., 2019). Consequently, protein antigens that exhibit high conservation across multiple pneumococcal serotypes hold the potential to provide serotype-independent protection against IPD, mitigating the risk of serotype replacement (Stanek et al., 2016). Numerous protein antigens have been investigated as potential vaccine targets,

including neuraminidase, LytA, Ply, CbpA, PspA, pneumococcal surface antigen A (PsaA), and polyhistidine triad protein D (PhtD) (Lock et al., 1988; McDaniel et al., 1991; Paton et al., 1993; Sampson et al., 1997; Chen et al., 2015; Pichichero, 2017; Afshar et al., 2020). These protein antigens are predicted to elicit a T-cell dependent response, resulting in long-term immunological memory.

Another promising approach to elicit non-serotype dependent protection involves using whole cell vaccines (WCVs). Modern WCVs are based on killed, non-encapsulated pneumococci, in which a wide range of surface protein antigens are exposed. Immunisation with these vaccines elicits a broad protection against pneumococcal surface proteins, resulting in an immune response that mimics natural human immunity, which develops in late childhood via natural exposure to pneumococci. Notably, the natural human immunity arises predominantly from anti-protein antibodies rather than anti-capsular antibodies (Wilson et al., 2015). Recent studies with a strain of un-encapsulated pneumococci, Rx1, expressing non-toxic Ply with a lytA-deletion have demonstrated that generating antibodies against a range of pneumococcal antigens can be effective in providing protection against both nasopharyngeal carriage and sepsis in murine models (Malley et al., 2001; Lu et al., 2010; Babb et al., 2016). WCVs have the potential for affordable, broad range protection against all pneumococci, irrespective of serotype (Morais et al., 2019), making them more suitable for widespread use, especially in developing countries. Both chemically killed (Moffit and Malley, 2016) and γ-irradiated (Babb et al., 2016; Babb et al., 2017; David et al., 2019; David et al., 2022) pneumococcal WCVs have been developed and have undergone or are currently undergoing clinical trials to assess their safety and efficacy in providing serotype-independent protection.

1.4.3. Host immune responses

1.4.3.1. Innate immunity

The innate immune system provides the first line of defence against infection by *S. pneumoniae*, by producing a rapid yet non-specific response that is initiated against any foreign invaders. This important defence mechanism is triggered by the recognition of pathogens, mediated by pattern recognition receptors (PRRs) located on the surfaces of host cells or within them. These receptors can identify pathogen-associated molecular patterns (PAMPs), resulting in the activation of a signalling cascade leading to what is known as the innate immune response (Paterson & Mitchell, 2006a; Murphy et al., 2008). Within the multiple PRRs identified, Toll-like receptors (TLRs) are

widely distributed across human immune cells and play critical roles in the recognition and response to pneumococcal infection (Koppe et al., 2012). Typically located bound to the cell membrane, with the exception of TLR9 (located on endosomes within cells), TLR2, TLR4 and TLR9, have a critical role in recognising pneumococci (Srivastava et al., 2005; Richard et al., 2014; Tomlinson et al., 2014). TLR2, TLR4 and TLR9 identify essential components of *S. pneumoniae* such as pneumococcal lipoproteins, the pneumococcal toxin Ply, and CpG-DNA, respectively. Upon recognition of these components, TLRs initiate an innate immune response to help combat infection. Beyond their role in the innate immune response, TLRs also play a vital role in shaping the adaptive immune response. Specifically, they facilitate the release of co-stimulatory molecules necessary for T-cell activation, a critical step in mounting an effective and long-lasting immune defence (Rahman et al., 2009).

Another important class of PRRs are the nucleotide-binding and oligomerisation domain- (NOD-) like receptors (NLRs), which play a crucial role in innate immunity with their ability to recognise bacterial cell wall components. Upon ligand binding, NLRs initiate several critical immune response, including the activation of NF-kB dependent proinflammatory gene expression, stimulation of the inflammasome, promotion of cytokine production and induction of inflammation (Franchi et al., 2009; Murray, 2009; Koppe et al., 2012; Rabes et al., 2016).

In response to the production of inflammatory mediators, various innate immune cells are recruited to the site where the pathogen was encountered. These cells include basophils, dendritic cells, eosinophils, Langerhans cells, mast cells, monocytes, macrophages, neutrophils, and natural killer (NK) cells. Of these cells, neutrophils and macrophages are of particular importance for the clearance of pneumococcal infection (Paterson & Mitchell, 2006a; Murphy et al., 2008; Craig et al., 2009; Dockrell & Brown, 2016). As the most abundant innate cell type, neutrophils are among the first responders to the site of infection (Craig et al., 2009; Kolaczkowska & Kubes, 2013). They are highly phagocytic cells that produce granules capable of breaking down the cell walls of pathogens (Falloon & Gallin, 1986; Kolaczkowska & Kubes, 2013). Moreover, neutrophils are capable of trapping pneumococci extracellularly using fibres made from DNA (Gardiner & Andrews, 2012). Macrophages, similarly phagocytic in nature, play a critical role in engulfing and eliminating pneumococci. They target opsonised cells through the complement system and Fcγ receptors (Dockrell and Brown, 2015), but they can also phagocytose non-opsonised antigens through their receptor, MARCO (macrophage receptor with a collagenous structure) (Kraal et al., 2000).

In addition to neutrophils and macrophages, respiratory epithelial cells contribute significantly to the defence against pneumococci. They have the ability to produce antimicrobial peptides, such as aoplactoferrin and lysozyme, which are capable of lysing bacterial cells, preventing growth and sequestering iron from pneumococci (André et al., 2015; Whitsett & Alenghat, 2015). These respiratory epithelial cells also release cytokines and chemokines, which play a critical role in the recruitment of additional immune cells to the site of infection (Whitsett & Alenghat, 2015).

1.4.3.2. Adaptive immunity

The adaptive immune response, also known as acquired immunity, takes longer to develop and initiate compared with the innate immune response, however it is highly effective, robust and pathogen-specific. There are two main types of adaptive response: cell-mediated immunity involving T-cells and humoral immunity involving the production of antigen-specific antibodies by B-cells.

The activation of B-cells and subsequent class switching are essential for producing highly functional and specific antibodies, primarily IgG and IgA, which promote phagocytosis by opsonising the target pathogen. In pneumococcal infections, control at mucosal sites is also achieved through secretory IgA, which also opsonise bacteria to promote phagocytosis (Mook-Kanamori et al., 2011).

Cell-mediated immunity relies on T-cells, which play a pivotal role in clearing pneumococcal infections. T-cells are further divided into two broad classes: helper CD4+ T-cells and cytotoxic CD8+ T-cells (Mook-Kanamori et al., 2011). T-cell activation occurs when they recognise their specific antigen presented on the major histocompatibility complex (MHC) of professional antigen-presenting cells (APCs), including macrophages, dendritic cells, and B-cells (Brooks & Mias, 2018). After activation, helper T-cells can differentiate into Th1, Th2 or Th17 subsets, each playing unique roles in the immune response. Th1 cells primarily produce anti-inflammatory cytokines that drive an inflammatory immune response and recruit additional immune cells to the site of infection. Th2 cells interact with B-cells to promote class switching and antibody production (Romagnani, 1999) The interleukin- (IL-) 17 producing T-helper cells, Th17 cells, have a significant role in anti-pneumococcal immunity. The release of IL-17 from these cells recruits monocytes, neutrophils, and macrophages to the infection site, facilitating pneumococcal clearance. Furthermore, Th17 responses have been linked to reduced pneumococcal carriage (Hoe et al., 2017). In contrast, CD8+ T-cells directly kill infected host cells, similar to NK T-cells (van der Poll & Opal, 2009).

Following an infection, subsets of both B-cells and T-cells differentiate into memory cells that continue to circulate within the body. In the event of re-infection, these memory cells can be rapidly activated, enabling a faster, pathogen-specific adaptive immune response, leading to enhanced pathogen clearance (Sprent, 1994).

1.5. Carbohydrate metabolism

S. pneumoniae, a strictly fermentative bacterium, relies solely on glycolysis for energy production due to the absence of genes involved in the tricarboxylic acid cycle and an electron transport chain (Hoskins et al., 2001; Tettelin et al., 2001). This metabolic characteristic underscores the critical role of carbohydrates as an energy source, as evident from the extensive array of sugar transporters encoded within the genomes, with over 30% of all transporters dedicated to carbohydrate uptake (Hoskins et al., 2001; Bidossi et al., 2012).

It is known that pneumococci import at least 32 different carbohydrates through 21 phosphotransferase systems (PTS) and 8 ATP-binding cassette (ABC) transporters (Puyet et al., 1993; Brown et al., 2002; R. Iyer & Camilli, 2007; McKessar & Hakenbeck, 2007; Marion, et al., 2011a; Marion, et al., 2011b; Bidossi et al., 2012). These two transporter families differ primarily in their mechanism of cargo translocation. ABC transporters consist of an extracellular solute binding domain, responsible for binding the solute and delivering it to the transporter. Subsequently, the solute transverses the membrane through the transmembrane domain (TMD). Situated directly beneath the TMD, is the nucleotide binding domain that hydrolyses ATP, providing the energy required for transportation (Marion, et al., 2011a; Buckwalter & King, 2012). On the other hand, the PTS are composed of two cytoplasmic proteins, Enzyme I and Histidine Protein (HPr) (Deutscher et al., 2005). These facilitate the transfer of phosphate groups from phosphoenolpyruvate to the multi-domain Enzyme II, a sugar-specific transporter responsible for importing the desired carbon source (Postma et al., 1993; Buckwalter & King, 2012).

The imported carbohydrates then undergo glycolysis, a process through which one molecule of glucose is converted into two molecules of pyruvate, yielding two ATP molecules and two NADH molecules in the process. Subsequently, pyruvate is primarily metabolised to lactate through the action of lactate dehydrogenase, a process that regenerates NAD^+ and helps maintain redox balance (Harris & Harper, 2005). The balance between NADH and NAD^+ appears to play a crucial role in regulating pneumococcal fermentation. When there is an excess of easily convertible sugars, like glucose, or when oxygen tension is low, there is a high NADH-NAD^+ ratio, leading to

homolactic fermentation, where two molecules of lactic acid are produced (Ganzle, 2015). In contrast, when glycolytic flux is low, as seen during an excess of non-readily convertible sugars, and oxygen tension is high, pneumococci undergo mixed acid fermentation, resulting in the production of ethanol, acetate, and formate (Kandler, 1983; Yesilkaya et al., 2009).

During colonisation and infection, *S. pneumoniae* encounters diverse environmental niches with varying nutrient compositions, including carbohydrates. As a result, pneumococci have developed the ability to ferment a wide range of carbohydrates (Bidossi et al., 2012). Among the available carbon sources, glucose stands out as the preferred choice for the pneumococcus, closely followed by sucrose (Carvalho et al., 2011). Glucose is typically found in the blood of the human host, with concentrations ranging from 3.5 mM to 5.5 mM in healthy adults and inflamed tissues, although its availability varies between different niches (Güemes et al., 2016). The uptake of glucose into the cell is primarily facilitated by the PTS MalN-MalLM system, in which the incoming glucose is phosphorylated to Glucose-1-phosphate, enabling its entry into the glycolytic pathway. Alternatively, it can be transported via an ABC transporter, in which it undergoes phosphorylation to become Glucose-6-phosphate by the glucokinase Gki before entering the glycolytic pathway (Bidossi et al., 2012).

When glucose or sucrose are present in the niche in which the pneumococcus is, the metabolic pathways required for utilising other non-preferred carbon sources are supressed to optimise growth so that only preferred carbon sources, such as glucose and to a lesser extent sucrose, may be used. This phenomenon, known as 'Carbon Catabolite Repression' (CCR), ensures metabolic efficiency by preventing simultaneous utilisation of sugars. This process involves the phosphorylation of the phosphoprotein Hpr by the kinase HPrK, mediating CCR via both carbon catabolite protein A- (CcpA-) dependent and independent mechanisms (Iyer et al., 2005; Carvalho et al., 2011; Fleming et al., 2015). During CCR mediated by CcpA-dependent mechanisms, the transcription factor CcpA binds to catabolite repression elements (*cre*) found in the promoter region of genes responsible for non-preferred carbon source utilisation, leading to their repression. This regulatory process plays a crucial role in pneumococcal disease progression, as demonstrated by murine model studies where *ccpA* deletion mutants were severely attenuated in nasopharyngeal colonisation and lung infection, suggesting a link between carbohydrate metabolism and pneumococcal virulence (Iyer et al., 2005).

However, glucose is not abundant in all anatomical niches of the human host. In niches such as the nasopharynx and respiratory tract, where pneumococci primarily reside, glucose concentrations are typically below 1 mM, as an important part of the lungs' defence against bacterial infection (Philips et al., 2003). Subsequently, *S. pneumoniae* scavenge for other carbohydrate sources in these anatomical niches where glucose concentrations are low. Pneumococci utilise a range of extracellular glycosidases, such as NanA, BgaA and StrH, which have the capability to cleave sugars from N-linked glycoconjugates present on host epithelial cells (King, 2010). This enzymatic activity liberates sugars that can be subsequently taken up by their corresponding PTS or ABC transporters, providing essential substrates to support energy production in the bacterium. The glycosidases in pneumococci also exhibit specificity towards particular sugar structures. The galactose, a monosaccharide sugar cleaved from N-linked glycoconjugates present on host epithelial cells in the upper respiratory tract, is then metabolised by pneumococci through either the Leloir pathway or the Tagatose-6-Phosphate (T6P) pathway during homolactic fermentation (Paixão et al., 2015). Recently, it has also been shown that during mixed acid fermentation, pneumococcal galactose catabolism is controlled by several transcriptional regulators acting on pyruvate formate lyase, with both feed-back inhibition and activation being involved in the process (Al-Bayati et al., 2017).

S. pneumoniae also demonstrates its adaptability by being able to grow solely on mucins, which are glycosylated macromolecules predominantly composed of carbohydrates, serving as an alternative carbon source (Rose and Voynow, 2006). Additionally, studies have shown that pneumococci can modify the lipopolysaccharide structures of other bacteria, such as *Neisseria meningitidis* and *Haemophilus influenzae*, via the neuraminidase NanA to compete for surface carbohydrates on the host (Shakhnovich et al., 2002). *S. pneumoniae* are also capable of utilising the purified capsule of Group A Streptococcus as a carbon source for growth (Marion et al., 2012). Furthermore, as a human-adapted bacterium, *S. pneumoniae* demonstrates the ability to take up and metabolise various plant-derived sugars, consumed by humans, indicating its ability to adapt to diverse environments and utilise various carbohydrate sources (Hiss, 1905; Rosenow et al., 1999; McKessar and Hakenbeck, 2007; Shafeeq et al., 2011; Bidossi et al., 2012).

The ability of *S. pneumoniae* to adapt its carbohydrate utilisation strategy depending on the concentrations of the available carbohydrates in different host niches underscores its metabolic versatility and its capacity to thrive in diverse environments. Other airway commensal and pathogenic bacteria, such as *N. meningitidis*, *H. influenzae* and *Moraxella catarrhalis*, have more

limited carbohydrate utilisation abilities, except for *Staphylococcus aureus*, impacting their ability to survive in different host niches, with a competitive disadvantage against other bacterial species (Egan and Morse, 1966; Macfadyen et al., 1996; Leighton et al., 2001; de Vries et al., 2010). It is likely that pneumococci's capacity to utilise a wider variety of carbohydrates confers a competitive advantage against other bacteria within human host niches.

1.5.1. Impact of carbohydrate utilisation on pneumococcal disease

A recent study by Im et al. (2022) compared the effect of the carbohydrates available in the human nasopharynx compared with the blood on pneumococcal virulence and fitness during colonisation and disease. It was found that when the pneumococcal strain TIGR4 was grown in chemically defined media (CDM) with carbohydrates (galactose and sialic acid) mimicking the nasopharyngeal environment the pneumococci displayed reduced metabolic activity and slower growth, engaging in mixed acid fermentation with notable hydrogen peroxide production. They were also in a state of carbon-catabolite de-repression compared to cells cultured in CDM with carbohydrates (glucose and sialic acid) mimicking the blood. Transcriptome sequencing further revealed that changes in gene expression primarily were related to carbohydrate metabolism, with these genes also including those encoding key virulence factors, including capsule and surface adhesins. Notably, anatomical site-specific carbohydrate availability directly influenced well-established pneumococcal virulence traits. Cells grown in the blood-mimicking medium formed shorter chains, produced more capsule, exhibited reduced adhesiveness and demonstrated higher resistance to macrophage attacks in opsonophagocytosis assays. Importantly, the pre-growth of pneumococci in nasopharynx or blood-mimicking media significantly affected their fitness in colonisation and disease murine models. Specifically, pneumococci grown in nasopharynx-mimicking media were 4.9-fold more abundant in the nasal wash fluid, whilst there were greater numbers of pneumococci pre-grown in blood-mimicking media in the blood of infected mice. Together, these results demonstrate that site-specific carbohydrate availability influences pneumococci's physiology and virulence, ultimately impacting its fitness at specific anatomical sites (Im et al., 2022).

The most prevalent localised pneumococcal disease is otitis media, however our understanding of the sugar availability within the middle ear remains limited. Furthermore, the precise mechanisms and the specific genes necessary for the development of OM are still shrouded in mystery, primarily due to the scarcity of dependable *in vivo* and *in vitro* models. However, recent research has highlighted that variation in the uptake and utilisation of the plant-derived trisaccharide raffinose, appears to have an impact on disease outcome in a murine model, although the exact mechanism

behind its role in disease has yet to be fully discerned (Minhas et al., 2019; Minhas et al., 2020; Agnew et al., 2022).

A separate systematic review of five clinical trials revealed that xylitol, a five-carbon sugar alcohol commonly present in various fruits and vegetables, successfully lowered the incidence of acute OM in healthy children from 30% to 22%. However, the results remain inconclusive as to the efficacy in preventing OM in children with respiratory infections or children prone to OM infections (Azarpazhooh et al., 2016).

As discussed earlier (Section 1.5), although glucose is readily available in both blood and inflamed tissues, it undergoes fluctuations in concentration as invasive disease progresses to different anatomical niches (Philips et al., 2003). While pneumococci may form static biofilms during nasopharyngeal carriage and OM, they adopt a more planktonic lifestyle during IPD (Oggioni et al., 2006). As a result, the metabolic requirements for pneumococci causing IPD differ from those during nasopharyngeal colonisation or middle ear infection.

In a signature-tagged mutagenesis screen followed by murine competition assays, it was discovered that transporter and metabolic genes associated with the utilisation of various sugars, such as glucose, galactose, lactose, cellobiose, mannitol, galactitol, fructose, and mannose, were essential for successful establishment of lung infections (Hava and Camilli, 2002). Furthermore, certain carbohydrate-related factors crucial for nasopharyngeal colonisation were also found to be indispensable during IPD. For instance, the sucrose-6-phosphate hydrolase, SusH, and its corresponding sucrose ABC transporter were identified as critical factors in murine lung infections (Iyer and Camilli, 2007). Meanwhile, the deletion of *lacD* and *galK*, encoding the tagatose-1,6-bisphosphate aldolase and galactokinase, respectively, were associated with increased survival times in intranasally infected mice (Paixão et al., 2015). Another study found that blocking phosphorylation at key sites of GalR, a galactose operon repressor, had a significant impact on both the Leloir and tagatose 6-phosphate galactose metabolic pathways, diminishing the pneumococci's capacity to successfully colonise the nasopharynx, middle ear and lungs of intranasally infected mice (McLean et al., 2020).

The deacetylation of sialic acid via esterases also resulted in greater survival time for mice infected intranasally (Kahya et al., 2017). Furthermore, a separate study found that the administration of free sialic acid before intranasal challenge resulted in elevated numbers of bacteria in the central nervous system, likely facilitated through spread from the nasopharynx via the olfactory neurons (Hatcher et al., 2016). Notably, individual gene deletions encoding proteins responsible for cleaving/trimming N-glycans, such as endo-β-N-acetylglucosaminidase and α-(1,2)-mannosidase,

also led to reduced pneumococcal counts in the blood whilst prolonging survival in murine models (Robb et al., 2017).

As mentioned earlier, the ability to metabolise the carbohydrate raffinose influenced pneumococcal survival in the ears of intranasally infected mice (Minhas et al., 2019; Agnew et al., 2022). In the study by Minhas et al. it was found that in closely related (serotype 14 ST15) blood and ear isolates a SNP in the *rafR* gene led to reduced raffinose utilisation in the ear isolates, allowing these strains to spread into the brain of intranasally infected mice. Conversely, the clonally related blood isolates with enhanced raffinose utilisation were able to persist in the lungs of mice following intranasal challenge (Minhas et al., 2019). In a subsequent study (Minhas et al., 2020) using dual RNAseq analysis during early infection of murine lungs, the *rafR* SNP not only influence bacterial genes related to raffinose but also impacted multiple sugar transporters and enzymes for other carbohydrates. Additionally, this genetic variation caused significant alterations in the host's transcriptional responses to infection, particularly in genes related to cytokines, chemokines, and receptors. The differing virulence characteristics of blood and ear isolates were largely attributed to their distinct abilities to activate IL-17 signalling pathways and recruit neutrophils to the lungs in the early stages of infection (Minhas et al., 2020).

1.6. Fatty acids

Host-derived free fatty acids play pivotal roles in the host's defence against a spectrum of pathogenic agents, including bacteria, viruses and fungi (Kohn et al., 1980; Zheng et al., 2005; Ells et al., 2009; Desbois and Smith, 2010). Their primary function lies in comprising the integrity of cellular membranes, as they are key components of phospholipids, which are the building blocks of cell membranes, influencing the fluidity and stability of membranes. However, a wealth of research spanning diverse bacterial species has unveiled the multifaceted impact of free fatty acids on various cellular processes. These include not only membrane disruption but also intricate modulation of energy production, nutrient uptake, and enzyme activity, all of which occur in context-specific and organism-dependent manners (Desbois and Smith, 2010). The versatile influence of free fatty acids extends to thwarting the colonisation efforts of pathogenic microbes at the host-pathogen interface, as evidenced by compelling findings (Barakat et al., 2015; Mil-Homens et al., 2016). However, the assessment of the antimicrobial effectiveness of free fatty acids is a nuanced challenge. The complexity arises from the fact that many bacterial pathogens possess the capacity to harness host fatty acids both as an energy source and as building blocks for their own membrane synthesis (Balemans et al., 2010).

The current understanding of the impact of fatty acids on *S. pneumoniae's* disease-causing capabilities is an area still being explored. The synthesis of essential pneumococcal cell membrane fatty acids is orchestrated through the type II fatty acid synthase (FASII) system (Zhang and Rock, 2008), an intricate process encoded within a singular gene cluster (*fab*-cluster) that involves the covalent attachment of an acyl carrier protein (ACP) to the carboxyl end of the fatty acid. This unique arrangement facilitates the enzymatic elongation steps and the incorporation of double bonds (desaturation). The ultimate length of the fatty acid chain is a product of both transcriptional feedback loops and enzymatic preferences, culminating in the production of specific fatty acids with distinct functions such as protein acylation, polyketide synthesis, and the formation of complex lipid molecules like membrane phospholipids. A MaR-type regulator, known as FabT, governs the regulation of the fab-cluster, inhibiting fab-cluster transcription upon fatty acid binding (Jerga and Rock, 2009).

Notably, the FASII system does not work in isolation, as the pneumococcus also exhibits the ability to assimilate exogenous fatty acids into its membrane using the FakA/B system (Parsons et al., 2015). The initial recognition and binding of free fatty acids are orchestrated by FakB, a fatty acid binding protein. This event is followed by the linkage of a phosphate headgroup, achieved through the kinase activity of FakA, a kinase domain protein. These crucial actions transpire on the intracellular side of the cell membrane (Parsons et al., 2014).

Of particular significance is the activation triggered by FakA and FakB, which triggers PlsX, a soluble acyl-acyl carrier protein (ACP):PO4 transacylase, to attach exogenously acquired fatty acids to ACP (Parsons et al., 2015). This process allows pneumococci to bypass the FASII pathway entirely in the presence of exogenous fatty acids (Yao and Rock, 2017).

Importantly, the functionality of both the FASII system and FakA/B system is critical for the organism's survival *in vivo* (van Opijnen and Camilli, 2012).

1.6.1. Correlation between fatty acids and bacterial quorum sensing

Studies conducted within a range of different bacterial species, both Gram-negative and Gram-positive have indicated that fatty acids can also affect quorum sensing and subsequent biofilm formation. In the Gram-negative species *Acinetobacter baumannii*, mono-unsaturated chain fatty acids are able to reduce bacterial biofilm formation by up to 38%, whilst also exhibiting a capacity to disperse existing biofilms and significantly impair bacterial motility. Strikingly, this reduction in biofilm formation was linked to the downregulation of the *abaR* regulator within the LuxIR-type QS system present in *A. baumannii*, resulting in a decrease of the signalling molecule produced by this

QS system. Another aspect of this study investigated the impact of these fatty acids on 22 clinical isolates. Importantly, the antibiofilm activity of the fatty acids was revealed to be strain-dependent (Nicol et al., 2018).

In *Vibrio harveyi* and *Escherichia coli*, both medium and long chain fatty acids, such as palmitic acid ($C_{16:0}$), stearic acid ($C_{18:0}$), oleic acid ($C_{18:1}\omega9$) and linoleic acid ($C_{18:2}\omega6$) were capable of inhibiting AI-2 based cell signalling and biofilm formation included. In *V. harveyi* the inhibitory effects of these fatty acids on AI-2 signalling ranged from 25 to 90%, with a mixture of fatty acids resulting in 52 to 65% inhibition of AI-2 activity. In *E. coli* K-12 cells, fatty acids derived from ground beef were found to interfere with biofilm formation without exerting any adverse effects on bacterial cell viability (Soni et al., 2008).

In the Gram-positive bacteria *Streptococcus gordonii* short-chain fatty acids (SCFAs) have been found to inhibit biofilm formation. SCFAs, including sodium acetate, sodium propionate and sodium butyrate, demonstrated effective inhibitory activity against the formation of biofilms in *S. gordonii*, without causing any reduction in bacterial growth. Notably, these SCFAs exhibited a prominent suppression of *S. gordonii* biofilm formation during its early stages yet had no impact on pre-existing biofilms (Park et al., 2021b). One regulatory mechanism for biofilm formation that exists within streptococcal species, including *S. gordonii,* is the quorum-sensing mechanism mediated by competence stimulating peptide (CSP) (Loo et al., 2000). In *S. gordonii* SCFAs significant decrease in the mRNA expression of both comD and comE, which respectively encode the CSP-sensing protein and its associated response regulator, crucial components of the CSP pathway. This effect is especially noteworthy as these components play pivotal roles in the regulation of biofilm formation. Notably, even when exogenous synthetic CSP was employed to enhance *S. gordonii* biofilm formation, the presence of SCFAs counteracted this effect. The exact mechanism of how SCFAs negatively regulating the CSP pathway results in poor biofilm formation for *S. gordonii*, has not been established (Park et al., 2021b). One theory suggested that when CSP is present it may result in the production of a biofilm regulation peptide, such as BriC, resulting in enhanced biofilm formation as seen in *S. pneumoniae* (Aggarwal et al., 2020), thus when the CSP pathway is negatively by SCFAs in *S. gordonii*, this pathway may be suppressed, ultimately resulting in less biofilm formed (Park et al., 2021b).

Adjacent to the *S. pneumoniae* FASII locus, responsible for fatty acid biosynthesis, lies the compact peptide BriC (biofilm regulator induced by competence), an integral player in pneumococcal

physiology. BriC, is classified within the family of ribosomally synthesised peptides with double-glycine motifs, assumes significance in the pneumococcal context (Aggarwal et al., 2020). Remarkably, the induction of *briC* expression is orchestrated by ComE, the quintessential orchestrator of competence, establishing a direct link between two pivotal regulatory pathways. The secretory route of BriC involves utilisation of the competence-associated ABC transporter, ComAB, as a means of dissemination. The synthesis and subsequent secretion of BriC act as catalysts for the advancement of late-stage biofilm development *in vitro*, indicating it is a key player in the intricate orchestration of these biofilm structures. This influence extends to the complex landscape of nasopharyngeal colonisation, as affirmed by murine models of pneumococcal carriage (Aggarwal et al., 2018).

Importantly, it has been found that *briC* is co-transcribed alongside the genes within the *fab* gene cluster and its expression regulates the composition of membrane fatty acids in *S. pneumoniae*. Consistent with BriC's role in promoting the formation of biofilms, reducing the levels of *briC* expression by uncoupling it from the fab gene cluster has a negative impact on biofilm development. Strains in which *briC* is knocked out show decreased *fabT* expression, leading to a noticeable shift in the composition of molecular species of membrane phospholipids. This indicates that BriC plays a role in regulating the FASII process in pneumococci, either directly or indirectly, through its influence on the transcription of the FabT regulon. Alternatively, it is possible that the increased cell-to-cell signalling via quorum sensing associated with biofilm growth mode intensifies the effects of BriC on lipid composition, thereby establishing a connection between biofilms and lipid makeup in *S. pneumoniae* (Aggarwal et al., 2021).

1.7. Biofilms

A crucial factor in the pathogenesis of *S. pneumoniae* is their remarkable ability to form biofilms. Biofilms comprise a diverse population of highly organised bacterial cells enclosed within a matrix of extracellular polymeric substances. These substances consist of a mixture of extracellular DNA, proteins and polysaccharides produced by the bacteria themselves. Pneumococci have been found to colonise the nasopharynx in the form of biofilms. This plays a critical role in the subsequent development of pneumococcal infections (Stoodley et al., 2004). Furthermore, studies have identified specific niches within the body that provide optimal conditions for biofilm formation (Oggioni et al., 2006; Muñoz-Elías et al., 2008; Marks et al., 2012a; Chao et al., 2014). Both the nasopharynx and middle ear are such locations, providing reservoirs from which pneumococci can disseminate from to cause disease (Chao et al., 2014).

These complex biofilm structures serve as a protective shield for bacteria, enabling their persistence within the human host by providing resistance against host immune responses and antimicrobial agents. Adding to this, the intricate channel system within biofilms allows for the exchange of nutrients and signalling molecules, facilitating genetic exchange amongst pneumococci (Costerton et al., 1999; Donlan and Costerton, 2002; Cho et al., 2007; Lewis, 2008; Marks et al., 2012b). Unfortunately, this can lead to increased antibiotic resistance, as the drugs are unable to penetrate these biofilm structures effectively, resulting in shifts in pneumococci's phenotype (Nguyen et al., 2011; de la Fuente-Núñez et al., 2013). Furthermore, within biofilms, bacterial replication can become quiescent, occurring at an extremely slow rate (Allan et al., 2014). This characteristic is significant as many antibiotics primarily target bacterial replication pathways. As a result of both the slowed replication and the protective biofilm matrix, pneumococci within biofilms become over a thousand times more resistant to antibiotics, contributing to the recurrence of diseases (Chao et al., 2014).

In practice, biofilms present a major challenge in medical treatment. As many bacterial species persist within the nasopharynx even after antibiotic treatment, it is difficult to completely clear infections (Cohen et al., 1997; Dabernat et al., 1998; Dagan et al., 1998; Garcia-Rodriguez and Fresnadillo Martinez, 2002). This is especially concerning in conditions like otitis media or chronic rhinosinusitis, where biofilms can act as reservoirs for virulent bacteria, allowing them to reseed and trigger infections under favourable conditions (Weimer et al., 2010; Sanchez et al., 2011).

Bacterial cells within biofilms exhibit close proximity to each other and to the surrounding DNA, creating an optimal environment for genetic material exchange, which facilitates their survival and adaptation to the host environment. Notably, studies have highlighted that pneumococci that disperse from biofilms have distinct phenotypes. In *in vivo* murine models, biofilm-dispersed pneumococci demonstrated a remarkable ability to colonise the nasopharynx at higher levels compared to pneumococci grown in broth (Trappetti et al., 2011b). Additionally, these dispersed bacteria showed heightened dissemination to the middle ear and lungs (Marks et al., 2013).
Histological examinations further revealed that mice infected with biofilm-dispersed pneumococci experiences increased levels of inflammation and leukocyte infiltrates in the lungs, blood and middle ear, when compared to counterparts infected with planktonic *S. pneumoniae* (Blanchette-Cain et al., 2013). These differences in virulence between biofilm, planktonic and biofilm-dispersed bacteria suggest significant transcriptomic variations (Sanchez et al., 2011). The regulation of biofilm dispersal appears to be influenced by various environmental changes, which trigger

transcriptional alterations. These environmental changes include factors such as fever, ion concentrations, nutrient availability and pro-inflammatory cytokines present in the host (Grebe et al., 2010; Weiser, 2010; Marks et al., 2013).

1.8. Quorum sensing

Quorum sensing (QS) is a communication process employed by both Gram-negative and Gram-positive bacteria to orchestrate population-wide responses, commonly within biofilms. This mechanism is governed by the coordinated sensing and release, in a density dependent manner, of small signalling molecules called autoinducers or pheromones (Miller and Bassler, 2001; von Bodman et al., 2008). QS is intimately linked to several critical features in the pneumococcus. It enables the bacteria to synchronize their activities and behaviour based on the local population density. As the biofilm grows and cell numbers increase, the concentration of autoinducers rises, triggering specific responses within the bacterial community. These responses include regulation of competence and gene expression, biofilm development, symbiosis, sporulation, secretion of virulence factors and initiation of dispersal events (Johnston et al., 2014). In essence, QS acts as a sophisticated communication system, allowing the pneumococcus to act collectively as a unified entity, efficiently adapting to changing environments and optimising survival strategies during infection.

There are three main types of QS systems used by bacteria: LuxI/LuxR-type in Gram-negative bacteria, oligopeptide two-component type in Gram-positive bacteria and LuxS-mediated autoinducer 2 (AI-2) QS system in both Gram-negative and Gram-positive bacteria (Rutherford and Bassler, 2012).

1.8.1. Oligopeptide two-component type QS

The oligopeptide two-component type QS system is a communication mechanism unique to Gram-positive bacteria, relying on an Autoinducer signalling peptide (AIP) and a two-component signal transduction system (TCSTS) (Novick, 2003; Claverys et al., 2006). TCSTSs are composed of a histidine kinase and a response regulator protein. Upon sensing the AIP, the histidine kinase transfers a phosphate group to the response regulator protein, leading to differential gene expression (Stock et al., 2000).

One of the well-known examples of the QS system is the CSP/Com system that controls genetic competence in pneumococci. In the CSP/Com system, when the AIP, competence stimulating

peptide (CSP), is detected by the histidine kinase, ComD, which initiates a cascade of molecular events. The phosphate group is transferred to the response regulator protein, ComE, resulting in the activation of specific genes that play a crucial role in the regulation of genetic competence (Stock et al., 2000; Vidal et al., 2013) (Section 1.8.1.1).

1.8.1.1. Competence and natural transformation

Competence is a key feature that governs the natural transformability of the pneumococcus, as well as various other bacterial species (Lee and Morrison, 1999; Claverys and Håvarstein, 2002; Håvarstein et al., 2006). This critical process enables bacterial cells to take up extracellular DNA (eDNA) and integrate it into their genomes through homologous recombination. This process not only facilitates the repair of damaged DNA but also allows the acquisition of new advantageous traits, such as antibiotic resistance and virulence proteins, from neighbouring cells (Alioing et al., 1996; Johnston et al., 2014; Moreno-Gámez et al., 2017).

In *S. pneumoniae*, the regulation of competence is controlled by the *comABCDE* operon. The process starts with ComC, which is encoded as pre-CSP and exported via the ComAB ABC transporter/protease. Upon entering the extracellular space, ComC is cleaved into the competence stimulating peptide (CSP) (Håvarstein et al., 1995). CSP accumulates outside the cell and binds to the ComD histidine kinase receptor, which is part of the ComDE two-component signal transduction system. This binding triggers ComD auto-phosphorylation and the subsequent transfer of the phosphoryl group to ComE to form ComE-P. ComE-P then activates early competence genes that contain the Ceb promoter sequence, including *comABCDE* genes, *comM* (providing cellular immunity against lytic enzymes), and *comX* (encoding an alternative sigma factor) (Peterson et al., 2004; Håvarstein et al., 2006; Martin et al., 2013). ComX, in turn, controls the activation of late competence genes required for DNA uptake, transformation and fratricide.

Fratricide is the process by which competent pneumococci selectively lyse non-competent siblings, facilitating access to highly homologous DNA (Steinmoen et al., 2002). This mechanism is essential for gene integration between pneumococci and contributes to their pathogenicity by regulating the release of virulence factors like Ply (Claverys and Håvarstein, 2007). Key players in the lysis of target cells during fratricide are the murein hydrolase choline binding protein D (CbpD) and the early immunity protein ComM (Kausmally et al., 2005; Eldholm et al., 2009). Recent research has shown that fratricide can also lead to the release by closely related species, such as *S. mitis* and *S. oralis*, through CbpD binding to choline-containing teichoic acids (Johnsborg et al., 2008; Eldholm et al., 2010). Interestingly, the competence genes *comD*, *comX*, *comW*, *cglA*, *dltA* and the

murein hydrolase *cbpD*, which is associated with fratricide-dependent DNA release, were all directly related to *luxS* expression, a component of another bacterial communication system (Trappetti et al., 2011c).

Furthermore, bacteriocins, which are small ribosomal peptide antibiotics, play a role in promoting antagonistic interactions between different bacterial species within the same ecological niches. This competitive advantage benefits pneumococci (Wang and Kuramitsu, 2005). Notably, competence in *S. pneumoniae* has been tightly linked to bacteriocin production through various regulatory pathways (Shanker and Federle, 2017). For instance, lysis of non-competent pneumococci is mediated by the two-peptide bacteriocin CibAB, which targets cells lacking the corresponding immunity factor CibC (Guiral et al., 2005).

Whilst competence has long been recognised as critical for the acquisition of new virulence genes (Zhu and Lau, 2011), recent studies have revealed that the competence regulon can also cross-regulate virulence (Lau et al., 2001; Ibrahim et al., 2004; Guiral et al., 2005; Claverys and Håvarstein, 2007; Kowalko and Sebert, 2008). Notably, investigations focusing on the role of ComB, a component of the ABC transporter essential for CSP export, have shown that loss of function of this protein results in the attenuation of *S. pneumoniae* in a murine model of infection (Lau et al., 2001). Similarly, pneumococci mutants lacking the histidine kinase ComD also exhibit attenuation in virulence (Lau et al., 2001).

1.8.1.2. BlpABCSRH system

In addition to the CSP/Com pathway, another significant QS system in the pneumococcus is the BlpABCSRH pathway. This pathway plays a comparable role as it regulates the production of class II bacteriocins and their corresponding immunity proteins (Knutsen et al., 2004). The BlpABCSRH pathway is activated by the peptide BlpC, which binds to and activates the histidine kinase receptor BlpH. This leads to the phosphorylation of the response regulator BlpR (de Saizieu et al., 2000). Upon BlpC induction, several genes, including *blpABC*, *blpXYZ* and *blpSRH*, along with various putative bacteriocins and related immunity proteins that constitute the Bacteriocin Immunity Region (BIR), are upregulated (de Saizieu et al., 2000; Dawid et al., 2007; Dawid et al., 2009).

Notably, it has been found that there is a link between the CSP/Com and BlpABCSRH QS systems. Exogenous CSP can upregulate the *blp* operon, even in the absence of the *comAB* locus, suggesting a crosstalk between these two QS pathways (Wholey et al., 2016).

1.8.2. S-ribosyl-homocysteine lyase (LuxS)-mediated Autoinducer 2 QS

The LuxS-mediated autoinducer 2 (AI-2) QS system represents a common communication mechanism shared by both Gram-negative and Gram-positive bacteria, enabling them to interact with neighbouring cells (Surette et al., 1999; Wang et al., 2012). This QS system relies on the synthesis of a keto-pentose sugar-like molecule called Autoinducer-2, and its production is dependent on the metabolic enzyme S-ribosyl-homocysteine lyase (LuxS). In the pneumococcus, LuxS generates the precursor to AI-2, called 4,5-dihydroxy-2,3-pentanedione (DPD), as a by-product of the conversion of S-ribosyl-homocysteine to homocysteine, which is an integral part of the activated methyl cycle (Winzer et al., 2003; Yadav et al., 2018).

LuxS homologues have been discovered in nearly all bacterial species, emphasising the highly conserved nature of this cell-to-cell communication method (Kaur et al., 2018). Despite its widespread occurrence, the specific mechanism by which AI-2 accumulation mediates transcriptional responses remains poorly understood, particularly in Gram-positive bacteria.

The AI-2 QS system plays a crucial role in bacterial adaptation and behaviour, influencing various cellular processes such as virulence regulation, biofilm formation, and interspecies interactions. Specifically, studies have shown that pneumococcal strains lacking *luxS* are less invasive during murine intranasal challenge compared with the parent strain (Stroeher et al., 2003). Furthermore, strains lacking *luxS* exhibit significant reductions in biofilm formation, whilst strains overexpressing *luxS* demonstrate enhanced biofilm formation (Trappetti et al., 2011, 2017). In a rat model of infection, it was demonstrated that *luxS* is essential for biofilm formation and colonisation of the middle ear epithelium, with wildtype D39 being able to infect the middle ears of rats, whilst the *luxS* deletion strain was less prominent in the middle ear (Yadav et al., 2018).

1.8.2.1. The interplay between galactose metabolism and QS

In a study by Trappetti et al. (2017), the relationship between the pneumococcal quorum sensing system LuxS/AI-2 and sugar metabolism was elucidated. Using a serotype 2 strain (D39) with the *luxS* gene deleted (Δ*luxS*), they discovered that the mutant exhibited reduced growth in the presence of galactose compared to the wildtype D39. Interestingly, the growth of the Δ*luxS* mutant in galactose could be “rescued” by the addition of the QS molecule AI-2 in finite amounts. This finding provided the first indication of a link between QS and carbohydrate metabolism, specifically in the context of galactose (as the Δ*luxS* mutant grew as well as the wildtype D39 in glucose).

Further investigations confirmed this link by quantifying the total capsule present on both the wildtype and Δ*luxS* strains in the presence of galactose. Whilst capsule is primarily produced from glucose metabolism, it able to be generated through the metabolism of galactose via the Leloir pathway. This metabolic pathway results in an important precursor for the synthesis of various nucleotide sugars required for CPS biosynthesis (Carvalho et al., 2011; Paixão et al., 2015). The Δ*luxS* mutant showed a significant decrease in the amount of total capsule compared to the wildtype, indicating less galactose is being metabolised via the Leloir pathway. Intriguingly, the addition of AI-2 resulted in an increase in total capsule on the Δ*luxS* strain, bringing it to a level comparable to that of wildtype D39, indicating that the Leloir pathway was being utilised for galactose metabolism. This observation reinforced the proposed connection between quorum sensing and sugar metabolism (Trappetti et al., 2017).

Another study by Yadav et al. investigated the role of LuxS/AI-2 on biofilm formation, colonisation and gene regulation in D39 and D39Δ*luxS.* Here similar results, in regard to biofilm formation and virulence, to those previously observed were found (Trappetti et al., 2011c; Trappetti et al., 2017), with 117 genes being differentially regulated between the wildtype and mutant strains. Of these, the galactose pathway genes, such as *lacB*, *lacC*, *lacD*, and *lacA* (of the tagatose-6-phosphate pathway), and *galM* (of the Leloir pathway) were downregulated in D39Δ*luxS* compared to wildtype D39, further highlighting the likelihood that LuxS/AI-2 is linked to galactose metabolism in pneumococci (Yadav et al., 2018).

Additional RNA sequencing, performed by Trappetti et al., in the presence of AI-2 revealed candidate genes potentially involved in this relationship. Among them, *fruA* exhibited a 1.7-fold change in expression between the wildtype and the Δ*luxS* mutant. Further capsule studies in a Δ*fruA* mutant strain revealed no change in the total amount of capsule in the presence or absence of AI-2, while gene expression studies showed no change in the expression of the Leloir pathway genes (*galR*, *galK* and *galT*), required for capsule biosynthesis, in the Δ*fruA* mutant in the presence of AI-2. These findings led to the proposal that FruA might play a role in the sensing and uptake of AI-2 into the cell. Specifically, it has been suggested that FruA-mediated import of AI-2 results in phosphorylation of the signalling molecule, preventing it from diffusing freely out of the cell and effectively trapping it intracellularly. This phosphorylated AI-2 (AI-2-P) may then directly or indirectly facilitate phosphorylation of GalR, the activator of the Leloir pathway, potentially by acting as a phosphate donor (McLean et al., 2020). This would lead to the upregulation of the Leloir pathway and an increase in galactose metabolism, subsequently resulting in heightened capsule production

and a hypervirulent phenotype (Nelson et al., 2007; Carvalho et al., 2011; Paixão et al., 2015; Trappetti et al., 2017).

1.9. Genetic diversity

S. pneumoniae boasts an astonishingly diverse genome, exhibiting over 12,000 distinct clonal clusters identified through multi-locus sequence typing (ST) as established by Enright and Spratt in 1990. The species' genomic composition is further enriched by the concept of the pangenome, wherein pneumococcal genes are distributed across the population. Notably, at least 20% of coding sequences in a given pneumococcal isolate are unique to that strain, forming part of the accessory genome, which is unevenly distributed among all isolates (Hiller et al., 2007; Donati et al., 2010). The presence of such an extensive accessory genome equips the pneumococcus with additional sets of accessory genes, facilitating optimal adaptation to various environmental conditions. The first pneumococcal genome sequenced, TIGR4, is approximately 2 megabases in length and contains roughly 2200 coding sequences (Tettelin et al., 2001). The pneumococcal genome is believed to encode 500-1100 clusters of orthologous genes, while the pangenome encompasses between 5000-7000 orthologous clusters (Donati et al., 2010; Croucher et al., 2013; Gladstone et al., 2015; van Tonder et al., 2017). This indicates that around 75% of all pneumococcal genes exhibit differential distribution across the species.

The accessory genome significantly influences pneumococcal characteristics, particularly its ability to exchange DNA in biofilm settings within the nasopharynx. This exchange often results in strains with novel gene combinations, offering potential advantages such as evading host immune responses, outcompeting other colonisers or evading antibiotics (Ehrlich et al., 2005). However, it is essential to recognise that the accessory genomes are not exclusively derived from pneumococcal genes; other upper respiratory tract colonisers like *S. mitis*, *S. pseudopneumoniae*, *S. oralis* and *S. infantis* also play a substantial role in shaping the pneumococcal pangenome (Kilian et al., 2008; Donati et al., 2010).

Plasmids additionally contribute to the genetic variation observed within pneumococcus. For instance, the plasmid pDP1 has been identified in approximately 3% of all tested isolates (Smith and Guild, 1979; Sibold et al., 1991). However, the specific function of this plasmid, as well as other unrelated plasmids, remains largely unknown (Oggioni et al., 1999).

S. pneumoniae's remarkable capacity for genetic exchange arises from a combination of intrinsic and extrinsic factors, as discussed earlier. The species' natural competence and biofilm lifestyle in

the upper respiratory tract play crucial roles in this process. Furthermore, human intervention, such as antibiotic use, can activate competence by indirectly increasing local CSP concentrations (Prudhomme et al., 2006; Stevens et al., 2011; Domenech et al., 2018).

Additionally, pneumococci employ a sophisticated mechanism to safeguard and utilise internalised single-stranded DNA (ssDNA). The production of single-stranded DNA binding proteins (SsbB) enables the protection of a significant amount of intracellular DNA, roughly equivalent to half a genome. These ssDNA-SsbB complexes act as reservoirs for subsequent recombination events (Attaiech et al., 2011). The recombination machinery of *S. pneumoniae* exhibits flexibility, allowing for the integration of highly divergent alleles or novel genes without requiring extended runs of identical sequences (Prudhomme et al., 2002).

Another important avenue for genetic exchange in *S. pneumoniae* is transduction, which involves horizontal gene transfer mediated by prophages with lytic and lysogenic life cycles. Prophages, present in up to 76% of tested strains, are integrates into the pneumococcal genome during the lysogenic phase and are excised during the lytic phase to infect other bacterial cells (Ramirez et al., 1999). The phage integrase governs the location where the prophage integrates into the genomes, with most pneumococcal prophages found in a few conserved locations (Brueggemann et al., 2017). The significance of prophage genes in the pneumococcal genome has been highlighted through numerous studies. For instance, the ϕMM1-like phage has been shown to increase adherence to pharyngeal cells and inert surfaces (Loeffler and Fischetti, 2006). The phage tail protein PblB promotes adherence to human epithelial cells and enhances nasopharyngeal colonisation and lung infection in murine pneumococcal disease models (Harvey et al., 2011; Hsieh et al., 2015). Moreover, the Spn1 prophage leads to defects in pneumococcal autolysis, increased chain length of pneumococci, decreased fitness in murine colonisation models and increased resistance to penicillin-mediated lysis (DeBardeleben et al., 2014). The genomes of *S. pneumoniae* also contain phage-related chromosomal islands (PRCIs) that are believed to hitchhike with prophages, although they lack lytic cycles (Novick et al., 2010). However, the distribution of PRCIs is less diverse compared to prophages, likely due to limited lateral transfer or specificities between PRCIs and subsets of prophages.

Pneumococci employs various mechanisms, including conjugation, for horizontal gene transfer, which contributes significantly to its genetic diversity and evolution. Conjugation involves direct contact between bacteria, enabling the transfer of genetic material, particularly integrative and

conjugative elements (ICEs). ICEs consist of conjugative transposons or integrative plasmids, which, once inserted into the genome, can be vertically transferred or horizontally exchanged between strains after excision from the recipient genome (Burrus et al., 2002). The presence of several kilobases of genomic material in ICEs allows for the emergence of significant genetic diversity from just one transfer event. Notably, ICEs have a marked tendency to carry drug resistance genes, including those conferring resistance to antibiotics likes macrolides, tetracycline and chloramphenicol (Ayoubi et al., 1991; Croucher et al., 2009; Chancey et al., 2015).

1.9.1. Phase variation

In 1994, Weiser and colleagues made a significant observation regarding colony morphologies of *S. pneumoniae* isolates. Two distinct phenotypes, based on opacity, were identified when the isolates were viewed on a transparent agar surface under oblique, transmitted light. These phenotypes were termed “transparent” and “opaque” (Weiser et al., 1994). Intriguingly, the isolates demonstrated spontaneous and reversible switching between these two phenotypes. The frequency of this phenomenon, known as phase variation, varied between 10^{-3} and 10^{-6} per generation, depending on the strain. Interestingly, phase variation had previously been described in other pathogenic bacteria, such as *Neisseria gonorrhoeae* and *Haemophilus influenzae* (Swanson, 1982; Weiser et al., 1990). Further analyses were performed by Weiser and others (Weiser et al., 1994; Chai et al., 2017) to understand the differences between the opaque and transparent variants. Electron micrographs of the transparent variant revealed several distinct features compared to the opaque variant. Notably, the transparent exhibited less well-defined surface structures and displayed cytoplasm separation from the cell, along with the presence of extracellular debris. These observations suggested that the transparent variant was more prone to autolysis, a process in which cells self-destruct.

In addition to morphological differences, variations in the levels of specific components in the two phenotypes was found (Weiser et al., 1994). The transparent variant showed reduced levels of PspA and CPS. On the other hand, the opaque variant exhibited decreased levels of teichoic acid (a component of the cell wall) and increased amounts of CPS and PspA (Weiser et al., 1994; Kim and Weiser, 1998). The differences in CPS content between the two phenotypes revealed that the CPS content of the opaque phenotypes was up to 5.6-fold higher than that of the transparent variant. Conversely, the teichoic acid content of the transparent strain was up to 3.8-fold higher than that of the opaque phenotype (Kim and Weiser, 1998).

In vivo studies have provided valuable insights into the distinct virulence phenotypes of the transparent and opaque variants of pneumococci (Weiser et al., 1994). When equal doses of transparent and opaque variants were separately introduced into the nasopharynx of infant rats, it was observed that the transparent variant displayed higher levels of colonisation at all time points (days 1, 3 and 7) compared to the opaque variant. Interestingly, by day 7, no opaque colonies were identified from the nasal washes of rats given the opaque phenotype. Moreover, *in vitro* experiments demonstrated that transparent variants exhibited greater adherence to buccal epithelial cells (Cundell et al., 1995).

In an intraperitoneal mouse challenge model, where the nasopharynx was bypassed, the opaque phenotype of the serotype 2 strain D39 showed significantly higher mortality rates compared to their transparent counterparts (Kim and Weiser, 1998). Together, with the results of the colonisation model, indicates that the virulence potential of the two phenotypes varies depending on the route of infection, with opaque phase colonies causing more invasive disease and the transparent variants being more likely to colonise the infected individual. This disparity in infection outcome is likely due to the opaque phenotype having more CPS compared with the transparent colonies, with higher levels of CPS previously being shown to aid in virulence and less capsule aiding in colonisation (Weiser et al., 1994; Wen et al., 2016; Zafar et al., 2017).

A comprehensive analysis of over 300 pneumococcal clinical isolates from cases of invasive disease belonging to over 10 serotypes revealed interesting patterns (Serrano et al., 2006). Approximately, 52% of the isolates were of the opaque phenotype, whilst only 26% were transparent. The remaining 22% consisted of either mixtures of different phenotypes or an intermediate phenotype. This study also confirmed predictions from animal models, showing that isolates recovered from invasive infections in humans predominantly display the opaque phenotype. However, it was noted that the recovery frequencies of each phase variant were heterogenous between serotypes, suggesting that specific serotypes may preferentially express distinct variant phenotypes (Weiser et al., 1994; Serrano et al., 2006). The differential prevalence of the transparent and opaque variants in the nasopharynx versus invasive sites underscores the importance of phase variation in pneumococcal pathogenesis. Both variants represent adaptations to different host niches encountered by the pneumococcus during the transition from carriage to disease.

Furthermore, it was found that pneumococci isolates from cases of otitis media, displayed a 10-fold higher frequency of the opaque phenotype compared to the transparent phenotype (Long et al., 2003).

Strikingly, it was found that the increased expression of CPS in the opaque variants confers high resistance to complement-mediated opsonophagocytosis. On the other hand, transparent variants with higher teichoic acid content are better equipped to adhere to the nasopharyngeal mucosa. Teichoic acid, a major component of the cell wall, is adorned with phosphorylcholine (ChoP), facilitating bacterial attachment to the receptor for platelet-activating factor on respiratory epithelial cells (Kadioglu et al., 2008).

The molecular basis for pneumococcal phase variation remains a complex and incompletely understood phenomenon. It has been shown that the differences in colony opacity between the transparent and opaque variants could not be directly attributed to environmental conditions, expression and type of CPS, or differences in the function/expression of the major amidase *lytA* (Weiser et al., 1996). However, repetitive intergenic box elements A and C, located immediately 3' to the *glpF* termination codon, were identified as important factors contributing to the high frequency of phase switching, although they were not directly responsible for the opacity phenotype itself (Saluja and Weiser, 1995). Previous studies have shown that another protein that is differentially expressed between opaque and transparent variants of serotypes 4, 6B, 9V and D39 is SpxB, a pyruvate oxidase (Overweg et al., 2000; Belanger et al., 2004; Allegrucci and Sauer, 2008; Chai et al., 2017). The deletion of *spxB* in D39 has been shown to result in a larger and hyper-opaque phenotype (Pericone et al., 2002; Allegrucci and Sauer, 2008; Ramos-Montañez et al., 2008; Carvalho et al., 2013; Chai et al., 2017), attributed to an increase in capsule production or as a result of reduced hydrogen peroxide production, consequently leading to more biomass production due to less cell death. However, despite the deletion of *spxB* resulting in opaque phenotype, it is unlikely that reduced *spxB* expression drives the switch between opaque and transparent phenotypes, as ectopic over-expression of SpxB in opaque variants of D39 did not results in a transparent phenotype, as would be expected if SpxB was driving the opacity phase variation (Chai et al., 2017). Further supporting that SpxB is not the sole driver of phase variation is the finding that opaque or transparent colonies transformed with the *spxB* from the opposing phase variant, reverted back to their original opacity phase variant. Together, these results suggest that *spxB* is not solely responsible for the opacity variation witnessed in pneumococci but may work together with other proteins to produce the opaque and transparent colony variants (Chai et al., 2017).

1.9.1.1. SpnIII Restriction modification system

Restriction-modification (RM) systems play a pivotal role in the defence mechanisms of prokaryotes against invading viral or foreign DNA, first being described in the 1950s (Luria and Human, 1952; Bertani and Weigle, 1953). RM systems typically operate via a restriction enzyme, which cleaves specific unmethylated DNA sequences, and a methyltransferase, that methylates specific DNA sequences to protect from cleavage (Rodic et al., 2017). DNA methylation can be described as a heritable phenomenon characterised by the binding of a DNA-binding protein and DNA methylase to a specific DNA sequence with an overlapping target methylation site. The methylation process subsequently regulates expression of certain genes within the organism (Loenen et al., 2014). The RM systems present in bacteria can be broadly categorised into 4 main types (I-IV), each characterised by distinct features such as subunit composition, sequence recognition, cleavage site, co-factor requirements, and substrate specificity (Roberts et al., 2003). Among these types, Type I systems stand out as the most intricate. They consist of three essential subunits encoded by host-specificity-determinant (*hsd*) genes. Specifically, the *hsdR* gene is responsible for the restriction activity, the *hsdM* gene encodes the methylase and *hsdS* determines the DNA sequence specificity (Boyer and Roulland-dussoix, 1969; Hubacek and Glover, 1970). In *Streptococcus pneumoniae* there exists a type I restriction-modification (RM) system, SpnD39III. This type I system consists of multiple duplicated *hsdS* genes, each containing inverted repeats (IRs). These *hsdS* genes possess two unique 5' target recognition domains (TRDs) and three distinct 3' TRDs (Manso et al., 2014). As a result, the SpnD39III system can transition between six distinct specificities through homologous recombination events involving the variable TRDs found in the expressed (*hsdS*), and silent (*hsdS'* and *hsdS''*) forms of these specificity genes. This recombination event is facilitated by a recombinase associated with the locus, *creX* (Li et al., 2016), as well as a recombinase not linked to the locus (Li et al., 2019). The six methyltransferase specificities attributed to the SpnD39III locus, designated as alleles A to F, each target a distinct DNA sequence, thus governing separate phasevarions. Consequently, this intricate mechanism gives rise to a population of pneumococci comprised of six distinct cellular subtypes (Manso et al., 2014).

Notably, a series of mutants, each locked in one of the six alternative SpnD39III arrangements, exhibited marked differences in the expression of several virulence-associated genes, including *luxS* and the *cps* operon (Manso et al., 2014). These changes in gene expression were also associated with differences in colony opacity *in vitro* and variations in virulence in murine models, wherein either carriage or invasive disease was favoured. Of note, the *spnIIID39A* allele was

associated with higher quantities of opaque phenotype pneumococci and were more invasive in mice. Conversely, the *spnIIID39B* allele was associated with greater nasopharyngeal colonisation and downregulation of genes involved in capsule production and carbohydrate metabolism, including *luxS*, which has a role in quorum sensing (Manso et al., 2014).

However, it is noteworthy that both the expressed SpnD39III allele and strain-specific differences, such as differences in serotype or sequence type, play a role in virulence factors such as opacity phenotype, capsule and biofilm formation. Studies across different strains, such as D39 and TIGR4, have shown varying colony opacity phenotypes even when the same SpnD39III allele is being expressed (Manso et al., 2014; Li et al., 2016; Oliver et al., 2017). This finding underscores the intricate interplay between the expression of different SpnD39III alleles and unique strain-related factors, ultimately contributing to the enhanced phenotypic diversity observed within different population of *S. pneumoniae*.

It is essential to note that SpnD39III-locked strains do not exist in nature. Instead, the rate of switching between the SpnD39III variants *in vivo* is sufficiently high, leading to the existence of pneumococci as mixed populations with heterogeneous genomic methylation patterns. Therefore, this diversity in methylation patterns may contribute to the coexistence of transparent and opaque variants in various host niches, due to differential gene expression. In line with the observations regarding the selection for opaque versus transparent phase variants in different host niches, changes in SpnD39III allele frequencies were detected during the course of experimental pneumococcal infection and between different host niches (Manso et al., 2014).

Despite these advances, the precise molecular mechanisms governing pneumococcal phase variation and its impact on virulence and adaptation to various host environments remain complex and require further investigation.

1.9.2. Serogroup 15

The landscape of IPD has shifted following the introduction of pneumococcal conjugate vaccines (PCVs), resulting in a notable alteration in its epidemiology. Specifically, on a global scale there has been a discernible rise in infections attributed to pneumococcal serotypes that were not encompassed within the conjugate vaccine formulations, including those of serogroup 15.

Serogroup 15 of *Streptococcus pneumoniae* stands as a distinctive and clinically relevant subset within the diverse pneumococcal serotype landscape. It encompasses a cluster of five distinct capsular polysaccharides: 15A, 15B, 15C, 15F and the more recently identified 15D (Pimenta et al., 2021). Among these serotypes, at least four (Perry et al., 1982; Caroff and Perry, 1984; Jones and Lemercinier, 2005; Li et al., 2021) exhibit a repeating unit composed of the same quintet of monosaccharide constituents. The identical pentasaccharide repeat unit gives rise to a consistent linear structure in both 15A and 15F serotypes, while adopting a distinguishable branched configuration in the cases of 15B and 15C (Mavroidi et al., 2007). The fundamental structural divergence between these two sets of closely related serotypes is primarily rooted in the presence of two distinct repeat oligosaccharide polymerase genes, namely *wzy15BC* and *wzy15AF* (Mavroidi et al., 2007). Notably, the variation between serotypes 15B and 15C emerges from the O-acetylation of the polysaccharide in 15B, orchestrated by the *wciZ*-encoded enzyme. Intriguingly, these two serotypes exhibit a propensity to interconvert, a phenomenon attributed to the reversible frameshifting of a TA repeat within *wciZ* (van Selm et al., 2003). A parallel scenario unfolds in the realm of serotype 15A, where the *wciZ* gene harbours multiple inactivating mutations in contrast to its functionally intact counterpart in serotype 15F (Aanensen et al., 2007; Mavroidi et al., 2007). Furthermore, at the terminus of the cps15F operon resides the putative O-acetyltransferase gene *wcjE* (Mavroidi et al., 2007), which has recently been shown to contribute to the discernible serological distinctions between serotypes 15A and 15F (Li et al., 2021).

Recent findings have shed light on the newly discovered serotype 15D, revealing intriguing parallels in its molecular makeup to the other members of serogroup 15. Specifically, investigations have shown that serotype 15D possesses remarkable similar Wzy polymerase and WciZ O-acetyltransferase to those found in serotype 15F, indicating that it also possesses the *wzy15AF* polymerase gene shared by serotypes 15A and 15F. Notably, the distinguishing factor lies in the absence of the WcjE O-acetyltransferase in serotype 15D, which is found in serotype 15F (Pimenta et al., 2021). As a consequence of these shared and unique elements, it is plausible to anticipate that the CPS structure of serotype 15D closely resembles that of 15F rather than 15A.

1.9.2.1. Emergence of Serogroup 15 in disease after vaccine introduction

As mentioned in Section 1.4.2, the introduction of PCV vaccines resulted in the phenomenon of serotype replacement, in which non-vaccine serotypes, including serogroup 15, have begun to cause higher incidences of disease.

In 2010, PCV7 was introduced in Japan, resulting in escalating instances of IPD in children due to non-PCV7 serotypes including 19A. 15A, 15B, 15C and 24 (Chiba et al., 2014). A similar trend was observed in the United States post PCV13 debut, where slight increments in non-PCV13 serotype isolates were recorded in 2011 among eight paediatric hospitals. Notably, common non-vaccine types (NVTs) encompassed serotypes 33F, 22F, 12, 15B, 15C, 23A and 11 (Kaplan et al., 2013). In Belgium, IPDs attributed to non-PCV13 surged from 31% to 49%, associated with serogroups 12, 8 and 15 (Henckaerts et al., 2021). In India, NVT cases accounted for 21% of IPD cases in children under 5 years, featuring serotypes such as 10F, 9N, 11A, 20 and 15B across seven national surveys from 2007 to 2016 (Singh et al., 2017). Japan's Hokkaido, the main northern island, experienced a dramatic surge in NVTs, particularly serotypes 15A, 23A, 11A, 10A and 35B, escalating from 39.7% to 75.1% between 2013 and 2014. Notably, serotypes 15A, 15B, 23A, 24 and 33F contributed to 27.9% of isolates from children (Kawaguchiya et al., 2016). Following PCV13 introduction in 2013, a nationwide outbreak of NVT-related pneumococcal disease was observed, with prominent serotypes including 19A, 24F and 15A. The prevalence of non-PCV13 serotypes surged from 51.6% in 2012 to 71.4% in 2014. Among non-IPD isolates, types 19A, 15A and 3 were frequently identified, with a worrisome increase in antimicrobial-resistant strains of serotype 15A (Nakano et al., 2016).

A continuous investigation in Hong Kong showcased the steady rise in NVT isolates among children under five years over many years. The proportion increased from 27.4% (1999-2000) to 56.4% (2010-2013). Common non-PCV13 types included 15B (10.3%), 15C (9.6%), 6C (7.1%) and 15A (5.1%), with a notable presence of serogroup 15 among vaccinated children (Ho et al., 2015). An investigation in Taiwan also revealed that the prevalent NVTs were primarily serotypes 15A/F and 15B/C (13.3%) followed by serotype 23A (6.7%) (Janapatla et al., 2017). Of significance, NVTs such as serotypes 15B/C, 6C, 23A, 23B and 24F, which previously had low IPD incidence, appeared to be emerging as significant causes of meningitis in adults in Israel (Regev-Yochay et al., 2015).

In addition to causing more incidences of IPD, serotype 19A and serogroups 11 and 15 took the lead as major nasopharyngeal-colonising bacteria in Korean children with otitis media, following PCV7 introduction (Han et al., 2017). Furthermore, Iceland observed a substantial rise in NVTs (serotypes 6C, 15B/C, 23A and 23B) in pneumococci isolates from middle ear infections in children between 2009 and 2017. Particularly noteworthy were the increases of serotypes 15B/C and 6C in children under 2 as well as children aged 2-4, post-PCV introduction (Quirk et al., 2018). In summary, the introduction of different pneumococcal vaccines (PCV7, PCV10 and PCV13) prompted notable shifts in the prevalence and impact of serotypes 15A, 15B, 15C and 15F, with

varying degrees of association with invasive diseases, colonisation and otitis media in different regions globally.

As these serotypes have emerged as prominent players in causing disease, with serotype 15B being associated with elevated case-fatality rates, instances of meningitis and antibiotic resistance (Harboe et al., 2009; Thigpen et al., 2011; Van Hoek et al., 2012; Olarte et al., 2015; Metcalf et al., 2016; Stanek et al., 2016; Tomczyk et al., 2016; Oligbu et al., 2017), 15B has been included in the latest version of the pneumococcal conjugate vaccine (PCV20) (Hao et al., 2022). Immunisation studies found that subjects immunised with PCV20, inclusive of the 15B capsular polysaccharide conjugate, exhibited considerable cross-functional opsonophagocytic antibody titres against 15C strains, whilst there were limited responses against 15A. Therefore, it is likely that PCV20 is capable of inducing a cross-functional immune response against serotype 15C, reflecting the genetic relatedness and structural similarity between the capsular polysaccharides of serotypes 15B and 15C, whilst only providing limited efficacy against serotype 15A, due to the diverse conformations of the random coil found in serotype 15A, which would evoke functionally distinct antibodies from those responsive to serotypes 15B and 15C (Hao et al., 2022).

1.10. Clinical isolates and laboratory strains: key phenotypical differences

Understanding the intricate complexities of diseases caused by *Streptococcus pneumoniae*, a bacterium of paramount medical significance, requires a meticulous and comprehensive approach. Central to this endeavour is the choice between investigating clinical isolates or laboratory-adapted strains. Whilst both avenues offer valuable insights, the investigation of clinical isolates stands as a pivotal and irreplaceable method in unravelling the true nature of the diseases caused by this pathogen. By delving into the genetic, phenotypic and epidemiological variations present within clinical isolates, we can attain a deeper comprehension of *S. pneumoniae's* adaptive strategies, virulence factors and the challenges posed by antibiotic resistance. This approach not only enhances our understanding of the spectrum of diseases caused by pneumococci, but also informs targeted interventions, treatment strategies and vaccine development, ultimately striving for improved public health outcomes.

1.10.1. Carbohydrate and vitamin metabolism in clinical isolates

The complex interplay of mechanisms governing pneumococcal disease remain a subject of intense scrutiny, with a notable gap in the investigation of carbohydrate metabolism within clinical *S. pneumoniae* isolates. While numerous studies have delved into various facets of pneumococcal

behaviour, a scarcity of research has focused on unravelling the implications of carbohydrate metabolism in clinical isolates and its potential role in shaping the course of pneumococcal diseases. Fortunately, in more recent years the investigation into carbohydrate metabolism in clinical isolates has made some headway.

In 2018, a study carried out by Hartmann et al., used clinical isolates to shed light on the role of riboflavin metabolism in *S. pneumoniae* and its implications for the host immune response, specifically how riboflavin metabolism affects mucosal-associated invariant T (MAIT) cells. Prominently present in the peripheral blood and tissues such as the lung, MAIT cells are a specialised subset of primarily $CD8^+$ T cells, which play a critical role in immune surveillance and defence against microbial pathogens. Upon maturation and emigration from the thymus, these cells are immediately able to release cytokines and other cytolytic factors (Gold et al., 2013). Their unique immunosurveillance mechanism relies of the recognition of small molecules that originate from the riboflavin metabolic pathway, presented by the nonpolymorphic major histocompatibility complex class I-like molecule MR1 (Kjer-Nielsen et al., 2012; Corbett et al., 2014). Many fungal and bacterial species, including *S. pneumoniae* encode the enzymes responsible for the synthesis of these small molecules (Tettelin et al., 2001). To delve into whether pneumococci were capable of producing the riboflavin-derived molecules necessary for the subsequent activation of MAIT cells, a comprehensive study was undertaken, involving 35 clinical isolates of serotype 19A (Hartmann et al., 2018). These isolates were characterised based on their origin – colonisers from the nasopharynx or invasive strains from sterile sites like blood or pleural fluid. Fascinatingly, although MAIT cells demonstrated MR1-dependent recognition and response to *S. pneumoniae*-infected cells, the clinical serotype 19A isolates exhibited differential recognition patterns, not due to differences in phagocytosis or bacterial killing. A closer examination revealed potential links between MAIT cell response and genetic background – highlighted by multilocus sequence typing (MLST). Specifically, isolates with similar MLST groups showcased consistent MAIT cell responses, suggesting a correlation between genetic makeup and MAIT cell reactivity. Further investigation into the molecular underpinnings brought to light the pivotal role of riboflavin metabolism. MAIT cell ligands, essential for their activation, emerge as products of this pathway. Notably, the expression of riboflavin-related genes, particularly *ribD*, emerged as a critical factor. Clinical isolates that triggered robust MAIT cell responses exhibited higher *ribD* expression, potentially leading to enhanced production of MAIT cell ligands.

Interestingly, it was found that the environment in which the pneumococci was grown in played a significant role in modulating riboflavin metabolism. Importantly, varying the availability of riboflavin

in culture media resulted in alterations of *ribD* expression and consequently the abundance of MAIT cell ligands. Crucially, these findings underscore the inherent diversity within clinical isolates of *S. pneumoniae*, where distinct genetic requirements for riboflavin metabolism drive the intricate dance of MAIT cell activation. Indeed, the differential expressions of riboflavin biosynthesis and transport genes across clinical isolates speak to the unique riboflavin needs that define their individual characteristics. Moreover, a multifaceted array of regulatory factors come into play, orchestrating the dynamic regulation of riboflavin metabolism across these isolates. The results of a murine *in vivo* model suggest that the influence of riboflavin availability is similar to what was observed *in vitro*. However, the translation of these observations to the complex human pulmonary environment remains an enigma, particularly given the potential influence of diet on riboflavin availability.
The results of this study yields two pivotal insights. Firstly, it underscores the genetic heterogeneity in riboflavin metabolism across clinical isolates of the same serotype. Secondly, this genetic divergence intricately shapes the MAIT cell response upon *S. pneumoniae* infection. These disparities emerge as crucial factors in delineating the role of MAIT cells in early responses to pneumococcal infections and predicting the development of invasive disease (Hartmann et al., 2018).

Another study that investigated the role of carbohydrate metabolism in determining disease outcome of clinical isolates discovered that raffinose metabolism may dictate the nature of the disease caused (Minhas et al., 2019). This study followed on from a study that found closely related pneumococci, which share the same capsular serotype and sequence type (ST), can exhibit different disease-causing behaviours in mice based on where they were isolated from in the human host (e.g., blood or ear), indicating specialised adaptation within a clonal lineage (Trappetti et al., 2013). In the study performed by Minhas et al., genetic analysis revealed differences in specific DNA variations (SNPs or Indels) between blood and ear isolates taken from different patients with different serotypes (serotype 14 ST15 or serotype 3 ST180). In both pairs, genetic variations in the raffinose uptake and utilisation genes, *rafR* or *rafK*, were present. Notably, ear isolates had consistent deficiencies in their ability to grow in media where raffinose was the sole carbon source and in the expression of genes related to the raffinose pathway (*aga*, *rafG* and *rafK*) compared to their blood counterparts with the matching serotypes and STs. Similar differences were also observed in serotype 23F ST81 isolates from blood and ear. Further investigations using mutants that had swapped the *rafR* gene between the blood and ear isolates in serotype 14 ST15 demonstrated that the specific genetic variation in *rafR* was solely responsible for the distinct behaviour observed in the lab. This genetic variation also determined whether the bacteria would

cause lung-related disease or affect the ear and brain in a mouse challenge model after intranasal challenge. These findings suggest that the capability of pneumococci to use raffinose as an energy source is a key factor influencing the nature of diseases they cause (Minhas et al., 2019). A further study was conducted in 2020 by Minhas et al., to determine how the variation in the ability to metabolise raffinose resulted in the different disease types. In this investigation, a dual RNA-seq approach was utilised to unveil the impact of the SNP in *rafR* on various facets of pneumococci disease progression, using the lungs of mice intranasally infected with pneumococci. The SNP was found to significantly impact the expression of genes encoding a range of transmembrane transporters, encompassing those responsible for various sugars. Moreover, it intricately refines the carbohydrate metabolism of pneumococcal strains. This effect underscores the notion that distinct expression profiles of sugar catabolism pathways confer specific advantages in diverse host niches, highlighting the varying availability of distinct carbohydrate sources within these niches. These variances, and their ensuing ramifications in pneumococci, ultimately register within host cells, including epithelial and immune cell. This phenomenon culminates in the discernible divergence of host responses to distinct strains, particularly in terms of the expression of genes governing cytokines and chemokine ligands, as well as those linked to programmed cell death. Through detailed analysis of the dual RNA-seq data, it was found that there was an enrichment in the expression of IL-17-related genes in mice infected with the ear strain carrying the D249 *rafR* allele, allowing the pneumococci to be cleared from the lungs within 24 hours post-challenge. It has been well established that IL-17 stimulates the recruitment of neutrophils to the lungs after infection (Lindén et al., 2005; Ritchie et al., 2018). Additionally, it was found that genes associated with neutrophil extravasation exhibit heightened activity in murine lungs within 48 h of challenge with pneumococci. Importantly, this study confirmed that neutrophils were more abundant in the lungs at 6 h post-challenge in mice infected with the ear strain compared to those infected with the blood strain (Minhas et al., 2020). The results of this study have used clinical pneumococci isolates to underscore the profound influence that even a solitary SNP can exert, steering the trajectory of disease outcomes based on carbohydrate metabolism. Furthermore, it emphasises the pivotal role that early-stage modulation of neutrophil recruitment assumes in shaping a specific *S. pneumoniae* strain's ability to endure within the lung environment, consequently influencing the eventual disease outcome.

1.10.2. Biofilm in clinical isolates

A particular aspect that has remained relatively unexplored in the realm of *Streptococcus pneumoniae* research is biofilm formation by clinical isolates. One of the first studies focusing on

biofilm formation in clinical isolates shed light on the connection between biofilm matrix degradation via DNase treatment and the consequential downregulation of the pathogen's capsule – a key virulence factor (Hall-Stoodley et al., 2008). This study used 6 clinical isolates from nasal washes of paediatric patients that were of 6 different serotypes: 9V, 14, 3, 23F, 6A and 19F.

The composition of biofilm matrix formed by clinical isolates varied between isolates. Those with a high biofilm forming index (BFI) exhibited biofilm composition that was more structurally complex and exhibited greater colocalization with a mix of five lectins: ConA (from *Canavalia ensiformis*), WGA (wheat germ agglutinin), GS II (from *Griffonia simplicifolia*), SBA (soybean agglutinin) and PNA (peanut agglutinin). Secondly, the study investigated the impact of DNase treatment on the biofilm matrix formed by the various clinical isolates. Here it was found that the DNase treatment led to a significant reduction in the biofilm matrix stability and biomass of all strains, indicating the pivotal role of extracellular DNA in maintaining the integrity of the pneumococcal biofilm, which has previously been seen for the bacteria *Pseudomonas aeruginosa* (Whitchurch et al., 2002).

Finally, an intriguing connection between decreased biofilm formation and the downregulation of capsule was discovered. Specifically, it was observed that the expression of the capsule gene, *cpsA*, among the clinical isolates was downregulated in bacteria in biofilms compared to those from planktonic growth. This suggests that biofilm formation and capsule expression may be interlinked and that disrupting the biofilm matrix could influence the virulence properties of *S. pneumoniae* (Hall-Stoodley et al., 2008).

Another study conducted using clinical isolates found that both biofilm formation and virulence phenotypes of *S. pneumoniae* strains was affected based on the anatomical niche from where the sample was obtained (Trappetti et al., 2013). The isolates used in this study were serotype 3, obtained from both blood (12 isolates) and ear (13 isolates) infections. The isolates were further categorised based on their MLST to remove differential genetic bias that could affect the interpretation of results, thus ensuring that any observed differences were due to factors that influenced the type of disease caused in the patient and consequent site of pneumococcal isolation. Interestingly, despite similar MLST distributions between blood and ear isolates, they displayed significant differences in their traits. Blood isolates were found to develop robust biofilms primarily under neutral pH conditions (pH 7.4), with enhanced growth when exposed to Fe (III) supplementation. In contrast, ear isolates formed biofilms under slightly acidic conditions (pH 6.8), but their growth was inhibited by Fe (III). Furthermore, using clinical isolates it was determined that there is a correlation between biofilm formation, the expression of *luxS* and genetic competence of the isolates. To assess whether site of isolation impacted their virulence, the isolates were tested

in an intranasal murine model, mimicking pneumonia. Here it was found that blood isolates did not efficiently colonise the nasopharynx but instead spread to the bloodstream without causing ear infections. On the other hand, ear isolates were better at nasopharyngeal colonisation and exhibited the ability to spread to the ear compartment. However, these ear isolates did not lead to bloodstream infections. This divergence in phenotypes among clinical isolates of the same serotype and MLST indicates a stable adaptation to specific anatomical niches within a clonal lineage.

1.10.3. Quorum sensing systems in clinical isolates

The exploration of quorum sensing systems within clinical *S. pneumoniae* strains remains a relatively uncharted territory, with a significant scarcity of studies delving into this subject. However, recently a study conducted by Tikhomirova et al. (2022) showed that the role of *luxS* in a pneumococcal clinical isolate obtained from the middle ear, labelled 947, differed from what has previously been seen in the laboratory strain D39 (Trappetti et al., 2011c). Within the middle ear isolate 947, it was discovered to have heightened expression of key genes, *luxS* and *fruA*, associated with AI-2 mediated QS when compared to the closely related blood isolate 4559. Intriguingly, the introduction of exogenous of external AI-2 had different impacts on isolates obtained from the middle ear and the blood. Specifically, while it curtailed the growth of 947 (middle ear isolate) when cultivated in galactose media, it conversely bolstered the growth of 4559 (blood isolate). This contrast in growth suggests the possibility of dose-dependent effects of AI-2 in strains that initially display varying expression patterns of QS-related genes. Moreover, these findings emphasise the strain-specific nature of *luxS* effects within these clinical isolates.

To further investigate the role of the LuxS/AI-2 QS system, a 947 *luxS*- (deletion) mutant was generated (Tikhomirova et al., 2022). Of note it was found that the 947 *luxS*- mutant had significantly diminished capacity for adherence to human respiratory cells. Intriguingly, this reduction in adherence did not correlate with a parallel attenuation in *in vitro* biofilm formation capabilities, suggesting a potentially more complex relationship between adherence and downstream biofilm formation within the *in vivo* milieu. Interestingly, it was demonstrated that while *luxS* exhibited no discernible impact on capsule production, with the wildtype and *luxS* deletion mutant displaying similar amounts of capsule, it did wield a notable influence on infection dynamics within our murine model. Notably, the 947 *luxS*- strain showcased heightened transit to the ear, a trend toward increased nasopharyngeal colonisation and an elevated propensity for passage to the brain. This increased migration of the *luxS*- strain to the ear and brain, coupled with its diminished adherence to epithelial cells, implicates functional *luxS* in promoting an adherent

lifestyle *in vivo* while mitigating transit to other host niches. These findings resonate with the characteristic patterns observed in localised or systemic invasive diseases such as meningitis or OM. Intriguingly, these dynamics contrast with the role of *luxS* in the invasive D39, where it appears to drive the transition to invasive disease (Trappetti et al., 2011c). Thus, these results underscore the divergent roles of *luxS* across strains, highlighting its strain-specificity, which may be intricately linked to the genomic makeup of the isolate and its ecological niche.

As an isolate originating from the middle ear, strain 947 appears to rely on *luxS* to foster adherence and restrict dissemination to more invasive sites. In contrast, the case of D39, a laboratory strain initially isolated from the blood, *luxS* seems to orchestrate the transition to invasive disease. Together the results of this study underpin the need for studying QS systems in clinical isolates, as they have diverse roles across both localised and invasive strains.

1.11. Research project

1.11.1. Rationale

As discussed in "Clinical isolates and laboratory strains: key phenotypical differences" (Section 1.10) studies using clinical *S. pneumoniae* isolates offers a unique perspective into many factors of this bacteria that influences their lifestyle and ultimate disease outcome.

Of particular interest are the studies that have used clinical isolates that have come from different incidences of disease or from different anatomical niches within a single patient. In these studies, various *in vitro* and *in vivo* behaviours were observed that were associated with their site of isolation in humans (Silva et al., 2006; Hall-Stoodley et al., 2008; Croucher et al., 2013; Trappetti et al., 2013; Amin et al., 2015; Hartmann et al., 2018; Minhas et al., 2019; Minhas et al., 2020; Tikhomirova et al., 2022). These studies explored the influence of niche adaptation on carbohydrate metabolism, biofilm formation, virulence in murine models and host immune responses. Notably, some of the differences observed *in vitro* and *in vivo* were found to be the result of small genetic variations between the closely related strains (Croucher et al., 2013; Amin et al., 2015; Minhas et al., 2019).

Through an international collaboration with the German National Reference Center for Streptococci in Aachen (Germany), our laboratory has acquired a valuable collection of clinical *S. pneumoniae* isolates. This comprehensive dataset spans a 20-year period, encompassing the years 2002 to 2022, and originates from diverse regions within Germany. These isolates, meticulously gathered from a range of medical cases, offer a unique window into the epidemiology and clinical impact of

pneumococcal infections. The cases encompass a broad spectrum of age groups, from infants as young as 4 months to children over 6 years old, who were admitted to hospitals due to various manifestations of disease, including otitis media, pneumonia, sepsis, and meningitis.

Of particular significance, children diagnosed with OM were subject to the collection of isolates from both their middle ear and nasopharynx, granting us a holistic view of colonisation dynamics and potential transmission routes. In instances of more severe conditions such as sepsis or meningitis, isolates were procured from both the blood and cerebrospinal fluid (CSF), offering a unique glimpse into the pathogen's behaviour within differing anatomical niches.

The compelling aspect of this collection is its dichotomy, encapsulating strains from both localised and invasive disease contexts.

By delving into the phenotypic, genetic and epigenetic characteristics of these isolates, key insights into the factors that underlie the choice of disease manifestation by *S. pneumoniae* may be uncovered. This investigative endeavour holds immense promise for deciphering the intricate interplay between bacterial traits and host susceptibility, ultimately shedding light on the intriguing phenomenon of disease tropism.

Initial characterisation of growth was performed on a range of closely related blood and ear isolates obtained from children with meningitis or otitis media, respectively. Based on these initial results (Appendix C), isolates (blood, CSF, ear and nasopharynx) of serotype 15C ST8711 were chosen to be investigated further due to their differential ability to metabolise raffinose, a similar finding to what was observed by Minhas et al. in 2019. However, in this case it was interesting to note that the blood and ear isolates (denoted 60B and 101E) displayed the opposite metabolic ability to what was observed by Minhas. Here, the blood isolate was unable to metabolise raffinose, whilst the ear isolate could – a direct contrast to what was observed in pairs of blood and ear isolates of both serotype 3 and serotype 14 (Minhas et al., 2019). Fascinatingly, the CSF isolate (60CSF) obtained from the same meningitis paediatric patient as 60B displayed the ability to metabolise raffinose, whilst the blood isolate was unable to.

This finding therefore formed the basis for this research project investigating two clinical strains, possessing identical serotype, sequence type, and antibiotic sensitivity profiles, isolated at the same time from the blood and CSF of a single paediatric patient presenting with meningitis.

1.11.2. Hypothesis and aims

The hypothesis and aims underpinning this investigation are as follows:

Hypothesis: Closely related strains isolated from the blood and cerebrospinal fluid at the same time from a single paediatric meningitis patient may contain distinct molecular differences that have arisen during the course of disease that could contribute to a change in lifestyle, resulting in the differential niche adaptation.

Aim 1: Characterise the *in vitro* phenotypic profile of clinical isolates taken from different anatomical niches that are of the same serotype and ST.

Aim 2: Characterise the *in vivo* phenotypic profile of clinical isolates taken from different anatomical niches that are of the same serotype and ST.

Aim 3: Determine the molecular features of the clinical isolates that dictate changes in phenotype.

Chapter 2: *Streptococcus pneumoniae* Strains Isolated From a Single Pediatric Patient Display Distinct Phenotypes

2.1 Statement of authorship

Statement of Authorship

Title of Paper	*Streptococcus pneumoniae* Strains Isolated From a Single Pediatric Patient Display Distinct Phenotypes
Publication Status	✓ ☐ Published
Publication Details	Agnew, H.N., et al. (2022). *Streptococcus pneumoniae* Strains Isolated From a Single Pediatric Patient Display Distinct Phenotypes. *Frontiers in cellular and infection microbiology* 12, 866259-866259. doi: 10.3389/fcimb.2022.866259

Principal Author

Name of Principal Author (Candidate)	Hannah N. Agnew		
Contribution to the Paper	Designed and performed experiments, performed analysis on and interpreted data, and aided in writing the manuscript.		
Overall percentage (%)	80%		
Certification:	This paper reports on original research I conducted during the period of my Higher Degree by Research candidature and is not subject to any obligations or contractual agreements with a third party that would constrain its inclusion in this thesis. I am the primary author of this paper.		
Signature		Date	31/10/2023

Co-Author Contributions

By signing the Statement of Authorship, each author certifies that:

i. the candidate's stated contribution to the publication is accurate (as detailed above);

ii. permission is granted for the candidate in include the publication in the thesis; and

iii. the sum of all co-author contributions is equal to 100% less the candidate's stated contribution.

Name of Co-Author	Erin B. Brazel		
Contribution to the Paper	Designed and performed experiments, performed analysis on and interpreted data, and aided in writing the manuscript.		
Signature		Date	16/10/2023

Name of Co-Author	Alexandra Tikhomirova		
Contribution to the Paper	Designed and performed experiments, assisted with writing the manuscript		
Signature		Date	17/10/2023

Name of Co-Author	Mark van der Linden		
Contribution to the Paper	Provided the clinical isolates investigated, performed initial characterisation of strains, and aided in writing the manuscript.		
Signature		Date	13.10.2023

Name of Co-Author	Kimberley T. McLean		
Contribution to the Paper	Designed and performed experiments		
Signature		Date	17/10/2023

Name of Co-Author	James C. Paton		
Contribution to the Paper	Designed experiments and aided in writing of the manuscript		
Signature		Date	16/10/2023

Name of Co-Author	Claudia Trappetti		
Contribution to the Paper	Designed and performed experiments, performed analysis on and interpreted data, and aided in writing the manuscript.		
Signature		Date	30/10/2023

2.2 Purpose of the article

As mentioned in Section 1.11.1, closely related *S. pneumoniae* isolates obtained from the blood and cerebrospinal fluid of a single paediatric meningitis patient exhibited variations in the metabolism of raffinose, a carbohydrate source previously associated with differences in niche adaptation (Minhas et al., 2019). The primary aim of this article is to investigate whether the capacity to utilise raffinose induces similar effects on niche adaptation within these clinical isolates, as previously observed, and to elucidate the molecular mechanisms underpinning these observed differences.

2.2.1 Thesis research aims addressed

Aim 1: Characterise the *in vitro* phenotypic profile of clinical isolates taken from different anatomical niches that are of the same serotype and ST.

Aim 2: Characterise the *in vivo* phenotypic profile of clinical isolates taken from different anatomical niches that are of the same serotype and ST.

Aim 3: Determine the molecular features of the clinical isolates that dictate changes in phenotype.

2.3 Article

frontiers in Cellular and Infection Microbiology

ORIGINAL RESEARCH
published: 31 March 2022
doi: 10.3389/fcimb.2022.866259

Streptococcus pneumoniae Strains Isolated From a Single Pediatric Patient Display Distinct Phenotypes

Hannah N. Agnew[1], Erin B. Brazel[1], Alexandra Tikhomirova[1], Mark van der Linden[2], Kimberley T. McLean[1], James C. Paton[1] and Claudia Trappetti[1*]*

[1] Research Centre for Infectious Diseases, Department of Molecular and Biomedical Science, The University of Adelaide, Adelaide, SA Australia, [2] German National Reference Center for Streptococci, University Hospital Rheinisch-Westfälische Technische Hochschule (RWTH) Aachen, Aachen, Germany

OPEN ACCESS

Edited by:
Sven Hammerschmidt, University of Greifswald, Germany

Reviewed by:
Krzysztof Trzcinski, University Medical Center Utrecht, Netherlands
Gustavo Gamez, University of Antioquia, Colombia
Elissavet Nikolaou, Royal Children's Hospital, Australia

***Correspondence:**
Claudia Trappetti
claudia.trappetti@adelaide.edu.au
James C. Paton
james.paton@adelaide.edu.au

Specialty section:
This article was submitted to Molecular Bacterial Pathogenesis, a section of the journal Frontiers in Cellular and Infection Microbiology

Received: *31 January 2022*
Accepted: *08 March 2022*
Published: *31 March 2022*

Citation:
Agnew HN, Brazel EB, Tikhomirova A, van der Linden M, McLean KT, Paton JC and Trappetti C (2022) Streptococcus pneumoniae Strains Isolated From a Single Pediatric Patient Display Distinct Phenotypes. Front. Cell. Infect. Microbiol. 12:866259. doi: 10.3389/fcimb.2022.866259

Streptococcus pneumoniae is the leading cause of bacterial paediatric meningitis after the neonatal period worldwide, but the bacterial factors and pathophysiology that drive pneumococcal meningitis are not fully understood. In this work, we have identified differences in raffinose utilization by *S. pneumoniae* isolates of identical serotype and sequence type from the blood and cerebrospinal fluid (CSF) of a single pediatric patient with meningitis. The blood isolate displayed defective raffinose metabolism, reduced transcription of the raffinose utilization pathway genes, and an inability to grow *in vitro* when raffinose was the sole carbon source. The fitness of these strains was then assessed using a murine intranasal infection model. Compared with the CSF isolate, mice infected with the blood isolate displayed higher bacterial numbers in the nose, but this strain was unable to invade the ears of infected mice. A premature stop codon was identified in the *aga* gene in the raffinose locus, suggesting that this protein likely displays impaired alpha-galactosidase activity. These closely related strains were assessed by Illumina sequencing, which did not identify any single nucleotide polymorphisms (SNPs) between the two strains. However, these wider genomic analyses identified the presence of an alternative alpha-galactosidase gene that appeared to display altered sequence coverage between the strains, which may account for the observed differences in raffinose metabolic capacity. Together, these studies support previous findings that raffinose utilization capacity contributes to disease progression, and provide insight into a possible alternative means by which perturbation of this pathway may influence the behavior of pneumococci in the host environment, particularly in meningitis.

Keywords: *Streptococcus pneumoniae*, virulence, raffinose, clinical isolates, carbohydrate metabolism, meningitis, bacteremia

INTRODUCTION

Streptococcus pneumoniae (the pneumococcus) is the world's foremost bacterial pathogen, causing approximately 1.2 million deaths each year with over 190 million infections (Lavelle and Ward, 2021). This Gram-positive bacterium can asymptomatically colonize the nasopharynx of humans at a very high rate of up to 95% of infants and 25% of adults (Trimble et al., 2020). However, in a

number of these carriers, pneumococci can disseminate from this niche to deeper mucosal sites within the body, such as the middle ear, to cause otitis media or they can invade sterile sites such as the lungs, blood, and brain, leading to invasive pneumococcal diseases (IPDs), such as pneumonia, bacteremia, and meningitis, respectively. Of the IPDs, meningitis has a high case fatality rate with 30% of cases in higher-income countries resulting in fatality and lower-income countries having a case fatality rate of 50% (Brouwer et al., 2010). Meningitis is caused by inflammation of the brain and spinal cord following bacterial infection. *S. pneumoniae* can disperse from the nasopharynx during colonization into the bloodstream, resulting in bacteremia. The bacteria carried in the blood cross the endothelial cell layer of the blood-brain barrier to invade the brain by receptor-mediated transcytosis, in which the bacterium binds a specific receptor on endothelial cells, facilitating the translocation through the barrier (Iovino et al., 2016). Replication of the pneumococci results in high levels of inflammation that damages the brain. Complications include cerebrospinal fluid pleocytosis, cochlear damage, hydrocephalus, and cerebrovascular complications. If left untreated, meningitis can result in severe health problems, including hearing loss, brain damage and death (Mook-Kanamori et al., 2011).

S. pneumoniae is a highly diverse and genetically plastic species, with at least 100 capsular serotypes superimposed on at least 16,000 sequence types (STs) (https://pubmlst.org/), identified by multilocus sequence typing (MLST) (Enright and Spratt, 1998; Kim and Weiser, 1998). The core genome is composed of approximately 1500 genes, accounting for ~70% of the genome, with the remaining ~30% made up of accessory regions (ARs), leading to increased diversity between STs (Obert et al., 2006). Capsule switching experiments have displayed that both serotype and genetic background (i.e. ST) affect virulence (Kelly et al., 1994; Mcallister et al., 2011), but strain complexity has made it difficult to determine if there is a link between ST/serotype and predisposition to cause invasive rather than localized disease, and the mechanisms by which pneumococci switch from commensalism to cause localized or invasive disease remain poorly understood.

Previous studies undertaken in our laboratory have demonstrated that *S. pneumoniae* clinical isolates of the same serotype and ST displayed different virulence phenotypes in mice, that correlated with their site of isolation in humans. Intranasal (i.n.) challenge in mice with clinical isolates of serotype 3 ST180, ST232 and ST233 showed that blood isolates preferentially spread to the blood, whilst ear isolates spread to the ear in a significant proportion of mice (Trappetti et al., 2013). Further studies using clinical isolates of serotype 14 ST15 showed that ear isolates were able to spread to the ear, whilst the blood isolates spread to the lungs of mice (Trappetti et al., 2013; Amin et al., 2015). Subsequent studies uncovered single nucleotide polymorphisms (SNPs) in matched blood and ear isolates of serotype 3 ST180 and serotype 14 ST15, including in genes within the raffinose uptake and utilization pathway for both STs, *rafK* and *rafR*, respectively. These SNPs affected growth when raffinose was the sole carbon source and influenced the expression of the raffinose utilization genes *aga, rafG* and *rafK* (Minhas et al., 2019). Exchanging these mutations between the serotype 14 strains showed that these phenotypes were attributable to the SNPs, uncovering novel and clinically relevant molecular features that favour distinct lifestyles of pneumococcal disease.

We have now sought to investigate the bacterial drivers of meningitis, using clinically relevant serotype 15C *S. pneumoniae* isolates obtained at the same time from a single patient, provided to us by the German National Reference Center for Streptococci (Aachen). Pneumococci serotype 15C blood and CSF isolates (designated 60B and 60CSF, respectively) were isolated in 2015 from a child, aged 2, admitted to hospital with meningitis. We have performed *in vitro* and *in vivo* phenotypic characterization and genome comparisons of these clinical isolates and found differences in carbohydrate metabolism and gene expression *in vitro*, and distinct pathogenic phenotype differences between the isolates *in vivo*.

MATERIALS AND METHODS

Bacterial Strains and Growth Conditions

The *S. pneumoniae* strains used in this study are serotype 15C clinical isolates 60B (SN69534) and 60CSF (SN69531) (isolated from blood and CSF, respectively), D39 (serotype 2 ST595), and Rx1 (unencapsulated). Cells were routinely grown on Columbia agar supplemented with 5% (vol/vol) horse blood (BA), with or without gentamicin (40 μg/mL), at 37°C in 5% CO_2 overnight (Mclean et al., 2020). Growth assays were performed with pneumococci grown in a chemically defined medium (CDM) (Kloosterman et al., 2006) comprising SILAC RPMI 1640 Flex Media, no glucose, no phenol red (Sigma), supplemented with amino acids (**Table 1A**), vitamins (**Table 1B**), uracil (0.01 mg/mL), adenine (0.01 mg/mL), choline chloride (0.005 mg/mL) and catalase (10 U/mL), and either 0.5% glucose, galactose, lactose, raffinose or melibiose.

MLST

To conduct MLST analysis, the *aroE, gdh, gki, recP, spi, xpt* and *ddl* genes of the blood strains were PCR amplified, purified using the QiaQuick Purification Kit (Qiagen), and sequenced as described previously (Enright and Spratt, 1998). Sanger sequencing was conducted by the Australian Genome Research Facility (AGRF). The sequence types (ST) of the pneumococci strains were determined by searching the MLST database (https://pubmlst.org/) for matching allelic profiles.

Growth Assays

Strains were grown in flat-bottom 96-well microtiter plates (Costar) with a final volume of 200 μL as previously described (Minhas et al., 2019). Strains were inoculated at a starting optical density at 600 nm (OD_{600}) of 0.05 in CDM supplemented with either 0.5% glucose, galactose, lactose, raffinose or melibiose, before being incubated at 37°C with 5% CO_2. The OD_{600} was measured every 30 min for a total of 24 h in a SpectroSTAR

TABLE 1 | Components for the CDM.

	Components	Concentration in final media (mg/mL)
A) Amino acids	Alanine	0.24
	Glutamine	0.39
	Asparagine	0.35
	Arginine	0.125
	Lysine	0.44
	Isoleucine	0.215
	Methionine	0.125
	Phenylalanine	0.275
	Serine	0.34
	Threonine	0.225
	Tryptophan	0.05
	Valine	0.325
	Glycine	0.175
	Histidine	0.15
	Leucine	0.475
	Proline	0.675
	Cysteine hydrochloride	0.3
	Aspartic acid	0.3
B) Vitamins	Pyridoxal HCl	0.0028
	Thiamine	0.0014
	Pantothenic acid (Ca)	0.0014
	Biotin	0.00014
	Niacinamide	0.0014
	Riboflavin	0.0014
	Folic acid	0.0014

Omega spectrophotometer (BMG Labtech). Assays were conducted in triplicate with at least three repeated independent experiments.

Phenotypic Microarrays

Carbon phenotype microarray (PM) analysis using the PM microplates PM1 and PM2a (Biolog Inc.) was performed on the strains to test for the catabolism of 190 different carbon sources as previously described (Minhas et al., 2019). Every well of the microarrays contained a different carbon source. Briefly, cells were inoculated to a final OD_{590} of 0.06 in the buffer provided, according to the manufacturer's instructions. This suspension was added in 100 µL aliquots to the wells, and the plate was incubated at 37°C, 5% CO_2. The OD_{590} was measured every 15 min for 24 h. Catabolic activity was measured through colorimetric analysis. During catabolism, NADH is produced which subsequently reduces a colorless tetrazolium dye, resulting in a color change. The level of metabolism for each carbon source was arbitrarily determined by comparison with the negative value.

Biofilm Assays

The formation of biofilms was measured in real time using the real time cell analyzer (RTCA) xCELLigence (Agilent Technologies Inc.) instrument, as described previously for *Streptococcus mutans* and *Staphylococcus* spp. (Gutierrez et al., 2016). This instrument detects variation in the impedance signal (expressed as the arbitrary cell index, CI) as bacterial cells attach and form biofilms on the gold-microelectrodes present in the bottom of the E-plates (Agilent Technologies Inc.) Briefly, strains were grown overnight on BA plates at 37°C with 5% CO_2. Cells were harvested and resuspended in 200 µL of CDM + 0.5% glucose or galactose a final OD_{600} of 0.2. To the wells of the E-plate, 150 µL CDM + 0.5% glucose or 0.5% galactose was added before placing the plate in the cradle of the RTCA-DP system, within a 37°C incubator without CO_2 supplementation. An initial baseline impedance reading was taken before the E-plates were removed and 50 µL of bacterial suspension was added to wells for a 1 in 4 dilution, bringing the starting OD_{600} to 0.05. For control wells, an additional 50 µL of CDM + 0.5% glucose or 0.5% galactose was added. E-plates were locked into the cradles of the RTCA-DP platform within the incubator and biofilm formation was monitored for 24 h by recording the impedance signal (CI) every 15 min. Assays were conducted in triplicate with at least two repeated independent experiments. Statistical analysis was performed using two-tailed Student's *t* test; P values < 0.05 were deemed statistically significant.

Adherence Assays

Adherence assays were carried out on the Detroit 562 human pharyngeal cell line as previously described (Trappetti et al., 2011). Briefly, cells were grown in Dulbecco's modified Eagle's medium (DMEM) supplemented with 10% fetal calf serum (FCS), 100 U/mL penicillin and 100 µg/mL streptomycin at 37°C in 5% CO_2. Wells of 24-well tissue culture trays were seeded with 2×10^5 Detroit cells in DMEM with 10% FCS and grown for 24 h before inoculation with pneumococci. These strains were grown overnight on BA plates, before being resuspended in CDM + 0.5% glucose or CDM + 0.5% galactose at a final OD_{600} of 0.2. 500 µL of each bacterial suspension was added to the washed Detroit cell monolayers. As a control, each bacterial suspension was added in the same volume to empty wells. After

incubation for 2 h at 37°C, wells were washed 3 times with PBS before cells were detached from the plate by treatment with 100 µL 0.25% trypsin-0.02% EDTA and 400 µL of 0.1% Triton X-100 (Sigma). Samples were plated on BA to determine the number of adherent bacteria. Assays were conducted in triplicate with at least two repeated independent experiments. Statistical analysis was performed using two-tailed Student's *t* test; *P* values < 0.05 were deemed statistically significant. Data are presented as percentage of adherent bacteria, calculated using the colony forming units per mL (CFU/mL) of adherent bacteria and the CFU/mL of bacteria from the control wells that underwent the 2 h incubation. Control wells were also used to monitor the growth of bacteria during the incubation time, ensuring that each strain had similar rates of growth.

Capsule Assay

A FITC-dextran exclusion assay was used to determine the capsule thickness of strains based on previous methods (Hathaway et al., 2012), using FITC-Dextran 2000 kDa (Sigma). Briefly, pneumococci were grown overnight on BA plates in 37°C at 5% CO_2. Cells were washed in PBS, before being resuspended to a final OD_{600} of 0.6 in 1 mL. A volume of 80 µL bacterial suspension was mixed with 20 µL FITC-dextran (10 mg/ml in MilliQ water). Each bacterial suspension was pipetted at a volume of 10 µL onto a microscope slide and a coverslip applied securely. Imaging was conducted on 3 separate days with freshly prepared bacterial suspensions each time. The slides were viewed and imaged using an Olympus FV3000 Laser Scanning microscope with a 60× objective (Adelaide Microscopy). The images were analyzed using Zeiss Zen imaging software. Statistical analysis was performed using the Kruskal-Wallis test; *P* values < 0.05 were deemed statistically significant.

Targeted Gene Sequencing (Sanger Sequencing)

Selected genes of the raffinose operon from the strains underwent Sanger sequencing through AGRF (Adelaide, Australia). Briefly, samples were prepared for sequencing by PCR amplification of the region of interest using the primers listed in **Table 2**. PCR products were analyzed by gel electrophoresis, and successfully amplified products were purified using the QIAquick PCR Purification Kit (Qiagen) as per the manufacturer's instructions. Purified PCR products were evaluated for DNA quantity and quality using a Nanodrop (Thermofisher). Samples were diluted in ultrapure nuclease-free water to a final concentration of either 18 ng/µL or 60 ng/µL depending on the size of the product, according to the Australian Genome Research Facility (AGRF) guidelines.

Genome Sequencing

S. pneumoniae strains were grown to mid-exponential phase in HI broth. Genomic DNA (gDNA) was extracted using the Promega Wizard® Genomic DNA Purification Kit according to the manufacturer's instructions, except the DNA pellet was rehydrated in ultrapure nuclease-free water. The lytic enzymes used were lysosome (30 mg/mL), 10 units mutanolysin and 0.1% sodium deoxycholate (DOC). The gDNA was sequenced at the South Australian Genomics Centre (South Australian Health & Medical Research Institute, Adelaide, South Australia) on an Illumina MiSeq (250-bp paired-end reads). Genome assemblies were generated using shovill v1.1.0 (Seemann, 2020a), a bacterial isolate *de novo* genome assembly pipeline based on SPAdes (Prjibelski et al., 2020). The resulting genome assemblies were annotated using Prokka v1.14.6 (Seemann, 2014). Variant analysis was conducted using Snippy v4.6.0 (Seemann, 2020b) by performing all pairwise combination of aligning reads from one sample to the genome assembly of another sample. Gene presence/absence analysis was determined with a reciprocal-best-hit approach applied to the Prokka-derived amino acid sequences using mmseqs2 v13.45111 (Steinegger and Söding, 2017). A 3-step iterative searching strategy was applied using the easy-rbh workflow of mmseqs2 using sensitivities of 1, 3 and 7 (command line arguments: –start-sens 1 –sens-steps 3 -s 7) using a k-mer length of 6 (command line argument: -k 6).

RNA Extraction and qRT-PCR

Strains were initially grown overnight on BA plates at 37°C with 5% CO_2. Cells were harvested, washed, and resuspended in 1 mL of CDM + 0.5% glucose or raffinose to a final OD_{600} of 0.2. Suspensions were incubated at 37°C with 5% CO_2 for 30 min. RNA was extracted using a Qiagen RNeasy Minikit as per the manufacturer's instructions. Differences in levels of gene expression were determined using one-step relative real-time qRT-PCR in a Roche LC480 real-time cycler, as previously described (Minhas et al., 2019). The specific primers used for the different genes are listed in **Table 2** and were used at a final concentration of 200 nM per reaction. Primers specific for *gyrA* mRNA were used an internal control. Amplification data were analyzed using the comparative critical threshold ($2^{-\Delta\Delta CT}$) method (Livak and Schmittgen, 2001). Assays were performed in triplicate with a minimum of two independent experiments. Statistical analyses were performed using two-tailed Student's *t* test; *P* values < 0.05 were defined as statistically significant.

Murine Infection Model

Animal experiments were approved by the University of Adelaide Animal Ethics Committee. Female outbred 4- to 6-week-old CD-1 (Swiss) mice were anaesthetized by intraperitoneal injection of ketamine (8 mg/mL) and xylazine (0.8 mg/mL), and were challenged intranasally with 50 µL of bacterial suspension containing 1×10^8 CFU in SB as previously described (Minhas et al., 2019). The challenge dose was retrospectively confirmed by serial dilution and plating on BA. At 24 h and 48 h, groups of 6 or 8 mice were euthanized by CO_2 asphyxiation before harvesting the blood, lungs, nasal tissue, ears, and brain. Tissues were homogenized and pneumococci enumerated as previously described by serial dilution and plating on BA plates containing 5 µg/mL gentamicin (Trappetti et al., 2011). Statistical analyses of log-transformed CFU data were performed using two-tailed Student's *t* test; *P* values < 0.05 were deemed statistically significant.

TABLE 2 | Oligonucleotide primers used in this study for PCRs.

OLIGO NAME	SEQUENCE (5' → 3')	Reference
seq_rafK_F	AGAATCCAGTCAAATGTAGTGGAG	This study
seq_rafK_R	AAGTCAGTAATCATACGTACGGC	This study
rafK_F	AACGACGTAGCTCCAAAAGA	Minhas et al., 2019
rafK_R	GCTGGTTTACGTTCCAAGAA	Minhas et al., 2019
seq_rafR_F	TGTTTCAAAAGTAAGTAGCCATTTCG	This study
seq_rafR_R	TTCTTCTAGAATCTCTGGAAGAATAAGG	This study
seq_rafEFG_F1	GGCGAAGTTTACTCAGGTGC	This study
seq_rafEFG_R1	GCTGAACTCTTCCTCTGTGTC	This study
seq_rafEFG_F2	CACCATTTGGAATTGCAGGTG	This study
seq_rafEFG_F3	GAAAGCGGATGTGGATTAGGAG	This study
seq_rafEFG_F4	GCCTTTGACCAAGTCTTTGC	This study
seq_rafEFG_F5	ATTCCAGAAAGTCTGGATGAAGC	This study
seq_rafK_F2	TCAAATGTAGTGGAGAATCAGCG	This study
seq_rafK_R2	CGAAGAGTATTAAAGAGCATCACAATATAG	This study
aga_F1	TTCTATTTTGGAAAGCGATTTCAGG	This study
aga_F2	CTTTAGTGACTCATTCAGATCAGGG	This study
aga_F3	CCGCAATATCACTAAGCTAGGG	This study
aga_F4	GAAGCAGCTGTACAATTTAATTACGG	This study
rafF_R	AGAAGGTTTGGCCTTTGATT	This study
aga_F_RT	GTCAGACTAAGTTGAGCCTTAG	Minhas et al., 2019
aga_R_RT	CCAACTATACAGGTTCAGCA	Minhas et al., 2019
rafG_F	CCTATGGCAGCCTACTCCATC	Minhas et al., 2019
rafG_R	GGGTCTGTGGAATCGCATAGG	Minhas et al., 2019
rafR_F	CCAGCCATTCGTGATACATA	This study
rafR_R	CCTCCAGTGATTCCTAACCA	This study
gyrA RT F	ACTGGTATCGCGGTTGGGAT	Mclean et al., 2020
gyrA RT R	ACCTGATTTCCCCATGCAA	Mclean et al., 2020

RESULTS

Initial Characterization of Serotype 15C Blood and CSF Clinical Isolates

We began characterization of serotype 15C blood and CSF isolates from the same patient, denoted 60B and 60CSF, by performing multi-locus sequence typing (MLST) to determine the sequence type (ST). Both 60B and 60CSF have the sequence type 8711 (ST8711). Additional information provided by the German National Reference Center for Streptococci included the antibiotic sensitivity of the isolates. Both isolates, 60B and 60CSF had the same MIC values for all the antibiotics tested, with all MICs falling below the clinical breakpoint (European Committee on Antimicrobial Susceptibility Testing; EUCAST), indicating full sensitivity for both the isolates (data not shown).

Blood and CSF Isolates Metabolize Carbohydrate Sources Differently

As previous research undertaken in our lab has shown that isolates of the same serotype/ST potentially metabolize the carbohydrate raffinose differentially, we investigated the carbohydrate metabolism capabilities of 60B and 60CSF. Two types of phenotypic microarray plates, PM1 and PM2a, with a total of 190 carbon sources were used to test the isolates' metabolic ability. A total of 29 of the carbon sources are metabolized by both 60B and 60CSF, 10 carbon sources were metabolized by just 60CSF and the remaining 151 carbon sources were unable to be metabolized (**Table 3**). In line with prior research implicating an role for raffinose metabolism in tissue tropism, raffinose, and one of its derivatives, melibiose, were metabolized by 60CSF but not 60B. Of the carbon sources that were differentially metabolized by 60B and 60CSF, we analysed the growth of these strains in chemically defined medium (CDM) with the clinically relevant sugars: raffinose, melibiose, lactose and galactose. The growth of 60B and 60CSF were comparable in CDM + glucose (**Figure 1**), and the growth pattern was consistent in CDM + galactose and CDM + lactose (data not shown). Altought the phenotypic microarray showed that 60CSF was able to metabolize melibiose, there was no growth for either strain in CDM + melibiose, implying that melibiose may not be able to support growth of pneumococci as the sole carbon source in the present conditions (data not shown). Despite this, 60CSF was able to grow in CDM + raffinose, whilst 60B displayed an inability to grow in this medium (**Figure 1**). This indicates that despite the strains coming from the same patient and being closely related, there is a marked difference in their capacity to utilize raffinose as a carbon source.

Targeted Sequencing of the Raffinose Operon Reveals That *aga* Has a Premature Stop Codon in Both Isolates

Considering that raffinose was only metabolized by and capable of supporting the growth of 60CSF, and not 60B, we performed Sanger sequencing targeting the genes, that are part of the core genome, that are critical for raffinose metabolism to investigate whether they were functional in both strains (**Figure 2**). The raffinose uptake and utilization operon consists of eight main genes encoding an α-galactosidase (*aga*), transcriptional regulators (*rafS* and *rafR*), an ABC transporter with solute-binding protein and two cognate permeases (*rafE*, *rafF* and *rafG*), a sucrose phosphorylase (*gtfA*), and a protein of unknown function (*rafX*). Additionally, further

TABLE 3 | Phenotype microarray results for 60B and 60CSF in Biolog PM1 and PM2a plates.

CARBON SOURCE	60B	60CSF
L-Arabinose	+	+
N-Acetyl-D-Glucosamine	+	+
D-Galactose	+	+
D-Trehalose	+	+
D-Mannose	+	+
Glycerol	+	+
D-Xylose	+	+
D-Ribose	+	+
L-Rhamnose	-	+
D-Fructose	+	+
α-D-Glucose	+	+
Maltose	+	+
D-Melibiose	-	+
α-D-Lactose	+	+
Lactulose	+	+
Sucrose	+	+
ß-Methyl-D- Glucoside	+	+
Maltotriose	+	+
D-Cellobiose	+	+
N-Acetyl-ß-D-Mannosamine	+	+
D-Psicose	+	+
L-Lyxose	+	+
Chondroitin sulfate c	-	+
Dextrin	+	+
Inulin	+	+
Pectin	+	+
N-Acetyl-D Galactosamine	+	+
N-Acetyl Neuraminic Acid	+	+
D-Arabinose	-	+
2-Deoxy-DRibose	-	+
3-0-B-D-Galactopyranosyl-DArabinose	-	+
Palatinose	+	+
D-Raffinose	-	+
Salicin	+	+
D-Tagatose	-	+
Turanose	-	+
D-Glucosamine	+	+
5-Keto-DGluconic Acid	+	+
Dihydroxy Acetone	-	+

Catabolism was measured through a colorless tetrazolium dye being reduced by NADH produced during catabolism. +, metabolism occurred; -, no metabolism occurred. Metabolism was determined by calculating the change in OD_{590} from the initial to final measurements. These values were then compared with the change in the negative control and an arbitrary value based on the change in negative control was used to determine if metabolism occurred. Carbon sources which neither strain metabolized are not shown. Bold font indicates carbon sources that were differentially metabolized by the strains.

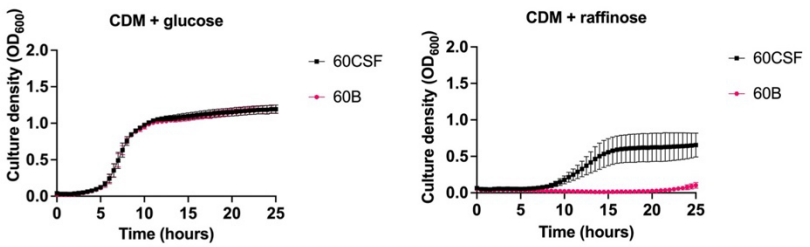

FIGURE 1 | Growth of 60B and 60CSF in CDM + glucose and CDM + raffinose. *S. pneumoniae* serotype 15C ST8711 blood isolate (60B) and CSF isolate (60CSF) were grown in 200 µL CDM supplemented with 0.5% glucose (CDM + glucose) or 0.5% raffinose (CDM + raffinose). OD_{600} was measured every 30 min for 24 h. Data are mean OD_{600} ± standard error mean (SEM) from three independent assays, each performed in triplicate.

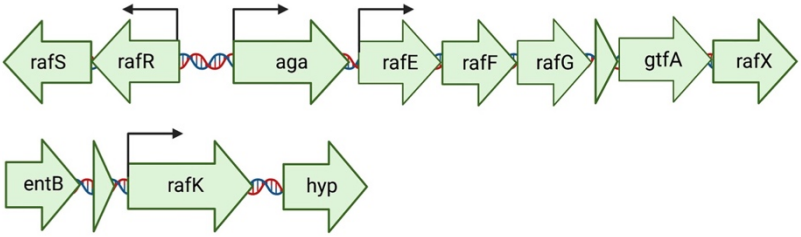

FIGURE 2 | Arrangement of the genetic loci required for the import and utilization of raffinose by *S. pneumoniae*. The main locus contains 8 genes: an ABC transporter with solute-binding protein and two cognate permeases (*rafE*, *rafF* and *rafG*); two transcriptional regulators, *rafS* (repressor) and *rafR* (activator), which control the expression of the gene encoding an α-galactosidase (*aga*); a sucrose phosphorylase (*gtfA*), and *rafX*, encoding a gene of unknown function. Further upstream is *rafK*, encoding an ATP-binding protein, essential for raffinose import into the cell (Rosenow et al., 1999). Arrows above the genes indicate locations of promoters. Created with BioRender.com.

upstream there is a gene encoding an ATP-binding protein (*rafK*), which is essential for import of raffinose into the bacteria (Rosenow et al., 1999) (**Figure 2**). The *aga, rafR, rafE, rafF, rafG* and *rafK* were sequenced. Each of these genes encode proteins with a critical role in raffinose uptake and utilization (**Figure 3**). The sequences of all the genes investigated were the identical between the 60B and 60CSF strains. However, for both 60B and 60CSF, there was a SNP in *aga* relative to the published D39 and TIGR4 genome sequences that resulted in an early stop codon, truncating the Aga protein at 213 a.a., compared with 721 a.a. for native Aga (**Supplementary Figure 1**). As the gene sequences involved in raffinose uptake and metabolism were the same between 60B and 60CSF, we investigated if the expression of these genes correlated with the capacity to utilize raffinose by performing quantitative real-time reverse transcription-PCR (qRT-PCR).

The Blood and CSF Isolates Display Differences in the Transcription of Raffinose Utilization Genes

To determine if the difference in ability to utilize raffinose between the blood and CSF isolates corresponded with raffinose operon gene expression, 60B and 60CSF strains were grown to the same OD_{600}

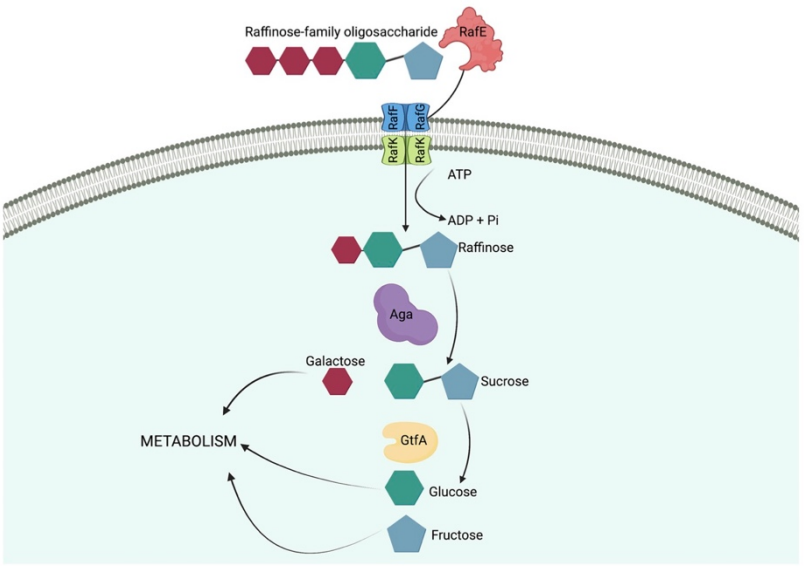

FIGURE 3 | Import and breakdown of raffinose in *S. pneumoniae*. A raffinose-family oligosaccharide (RFO) is delivered to the ABC transporter cell membrane components, RafF and RafG, by the solute-binding protein, RafE. The RFO is imported into the cell using the energy produced from the ATP-binding protein, RafK, with concomitant ATP hydrolysis. In the cytoplasm of the cell raffinose is sequentially degalactosylated by an α-galactosidase, Aga, releasing galactose, which can enter other metabolic pathways, and sucrose. A sucrose phosphorylase, GtfA, cleaves sucrose into glucose and fructose, both of which can enter further metabolic pathways and be utilized by the cell. (Hobbs et al., 2019). Created with BioRender.com.

(0.2) in CDM + Glucose and then washed and resuspended in CDM + Raffinose and incubated for a further 30 min. RNA was then extracted, and levels of *rafR*, *aga*, *rafK*, and *rafG* mRNA, representative of each of the three RafR-regulated transcriptional units, were then measured relative to *gyrA* mRNA by qRT-PCR. Although *rafR* was not expressed at detectable levels in either strain (data not shown), the expression levels of the α-galactosidase (*aga*) and the ATP binding protein component of the transporter (*rafK*) were significantly up-regulated in the CSF isolate compared to the blood isolate ($P < 0.05$), while the expression level of the putative permease (*rafG*) was comparable in both strains (**Figure 4**). These results indicate that, while the component of the raffinose ABC transporter gene (*rafG*) was equally expressed in both strains, the uptake of raffinose may be limited by the reduced transcription of the gene encoding the ATP binding protein *rafK* required to energize this transporter.

The Blood and CSF Isolates Display Altered Tissue Tropism

We next explored whether the two clinical isolates displayed any differences in disease phenotype using a mouse model of infection. Mice were intranasally challenged with 10^8 CFU of each strain and the bacterial burden in the blood, brain, ears, lungs, and nose were assessed at 24 and 48 h post challenge. Mice challenged with either strain showed no detectable bacteria present in the blood at either time point (data not shown). At 24 h post challenge, there was no significant difference in the relative bacterial burden between the mice infected with the 60B or 60CSF isolates in the brain or lungs (**Figure 5**). No bacteria for the 60B isolate were detected in the ears at 24 h post challenge (**Figure 5**), while bacteria were present in the ears of over 85% of the mice for the 60CSF strain (**Figure 5**; $P < 0.0001$). Conversely, the bacterial burden in the nose was higher for the 60B strain compared with the 60CSF strain (**Figure 5**; $P < 0.0001$). At 48 h post challenge, there were no observed significant differences between the two strains in any niche (data not shown).

Given the observed niche preferences for the strains at the 24 h time point, where the 60B strain was higher in the nose, while 60CSF higher in the ear, we investigated whether these strains produced varied amounts of capsule that may account for these differences. We analyzed the relative capsule abundance by measuring the FITC-Dextran exclusion area of the two isolates, as well as D39 and Rx1 as encapsulated and unencapsulated control strains, respectively. No significant difference in the mean FITC-Dextran exclusion area was observed between the 60B and 60CSF strains (**Figure 6**). The unencapsulated control strain Rx1 displayed a significantly lower mean capsule area compared with the D39 strain ($P < 0.01$), which showed a mean area comparable to that of the 60B strain, while there was a minor but significant difference compared with the 60CSF strain (**Figure 6**; $P < 0.01$). We next considered whether the difference in tissue tropism could be due to an altered capacity of the bacterial strains to adhere to the nasopharyngeal epithelium. The *in vitro* adherence of each strain to Detroit 562 pharyngeal cells was explored in the presence of glucose or galactose as the sole carbon source, the latter representing the prevalent sugar present in the nasopharynx (Paixão et al., 2015). No significant difference in the total number of adherent cells was observed between the strains in either carbon source (**Figure 7**). Together, these data suggest that the differences in tissue tropism are not merely a consequence of altered capsule expression or nasopharyngeal adherence capabilities between the strains. To determine whether the 60B and 60CSF strains displayed a difference in biofilm formation capacity, we performed an assessment of their biofilm formation with the xCELLigence instrument. An analysis of biofilm formation was performed in glucose, the preferred carbon source, and galactose, a carbon source accessible during nasopharyngeal colonization, where biofilm formation is thought to occur. No significant difference in the rate of biofilm formation over a 24h period was observed between the strains (data not shown). Furthermore, although the maximum biofilm formation in 60CSF appeared higher than in 60B, with higher biofilm levels in the galactose medium, this difference was not statistically significant (**Figure 8**).

Genomic Analyses Identify a Putative Alpha-Galactosidase That May Contribute to Phenotypic Differences Between the Blood and CSF Strains

As we have previously shown niche-adaptation differences between closely related isolates (Minhas et al., 2019) and isolates from the same patient (Tikhomirova et al., 2021) to be driven by a SNPs in

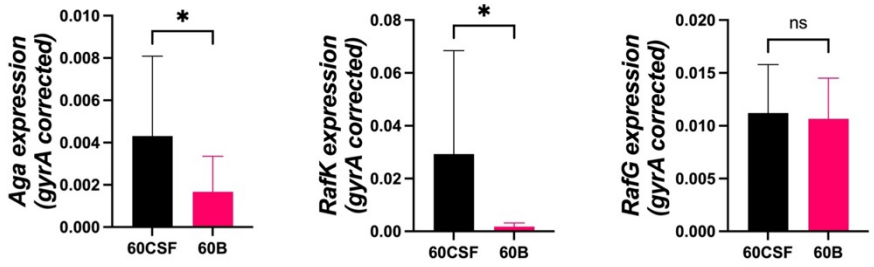

FIGURE 4 | Expression of RafR-regulated raffinose pathway genes by 60B and 60CSF isolates. Strains were grown to OD_{600} 0.2 in CDM + glucose and then washed and resuspended in CDM + raffinose and incubated at 37°C for a further 30 min. RNA was then extracted, and levels of *aga*, *rafK*, and *rafG* mRNA were analyzed by qRT-PCR using *gyrA* rRNA as an internal control (see *Materials and Methods*). Data are mean OD_{600} ± standard deviation (SD) from two independent assays. Significance of differences in gene expression between isolates was determined using two-tailed Student's *t* test; *$P < 0.05$. ns, not significant.

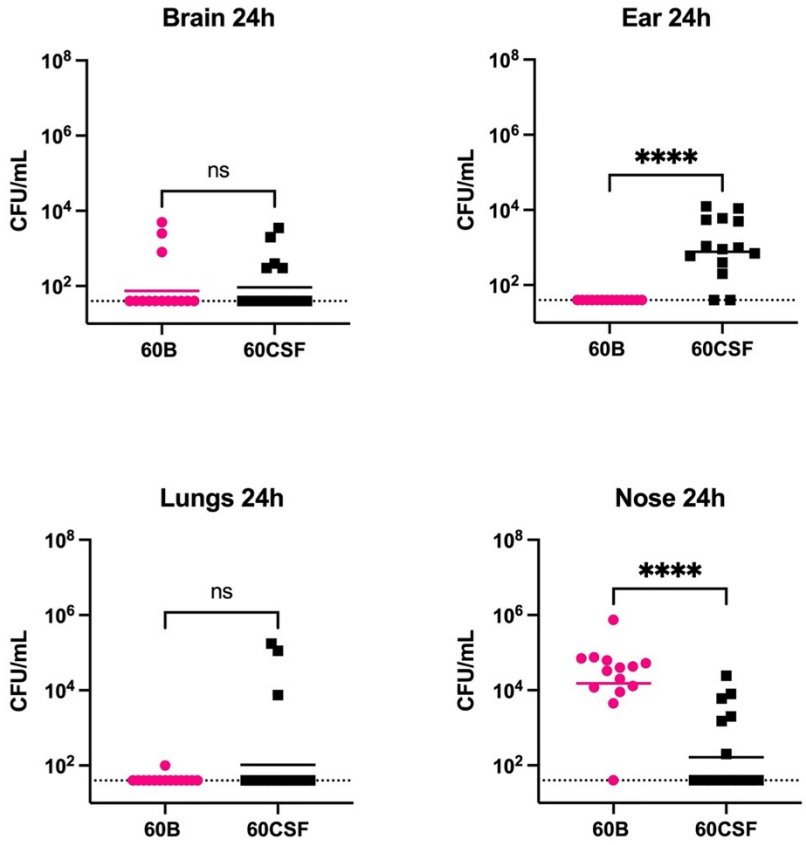

FIGURE 5 | Virulence phenotypes of blood and CSF isolates. In 2 separate experiments groups of 6 or 8 mice were infected intranasally with 10^8 CFU of the indicated strain. At 24 h, mice from each group were humanely euthanized and pneumococci in the brain, ear, lungs and nasal tissue were enumerated. Viable bacterial counts are displayed for each mouse in each niche; horizontal bars indicate the geometric mean (GM) CFU for each group; the dotted line indicates the detection threshold. Significance of differences in bacterial load between groups was determined using two-tailed Student's t test; ****$P < 0.0001$. ns, not significant.

loci responsible for uptake and utilization of raffinose, we performed whole genome sequencing of 60B and 60CSF on the Illumina platform, to determine whether the phenotypic differences observed here were a product of similar genomic events. SNP analysis comparing 60B and 60CSF sequences revealed that no SNPs were present in the well characterized raffinose locus or in any other coding regions. However, reciprocal best hit-based analysis revealed that there may be different fragments of a gene, encoding a putative glycosyl hydrolase family 36 (GH36) alpha-galactosidase, present between the blood and CSF isolates. The nucleotide and amino acid sequences shared no sequence similarity with the *aga* gene sequenced at the *raf* locus of these strains. We performed a BLASTn search using the nucleotide sequence for the largest fragment from the CSF isolate. This region showed 100% sequence identity to the latter 75% of an alpha-galactosidase gene that was present as part of the accessory genome in 68 out of 9029 other pneumococcal strains (0.75%), including the *S. pneumoniae* 4559, EF3030, and 947 strains (Junges et al., 2019; Minhas et al., 2019). Based on the short-read sequencing, obtained with the Illumina platform, the blood isolate appeared to possess two fragments spanning a 594 bp and 967 bp region of the alpha-galactosidase (**Supplementary Figure 2**), while the CSF isolate possessed one larger gene fragment encompassing 1680 bp in total (**Figure 9**). The sequencing did not identify regions with similarity to the first 537 bp of this full-length gene in either isolate. However, the fragments in the CSF isolate encompassed the remainder of the gene, while the contigs from the Illumina sequencing did not yield sequences that correspond to the final 132 bp of this gene for the 60B strain. We conducted further analyses of the alpha-galactosidase gene in the *S. pneumoniae* 4559 blood isolate. The alpha-galactosidase gene, depicted as a pink arrow (Protein ID WP_000158269.1; **Figure 10**), was present in a ~13 kb region of DNA that possessed a relatively low GC content (33% GC) to that of the upstream and downstream DNA (40.4% GC and 40% GC, respectively), suggesting a possible horizontal gene transfer event may have occurred. However, there were no other genes or features

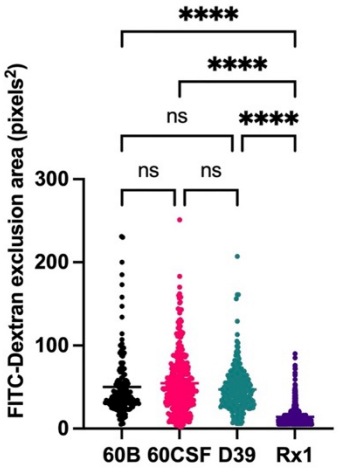

FIGURE 6 | Capsule area of blood and CSF isolates, measured using FITC-dextran exclusion assay. *S. pneumoniae* D39, Rx1, serotype 15C ST8711 blood isolate (60B) and CSF isolate (60CSF) were grown overnight before being resuspended to an OD_{600} of 0.6 in 1 mL PBS. 80μL of bacterial suspension was added to 20μL FITC-dextran (10mg/mL in MilliQ water). A volume of 10 μL of the bacterial FITC-dextran suspension was pipetted onto microscope slides, fixed with a coverslip, and imaged using a laser scanning microscope. Statistical analysis was performed using Kruskal-Wallis test; ****$P < 0.0001$. Imaging was conducted on 3 separate days with fresh bacterial suspensions prepared each time. ns, not significant.

identified nearby that would indicate that this region was a mobile genetic element. This ~13 kb region of *S. pneumoniae* 4559 contained nine genes in total, including genes with putative functions such as a NPCBM/NEW2 domain-containing glycoside hydrolase family 27 protein (WP_001813616.1), an additional alpha-galactosidase (WP_000687798.1), an alpha-L-fucosidase (WP_000683280.1), two carbohydrate ABC transporter permeases, (WP_001812774.1 and WP_000057512.1), an ABC transporter substrate binding protein (WP_001036442.1), and a rhamnulokinase (WP_000388563.1) (**Figure 10**). In *S. pneumoniae* 4559, this region was situated adjacent to the zinc acquisition pathway genes, *adcCBA*. We then examined whether either the 60B or 60CSF contigs contained the adjacent gene sequences. Both isolates contained contigs with sequence identity to the glycoside hydrolase family 27 and alpha-galactosidase genes.

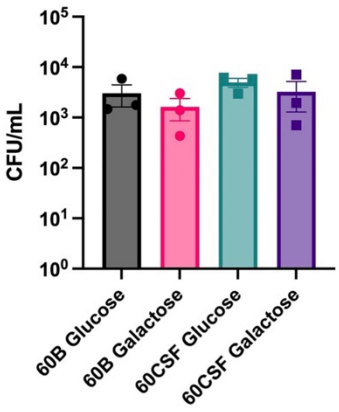

FIGURE 7 | Adherence of 60B and 60CSF to Detroit 562 cells. *S. pneumoniae* strains 60B and 60CSF at OD_{600} 0.2 were inoculated onto monolayers of Detroit 562 cells in CDM + glucose or CDM + galactose, and incubated for 2 h before being tested for adherent bacteria. Data are mean adherent bacteria ± standard error mean (SEM) from three independent assays, each performed in triplicate. Statistical analysis was performed using two-tailed Student's *t* test. No significant differences were detected between the adherence of the strains in different conditions.

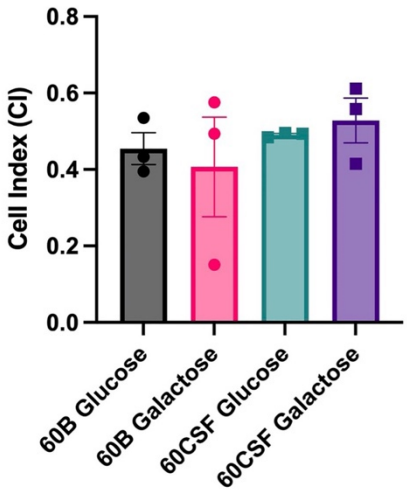

FIGURE 8 | Maximum biofilm formation by 60B and 60CSF. 60B and 60CSF were cultured overnight on BA plates before being diluted to a final OD_{600} of 0.05 in CDM + 0.5% glucose or CDM + 0.5% galactose. 200 µL of each bacterial strain in each sugar was placed into wells of a xCELLigence E-plate, with the plate being placed in the cradles of the RTCA-DP platform, and incubated at 37°C. Biofilm formation was determined by measuring cell index (CI) every 15 min over 24 h using real-time cell analysis (RTCA) xCELLigence technology. Data are mean maximum CI ± standard error mean (SEM) from three independent assays, each performed in triplicate. Statistical analysis was performed using two-tailed Student's *t* test. No significant differences were detected between the biofilm formation of the strains in different carbon sources.

DISCUSSION

Over the past 20 years marked reductions in total death rates were achieved for many of the world's most important communicable diseases including malaria, tuberculosis and diarrhea, but the mortality due to lower respiratory infections and meningitis remained fairly constant (GBD 2015 Child Mortality Collaborators, 2016). Notably, the decrease in pneumococcal isolates with serotypes covered by currently available conjugate vaccines, which often cause bacteremic disease, was counterbalanced by an increase in cases of meningitis associated with strains less likely to cause

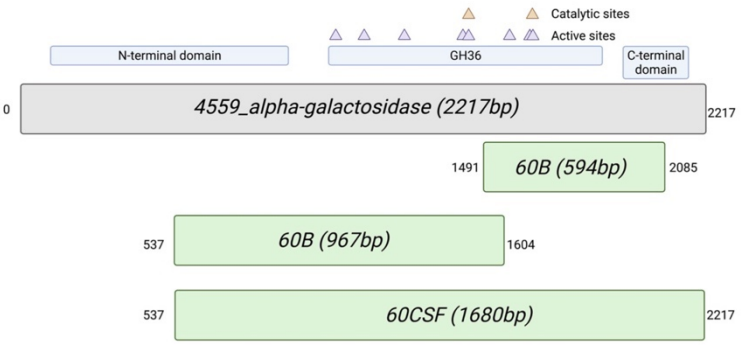

FIGURE 9 | Alignment of the alternative alpha-galactosidase gene with putative gene fragments. Gene fragments of 60B and 60CSF that correspond to an alternative alpha-galactosidase (protein ID: WP_000158269.1; locus tag: FJH52_RS10440; gene ID: GI:446080414) found in *S. pneumoniae* strain 4559. The blood isolate, 60B, contained fragments that were 594bp and 967bp in length, whilst the CSF isolate, 60CSF, contained a single fragment of 1680bp. Numbers outside of gene fragments correspond to nucleotide position within strain 4559 alpha-galactosidase. A conserved domain search was performed on using NCBI conserved domain search (Lu et al., 2020). A glycosyl hydrolase family 36 (GH36) motif was found in strain 4559 alternative alpha-galactosidase. Two aspartic acid residues have been identified as the catalytic nucleophile and the acid/base, respectively, as indicated by the orange triangles. Active sites within the GH36 motif are indicated by purple triangles. A glycosyl hydrolase family 36 N-terminal domain, with a beta-supersandwich fold, and a glycosyl hydrolase family 36 C-terminal domain, with a beta-sandwich structure with a Greek key motif, were also located within the strain 4559 alternative alpha-galactosidase.

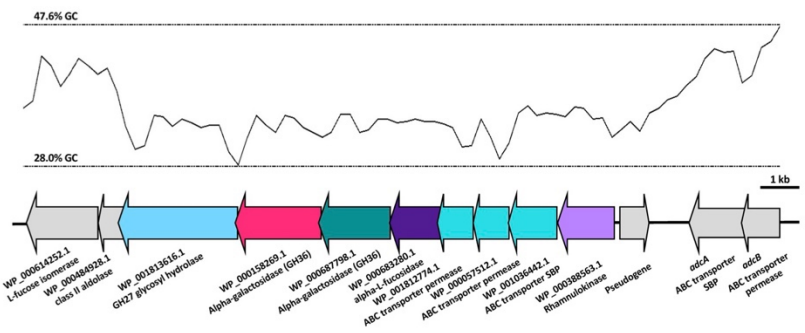

FIGURE 10 | Organisation of the *S. pneumoniae* 4559 alpha-galactosidase region. The GC content of the DNA is shown as a black line, with the upper and lower limits for this region as dotted lines. Open reading frames of genes are depicted in the direction of transcription, with genes in the lower GC region shown as colored arrows and genes adjacent to this region as grey arrows. The protein identification (ID) or name (if known), and putative function are indicated below the genes. Genes have been drawn to scale.

bacteremia (Mukerji and Briles, 2020). The lack of reduction in death rates of the diseases caused by the pneumococcus, despite the availability of an effective vaccine and suitable antimicrobial therapy, indicates that invasive pneumococcal disease is less well understood than we thought.

Understanding the bacterial features that dictate disease progression and phenotype is complicated by the high genetic diversity of *S. pneumoniae*. Certain serotypes have been associated with specific disease types, but non-capsular differences also contribute to disease progression. We have previously identified genetic and metabolic differences between clinical isolates of the same sequence type that were derived from the blood and ear of different patients. While these isolates exhibited related genetic backbones, these strains were isolated from distinct patients and possessed many additional gene alterations. In this study, we explored two clinical strains, possessing identical serotype, sequence type, and antibiotic sensitivity profiles, isolated at the same time from the blood and CSF of a single pediatric patient presenting with meningitis. These strains provided a unique opportunity to investigate whether differences may have arisen during the course of disease that could contribute to a change in lifestyle, such as permitting transfer across the blood-brain barrier or altered survival in the brain and CSF environment.

In vitro phenotypic characterization of these strains identified major differences in the metabolic capacity of the blood and CSF isolates. Compared with the isolate from the CSF, the blood isolate was unable to metabolize a range of carbohydrates, including L-rhamnose, 2-deoxy-D-ribose, D-arabinose, chondroitin sulfate c, D-tagatose, turanose and dihydroxy acetone and the two alpha-galactoside sugars, raffinose and melibiose. Importantly, we found that the blood isolate was unable to grow when raffinose was the sole carbon source.

This is distinct from our previous findings for serotype 14 ST15 strains, in which a pneumococcal blood isolate was able to grow in raffinose, while an ear isolate displayed perturbed growth (Minhas et al., 2019). In the current study, the CSF and blood isolates appeared to possess extensive genomic similarity, with short-read genomic analyses identifying no SNPs in the coding regions of genes between these two strains. However, we found that despite the observed capacity for raffinose to be metabolized and sustain growth of the CSF isolate, both of the strains possessed a premature stop codon in the *aga* gene. The impact of the premature stop codon on the stability of the *aga* mRNA is unclear, but a truncated protein lacking the C-terminal region that harbors the catalytic and active sites suggest this protein would lack functionality. While the nucleotide sequence of this *aga* gene at the *raf* locus most closely resembled the D39 (SPD_1678) and TIGR4 (SP_1898) sequences, we also identified fragments of an alternative alpha-galactosidase gene region that was differentially present in the two strains. These fragments shared 100% identity with a portion of a gene encoding an alternative alpha-galactosidase that was present in strains including *S. pneumoniae* strain 4559, EF3030, 947, and 70585.

We performed a conserved domain search to determine whether the C-terminal region of this protein, which was not detected in the blood isolate, might be of functional significance. The region missing from the larger fragment of the blood isolate corresponded to a putative glycosyl hydrolase family 36 (GH36) motif, which contains three out of the eight putative active site residues, including one of the catalytic aspartic acid residues. By comparison, the first 538 bp region (~179 N-terminal amino acids) that were not detected in either isolate did not contain any of the putative active site residues. The gene regions identified did not possess significant similarity to any other related Streptococcal species, but the identification of similarity in other pneumococcal isolates points to the acquisition of this gene through a recombination event with another pneumococcal strain, possibly during nasopharyngeal colonization. In *S. pneumoniae* 4559, the sequence of DNA including the adjacent genes possesses a lower GC content, which suggests that it may have originally been acquired from another species with a relatively lower GC%. Despite the absence of features

consistent with a mobile genetic element, the pneumococcus is naturally transformable and will readily incorporate DNA from the environment. However, both the 60B and 60CSF appear to possess sequences that align with the genes upstream and downstream of this alpha-galactosidase. As a result, these findings must be validated by long-read sequencing to have confidence in the sequence and precise location of this region in both strains. Nevertheless, as these isolates were obtained from different sites of the same patient, it is possible that after transition to the brain, the 60B strain lost the C-terminal region of this additional alpha-galactosidase gene, resulting in abolished raffinose utilization capacity.

Notwithstanding the above differences in the *aga* gene sequences, the blood isolate also showed reduced transcription of *aga* at the *raf* locus, as well as *rafK*, which encodes the ATP-binding component of the raffinose importer. No difference in expression was observed for the permease component (*rafG*), but as RafK is required to energize the transport of raffinose by this pathway, these data point to a likely reduction in the import of raffinose in the isolate from the blood compared with the CSF isolate, which may further compound growth defect and reduced transcription of the *rafK* gene observed. Unexpectedly, we found that the expression of the gene encoding the transcriptional activator of these operons, *rafR*, was undetectable in both isolates. The *rafR* gene is co-transcribed with *rafS*, and their gene products regulate the raffinose-dependent stimulation of a divergently transcribed second promoter (P_A) directing the expression of *aga* (Rosenow et al., 1999). As a result, the regulation of this operon may be largely dependent on the levels of raffinose in the cell. Thus, the observed reduced transcription of the raffinose uptake genes in the blood isolate may be a consequence of increased accumulation of raffinose due to the potential inactivity of the alpha-galactosidase, whereby excess uncleaved raffinose may directly interact with the regulatory protein, leading to repression of these genes in the blood isolate, compared with the CSF isolate.

In addition to the metabolic differences observed *in vitro*, these strains possessed markedly different virulence profiles in mice. No mice challenged with the blood isolate had detectable levels of pneumococci in the ears, while we recovered the CSF isolate from the ears of >85% of the infected mice. In this study, the blood isolate displayed an inability to transit to the ear after intranasal challenge. These data are consistent with previous findings in other serotypes and sequence types, in which bacteria isolated from the blood typically display lower bacterial loads in the ears of mice post-challenge, compared with bacteria from other isolation sites (Amin et al., 2015; Minhas et al., 2019). In our previous study, increased capacity to metabolize raffinose correlated with reduced ear titers, but the defect in raffinose utilization was attributed to SNPs present in the regulator RafR or the import protein component RafK (Minhas et al., 2019). Another distinction between this study and the previous is that the isolates were obtained from the same patient. Although it is not known whether the blood strain originated from the CSF isolate or vice versa, this approach resulted in substantially reduced background genetic differences, including an absence of detectable SNPs. In this study, the inability of the blood strain to utilize raffinose is likely a consequence of impaired alpha-galactosidase activity and is correlated with reduced ear titers. Together, these data suggest that perturbation of this pathway at distinct stages may result in substantially different virulence phenotypes. The burden of bacteria in the nasopharynx was higher for the blood isolate than the CSF isolate, suggesting that a defect in alpha-galactosidase activity may favour survival in this niche, or perturb transit to alternate sites. Overall, these findings expand our understanding of the pneumococcal factors that may dictate disease types in humans, pointing to possible new features of clinical significance.

The basis for the involvement of a raffinose utilization pathway in pneumococcal virulence remains unclear, but there are two prevailing hypotheses. First, that pneumococci may be exposed to raffinose in the oropharynx from dietary sources (generally plants). Consistent with this, many other streptococcal species, including *Streptococcus mutans*, and lactic acid bacteria possess loci with similar genes and gene organization to the pneumococcal raffinose locus. Alternatively, this pathway may function to import and utilize structurally related human glycans. Aga has been shown to effectively cleave a galactose unit from a linear blood group antigen, suggesting a possible alternative physiological substrate of this pathway, but as recent studies showed that Aga is localized intracellularly, the role of this protein in host glycan processing is also dependent on the efficient uptake of the glycan from the environment (Hobbs et al., 2019). However, these studies were performed on the Aga protein from the TIGR4 strain, which possesses limited (44%) amino acid sequence identity to the alternative alpha-galactosidase discussed here. While humans lack the capacity to metabolize raffinose, there is evidence that pneumococci require this pathway during disease, as detectable expression of the *raf* genes was observed in bacteria isolated from the lungs of mice (Minhas et al., 2020). Further studies of the full-length and truncated variants of this alternative alpha-galactosidase enzyme are required to elucidate the potential substrates and possible role *in vivo*. It is possible that the alpha-galactosidase variant described herein displays an altered specificity for an as yet unidentified substrate that is crucial during disease.

In a previous study, we found that during infection of the host, *S. pneumoniae* display two main patterns of gene expression; one was characteristic of bacteria in blood and one of bacteria in tissue, such as lungs and brain (Oggioni et al., 2006). In the present study, two clinical strains originated from the blood (planktonic state) and the brain (biofilm state) of a 2-year-old child admitted to hospital with suspected meningitis, showed the same capability to form *in vitro* biofilm. Biofilm formation is one of the most important virulence traits for the bacteria. Biofilms act as a reservoir for organisms, enabling escape from the action of host antibodies or antibiotics, as well as facilitating production of toxins and generation of resistant organisms. Bacteria in biofilms may also detach and cause bloodstream infections. The biofilm state is often associated with solid-tissue related infections; in cystic fibrosis, chronic

lung infections are due to *P. aeruginosa*, *Staphylococcus aureus* and *Haemophilus influenzae*, which reside in the airway in biofilms (Smyth, 2006; Starner et al., 2006). Otitis media is caused by nontypeable *H. influenzae* and pneumococcus living within a biofilm (Murphy, 2003; Weimer et al., 2010; Cevizci et al., 2015) and finally, endocarditis is considered to be a biofilm-related infection caused by staphylococci or streptococci (Donlan and Costerton, 2002). However, recent clinical studies of purpura fulminans, a disease state associated with meningococcal sepsis, showed that bacteria are mostly grouped in microcolonies in these lesions (Harrison et al., 2002). Thus, a new aspect of biofilm formation that remains poorly characterized may explain the unexpected findings for biofilm capacity obtained with the blood isolate. Importantly, the CSF and blood strains used in this study, were collected from the same patient who was admitted to the hospital with suspected meningitis and it is unknown whether the blood stain originated from the CSF isolate or vice versa. While the hematogenous route was for many years believed to be the only mode for the bacteria to enter the CSF, clinical studies in adult and neonatal human meningitis have shown that *S. pneumoniae* can travel directly from the nasopharyngeal tissue to the brain without any bloodstream invasion (Garges et al., 2006). Experimental infections have confirmed that initial nasopharyngeal colonization could be followed by isolation of high number of bacteria from olfactory epithelium, brain, olfactory bulbs and trigeminal ganglia in the absence of bacteremia (Van Ginkel et al., 2003). *In vivo* imaging also showed that pneumococci were able to directly localize in mice to the olfactory bulb and the brain, in the absence of detectable bacteremia (Marra and Brigham, 2001).

S. pneumoniae is an important commensal resident of the human nasopharynx, and like other commensals in this niche, colonisation is dependent on the capacity to adhere to the epithelium and exist within the nasal mucus. In our murine model of infection, we found that the blood isolate was better able to survive in the nasopharynx of the mice compared to the CSF strain. However, when the adherence of each strain was explored using *in vitro* cultured human nasopharyngeal epithelial cells, no significant difference in the total number of adherent cells was observed between the strains. In the nasopharynx, bacteria are predominantly embedded in the mucin glycans and pneumococci possess several surface components, such as surface-located pneumococcal adherence and virulence protein A (PavA), PavB and enolase (Eno), that enable persistance in this niche for weeks or months. Thus, inconsistencies between *in vitro* and *in vivo* results are likely due to the difference in available carbohydrates and the lack of expression of key pneumococcal surface adhesins in the *in vitro* assays. These adhesive interactions with the epithelial surface may be needed not only for colonization, but also for the initial step in the invasion process.

The pathophysiology of pneumococcal meningitis is not fully understood. In this study, we found that strains isolated from the brain and the blood of a single paediatric patient with meningitis and bacteraemia, showed remarkable differences *in vitro* and *in vivo* assays. Importantly, we found that the CSF strain could metabolize raffinose, while the blood isolate lacks this ability. Progression from carriage to invasive disease exposes the pneumococcus to markedly different micro-environments to which the organism must adapt, and this might explain the loss or the acquisition of one gene or another. The exact role of raffinose in disease progression, particularly in meningitis, is still unclear and further studies using comparative genomic and transcriptomic analyses of other *S. pneumoniae* serotypes and/or other meningitis-causing bacteria, are needed.

DATA AVAILABILITY STATEMENT

The datasets presented in this study can be found in online repositories. The name of the repository and accession number can be found below: NCBI; PRJNA803929.

ETHICS STATEMENT

Animal experiments were approved by the University of Adelaide Animal Ethics Committee.

AUTHOR CONTRIBUTIONS

Conceptualization, HA, EB, AT, JP, and CT. Methodology, HA, EB, KM, AT, and CT. Investigation, HA, EB, KM, AT, ML, and CT. Formal analysis, HA, EB, AT, JP, and CT. Data curation, HA, EB, AT, JP, and CT. Writing—original draft preparation. HA, EB, AT, JP, and CT. All authors have read and agreed to the published version of the manuscript.

FUNDING

This work was supported by the National Health and Medical Research Council (NHMRC) Investigator grant 1174876 to JP, and by the Australian Research Council (ARC) Discovery Project DP190102980 to CT and JP.

ACKNOWLEDGMENTS

We would like to acknowledge Jane Sibbons and Adelaide Microscopy for assistance with the microscopy.

SUPPLEMENTARY MATERIAL

The Supplementary Material for this article can be found online at: https://www.frontiersin.org/articles/10.3389/fcimb.2022.866259/full#supplementary-material

REFERENCES

Amin, Z., Harvey, R. M., Wang, H., Hughes, C. E., Paton, A. W., Paton, J. C., et al. (2015). Isolation Site Influences Virulence Phenotype of Serotype 14 *Streptococcus Pneumoniae* Strains Belonging to Multilocus Sequence Type 15. *Infect. Immun.* 83, 4781–4790. doi: 10.1128/IAI.01081-15

Brouwer, M. C., Tunkel, A. R., and Van De Beek, D. (2010). Epidemiology, Diagnosis, and Antimicrobial Treatment of Acute Bacterial Meningitis. *Clin. Microbiol. Rev.* 23, 467–492. doi: 10.1128/CMR.00070-09

Cevizci, R., Duzlu, M., Dundar, Y., Noyanalpan, N., Sultan, N., Tutar, H., et al. (2015). Preliminary Results of a Novel Quorum Sensing Inhibitor Against Pneumococcal Infection and Biofilm Formation With Special Interest to Otitis Media and Cochlear Implantation. *Eur. Arch. Otorhinolaryngol.* 272, 1389–1393. doi: 10.1007/s00405-014-2942-5

GBD 2015 Child Mortality Collaborators (2016). Global, Regional, National, and Selected Subnational Levels of Stillbirths, Neonatal, Infant, and Under-5 Mortality 1980-2015: A Systematic Analysis for the Global Burden of Disease Study 2015. *Lancet* 388, 1725–1774. doi: 10.1016/S0140-6736(16)31575-6

Donlan, R. M., and Costerton, J. W. (2002). Biofilms: Survival Mechanisms of Clinically Relevant Microorganisms. *Clin. Microbiol. Rev.* 15, 167–193. doi: 10.1128/CMR.15.2.167-193.2002

Enright, M. C., and Spratt, B. G. (1998). A Multilocus Sequence Typing Scheme for *Streptococcus Pneumoniae*: Identification of Clones Associated With Serious Invasive Disease. *Microbiol. (Soc. Gen. Microbiol.)* 144, 3049–3060. doi: 10.1099/00221287-144-11-3049

Garges, H. P., Moody, M. A., Cotten, C. M., Smith, P. B., Tiffany, K. F., Lenfestey, R., et al. (2006). Neonatal Meningitis: What is the Correlation Among Cerebrospinal Fluid Cultures, Blood Cultures, and Cerebrospinal Fluid Parameters? *Pediatrics* 117, 1094–1100. doi: 10.1542/peds.2005-1132

Gutierrez, D., Hidalgo-Cantabrana, C., Rodriguez, A., Garcia, P., and Ruas-Madiedo, P. (2016). Monitoring in Real Time the Formation and Removal of Biofilms From Clinical Related Pathogens Using an Impedance-Based Technology. *PloS One* 11, e0163966–e0163966. doi: 10.1371/journal.pone.0163966

Harrison, O. B., Robertson, B. D., Faust, S. N., Jepson, M. A., Goldin, R. D., Levin, M., et al. (2002). Analysis of Pathogen-Host Cell Interactions in Purpura Fulminans: Expression of Capsule, Type IV Pili, and PorA by *Neisseria Meningitidis In Vivo*. *Infect. Immun.* 70, 5193–5201. doi: 10.1128/IAI.70.9.5193-5201.2002

Hathaway, L. J., Brugger, S. D., Morand, B., Bangert, M., Rotzetter, J. U., Hauser, C., et al. (2012). Capsule Type of *Streptococcus Pneumoniae* Determines Growth Phenotype. *PloS Pathog.* 8, e1002574–e1002574. doi: 10.1371/journal.ppat.1002574

Hobbs, J. K., Meier, E. P. W., Pluvinage, B., Mey, M. A., and Boraston, A. B. (2019). Molecular Analysis of an Enigmatic *Streptococcus Pneumoniae* Virulence Factor: The Raffinose-Family Oligosaccharide Utilization System. *J. Biol. Chem.* 294, 17197–17208. doi: 10.1074/jbc.RA119.010280

Iovino, F., Seinen, J., Henriques-Normark, B., and Van Dijl, J. M. (2016). How Does *Streptococcus Pneumoniae* Invade the Brain? *Trends Microbiol. (Regular ed.)* 24, 307–315. doi: 10.1016/j.tim.2015.12.012

Junges, R., Maienschein-Cline, M., Morrison, D. A., and Petersen, F. C. (2019). Complete Genome Sequence of *Streptococcus Pneumoniae* Serotype 19F Strain EF3030. *Microbiol. Resour. Announc.* 8,. doi: 10.1128/MRA.00198-19

Kelly, T., Dillard, J. P., and Yother, J. (1994). Effect of Genetic Switching of Capsular Type on Virulence of *Streptococcus Pneumoniae*. *Infect. Immun.* 62, 1813–1819. doi: 10.1128/iai.62.5.1813-1819.1994

Kim, J. O., and Weiser, J. N. (1998). Association of Intrastrain Phase Variation in Quantity of Capsular Polysaccharide and Teichoic Acid With the Virulence of *Streptococcus Pneumoniae*. *J. Infect. Dis.* 177, 368–377. doi: 10.1086/514205

Kloosterman, T. G., Bijlsma, J. J. E., Kok, J., and Kuipers, O. P. (2006). To Have Neighbour's Fare: Extending the Molecular Toolbox for *Streptococcus Pneumoniae*. *Microbiol. (Soc. Gen. Microbiol.)* 152, 351–359. doi: 10.1099/mic.0.28521-0

Lavelle, E. C., and Ward, R. W. (2021). Mucosal Vaccines — Fortifying the Frontiers. *Nat. Rev. Immunol.* doi: 10.1038/s41577-021-00583-2

Livak, K. J., and Schmittgen, T. D. (2001). Analysis of Relative Gene Expression Data Using Real-Time Quantitative PCR and the 2–ΔΔCT Method. *Methods (San Diego Calif.)* 25, 402–408. doi: 10.1006/meth.2001.1262

Lu, S., Wang, J., Chitsaz, F., Derbyshire, M. K., Geer, R. C., Gonzales, N. R., et al. (2020). CDD/SPARCLE: The Conserved Domain Database in 2020. *Nucleic Acids Res.* 48, D265–D268. doi: 10.1093/nar/gkz991

Marra, A., and Brigham, D. (2001). *Streptococcus Pneumoniae* Causes Experimental Meningitis Following Intranasal and Otitis Media Infections *via* a Nonhematogenous Route. *Infect. Immun.* 69, 7318–7325. doi: 10.1128/IAI.69.12.7318-7325.2001

Mcallister, L. J., Ogunniyi, A. D., Stroeher, U. H., Leach, A. J., and Paton, J. C. (2011). Contribution of Serotype and Genetic Background to Virulence of Serotype 3 and Serogroup 11 Pneumococcal Isolates. *Infect. Immun.* 79, 4839–4849. doi: 10.1128/IAI.05663-11

Mclean, K. T., Tikhomirova, A., Brazel, E. B., Legendre, S., Haasbroek, G., Minhas, V., et al. (2020). Site-Specific Mutations of GalR Affect Galactose Metabolism in *Streptococcus Pneumoniae*. *J. Bacteriol.* 203, e00180-20. doi: 10.1128/JB.00180-20

Minhas, V., Aprianto, R., Mcallister, L. J., Wang, H., David, S. C., Mclean, K. T., et al. (2020). *In Vivo* Dual RNA-Seq Reveals That Neutrophil Recruitment Underlies Differential Tissue Tropism of *Streptococcus Pneumoniae*. *Commun. Biol.* 3, 293–293. doi: 10.1038/s42003-020-1018-x

Minhas, V., Harvey, R. M., Mcallister, L. J., Seemann, T., Syme, A. E., Baines, S. L., et al. (2019). Capacity to Utilize Raffinose Dictates Pneumococcal Disease Phenotype. *mBio* 10, e02596–e02518. doi: 10.1128/mBio.02596-18

Mook-Kanamori, B. B., Geldhoff, M., van der Poll, T., and Van De Beek, D. (2011). Pathogenesis and Pathophysiology of Pneumococcal Meningitis. *Clin. Microbiol. Rev.* 24, 557–591. doi: 10.1128/CMR.00008-11

Mukerji, R., and Briles, D. E. (2020). New Strategy is Needed to Prevent Pneumococcal Meningitis. *Pediatr. Infect. Dis. J.* 39, 298–304. doi: 10.1097/INF.0000000000002581

Murphy, T. F. (2003). Respiratory Infections Caused by non-Typeable *Haemophilus Influenzae*. *Curr. Opin. Infect. Dis.* 16, 129–134. doi: 10.1097/00001432-200304000-00009

Obert, C., Sublett, J., Kaushal, D., Hinojosa, E., Barton, T., Tuomanen, E. I., et al. (2006). Identification of a Candidate *Streptococcus Pneumoniae* Core Genome and Regions of Diversity Correlated With Invasive Pneumococcal Disease. *Infect. Immun.* 74, 4766–4777. doi: 10.1128/IAI.00316-06

Oggioni, M. R., Trappetti, C., Kadioglu, A., Cassone, M., Iannelli, F., Ricci, S., et al. (2006). Switch From Planktonic to Sessile Life: A Major Event in Pneumococcal Pathogenesis. *Mol. Microbiol.* 61, 1196–1210. doi: 10.1111/j.1365-2958.2006.05310.x

Paixão, L., Oliveira, J., Veríssimo, A., Vinga, S., Lourenço, E. C., Ventura, M. R., et al. (2015). Host Glycan Sugar-Specific Pathways in *Streptococcus Pneumonia*: Galactose as a Key Sugar in Colonisation and Infection. *PloS One* 10, e0121042. doi: 10.1371/journal.pone.0121042

Prjibelski, A., Antipov, D., Meleshko, D., Lapidus, A., and Korobeynikov, A. (2020). Using SPAdes *De Novo* Assembler. *Curr. Protoc. Bioinf.* 70, e102. doi: 10.1002/cpbi.102

Rosenow, C., Maniar, M., and Trias, J. (1999). Regulation of the Alpha-Galactosidase Activity in *Streptococcus Pneumoniae*: Characterization of the Raffinose Utilization System. *Genome Res.* 9, 1189–1197. doi: 10.1101/gr.9.12.1189

Seemann, T. (2014). Prokka: Rapid Prokaryotic Genome Annotation. *Bioinformatics* 30, 2068–2069. doi: 10.1093/bioinformatics/btu153

Seemann, T. (2020a) *Shovill*. Available at: https://github.com/tseemann/shovill (Accessed 2021).

Seemann, T. (2020b) *Snippy*. Available at: https://github.com/tseemann/snippy (Accessed 2021).

Smyth, A. (2006). Update on Treatment of Pulmonary Exacerbations in Cystic Fibrosis. *Curr. Opin. Pulm Med.* 12, 440–444. doi: 10.1097/01.mcp.0000245711.43891.16

Starner, T. D., Zhang, N., Kim, G., Apicella, M. A., and Mccray, P. B.Jr. (2006). Haemophilus Influenzae Forms Biofilms on Airway Epithelia: Implications in Cystic Fibrosis. *Am. J. Respir. Crit. Care Med.* 174, 213–220. doi: 10.1164/rccm.200509-1459OC

Steinegger, M., and Söding, J. (2017). MMseqs2 Enables Sensitive Protein Sequence Searching for the Analysis of Massive Data Sets. *Nat. Biotechnol.* 35, 1026–1028. doi: 10.1038/nbt.3988

Tikhomirova, A., Trappetti, C., Paton, J. C., Watson-Haigh, N., Wabnitz, D., Jervis-Bardy, J., et al. (2021). A Single Nucleotide Polymorphism in an IgA1 Protease Gene Determines *Streptococcus Pneumoniae* Adaptation to the Middle Ear During Otitis Media. *Pathog. Dis.* 79, 1–8. doi: 10.1093/femspd/ftaa077

Trappetti, C., Ogunniyi, A. D., Oggioni, M. R., and Paton, J. C. (2011). Extracellular Matrix Formation Enhances the Ability of *Streptococcus Pneumoniae* to Cause Invasive Disease. *PloS One* 6, e19844–e19844. doi: 10.1371/journal.pone.0019844

Trappetti, C., van der Maten, E., Amin, Z., Potter, A. J., Chen, A. Y., Van Mourik, P. M., et al. (2013). Site of Isolation Determines Biofilm Formation and Virulence Phenotypes of *Streptococcus Pneumoniae* Serotype 3 Clinical Isolates. *Infect. Immun.* 81, 505–513. doi: 10.1128/IAI.01033-12

Trimble, A., Connor, V., Robinson, R. E., Mclenaghan, D., Hancock, C. A., Wang, D., et al. (2020). Pneumococcal Colonisation is an Asymptomatic Event in Healthy Adults Using an Experimental Human Colonisation Model. *PloS One* 15, 1–12. doi: 10.1371/journal.pone.0229558

Van Ginkel, F. W., Mcghee, J. R., Watt, J. M., Campos-Torres, A., Parish, L. A., and Briles, D. E. (2003). Pneumococcal Carriage Results in Ganglioside-Mediated Olfactory Tissue Infection. *Proc. Natl. Acad. Sci. U.S.A.* 100, 14363–14367. doi: 10.1073/pnas.2235844100

Weimer, K. E., Armbruster, C. E., Juneau, R. A., Hong, W., Pang, B., and Swords, W. E. (2010). Coinfection With *Haemophilus Influenzae* Promotes Pneumococcal Biofilm Formation During Experimental Otitis Media and Impedes the Progression of Pneumococcal Disease. *J. Infect. Dis.* 202, 1068–1075. doi: 10.1086/656046

Conflict of Interest: The authors declare that the research was conducted in the absence of any commercial or financial relationships that could be construed as a potential conflict of interest.

Publisher's Note: All claims expressed in this article are solely those of the authors and do not necessarily represent those of their affiliated organizations, or those of the publisher, the editors and the reviewers. Any product that may be evaluated in this article, or claim that may be made by its manufacturer, is not guaranteed or endorsed by the publisher.

2.4 Supplementary material

Supplementary Material

Supplementary Figure 1: Sequence alignment of the *aga* gene in 60B and 60CSF. Sanger sequencing was used to generate the *aga* sequence for both 60B and 60CSF. At position 638, C has changed to an A (bold font), resulting in a premature stop codon in both 60B and 60CSF. Underlined bases indicate the start codon and stop codons, including both the premature stop codon and stop codon for the full-length product.

```
60B_aga         ATGGGAGTTAGGATAGAGAATAATCTATTTTATGTTGAGAGTAAAAATCTAAGTTTGATT  60
60CSF_aga       ATGGGAGTTAGGATAGAGAATAATCTATTTTATGTTGAGAGTAAAAATCTAAGTTTGATT  60
                ************************************************************

60B_aga         ATTGAAAATCGAAATGGCTACTTACTTTTGAAACATTTAGGAAAGACTATTAAGAACTAT  120
60CSF_aga       ATTGAAAATCGAAATGGCTACTTACTTTTGAAACATTTAGGAAAGACTATTAAGAACTAT  120
                ************************************************************

60B_aga         AAAGGTTCCAATAGTGTTTATGAACGAGACCATGCCTTTTCAGGAAATCCAACGGCTACT  180
60CSF_aga       AAAGGTTCCAATAGTGTTTATGAACGAGACCATGCCTTTTCAGGAAATCCAACGGCTACT  180
                ************************************************************

60B_aga         AATCGAACCTTTAGTTTAGATACTCAGCGACAGATTTTTGGACAACATGGCTTAGGAGAT  240
60CSF_aga       AATCGAACCTTTAGTTTAGATACTCAGCGACAGATTTTTGGACAACATGGCTTAGGAGAT  240
                ************************************************************

60B_aga         TTTAGGAAACCAACCATACAGGTTCAGCATAGTGTAACTGAAGTAACAGACTTTCGATTT  300
60CSF_aga       TTTAGGAAACCAACCATACAGGTTCAGCATAGTGTAACTGAAGTAACAGACTTTCGATTT  300
                ************************************************************

60B_aga         GTAGAAGCAAAGATTTTAAAAGGTCAGAATGGTCCACAGGGCTTACCTTCTCCACATAGC  360
60CSF_aga       GTAGAAGCAAAGATTTTAAAAGGTCAGAATGGTCCACAGGGCTTACCTTCTCCACATAGC  360
                ************************************************************

60B_aga         ATGGACGATACAGAGACTCTTGTCTTAATGTTAGAAGATTCTAAGGCTCAACTTAGTCTG  420
60CSF_aga       ATGGACGATACAGAGACTCTTGTCTTAATGTTAGAAGATTCTAAGGCTCAACTTAGTCTG  420
                ************************************************************

60B_aga         ACTTTGTATTATACTACTTTTAATAATGATGCGACTATTGCTAGCTACAGTAAATTAGAT  480
60CSF_aga       ACTTTGTATTATACTACTTTTAATAATGATGCGACTATTGCTAGCTACAGTAAATTAGAT  480
                ************************************************************

60B_aga         AATAATAGTAATCAGGAAGTTGTCATCCATAAAGATTTTTCTTTTATGGCTGATTTTCCA  540
60CSF_aga       AATAATAGTAATCAGGAAGTTGTCATCCATAAAGATTTTTCTTTTATGGCTGATTTTCCA  540
                ************************************************************

60B_aga         GCTGCAGATTACGAAATAGTAACTCTGCAGGGTGCTTATGCTCGTGAAAAGACTGTTAGA  600
60CSF_aga       GCTGCAGATTACGAAATAGTAACTCTGCAGGGTGCTTATGCTCGTGAAAAGACTGTTAGA  600
                ************************************************************

60B_aga         CGTCAACAGGTAGAACAAGGAATCTTTTCGATTAGCTAAAACCGAGGTGCTTCTGGTCAT  660
60CSF_aga       CGTCAACAGGTAGAACAAGGAATCTTTTCGATTAGCTAAAACCGAGGTGCTTCTGGTCAT  660
                ****************************************************************

60B_aga         GCTCAAACACCAGCTCTTCTACTATGCGAACAAGGAGTCACAGAGGATGCTGGGAATGTG  720
60CSF_aga       GCTCAAACACCAGCTCTTCTACTATGCGAACAAGGAGTCACAGAGGATGCTGGGAATGTG  720
                ************************************************************

60B_aga         TTTGCTATTCAACTAATGTATAGTGGCAACTTTGAAGCTTTTGTTCAAAAAAATCAATTG  780
60CSF_aga       TTTGCTATTCAACTAATGTATAGTGGCAACTTTGAAGCTTTTGTTCAAAAAAATCAATTG  780
                ************************************************************
```

```
60B_aga         AATGAAGTTCGGGTGGCTATTGGCATTAATCCAGAAAACTTTTCTTGGAAGTTAGCTCCT  840
60CSF_aga       AATGAAGTTCGGGTGGCTATTGGCATTAATCCAGAAAACTTTTCTTGGAAGTTAGCTCCT  840
                ************************************************************

60B_aga         GAGGAATACTTTGAAACACCGGTAGCTTTAGTGACCCATTCAGATCAGGGATTAACTGGT  900
60CSF_aga       GAGGAATACTTTGAAACACCGGTAGCTTTAGTGACCCATTCAGATCAGGGATTAACTGGT  900
                ************************************************************


60B_aga         ATTAGTCATGAAAGTCAGAATTTTGTACTGAAGCACATTATGCTAAGTGAATTTTCTAAA  960
60CSF_aga       ATTAGTCATGAAAGTCAGAATTTTGTACTGAAGCACATTATGCTAAGTGAATTTTCTAAA  960
                ************************************************************

60B_aga         AAAGAACGTCCAATTCTAATCAATAACTGGGAAGCTACTTACTTTGACTTTCAGAGAGAA  1020
60CSF_aga       AAAGAACGTCCAATTCTAATCAATAACTGGGAAGCTACTTACTTTGACTTTCAGAGAGAA  1020
                ************************************************************

60B_aga         AAACTGTTAGAGTTAGCAGATGAAGCTAAGAAAGTTGGCATTGAACTTTTTGTATTAGAT  1080
60CSF_aga       AAACTGTTAGAGTTAGCAGATGAAGCTAAGAAAGTTGGCATTGAACTTTTTGTATTAGAT  1080
                ************************************************************

60B_aga         GATGGTTGGTTTGGCAATCGTTTTGATGATAATCGTGCTTTAGGTGATTGGGTTGTTAAT  1140
60CSF_aga       GATGGTTGGTTTGGCAATCGTTTTGATGATAATCGTGCTTTAGGTGATTGGGTTGTTAAT  1140
                ************************************************************

60B_aga         GAGGAAAAACTGGGTGGAAGTCTAGAAAGTCTGATTTCAGCTATCCATGAAAGAGGTTTG  1200
60CSF_aga       GAGGAAAAACTGGGTGGAAGTCTAGAAAGTCTGATTTCAGCTATCCATGAAAGAGGTTTG  1200
                ************************************************************

60B_aga         CAGTTTGGACTTTGGTTAGAACCCGAAATGATTTCTGTAGATAGTGATTTGTATCGTCAA  1260
60CSF_aga       CAGTTTGGACTTTGGTTAGAACCCGAAATGATTTCTGTAGATAGTGATTTGTATCGTCAA  1260
                ************************************************************

60B_aga         CATCCTGACTGGGCTATTCAGGTTCCTGGCTATGAGCATACTTATTCTCGGAATCAATTA  1320
60CSF_aga       CATCCTGACTGGGCTATTCAGGTTCCTGGCTATGAGCATACTTATTCTCGGAATCAATTA  1320
                ************************************************************

60B_aga         GTACTTAATCTTGCCAATCCTCAGGTAGTAGAATACTTGAAAAGTGTCTTAGATCAACTC  1380
60CSF_aga       GTACTTAATCTTGCCAATCCTCAGGTAGTAGAATACTTGAAAAGTGTCTTAGATCAACTC  1380
                ************************************************************

60B_aga         CTATCTTATCATGATATTGATTACATTAAATGGGATATGAACCGCAATATCACTAAGCTA  1440
60CSF_aga       CTATCTTATCATGATATTGATTACATTAAATGGGATATGAACCGCAATATCACTAAGCTA  1440
                ************************************************************

60B_aga         GGGAATGGATTAACTTATCTAGAGACACAGATGCAATCTCATCAGTACATGCTGGGGCTT  1500
60CSF_aga       GGGAATGGATTAACTTATCTAGAGACACAGATGCAATCTCATCAGTACATGCTGGGGCTT  1500
                ************************************************************

60B_aga         TACGAACTCGTTTCTTATCTGACAGAGAAGCACAGCCATATTCTCTTTGAGTCCTGCTCT  1560
60CSF_aga       TACGAACTCGTTTCTTATCTGACAGAGAAGCACAGCCATATTCTCTTTGAGTCCTGCTCT  1560
                ************************************************************

60B_aga         GGTGGTGGTGGACGAAATGATCTTGGTATGATGCGCTATTTCCCACAAGTCTGGGCTAGT  1620
60CSF_aga       GGTGGTGGTGGACGAAATGATCTTGGTATGATGCGCTATTTCCCACAAGTCTGGGCTAGT  1620
                ************************************************************

60B_aga         GATAATACAGATGCTATTGCACGTTTACCAATTCAATACGGTTCATCCTATCTCTATCCA  1680
60CSF_aga       GATAATACAGATGCTATTGCACGTTTACCAATTCAATACGGTTCATCCTATCTCTATCCA  1680
                ************************************************************

60B_aga         ACCATTTCTATGGGGGCTCATGTGTCAGCAGTACCGAATCATCAGATGGGGCGAACGACA  1740
60CSF_aga       ACCATTTCTATGGGGGCTCATGTGTCAGCAGTACCGAATCATCAGATGGGGCGAACGACA  1740
                ************************************************************
```

```
60B_aga         CCATTAGAAACACGTGGCCTTGTAGCAATGATGGGAAATTTGGGCTATGAACTTGATTTG  1800
60CSF_aga       CCATTAGAAACACGTGGCCTTGTAGCAATGATGGGAAATTTGGGCTATGAACTTGATTTG  1800
                ************************************************************

60B_aga         ACAAATTTATCAGATGAAGAGAAAGCTACGATTGCTAATCAGGTGAACTTGTATAAAGAA  1860
60CSF_aga       ACAAATTTATCAGATGAAGAGAAAGCTACGATTGCTAATCAGGTGAACTTGTATAAAGAA  1860
                ************************************************************

60B_aga         TTACGACCAGTAGTTCAGTTAGGACAACAGTATAGACTAATTAATCCTGATACTGCATCC  1920
60CSF_aga       TTACGACCAGTAGTTCAGTTAGGACAACAGTATAGACTAATTAATCCTGATACTGCATCC  1920
                ************************************************************

60B_aga         AATGAAGCTGCTGTACAATTTAATTACAAAAATCAAACGATTGTAACCTACGTTCGCGTT  1980
60CSF_aga       AATGAAGCTGCTGTACAATTTAATTACAAAAATCAAACGATTGTAACCTACGTTCGCGTT  1980
                ************************************************************

60B_aga         TTATCTGTTGTAGAGACCATGGAAACAACTTTAAAGTTAAAAGATTTGGATGAAGAGGGA  2040
60CSF_aga       TTATCTGTTGTAGAGACCATGGAAACAACTTTAAAGTTAAAAGATTTGGATGAAGAGGGA  2040
                ************************************************************

60B_aga         CTATATGAATTACAGGAAAATGGCGAAGTTTACTCAGGTGCAGAACTCATGTATGCGGGT  2100
60CSF_aga       CTATATGAATTACAGGAAAATGGCGAAGTTTACTCAGGTGCAGAACTCATGTATGCGGGT  2100
                ************************************************************

60B_aga         TTAACTGTTATTTTATCCCAAGGAGATTTTTTGAGTAAACAGTATATTTTTAGAAGACTA  2160
60CSF_aga       TTAACTGTTATTTTATCCCAAGGAGATTTTTTGAGTAAACAGTATATTTTTAGAAGACTA  2160
                ************************************************************

60B_aga         TAA         2163
60CSF_aga       TAA         2163
                ***
```

Supplementary Figure 2: Sequence alignment of the 60B and 60CSF *aga* gene fragments with *aga* in *S. pneumoniae* strain 4559. Reciprocal best hit -based analysis on results from Illumina sequencing revealed *aga* gene fragments in 60B and 60CSF. These fragments did not correspond to the *aga* gene previously sequenced at the raf locus but instead shared 100% identity with a portion of a gene encoding an alternative alpha-galactosidase (2217bp) that was present in *S. pneumoniae* strain 4559 (labelled 4559_2217bp). The blood isolate, 60B, contained fragments that were 594bp and 967bp in length, whilst the CSF isolate, 60CSF, contained a single fragment of 1680bp.

```
60B_594bp          ------------------------------------------------------------      0
60B_967bp          ------------------------------------------------------------      0
60CSF_1680bp       ------------------------------------------------------------      0
4559_2217bp        ATGACGATTTATATTAATAAGGACGAGACCGTTTTTCATTTGGCAATGAAAGATAGTAGT      60

60B_594bp          ------------------------------------------------------------      0
60B_967bp          ------------------------------------------------------------      0
60CSF_1680bp       ------------------------------------------------------------      0
4559_2217bp        TATATTTTTAGAATTTTAGAAAATGGGGAACTTCAACATCTACATTTTGGGAAAAGGATT      120

60B_594bp          ------------------------------------------------------------      0
60B_967bp          ------------------------------------------------------------      0
60CSF_1680bp       ------------------------------------------------------------      0
4559_2217bp        CATGTCAAGGAAAATTATAACCAATTGATGGCCTATGAAAAAAGAGGATTTGAAGTATCT      180

60B_594bp          ------------------------------------------------------------      0
60B_967bp          ------------------------------------------------------------      0
60CSF_1680bp       ------------------------------------------------------------      0
4559_2217bp        TTTTCTGAAGAATTTGAGGATATTCAACAGTCTATGATACAAAATGAATATTCTTCATAT      240

60B_594bp          ------------------------------------------------------------      0
60B_967bp          ------------------------------------------------------------      0
60CSF_1680bp       ------------------------------------------------------------      0
4559_2217bp        GGGAAAGGAGATTTTCGGCATCCAGCCTTTCAAGTTCAAGGAATGAATGGTAGTAGGATA      300

60B_594bp          ------------------------------------------------------------      0
60B_967bp          ------------------------------------------------------------      0
60CSF_1680bp       ------------------------------------------------------------      0
4559_2217bp        ACGACACTAAAATATCAAGGTTTTGAACTTGAAAAAGGGAAAAATCGTCTTAACTCTCTA      360

60B_594bp          ------------------------------------------------------------      0
60B_967bp          ------------------------------------------------------------      0
60CSF_1680bp       ------------------------------------------------------------      0
4559_2217bp        CCTTCAACATTTGATGATATTGGTCAGTGTGCGGAAACATTAACGATTATTTTAACAGAT      420

60B_594bp          ------------------------------------------------------------      0
60B_967bp          ------------------------------------------------------------      0
60CSF_1680bp       ------------------------------------------------------------      0
4559_2217bp        TCCATATTAGATTTAACTGTTAGACTAAATTACACAATTTTTCCGGAATACAATGTCTTA      480

60B_594bp          ------------------------------------------------------------      0
60B_967bp          ------------------------------------------------------------ATG      3
60CSF_1680bp       ------------------------------------------------------------ATG      3
```

```
4559_2217bp       GTTAGAAATACGGAATTTTTAAATAATAGCAATAATAAGTTGACTCTTTTGAAAGCAATG       540


60B_594bp         ------------------------------------------------------------       0
60B_967bp         AGCTTACAGCTAGATCTACCTGATAGTCAATATGACTTTATTCAATTTTCTGGAGCATGG       63
60CSF_1680bp      AGCTTACAGCTAGATCTACCTGATAGTCAATATGACTTTATTCAATTTTCTGGAGCATGG       63
4559_2217bp       AGCTTACAGCTAGATCTACCTGATAGTCAATATGACTTTATTCAATTTTCTGGAGCATGG       600


60B_594bp         ------------------------------------------------------------       0
60B_967bp         CTGAGGGAACGTCAGTTATATAGAACTTCGCTTAGACCAGGTATTCAAGCAATAGATAGC       123
60CSF_1680bp      CTGAGGGAACGTCAGTTATATAGAACTTCGCTTAGACCAGGTATTCAAGCAATAGATAGC       123
4559_2217bp       CTGAGGGAACGTCAGTTATATAGAACTTCGCTTAGACCAGGTATTCAAGCAATAGATAGC       660


60B_594bp         ------------------------------------------------------------       0
60B_967bp         TTGAGATACTCATCAAGTCCTCAGCAAAATCCTTTCTTTATGCTATCAAGGAGGGAAACT       183
60CSF_1680bp      TTGAGATACTCATCAAGTCCTCAGCAAAATCCTTTCTTTATGCTATCAAGGAGGGAAACT       183
4559_2217bp       TTGAGATACTCATCAAGTCCTCAGCAAAATCCTTTCTTTATGCTATCAAGGAGGGAAACT       720


60B_594bp         ------------------------------------------------------------       0
60B_967bp         ACAGAGCATAGTGGTGAGGTTTATGGTTTTAACTTTATCTATTCTGGAAATTTTCAAAAT       243
60CSF_1680bp      ACAGAGCATAGTGGTGAGGTTTATGGTTTTAACTTTATCTATTCTGGAAATTTTCAAAAT       243
4559_2217bp       ACAGAGCATAGTGGTGAGGTTTATGGTTTTAACTTTATCTATTCTGGAAATTTTCAAAAT       780


60B_594bp         ------------------------------------------------------------       0
60B_967bp         ATGATTGAAGTTGACCATTTTGACACCGCTAGAGTAACGGTAGGAATAAATCCAGTAGAA       303
60CSF_1680bp      ATGATTGAAGTTGACCATTTTGACACCGCTAGAGTAACGGTAGGAATAAATCCAGTAGAA       303
4559_2217bp       ATGATTGAAGTTGACCATTTTGACACCGCTAGAGTAACGGTAGGAATAAATCCAGTAGAA       840


60B_594bp         ------------------------------------------------------------       0
60B_967bp         TTTCGTTTTTTATTAAATCCTGCCGAAAGTTTTGTGACACCAGAAGCAATTGTGATCTAT       363
60CSF_1680bp      TTTCGTTTTTTATTAAATCCTGCCGAAAGTTTTGTGACACCAGAAGCAATTGTGATCTAT       363
4559_2217bp       TTTCGTTTTTTATTAAATCCTGCCGAAAGTTTTGTGACACCAGAAGCAATTGTGATCTAT       900


60B_594bp         ------------------------------------------------------------       0
60B_967bp         TCTGATCAAGGGATGAATCAGATGAGCCAACAACTATCAGATTTTTATCGACATCATTTA       423
60CSF_1680bp      TCTGATCAAGGGATGAATCAGATGAGCCAACAACTATCAGATTTTTATCGACATCATTTA       423
4559_2217bp       TCTGATCAAGGGATGAATCAGATGAGCCAACAACTATCAGATTTTTATCGACATCATTTA       960


60B_594bp         ------------------------------------------------------------       0
60B_967bp         GTTAATCCTAATTTTTCTCAAGCTAGTCGTCCTATAATACTCAATAGTTGGGAAACATTT       483
60CSF_1680bp      GTTAATCCTAATTTTTCTCAAGCTAGTCGTCCTATAATACTCAATAGTTGGGAAACATTT       483
4559_2217bp       GTTAATCCTAATTTTTCTCAAGCTAGTCGTCCTATAATACTCAATAGTTGGGAAACATTT       1020


60B_594bp         ------------------------------------------------------------       0
60B_967bp         TATTTTGACTTGAGTACAGAAAAAATTTTAGATTTAGCAAAGGCTGCTAAAGATTTAGGG       543
60CSF_1680bp      TATTTTGACTTGAGTACAGAAAAAATTTTAGATTTAGCAAAGGCTGCTAAAGATTTAGGG       543
4559_2217bp       TATTTTGACTTGAGTACAGAAAAAATTTTAGATTTAGCAAAGGCTGCTAAAGATTTAGGG       1080


60B_594bp         ------------------------------------------------------------       0
60B_967bp         ATAGAATTATTTGTACTGGATGATGGTTGGTTTGGTCATAGGAAAGATGACAAAAGTTCT       603
60CSF_1680bp      ATAGAATTATTTGTACTGGATGATGGTTGGTTTGGTCATAGGAAAGATGACAAAAGTTCT       603
4559_2217bp       ATAGAATTATTTGTACTGGATGATGGTTGGTTTGGTCATAGGAAAGATGACAAAAGTTCT       1140


60B_594bp         ------------------------------------------------------------       0
60B_967bp         CTGGGTGATTGGGTAACAGATAGAAGTCGCCTTCCTGAAGGTATTGGATTTCTTGCAGAT       663
```

```
60CSF_1680bp      CTGGGTGATTGGGTAACAGATAGAAGTCGCCTTCCTGAAGGTATTGGATTTCTTGCAGAT      663
4559_2217bp       CTGGGTGATTGGGTAACAGATAGAAGTCGCCTTCCTGAAGGTATTGGATTTCTTGCAGAT      1200

60B_594bp         ------------------------------------------------------------      0
60B_967bp         GAAATTCACAAAATAGGTTTACAATTTGGTTTGTGGTTTGAGCCTGAAATGATTTCTATT      723
60CSF_1680bp      GAAATTCACAAAATAGGTTTACAATTTGGTTTGTGGTTTGAGCCTGAAATGATTTCTATT      723
4559_2217bp       GAAATTCACAAAATAGGTTTACAATTTGGTTTGTGGTTTGAGCCTGAAATGATTTCTATT      1260

60B_594bp         ------------------------------------------------------------      0
60B_967bp         GATAGTGATTTGTACAAGAATCATGCCGATTGGACTATCCATTTGTTAGACAGAGAGAAG      783
60CSF_1680bp      GATAGTGATTTGTACAAGAATCATGCCGATTGGACTATCCATTTGTTAGACAGAGAGAAG      783
4559_2217bp       GATAGTGATTTGTACAAGAATCATGCCGATTGGACTATCCATTTGTTAGACAGAGAGAAG      1320

60B_594bp         ------------------------------------------------------------      0
60B_967bp         TCAGTAGGAAGAAATCAATATGTGTTGGATTTGACGAGACAGGAAGTTGTTGATTATCTT      843
60CSF_1680bp      TCAGTAGGAAGAAATCAATATGTGTTGGATTTGACGAGACAGGAAGTTGTTGATTATCTT      843
4559_2217bp       TCAGTAGGAAGAAATCAATATGTGTTGGATTTGACGAGACAGGAAGTTGTTGATTATCTT      1380

60B_594bp         ------------------------------------------------------------      0
60B_967bp         TTTGATTCTATTTCTAAAATCATAATCAAAACAAATCTGGATTATATCAAATGGGATATG      903
60CSF_1680bp      TTTGATTCTATTTCTAAAATCATAATCAAAACAAATCTGGATTATATCAAATGGGATATG      903
4559_2217bp       TTTGATTCTATTTCTAAAATCATAATCAAAACAAATCTGGATTATATCAAATGGGATATG      1440

60B_594bp         ----------------------------------------------------ATGGAATTT      9
60B_967bp         AATCGTCATATAACAGATATTTATAGTATTGAACTTGATTCTGAACAGCAGATGGAATTT      963
60CSF_1680bp      AATCGTCATATAACAGATATTTATAGTATTGAACTTGATTCTGAACAGCAGATGGAATTT      963
4559_2217bp       AATCGTCATATAACAGATATTTATAGTATTGAACTTGATTCTGAACAGCAGATGGAATTT      1500
                                                                  *********

60B_594bp         GGTCATCGATATATCTTAGGTCTTTATCAGTTATTAGATCGTTTAATAACTAAGTTCCCT      69
60B_967bp         GGTC------------------------------------------------------      967
60CSF_1680bp      GGTCATCGATATATCTTAGGTCTTTATCAGTTATTAGATCGTTTAATAACTAAGTTCCCT      1023
4559_2217bp       GGTCATCGATATATCTTAGGTCTTTATCAGTTATTAGATCGTTTAATAACTAAGTTCCCT      1560
                  ****

60B_594bp         TCAGTTCTATTTGAATCTTGTTCTTCAGGTGGTGGACGTTTTGATTTAGGACTTATGTAT      129
60B_967bp         ------------------------------------------------------------      967
60CSF_1680bp      TCAGTTCTATTTGAATCTTGTTCTTCAGGTGGTGGACGTTTTGATTTAGGACTTATGTAT      1083
4559_2217bp       TCAGTTCTATTTGAATCTTGTTCTTCAGGTGGTGGACGTTTTGATTTAGGACTTATGTAT      1620

60B_594bp         TATGCACCGCAAGCGTGGACGAGTGATGATACGGACCCGATAGAAAGATTGAAAATTCAG      189
60B_967bp         ------------------------------------------------------------      967
60CSF_1680bp      TATGCACCGCAAGCGTGGACGAGTGATGATACGGACCCGATAGAAAGATTGAAAATTCAG      1143
4559_2217bp       TATGCACCGCAAGCGTGGACGAGTGATGATACGGACCCGATAGAAAGATTGAAAATTCAG      1680

60B_594bp         CATGGAACTTCTTATGGATATTCTCCATCAATGATGACAGCCCATGTTTCTATTTCTCCA      249
60B_967bp         ------------------------------------------------------------      967
60CSF_1680bp      CATGGAACTTCTTATGGATATTCTCCATCAATGATGACAGCCCATGTTTCTATTTCTCCA      1203
4559_2217bp       CATGGAACTTCTTATGGATATTCTCCATCAATGATGACAGCCCATGTTTCTATTTCTCCA      1740

60B_594bp         AATGAACAAAGTGGAAGACAAACGAGTTTGGACACTAGGACAAATGTAGCTTATTTTAGT      309
60B_967bp         ------------------------------------------------------------      967
60CSF_1680bp      AATGAACAAAGTGGAAGACAAACGAGTTTGGACACTAGGACAAATGTAGCTTATTTTAGT      1263
4559_2217bp       AATGAACAAAGTGGAAGACAAACGAGTTTGGACACTAGGACAAATGTAGCTTATTTTAGT      1800
```

```
60B_594bp          TCTTTCGGTTATGAATTAGATGTTACGAGATTGTCGGTAGAAGAAAAAGAACAAGTGAGA       369
60B_967bp          ------------------------------------------------------------       967
60CSF_1680bp       TCTTTCGGTTATGAATTAGATGTTACGAGATTGTCGGTAGAAGAAAAAGAACAAGTGAGA       1323
4559_2217bp        TCTTTCGGTTATGAATTAGATGTTACGAGATTGTCGGTAGAAGAAAAAGAACAAGTGAGA       1860

60B_594bp          GAACAAATTCAGTTTTATAAAAAATATCGTTCATTGCTTCAATATGGGGATTTCTATAGG       429
60B_967bp          ------------------------------------------------------------       967
60CSF_1680bp       GAACAAATTCAGTTTTATAAAAAATATCGTTCATTGCTTCAATATGGGGATTTCTATAGG       1383
4559_2217bp        GAACAAATTCAGTTTTATAAAAAATATCGTTCATTGCTTCAATATGGGGATTTCTATAGG       1920

60B_594bp          ATAAACAGTCCTTTTAGTTGTGATTCTGCTAGTTGGCAAGTTGTTTCAAAAGATAAATGC       489
60B_967bp          ------------------------------------------------------------       967
60CSF_1680bp       ATAAACAGTCCTTTTAGTTGTGATTCTGCTAGTTGGCAAGTTGTTTCAAAAGATAAATGC       1443
4559_2217bp        ATAAACAGTCCTTTTAGTTGTGATTCTGCTAGTTGGCAAGTTGTTTCAAAAGATAAATGC       1980

60B_594bp          CAATCGATTTTATTGTATGCTCAATTGAATAGTAAGTTGAATCCAGGTTATACAAGAGTT       549
60B_967bp          ------------------------------------------------------------       967
60CSF_1680bp       CAATCGATTTTATTGTATGCTCAATTGAATAGTAAGTTGAATCCAGGTTATACAAGAGTT       1503
4559_2217bp        CAATCGATTTTATTGTATGCTCAATTGAATAGTAAGTTGAATCCAGGTTATACAAGAGTT       2040

60B_594bp          TATTTTAGTGGTTTAGATAAAGATCTGTCTCTTATACACATCTGA---------------       594
60B_967bp          ------------------------------------------------------------       967
60CSF_1680bp       TATTTTAGTGGTTTAGATAAAGATAAATGCTATTCCGTCTCTGGATTTGATGAGTTCTTT       1563
4559_2217bp        TATTTTAGTGGTTTAGATAAAGATAAATGCTATTCCGTCTCTGGATTTGATGAGTTCTTT       2100

60B_594bp          ------------------------------------------------------------       594
60B_967bp          ------------------------------------------------------------       967
60CSF_1680bp       TATGGAGATGAATTAATGAATGCTGGAATAAAAGTAAGTTTAAGTAATTTAGCACTTTGT       1623
4559_2217bp        TATGGAGATGAATTAATGAATGCTGGAATAAAAGTAAGTTTAAGTAATTTAGCACTTTGT       2160

60B_594bp          ------------------------------------------------------------  594
60B_967bp          ------------------------------------------------------------  967
60CSF_1680bp       GTTCCAGAATATCTTACAAAATTATTTGTTATTGAAGAAGTTGTATGTAAATATTGA  1680
4559_2217bp        GTTCCAGAATATCTTACAAAATTATTTGTTATTGAAGAAGTTGTATGTAAATATTGA  2217
```

Chapter 3: Uncovering the link between the SpnIII restriction modification system and LuxS in *Streptococcus pneumoniae* meningitis isolates

3.1 Statement of authorship

Statement of Authorship

Title of Paper	Uncovering the link between the *SpnIII* restriction modification system and LuxS in *Streptococcus pneumoniae* meningitis isolates
Publication Status	✓ ☐ Published
Publication Details	Agnew, H.N., et al. (2023). Uncovering the link between the SpnIII restriction modification system and LuxS in *Streptococcus pneumoniae* meningitis isolates. *Frontiers in Cellular and Infection Microbiology* 13. doi: 10.3389/fcimb.2023.1177857

Principal Author

Name of Principal Author (Candidate)	Hannah N. Agnew		
Contribution to the Paper	Designed and performed experiments, performed analysis on and interpreted data, and aided in writing the manuscript.		
Overall percentage (%)	80		
Certification:	This paper reports on original research I conducted during the period of my Higher Degree by Research candidature and is not subject to any obligations or contractual agreements with a third party that would constrain its inclusion in this thesis. I am the primary author of this paper.		
Signature		Date	31/10/2023

Co-Author Contributions

By signing the Statement of Authorship, each author certifies that:

i. the candidate's stated contribution to the publication is accurate (as detailed above);
ii. permission is granted for the candidate in include the publication in the thesis; and
iii. the sum of all co-author contributions is equal to 100% less the candidate's stated contribution.

Name of Co-Author	John M. Atack		
Contribution to the Paper	Designed and performed experiments, and performed analysis on and interpreted subsequent data		
Signature		Date	16th October 2023

Name of Co-Author	Ann R.D. Fernando		
Contribution to the Paper	Designed and performed experiments, performed analysis on and interpreted data, and aided in writing the manuscript.		
Signature		Date	16/10/2023

Name of Co-Author	Sophie N. Waters		
Contribution to the Paper	Designed and performed experiments, performed analysis on and interpreted data		
Signature		Date	21/10/2023

Name of Co-Author	Mark van der Linden		
Contribution to the Paper	Provided the clinical isolates investigated, performed initial characterisation of strains, and aided in writing the manuscript.		
Signature		Date	13.10.2023

Name of Co-Author	Erin Smith		
Contribution to the Paper	Synthesised and provided AI-2/DPD		
Signature		Date	18/10/2023

Name of Co-Author	Andrew D. Abell		
Contribution to the Paper	Synthesised and provided AI-2/DPD		
Signature		Date	18/10/2023

Name of Co-Author	Erin B. Brazel		
Contribution to the Paper	Contributed to interpretation of results and aided in writing of the manuscipt.		
Signature		Date	16/10/2023

Name of Co-Author	James C. Paton
Contribution to the Paper	Designed experiments and aided in writing of the manuscript

Signature		Date	16/10/2023

Name of Co-Author	Claudia Trappetti
Contribution to the Paper	Designed and performed experiments, performed analysis on and interpreted data, and aided in writing the manuscript

Signature		Date	30/10/2023

3.2 Purpose of the article

In Chapter 2 distinct *in vivo* disparities between strains 60B and 60CSF were uncovered, with 60B demonstrating an inability to survive within the ears of intranasally infected mice, as opposed to 60CSF. As genomic analysis failed to provide a definitive explanation for these distinctions, this study delves into the potential influence that variants of a methyltransferase might exert on the virulence phenotype of these clinical *S. pneumoniae* isolates. As described in the introduction (Section 1.9.1.1), the *spnIII* restriction-modification type I system can give rise to subpopulations of *S. pneumoniae* due to different methylation patterns, with the resulting subpopulations being characterised by unique virulence phenotypes. For example, the *spnIIIB* allele has been associated with the downregulation of *luxS*, a gene of the LuxS/Autoinducer-2 quorum sensing system that has been shown to have a role in biofilm formation. In turn biofilm formation can act as a reservoir from which pneumococci can disseminate to cause more invasive pneumococcal disease. Therefore, this article has characterised the variants of the methyltransferase within the *spnIII* restriction-modification type I system in these strains. Furthermore, greater insight into the poorly understood link between the *spnIII* system and the LuxS/Autoinducer-2 system was gained, uncovering the role of LuxS in enabling these strains to cause disease.

3.2.1 Thesis research aims addressed

Aim 3: Determine the molecular features of the clinical isolates that dictate changes in phenotype.

frontiers | Frontiers in Cellular and Infection Microbiology

TYPE Original Research
PUBLISHED 01 May 2023
DOI 10.3389/fcimb.2023.1177857

OPEN ACCESS

EDITED BY
Michael Otto,
National Institutes of Health (NIH),
United States

REVIEWED BY
M. Ammar Zafar,
Wake Forest University, United States
Justin A. Thornton,
Mississippi State University, United States

*CORRESPONDENCE
Claudia Trappetti
claudia.trappetti@adelaide.edu.au
James C. Paton
james.paton@adelaide.edu.au

RECEIVED 02 March 2023
ACCEPTED 17 April 2023
PUBLISHED 01 May 2023

CITATION
Agnew HN, Atack JM, Fernando ARD, Waters SN, van der Linden M, Smith E, Abell AD, Brazel EB, Paton JC and Trappetti C (2023) Uncovering the link between the *SpnIII* restriction modification system and LuxS in *Streptococcus pneumoniae* meningitis isolates. *Front. Cell. Infect. Microbiol.* 13:1177857. doi: 10.3389/fcimb.2023.1177857

Uncovering the link between the *SpnIII* restriction modification system and LuxS in *Streptococcus pneumoniae* meningitis isolates

Hannah N. Agnew[1], John M. Atack[2,3], Ann R.D. Fernando[1], Sophie N. Waters[1], Mark van der Linden[4], Erin Smith[5], Andrew D. Abell[5], Erin B. Brazel[1], James C. Paton[1*] and Claudia Trappetti[1*]

[1]Research Centre for Infectious Diseases, Department of Molecular and Biomedical Science, University of Adelaide, Adelaide, SA, Australia, [2]Institute for Glycomics, Griffith University, Gold Coast, QLD, Australia, [3]School of Environment and Science, Griffith University, Gold Coast, QLD, Australia, [4]German National Reference Center for Streptococci, University Hospital Rheinisch-Westfälische Technische Hochschule (RWTH) Aachen, Aachen, Germany, [5]School of Physical Sciences, Faculty of Sciences, Engineering and Technology, University of Adelaide, Adelaide, SA, Australia

Streptococcus pneumoniae is capable of randomly switching their genomic DNA methylation pattern between six distinct bacterial subpopulations (A-F) via recombination of a type 1 restriction-modification locus, *spnIII*. These pneumococcal subpopulations exhibit phenotypic changes which favor carriage or invasive disease. In particular, the *spnIIIB* allele has been associated with increased nasopharyngeal carriage and the downregulation of the *luxS* gene. The LuxS/AI-2 QS system represent a universal language for bacteria and has been linked to virulence and biofilm formation in *S. pneumoniae*. In this work, we have explored the link between *spnIII* alleles, the *luxS* gene and virulence in two clinical pneumococcal isolates from the blood and cerebrospinal fluid (CSF) of one pediatric meningitis patient. The blood and CSF strains showed different virulence profiles in mice. Analysis of the *spnIII* system of these strains recovered from the murine nasopharynx showed that the system switched to different alleles commensurate with the initial source of the isolate. Of note, the blood strain showed high expression of *spnIIIB* allele, previously linked with less LuxS protein production. Importantly, strains with deleted *luxS* displayed different phenotypic profiles compared to the wildtype, but similar to the strains recovered from the nasopharynx of infected mice. This study used clinically relevant *S. pneumoniae* strains to demonstrate that the regulatory network between *luxS* and the type 1 restriction-modification system play a key role in infections and may support different adaptation to specific host niches.

KEYWORDS

***Streptococcus pneumoniae* (pneumococcus), virulence, clinical isolates bacterial, Quorum sensing, biofilm**

1 Introduction

Streptococcus pneumoniae (the pneumococcus) is a Gram-positive bacterium that asymptomatically colonizes the nasopharynx in up to 95% of infants and 25% of adults (Trimble et al., 2020). However, it can migrate to other niches in the body and cause localized diseases, such as otitis media and sinusitis, or it can disseminate to sterile sites to cause invasive pneumococcal diseases (IPD) such as pneumonia, bacteremia and meningitis. The broad range of both localized and invasive diseases it causes, results in more than 190 million infections with 1.2 million deaths worldwide each year, making it one of the most pathogenic bacterial species (Lavelle and Ward, 2022).

The mechanism by which *S. pneumoniae* transit from colonizer to pathogen is not well understood. However, pneumococci are capable of randomly switching their genomic DNA methylation pattern between six distinct bacterial subpopulations (A-F) via recombination of a type 1 restriction-modification locus, *spnIII*, with any given culture comprising a mixture of genotypes. These pneumococcal subpopulations exhibit phenotypic changes which favor carriage or invasive disease. Of particular interest, the *spnIIIA* allele was found to be associated with higher quantities of opaque phase pneumococcal colonies and had a more invasive phenotype. In contrast, the *spnIIIB* allele has been associated with increased nasopharyngeal carriage and the downregulation of the *luxS* gene (Manso et al., 2014).

LuxS is an essential component of the "universal" Quorum sensing (QS) LuxS/Autoinducer-2 (AI-2) system present in both Gram-positive and Gram-negative bacteria (Miller and Bassler, 2001; Von Bodman et al., 2008). The metabolic enzyme LuxS (an S-ribosylhomocysteine lyase) synthesizes AI-2 as a by-product of the conversion of S-ribosyl-homocysteine to homocysteine, an essential reaction of the activated methyl cycle. There are numerous QS systems, each allowing bacteria to detect stimuli, through autoinducers, and respond by inducing changes in gene expression of target cells (De Kievit and Iglewski, 2000). Although, the response to the LuxS/AI-2 system has been well characterized in Gram-negative bacteria (Vendeville et al., 2005), it is not well understood in Gram-positive bacteria, and in particular *S. pneumoniae*. Importantly in pneumococci, the LuxS/AI-2 QS system has been linked to virulence and biofilm formation (Stroeher et al., 2003; Trappetti et al., 2011a).

Biofilms can be defined as highly complex and dynamic surface associated structures, which provide *S. pneumoniae* a means of evading the host immune response and antimicrobial treatment, making biofilms indispensable for the persistence of pneumococcal disease (Costerton et al., 1999; Kolenbrander, 2000). In the laboratory strain D39, addition of extracellular AI-2 induced biofilm formation, with a deletion of the *luxS* gene resulting in decreased biofilm formation (Trappetti et al., 2011b) and decreased virulence in a murine model (Stroeher et al., 2003). The effect of *luxS* expression on biofilm formation has also been assessed in clinical isolates (Trappetti et al., 2013; Tikhomirova et al., 2022). We have previously found that serotype 3 pneumococcal isolates from the blood of 12 distinct patients had higher levels of *luxS* expression compared with isolates from the ears of 13 distinct patients, indicating that the role of *luxS* in biofilm formation may differ depending on the site of isolation (Trappetti et al., 2013). Recently we have investigated the role of LuxS in the middle ear isolate 947 serotype 14 sequence type (ST) 15 (Tikhomirova et al., 2022). We found that while biofilm formation was similar between the wildtype 947 strain and the *luxS* deletion mutant, the *luxS* mutant appeared more virulent than the parent strain in an intranasal murine infection model. These findings suggest that LuxS/AI-2 QS system in the middle ear isolate may have an opposite effect to that of the invasive strain D39 (Stroeher et al., 2003; Tikhomirova et al., 2022).

In the current study, we have characterized *luxS* in two *S. pneumoniae* clinical isolates obtained at the same time from the blood and cerebral spinal fluid (serotype 15C, ST 8711) of a single pediatric meningitis patient. Previously we have shown that these clinical isolates display different virulence phenotypes in a murine infection model (Agnew et al., 2022). Here, we aimed to investigate the role of *luxS* in these two clinical isolates.

2 Materials and methods

2.1 Bacterial strains and growth conditions

The wildtype *S. pneumoniae* strains used in this study (Table 1) were provided to us by the German National Reference Center for Streptococci (Aachen) (Agnew et al., 2022). Pneumococci serotype 15C blood and CSF isolates (designated 60B and 60CSF, respectively) were isolated in 2015 from a child, aged 2, admitted to hospital with meningitis. The cells were routinely grown on Columbia agar supplemented with 5% (vol/vol) horse blood (BA), with or without gentamicin (5 μg/mL) or spectinomycin (200 μg/mL), at 37°C in 5% CO_2 overnight. Growth assays were carried out using pneumococci grown in a chemically defined media (CDM) which is composed of SILAC RPMI 1640 Flex Media supplemented with amino acids, vitamins, choline chloride and catalase (10 U/mL) as described previously (Agnew et al., 2022), and either 0.5% (w/v) glucose or 0.5% (w/v) galactose.

2.2 Construction of mutant strains

The *luxS* gene was deleted from *S. pneumoniae* 60B and 60CSF strains and replaced with a spectinomycin resistance cassette by transformation. A linear DNA fragment containing the resistance cassette was constructed by overlap extension PCR (Iannelli and Pozzi, 2004), using primers listed in Table 1.

2.3 Growth assays

The strains were grown in flat-bottom 96-well microtiter plates (Costar) with a final volume of 200 μL as previously described (Minhas et al., 2019). Bacterial strains were inoculated at a starting optical density at 600 nm (OD_{600}) of 0.05 in CDM supplemented with either 0.5% (w/v) glucose or 0.5% (w/v) galactose and AI-2 (refer to

TABLE 1 *S. pneumoniae* strains and oligonucleotide primers used in this study.

Strain or primer	Description or sequence (5′➔3′)	Source or reference
Strains		
60B	Clinical isolate from blood (serotype 15C, sequence type 8711) (SN69534)	Agnew et al., 2022
60CSF	Clinical isolate from cerebral spinal fluid (serotype 15C, sequence type 8711) (SN69531)	Agnew et al., 2022
60BΔluxS	*luxS* deletion-replacement mutant (spec^r)	This study
60CSFΔluxS	*luxS* deletion-replacement mutant (spec^r)	This study
Primers		
Oligo name	Sequence (5′ ➔ 3′)	Reference
luxS for	TGGACCAGCCCTAGCCTTTGAA	Trappetti et al., 2017
luxS Rev	CACACTTGACTAAGGAAGAC	Trappetti et al., 2017
luxS spec for	AAATAACAGATTGAAGAAGGTATAATCTCACACCACCGTACGTA	Trappetti et al., 2017
luxS spec Rev	TATGTATTCATATATATCCTCCTCGTTGCTCCTGAGACAGA	Trappetti et al., 2017
luxS-RT-F	CCCTATGTTCGCTTGATTGGGG	Trappetti et al., 2011b
luxS-RT-R	AGTCAATCATGCCGTCAATGCG	Trappetti et al., 2011b
gyr-RT-F	ACTGGTATCGCGGTTGGGAT	Mclean et al., 2020
gyr-RT-R	ACCTGATTTCCCCATGCAA	Mclean et al., 2020

Supplementary data for synthesis of AI-2) at concentrations of 4 μM, 10 μM, 100 μM and 200 μM, then incubated at 37°C with 5% CO_2. The OD_{600} was measured every 30 min for a total of 24 h in a SpectroSTAR Omega spectrophotometer (BMG Labtech). Assays were conducted in triplicate with at least two repeated independent experiments. Statistically significant differences in both final OD_{600} and mid-exponential phase OD_{600} between strains was determined using two-tailed Student's *t* test; $P < 0.05$ were deemed statistically significant.

2.4 RNA extraction and qRT-PCR

Strains were grown overnight on BA plates at 37°C with 5% CO_2. Cells were harvested, washed and resuspended in 1 mL of CDM to a final OD_{600} of 0.2. Bacterial suspensions were incubated at 37°C with 5% CO_2. RNA extractions were carried our using a Qiagen RNeasy Minikit as per the manufacturer's instructions. Differences in gene expression levels were determined using one-step relative real-time qRT-PCR in a Roche LC480 real-time cycler, as described previously (Minhas et al., 2019). Primers used for *luxS* and *gyrA* (internal control) are listed in Table 1 and were used at a final concentration of 200 nM per reaction. Amplification data were analyzed using the comparative critical threshold ($2^{-\Delta\Delta CT}$) method (Livak and Schmittgen, 2001). Assays were performed in triplicate and statistical analyses were performed using two-tailed Student's *t* test; *P* values < 0.05 were deemed as statistically significant.

2.5 Phenotypic microarrays

Carbon phenotype microarray (PM) analysis using the PM microplate PM1 (Biolog Inc.) was performed on the strains to test for catabolism of 95 different carbon sources as previously described (Minhas et al., 2019). Each well in the microplate contained a different carbon source. The cells were inoculated to a final OD_{590} of 0.06 in the buffer provided, in accordance with the manufacturer's instructions. This suspension was added in 100 μL aliquots to the wells, and the plate was incubated at 37°C, 5% CO_2. The OD_{590} was measured every 15 min for 24 h. Catabolic activity was measured through colorimetric analysis, in which a colorless tetrazolium dye was reduced by NADH produced during catabolism. The level of metabolism for each carbon source was arbitrarily determined by comparison with the zero carbon source blank.

2.6 Biofilm assays

Biofilm formation was measured in real-time with the real-time cell analyzer (RTCA) xCELLigence (Agilent Technologies Inc.) instrument as previously described (Agnew et al., 2022; Tikhomirova et al., 2022). This instrument detects variations in the impedance signal (expressed as the arbitrary cell index, CI) as bacterial cells attach and form biofilms on the gold-microelectrodes present at the bottom of the E-plates (Agilent Technologies Inc.). Bacterial strains were grown overnight on BA plates at 37°C with 5% CO_2. The cells were harvested and resuspended in 200 μL of CDM + 0.5% (w/v) glucose or 0.5% (w/v) galactose to a final OD_{600} of 0.2. To the wells of the E-plate, 150 μL CDM + 0.5% (w/v) glucose or 0.5% (w/v) galactose ± 10μM AI-2 was added, before being placed in the cradle of the RTCA-DP system, within a 37°C incubator with 5% CO_2 supplementation. An initial baseline impedance reading was taken before the E-plates were removed and 50 μL of bacterial suspension added to the wells for a 1 in 4 dilution, reducing the starting OD_{600} to 0.05. An additional 50 μL of

CDM + 0.5% (w/v) glucose or 0.5% (w/v) galactose ± 10 μM AI-2 was added to the control wells. The E-plates were locked into the cradles of the RTCA-DP platform within the incubator and the impedance signal (CI) was recorded every 15 min for 24 h to monitor biofilm formation. Assays were conducted in duplicate with at least two repeated independent experiments. Statistical analysis was carried out using a two-tailed Student's *t* test; *P* values < 0.05 were deemed statistically significant.

2.7 Adherence and invasion assays

Adherence and invasion assays were carried out using the Detroit 562 human pharyngeal cell line as previously described (Trappetti et al., 2011a; Amin et al., 2015). Detroit 562 human pharyngeal cells were grown in Dulbecco's modified Eagle's medium (DMEM) supplemented with 10% fetal calf serum (FCS), 100 U/mL penicillin and 100 μg/mL streptomycin at 37°C in 5% CO_2. Wells of 24-well tissue culture trays were seeded with Detroit cells in DMEM with 10% FCS as described previously (Trappetti et al., 2011a) and left to grow overnight. Cells were inoculated with 500 μL of each bacterial suspension grown overnight on BA plates and resuspended in CDM ± 10μM AI-2 at a final OD_{600} of 0.2. The same volume of each bacterial strain was added to empty wells as a control. Adherence assays were conducted after incubation of the bacteria with the Detroit cells for 2 h at 37°C. The wells were washed 3 times with PBS, the cells were detached from the plate by treatment with 100 μL 0.25% trypsin-0.02% EDTA and 400 μL of 0.1% Triton X-100 (Sigma), and samples were plated on BA plates to determine the number of adherent bacteria. Invasion assays were carried out essentially as described above. After the post-adherence washing step, cultures were incubated for 1 h in fresh media supplemented with 200 μg/mL gentamicin and 10 μg/mL penicillin to kill extracellular bacteria. Monolayers were again washed, lysed, serially diluted, and plated on BA, as described above. The assays were conducted in triplicate with at least two repeated independent experiments. Statistical analysis was carried out using a two-tailed Student's *t*-test; *P* values < 0.05 were considered statistically significant. Data collected are presented as mean adherent or invasive bacteria ± standard error mean (SEM) in CFU/mL. The controls were used to monitor bacterial growth during the 2 h incubation period, ensuring strains grew at similar rates.

2.8 Murine infection model

Animal experiments were approved by the University of Adelaide Animal Ethics Committee (approval number S-2022-029). Female outbred 4- to 6-week-old CD-1 (Swiss) mice were anaesthetized by intraperitoneal injection of ketamine (8 mg/mL) and xylazine (0.8 mg/mL), and were challenged intranasally with 50 μL of bacterial suspension containing 1 x 10^8 CFU in serum broth (SB) as previously described (Minhas et al., 2019). The challenge dose was retrospectively confirmed by serial dilution and plating on BA. At 24 h, groups of 8 mice were euthanized by CO_2 asphyxiation before the blood, lungs, nasal tissue, ears, and brain were collected. Tissue samples were homogenized in 1 mL PBS, serially diluted and plated on BA plates containing 5 μg/mL gentamicin to enumerate pneumococci as previously described (Trappetti et al., 2011a). Statistical analyses of log-transformed CFU data were performed using two-tailed Student's *t* test; *P* values < 0.05 were deemed statistically significant.

2.9 *spnIII* allele quantification

Female outbred 4- to 6-week-old CD-1 (Swiss) mice were anaesthetized and intranasally challenged as described above. The nasal tissue was harvested 24 h post infection, processed and plated as above. DNA extraction was performed on the *luxS* mutants, WT original challenge inoculum and colonies grown overnight on BA plates supplemented with 5 μg/mL gentamicin, using a Qiagen DNeasy Blood & Tissue kit as per the manufacturer's instructions. The variant *spnIII* alleles were quantified as previously described (Manso et al., 2014). Statistical analyses were performed using two-way analysis of variance and a Tukey post-comparison test; *P* values < 0.05 were deemed statistically significant.

2.10 Isolation of bacteria from nasopharynx of infected mice

Female outbred 4- to 6-week-old CD-1 (Swiss) mice were anaesthetized and intranasally challenged as described above. The nasal tissue was harvested 24 h post infection, processed and plated as above. Bacterial colonies from each mouse (n = 5 for 60CSF, n = 6 for 60B) were resuspended in serum broth and stored at -80°C. Biolog assays were performed as above on bacteria from a single mouse, representative for each strain.

3 Results

3.1 Blood and CSF strain have different proportions of *spnIII* alleles

Previously, we have shown that while the CSF clinical *S. pneumoniae* isolate (60CSF) is found in the ears of infected mice 24 h post intranasal infection, the blood isolate (60B) was unable to survive in this niche (Agnew et al., 2022). To determine whether the observed different virulence phenotypes of 60B and 60CSF in mice could be mediated by rearrangements in the *spnIII* Type I restriction-modification (RM) system, the *spnIII* allele distribution was assessed from pneumococcal DNA extracted from the nasopharynx of intranasally infected animals. Mice were intranasally challenged with 10^8 colony forming units (CFU) of each strain and the bacteria were taken from the nose 24 h post-infection. The DNA was isolated and the *spnIII* alleles were quantified for the inoculum and recovered bacteria for both strains. The 60B inoculum used to challenge the mice had predominantly *spnIIIB* (21% *spnIIIA*, 39% *spnIIIB*, 9% *spnIIIC*, 7% *spnIIID*, 22% *spnIIIE* and 2% *spnIIIF*), while the 60CSF

inoculum was skewed towards *spnIIIA* (33% *spnIIIA*, 27% *spnIIIB*, 7% *spnIIIC*, 15% *spnIIID*, 17% *spnIIIE* and 1% *spnIIIF*) (Figure 1). The bacteria recovered from the nasopharynx of both groups of mice, showed no change in the *spnIII* allele distribution. The *spnIIIB* allele remained the predominant allele in all samples from the nasopharynx of mice challenged with 60B (23% *spnIIIA*, 44% *spnIIIB*, 12% *spnIIIC*, 9% *spnIIID*, 10% *spnIIIE* and 2% *spnIIIF*), while mice challenged with 60CSF, showed a similar proportion of *spnIIIA* and *spnIIIB* (32% *spnIIIA*, 28% *spnIIIB*, 7% *spnIIIC*, 10% *spnIIID*, 16% *spnIIIE* and 7% *spnIIIF*). Interestingly, when comparing the bacteria recovered from the noses of infected mice, 60B had a significantly higher proportion of the *spnIIIB* allele compared to 60CSF (Figure 1).

3.2 Downregulation of the *luxS* gene in 60B strain

We have previously reported that cell-cell signaling via the autoinducer 2 (AI-2)/LuxS quorum-sensing system is linked to the *spnIIIB* variant in *S. pneumoniae*. In particular, the *luxS* gene was found to be downregulated in SpnD39IIIB locked strain compared to the other SpnD39III locked strains (Manso et al., 2014). As reported above, the 60B strain has higher proportion of *spnIIIB* allele, while 60CSF has comparable level of *spnIIIA* and *spnIIIB* allele (Figure 1). Thus, we analyzed *luxS* gene expression in the 60B and 60CSF strains. Importantly, we found downregulation of the *luxS* gene in the 60B strain in which the *spnIIIB* allele is the predominant allele (Figure 2).

3.3 *luxS* mutants displayed similar metabolic profile of strains recovered from the nasopharynx of infected mice

LuxS regulates key aspects of carbohydrate metabolism in *S. pneumoniae* and the capacity to utilize different carbon sources is crucial for nasopharyngeal colonization (Minhas et al., 2019; Mclean et al., 2020; Agnew et al., 2022). Thus, we employed a phenotypic microarray to compare the capacity of strains recovered from the nasopharynx of mice infected with either 60B or 60CSF to metabolize 95 different carbohydrates (see Materials and Methods). Interestingly, strains recovered from the nose of mice infected with either 60B or 60CSF showed a distinct metabolic profile to that of the inoculum strains. Importantly, the nasopharyngeal strains were now able to metabolize L-fucose, but unable to metabolize D-psicose (Supplementary Table 1).

We then created a *luxS* deletion mutant in both 60B and 60CSF. The metabolic profiles of these mutants were then assessed with the phenotypic microarray. Surprisingly, we found that these strains paralleled the metabolic profiles of the strains recovered from mice and not that of the original inoculating strains (Supplementary Table 1). These results indicate that the strains may undergo a change in the nose of mice that results in an increase of the *spnIIIB* allele to aid their colonization and resulting in reduced *luxS* expression, consequently leading to a similar metabolic profile to that of the *luxS* mutants. Thus, there appears to be an unknown link between LuxS and the *spnIIIB* allele, which merits further investigation.

3.4 The *luxS* mutants display a dramatic shift in proportion of *spnIII* alleles

Based on the results obtained in Section 3.3, we investigated the *spnIII* allele profiles of the *luxS* deletion mutants in 60B and 60CSF. As shown in Figure 3, it was found that 60BΔluxS possessed only *spnIIIC* and *spnIIID* (0% *spnIIIA*, 0% *spnIIIB*, 84.15% *spnIIIC*, 15.85% *spnIIID*, 0% *spnIIIE* and 0% *spnIIIF*), similar to

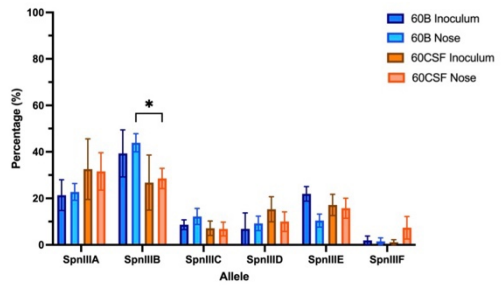

FIGURE 1
spnIII allele frequencies of 60B and 60CSF recovered post intranasal murine infection. Mice were intranasally challenged with 10^8 CFU *S. pneumoniae* serotype 15C ST8711 blood isolate (60B) or CSF isolate (60CSF). At 24 h, mice from each group were humanely euthanized and pneumococci in the nasal tissue were harvested. *spnIII* allele quantification was performed on DNA extracted from the original inoculum and colonies grown from nasopharynx samples. Allele percentages for original inoculum and bacteria recovered from noses are represented. Statistical analysis was performed using two-way analysis of variance and a Tukey post-comparison test; *$P < 0.05$.

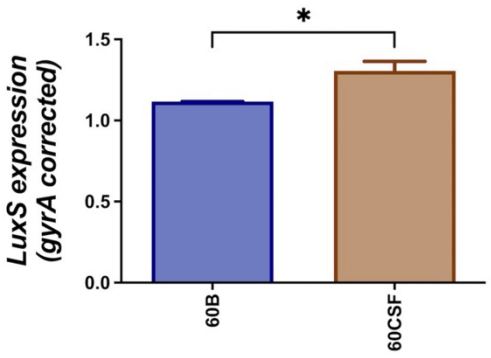

FIGURE 2
Expression of *luxS* by 60B and 60CSF isolates. Strains were resuspended in CDM at OD_{600} 0.2 and incubated at 37°C with 5% CO_2 for 30 min. RNA was extracted and *luxS* mRNA levels were analyzed by qRT-PCR using *gyrA* rRNA as an internal control (see Materials and Methods). Data are mean OD_{600} ± standard error mean (SEM) from three biological replicates. Significance of differences in gene expression between isolates was determined using two-tailed Student's t test; *$P < 0.05$.

60CSFΔluxS (0% *spnIIIA*, 4.36% *spnIIIB*, 79.39% *spnIIIC*, 16.25% *spnIIID*, 0% *spnIIIE* and 0% *spnIIIF*). Compared to the WT 60B and 60CSF inoculums, both *luxS* mutants had no *spnIIIA* present and *spnIIIB* was only present in 60CSFΔluxS at a very low proportion. Interestingly, we found both mutants were now predominantly expressing *spnIIIC*. Similar results were seen when comparing the *luxS* deletion mutants with the WT strains recovered from the nose of infected mice, in which the *luxS* mutants had more *spnIIIC*, little to no *spnIIIB* and no *spnIIIA* (Supplementary Figure 1). These results support the link between LuxS and the *spnIII* locus, with a complete absence of LuxS resulting in a shift towards high proportions of *spnIIIC* and a severe decrease in *spnIIIA* and *spnIIIB*.

3.5 *luxS* has a different impact in the 60B and 60CSF strains

S. pneumoniae is unable to grow with fucose as the sole carbon source, therefore, none of our established assays could be used for further analysis (Higgins et al., 2014). Similarly, D-Psicose is a low energy hexoketose monosaccharide, which is a C-3 epimer of D-fructose and is rarely found in nature, thus it is unlikely to play a role in pneumococcal virulence (Matsuo et al., 2002). Therefore, to further characterize our *luxS* mutant we used a different approach. LuxS QS boosts the capacity of *S. pneumoniae* to utilize galactose as a carbon source by upregulation of the Leloir pathway, so we then assessed the capacity of the *luxS* mutants to grow in galactose. Glucose was used as a control sugar, as it is the major sugar present in blood (Paixão et al., 2015). In CDM + glucose or galactose, wildtype (WT) strains showed comparable growth (Supplementary Figure 2). In Figure 4A, in CDM + glucose the 60B *luxS* deletion mutant (60BΔ*luxS*) had a slight reduction in the final cell density (*P* value = 0.0329), while in CDM + galactose the observed reduction is more prominent (*P* value = 0.0257). Interestingly, the 60CSF *luxS* deletion mutant (60CSFΔ*luxS*) showed comparable growth to that of the WT 60CSF in CDM + glucose (Figure 4B; *P* value = 0.3057), but an increased generation time compared to 60CSF in CDM + galactose was observed (*P* value = 0.0493). These results show that *luxS* deletion has a different impact in the two closely related strains.

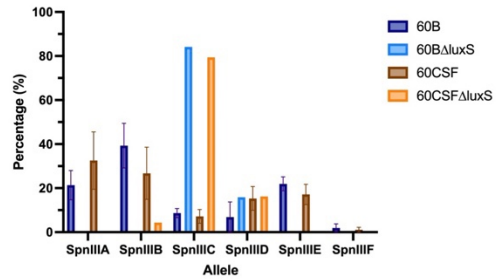

FIGURE 3
spnIII allele frequencies of 60B, 60CSF and *luxS* mutants. *spnIII* allele quantification was performed on DNA extracted from 60B, 60CSF, 60BΔluxS and 60CSFΔluxS colonies grown on BA plates overnight at 37°C with 5% CO_2. Allele percentages are displayed for WT original inoculum (Figure 1) and *luxS* mutants from frozen stock.

3.6 Higher doses of AI-2 negatively impacts growth of 60CSF

It has previously been demonstrated that the addition of 10 μM exogenous AI-2 was able to moderately restore the defective growth of a D39 *luxS* deletion strain (Trappetti et al., 2017). However, it was also shown in two serotype 14 blood and ear isolates that the addition of exogenous AI-2 reduces the growth in a dose-dependent manner (Tikhomirova et al., 2022). Therefore, the effects of different concentrations of exogenous AI-2 on the growth of the blood (60B) and CSF (60 CSF) strains was assessed. In CDM + glucose, for both 60B and 60CSF strains the addition of 4 and 10 μM AI-2 had little or no effect on growth, but at the higher concentrations of 100 μM and 200 μM AI-2, reduction in growth was observed (Figure 5A). Interestingly, in CDM + galactose the addition of AI-2 caused reduced growth of 60CSF for all concentrations (4, 10, 100 and 200 μM) tested, whilst in 60B the reduced growth was only different when higher concentration of AI-2 (100 and 200 μM) were added to the media (Figure 5B).

3.7 Addition of exogenous AI-2 enhances growth in 60B *luxS* deletion mutant

As the addition of AI-2 caused a growth defect in the WT 60B and 60CSF strains (Figure 5), we examined the capacity of exogenous AI-2 to complement the growth defect of *luxS* deletion strain. In Figure 6, addition of exogenous AI-2 to 60BΔ*luxS* and 60CSFΔ*luxS* had no effect in CDM + glucose, while it enhanced the growth of the 60BΔ*luxS* mutant in CDM + galactose. These results confirmed a dose-dependent effect previously observed in the D39 strain (Trappetti et al., 2017).

3.8 *luxS* plays a key role in the blood and CSF strains' ability to form a biofilm

Previously, *luxS* has been shown to play a key role in the ability of D39 to form a biofilm (Trappetti et al., 2011b). Therefore, we assessed the ability of WT 60B, 60CSF and *luxS* deletion mutants to form biofilm in real-time using CDM + glucose and CDM + galactose, with or without supplementation of 10 μM AI-2. In CDM + glucose and CDM + galactose both 60B and 60CSF showed the same capacity to form a biofilm (Supplementary Figure 3). The 60BΔ*luxS* mutants formed a biofilm at a slightly increased rate compared to WT 60B in CDM + glucose (Figure 7A). Interestingly, the 60CSFΔ*luxS* mutant had delayed biofilm formation compared to WT in CDM + glucose (Figure 7B). Addition of exogenous AI-2 greatly enhanced biofilm formation of WT strains but had no impact on *luxS* mutant strains (Figures 7A, B). In CDM +

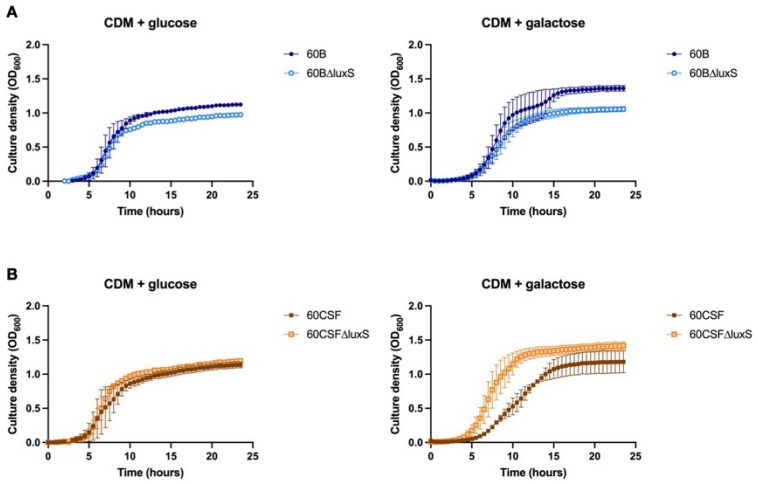

FIGURE 4
Growth of 60B, 60CSF and *luxS* mutants in CDM + glucose and CDM + galactose. 60B and its *luxS* mutant 60BΔluxS **(A),** and 60CSF and its *luxS* mutant 60CSFΔluxS **(B)** were grown in 200 µL CDM supplemented with 0.5% glucose (CDM + glucose) or 0.5% galactose (CDM + galactose). OD_{600} was measured every 30 min for 24 (h) Data are mean OD_{600} ± standard error mean (SEM) from two independent assays, each performed in triplicate.

galactose, both *luxS* mutants (60BΔ*luxS* & 60CSFΔ*luxS*) had delayed biofilm formation compared to their WT counterparts (Figures 7C, D), with 60CSFΔ*luxS* forming more biofilm than WT 60CSF. Similar to the earlier results in glucose, addition of AI-2 increased the biofilm formation of the WT 60B and 60CSF strains whilst appearing to have no impact in the *luxS* mutants.

luxS has been found to be crucial for adherence to epithelial cells (Tikhomirova et al., 2022). Therefore, we investigated the role of LuxS in adherence to, and invasion of, human epithelial cells, using the human nasopharyngeal Detroit 562 cell line in CDM with or without 10 µM AI-2 supplementation. No significant differences in the total number of adherent and invasive cells were observed between the WT strains and the *luxS* deletion mutants in CDM, with or without the addition of AI-2 (Supplementary Figure 4). These results are similar to those previously found for a D39 *luxS* deletion mutant in which there was no difference between WT and mutant in adherence to lung (A549) or larynx (HEp-2) derived cell lines (Stroeher et al., 2003).

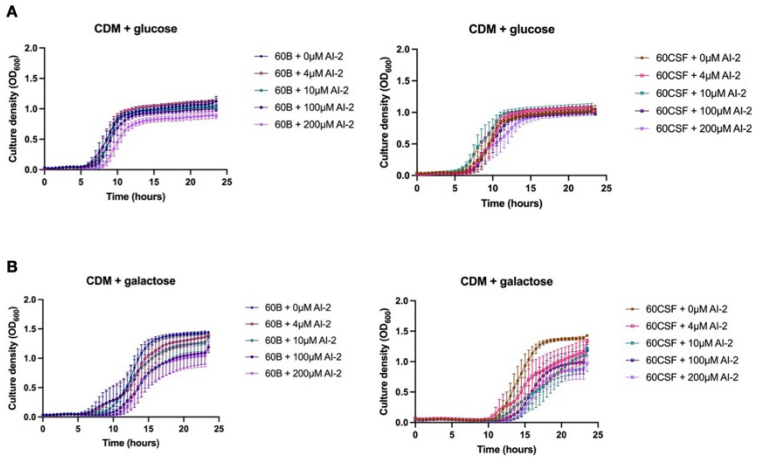

FIGURE 5
Growth of 60B and 60CSF with AI-2 supplementation at different concentrations. 60B and 60CSF were cultured in CDM + glucose **(A)** or CDM + galactose **(B)** supplemented with 0, 4, 10, 100 or 200 µM. OD_{600} was measured every 30 min for 24 (h) Data are mean OD_{600} ± standard error mean (SEM) from three independent assays, each performed in triplicate.

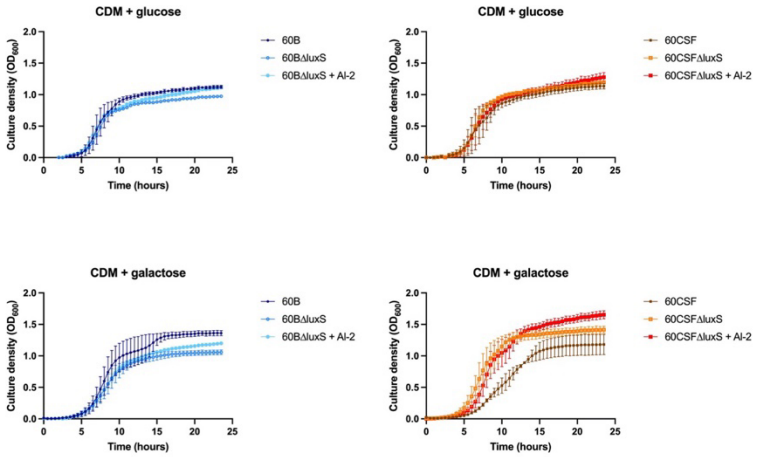

FIGURE 6
Impact of AI-2 on growth of *luxS* mutants. 60B, 60CSF, 60BΔluxS and 60CSFΔluxS were grown in 200 µL CDM supplemented with 0.5% glucose (CDM + glucose) or 0.5% galactose (CDM + galactose). OD_{600} was measured every 30 min for 24 h. Data are mean OD_{600} ± standard error mean (SEM) from two independent assays, each performed in triplicate.

3.9 Deletion of *luxS* in blood and CSF strains affects virulence in a murine model

The ability of *S. pneumoniae* to metabolise specific carbohydrates has previously been linked to pneumococci disease phenotype in a murine model (Minhas et al., 2019; Agnew et al., 2022). As *luxS* may play a role in carbohydrate metabolism in pneumococci, their virulence phenotypes were assessed in a murine model. It has previously been shown that *luxS* plays a role in the pathogenesis of *S. pneumoniae* D39 and ear isolate 947 (Stroeher et al., 2003; Tikhomirova et al., 2022). Specifically, in the 947 strain, deletion of *luxS* resulted in a significantly higher bacterial burden in the ears of infected mice (Tikhomirova et al., 2022). An earlier study of the blood and CSF strains has shown that they behave differently in a murine model, whereby 60B was unable to survive in the ear (Agnew et al., 2022). Here, we extended these studies by exploring the 60B and 60CSF *luxS* deletion strains in our intranasal murine infection model. CD-1 Swiss mice were intranasally challenged with

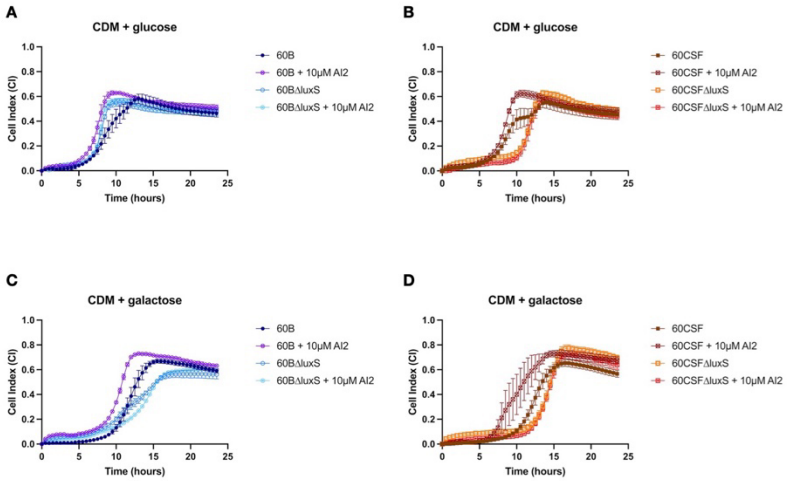

FIGURE 7
Biofilm formation of 60B, 60CSF, 60BΔluxS and 60CSFΔluxS strains. Bacteria were cultured overnight on BA plates before being diluted to a final OD_{600} of 0.05 in CDM + 0.5% glucose ± 10 µM AI-2 **(A, B)** or CDM + 0.5% galactose ± 10 µM AI-2 **(C, D)**. 200 µL of each bacterial strain in each culture medium was placed into wells of a xCELLigence E-plate, with the plate being placed in the cradles of the RTCA-DP platform and incubated at 37°C with 5% CO_2. Biofilm formation was determined by measuring cell index (CI) every 15 min over 24 h using real-time cell analysis (RTCA) xCELLigence technology. Data are mean CI ± standard error mean (SEM) from three independent assays, each performed in triplicate.

10^8 CFU of each strain (60B, 60CSF, 60BΔ*luxS* & 60CSFΔ*luxS*) and the bacterial burden in the blood, brain, ears, lungs, and nose was assessed at 24 h post challenge. At 24 h post infection, there were no significant differences observed in the bacterial burdens in the brain and nasopharynx between mice infected with WT or *luxS* deletion strains (Supplementary Figure 5). Consistent with previous work (Agnew et al., 2022), no bacteria were detected in the ears of mice challenged with 60B, whilst bacteria were present in the ears of 50% of the mice infected with 60CSF (Figure 8; $P < 0.05$). Strikingly, the bacterial burden in the ears of mice challenged with 60BΔ*luxS* was significantly higher than the bacteria detected in both 60B ($P < 0.0001$) and 60CSF (Figure 8; $P < 0.05$). There was no significant difference between the number of 60CSFΔ*luxS* and WT 60CSF pneumococci present in the ears of mice, with the 60CSFΔ*luxS* strain proliferating in this niche at a slightly higher number compared to the wildtype.

Interestingly, in the lungs of mice infected with 60CSFΔ*luxS*, there was a significantly higher bacterial burden compared to mice challenged with 60CSF (Figure 8; $P < 0.05$). A similar trend was observed in the lungs of mice infected with 60BΔ*luxS*, although the difference in bacterial numbers recovered from this niche did not reach statistical significance.

4 Discussion

The LuxS/AI-2 QS system is dependent on the universal Autoinducer-2 (AI-2) signaling molecule, produced by LuxS. Previous studies on the pneumococcal LuxS QS system have shown that a *luxS* mutant strain is defective in biofilm formation and is less able to cause invasive diseases compared with wildtype pneumococci in the laboratory strain D39 (Trappetti et al., 2011b; Vidal et al., 2011). The opposite has been shown for the clinical ear isolate 947, where the *luxS* mutant was more able to cause invasive disease compared to the WT strain and no effect was observed on biofilm formation. In this work, we demonstrate that the different pathogenic profile previously observed in strains collected from a single pediatric patient (Agnew et al., 2022) might by linked to *luxS* and the restriction-modification (RM) locus *spnIII*.

S. pneumoniae is able to randomly switch its genomic DNA methylation pattern between six distinct states (*spnIIIA-F*) via recombination at the *spnIII* locus. Importantly, we previously found that these pneumococcal subpopulations exhibit phenotypic changes which have a major impact on bacterial virulence (Manso et al., 2014). This system, referred to as phasevarion (for phase-variable regulon), allows bacteria to generate a range of phenotypic variants within a population to act as an extra survival strategy (Phillips et al., 2019; Seib et al., 2020). Phasevarions have been characterized in multiple bacterial species such as *H. influenzae* (ModA) (Srikhanta et al., 2005; Fox et al., 2007; Atack et al., 2015), *M catarrhalis* (ModM) (Seib et al., 2002; Blakeway et al., 2014) the pathogenic *Neisseriae* (ModA, ModB, ModD) (Srikhanta et al., 2009; Seib et al., 2011; Seib et al., 2015; Tan et al., 2016), *Helicobacter pylori* (ModH) (Srikhanta et al., 2011), *Streptococcus suis* (Atack et al., 2018), and *Actinobacillus pleuropneumoniae* (Nahar et al., 2023). Analyzing the impact of altered methylase specificity on global transcriptomic patterns is complicated by the presence of multiple *spnIII* alleles in any culture. However, in a previous study, analysis of global gene expression was examined in a set of D39 *spnIII* mutants that were locked in a single specificity (Manso et al., 2014). RNA-seq identified only two major differences between the strains; the capsular polysaccharide serotype 2 biosynthesis operon *csp2* and the *luxS* gene, with both of these genes significantly downregulated in the *SpnIIIB*-locked mutant compared to all the other locked strains analyzed. Previously, we have shown that two clinical isolates 60B and

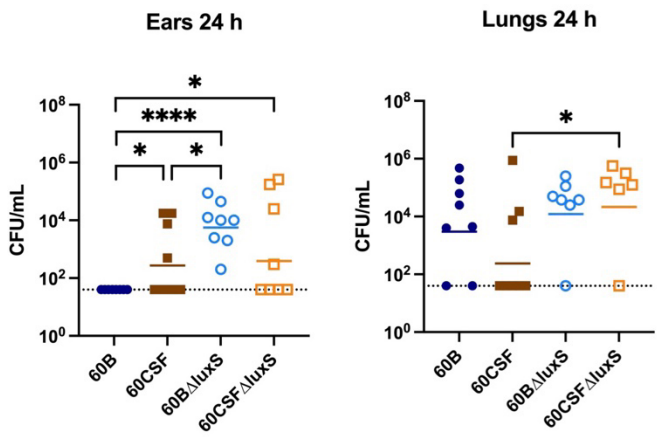

FIGURE 8
Virulence phenotypes of 60B, 60CSF, 60BΔluxS and 60CSFΔluxS strains. Groups of 8 mice were infected intranasally with 10^8 CFU of the indicated strain. At 24 h, mice from each group were humanely euthanized and pneumococci in the brain, ear, lungs and nasal tissue were enumerated. Viable bacterial counts are displayed for each mouse in the ears and lungs (brain and nose data in Supplementary Figure 5); horizontal bars indicate the geometric mean (GM) CFU for each group; the dotted line indicates the detection threshold. Significance of differences in bacterial load between groups was determined using two-tailed Student's *t* test; *$P < 0.05$, ****$P < 0.0001$.

60CSF (serotype 15C, sequence type 8711) that were isolated from the blood and cerebral spinal fluid (CSF), respectively, of a single pediatric meningitis patient exhibit distinct virulence phenotypes in an intranasal murine infection model (Agnew et al., 2022). The two strains expressed similar amounts of capsular polysaccharide, but different ability to colonize the nasopharynx and the ear of mice. The first step in development of pneumococcal disease is the colonization of the human nasopharynx. *S. pneumoniae* is part of the commensal flora of the upper respiratory tract and shares this niche with other potentially pathogenic bacteria including Gram-negative bacteria such as *Haemophilus influenzae*, *Neisseria meningitidis*, and other Gram-positive bacteria, such as *Staphylococcus aureus*, and other streptococci (Faden et al., 1990). The nasopharyngeal flora is established in the first months of life (Faden et al., 1997) and it has a large turnover of colonizing species and serotypes that occupy the niche during the early years, but a balance is usually reached. In this community bacteria need to communicate to each other and thus Quorum sensing systems play a key role in this environment. In particular, the LuxS/AI-2 QS is the only QS shared between Gram-positive and Gram-negative bacteria. Apart from its role in quorum sensing, the enzyme LuxS is tightly coupled to the S-adenosylmethionine (SAM) utilization pathway. The metabolic enzyme LuxS synthesizes AI-2 as a by-product of the conversion of *S*-ribosyl-homocysteine to homocysteine, an integral reaction of the activated methyl cycle (AMC). Thus, the LuxS enzyme has dual roles, firstly as a critical enzyme in the AMC and secondly as an enzyme that produces the QS molecule AI-2. Homocysteine can be generated from S-adenosyl homocysteine (SAH) through two independent pathways: A) Most Gram-positive and Gram-negative bacteria use the enzyme Pfs to first produce *S*-ribosylhomocysteine (SRH), then LuxS catalyzes the conversion to homocysteine, simultaneously generating 4,5-dihydroxy-2,3-pentanedione (DPD), which is spontaneously converted to AI-2. B) Alternatively, bacteria such as *P. aeruginosa* use the enzyme SAH hydrolase (SahH) to generate homocysteine directly without generating DPD. Despite intensive research on luxS and AI-2 in the past few years, a clear separation of the possible metabolic role of AI-2 from its signaling activity, or by AMC metabolic pathway disruption, could not be achieved. In our previous paper we have shown chemical complementation of a D39Δ*luxS* mutant with exogenous AI-2 and identified the AI-2 receptor (Trappetti et al., 2017). Thus, unequivocally proving the role of AI-2 as a QS system in *S. pneumoniae* D39 strain.

In this current study, we investigated the role of *luxS* in the clinical isolates, 60B and 60CSF (Agnew et al., 2022). We quantified the *spnIII* alleles of the bacteria recovered from the nasopharynx of mice intranasally challenged with either 60B or 60CSF strains. Interestingly, bacteria recovered from mice infected with 60B had a higher proportion of the *spnIIIB* allele, corresponding to a low expression level of *luxS*, previously observed in the SpnD39IIIB locked strain (Manso et al., 2014). In contrast bacteria isolated from mice infected with 60CSF, had higher proportions of the *spnIIIA* and *spnIIIB* alleles. Importantly, when the *luxS* gene was deleted from 60B and 60CSF, the mutants had significantly reduced proportions of *spnIIIA* and *spnIIIB* and now had predominantly *spnIIIC*. These results indicate that the presence of LuxS is essential for the *spnIII* locus to switch to the *spnIIIA* and *spnIIIB* alleles, with the complete absence resulting in a switch to *spnIIIC* and *spnIIID*. The exact nature of this link between LuxS and the *spnIII* locus will require further characterization, to establish the mechanism by which LuxS influences the switching of alleles. In addition to differences in *spnIII* allele proportions, 60BΔluxS showed reduced ability to grow in media with only galactose. The opposite was true for 60CSF where deletion of the *luxS* gene improved the growth. Therefore, distinct mechanisms seem to be operating in these strains. In the case of 60B, mutation in the *luxS* gene decreases its ability to grow (as previously observed for the virulent strain D39 and for the ear isolate 947), while in 60CSF, deletion of *luxS* increased the ability of the strain to grow in galactose media. This suggested a strain-specific effect of *luxS* in these clinical isolates. When the ability of the strains to form a biofilm was tested, we found that both strains could form biofilm at comparable rates, but again *luxS* mutation was deleterious for the 60B strain, whilst improving the biofilm formation capacity of the 60CSF strain. Addition of AI-2 improved the biofilm capacity in both WT strains, while interestingly chemical complementation of the *luxS* mutants with exogenous AI-2 could not be achieved. Thus, LuxS seems to have more of a metabolic role rather than a role in QS in these clinical isolates, dissimilar to the findings in D39 (Trappetti et al., 2017). In a murine infection model the 60BΔ*luxS* strain displayed an enhanced transit to the ear compared to the WT, and increased transit to the lungs for the 60CSFΔ*luxS* strain (Figure 8). An increased transit of the 60BΔ*luxS* strain to the ear together with the reduced capacity of the strain to form a biofilm, suggests that functional *luxS* may act to facilitate adherence to the nasopharynx, but may interfere with transit to other host niches, like the ear compartment. However, in the 60CSF strain, deletion of *luxS* increased its ability to form a biofilm and also increased the ability of the strain to persist in the lung.

These results suggested an opposite role for *luxS* in the infection profiles of 60B in comparison to 60CSF, with a potential role in metabolism. We then analyzed the metabolic profiles of the *luxS* mutants and importantly, both *luxS* mutants displayed the same metabolic profile, having lost the ability to metabolise psicose and having acquired the ability to metabolise fucose in comparison to the wildtype. Most importantly, strains recovered from the nasopharynx of mice intranasally infected with 60B or 60CSF displayed the same changes in metabolic profile as the *luxS* mutants, indicating that *luxS* may be downregulated in these strains during nasopharyngeal colonization. Our earlier analysis of the *spnIII* allele variants in 60B and 60CSF isolated from murine nasal tissue indicated both had high proportions of *spnIIIB*, which is associated with increased colonization ability and downregulation of *luxS*. Therefore, during colonization of the nasopharynx 60B and 60CSF undergo changes to increase their proportion of *spnIIIB* allele to aid their colonization, likely resulting in a downregulation of *luxS*, thereby altering their ability to metabolise fucose and psicose in a similar way as was observed for the *luxS* mutants. Furthermore, other factors may be contributing to the observed different phenotypes that have yet to be identified. It is important that previous and future studies on pneumococcal *luxS* and its involvement in virulence be interpreted in the context of the potential switching between epigenetically-different subpopulations during the course of any experimental infection study.

Data availability statement

The raw data supporting the conclusions of this article will be made available by the authors, without undue reservation.

Ethics statement

The animal study was reviewed and approved by University of Adelaide Animal Ethics Committee.

Author contributions

Conceptualization, HA, EB, JP, and CT; methodology, HA, JA, AF, SW, and CT; investigation, HA, JA, AF, MvdL, and CT; synthesis of AI-2/DPD, ES and AA; data curation, HA and CT; writing—original draft preparation, HA, EB, JP, and CT. All authors contributed to the article and approved the submitted version.

Funding

This work was supported by the National Health and Medical Research Council (NHMRC) Investigator Grant 1174876 to JP, by the Australian Research Council (ARC) Discovery Project DP190102980 to CT and JP, and by the Channel 7 Children's Research Foundation Grant 20656402 to EB.

Acknowledgments

We would like to acknowledge Peter S Zilm for access and assistance with the xCELLigence (Agilent Technologies, USA) biofilm formation system.

Conflict of interest

The authors declare that the research was conducted in the absence of any commercial or financial relationships that could be construed as a potential conflict of interest.

Publisher's note

Supplementary material

The Supplementary Material for this article can be found online at: https://www.frontiersin.org/articles/10.3389/fcimb.2023.1177857/full#supplementary-material

References

Agnew, H. N., Brazel, E. B., Tikhomirova, A., van der Linden, M., Mclean, K. T., Paton, J. C., et al. (2022). Streptococcus pneumoniae strains isolated from a single pediatric patient display distinct phenotypes. *Front. Cell. Infect. Microbiol.* 12. doi: 10.3389/fcimb.2022.866259

Amin, Z., Harvey, R. M., Wang, H., Hughes, C. E., Paton, A. W., Paton, J. C., et al. (2015). Isolation site influences virulence phenotype of serotype 14 streptococcus pneumoniae strains belonging to multilocus sequence type 15. *Infection Immun.* 83, 4781–4790. doi: 10.1128/IAI.01081-15

Atack, J. M., Srikhanta, Y. N., Fox, K. L., Jurcisek, J. A., Brockman, K. L., Clark, T. A., et al. (2015). A biphasic epigenetic switch controls immunoevasion, virulence and niche adaptation in non-typeable haemophilus influenzae. *Nat. Commun.* 6, 7828. doi: 10.1038/ncomms8828

Atack, J. M., Weinert, L. A., Tucker, A. W., Husna, A. U., Wileman, T. M., Hadjirin, N. F., et al. (2018). Streptococcus suis contains multiple phase-variable methyltransferases that show a discrete lineage distribution. *Nucleic Acids Res.* 46, 11466–11476. doi: 10.1093/nar/gky913.

Blakeway, L. V., Power, P. M., Jen, F. E., Worboys, S. R., Boitano, M., Clark, T. A., et al. (2014). ModM DNA methyltransferase methylome analysis reveals a potential role for moraxella catarrhalis phasevarions in otitis media. *FASEB J.* 28, 5197–5207. doi: 10.1096/fj.14-256578

Costerton, J. W., Stewart, P. S., and Greenberg, E. P. (1999). Bacterial biofilms: a common cause of persistent infections. *Science* 284, 1318–1322. doi: 10.1126/science.284.5418.1318

De Kievit, T. R., and Iglewski, B. H. (2000). Bacterial quorum sensing in pathogenic relationships. *Infection Immun.* 68, 4839–4849. doi: 10.1128/IAI.68.9.4839-4849.2000

Faden, H., Duffy, L., Wasielewski, R., Wolf, J., Krystofik, D., and Tung, Y. (1997). Relationship between nasopharyngeal colonization and the development of otitis media in children. *J. Infect. Dis.* 175, 1440–1445. doi: 10.1086/516477

Faden, H., Stanievich, J., Brodsky, L., Bernstein, J., and Ogra, P. L. (1990). Changes in nasopharyngeal flora during otitis media of childhood. *Pediatr. Infect. Dis. J.* 9, 623–626.

Fox, K. L., Dowideit, S. J., Erwin, A. L., Srikhanta, Y. N., Smith, A. L., and Jennings, M. P. (2007). Haemophilus influenzae phasevarions have evolved from type III DNA restriction systems into epigenetic regulators of gene expression. *Nucleic Acids Res.* 35, 5242–5252. doi: 10.1093/nar/gkm571

Higgins, M. A., Suits, M. D., Marsters, C., and Boraston, A. B. (2014). Structural and functional analysis of fucose-processing enzymes from streptococcus pneumoniae. *J. Mol. Biol.* 426, 1469–1482. doi: 10.1016/j.jmb.2013.12.006

Iannelli, F., and Pozzi, G. (2004). Method for introducing specific and unmarked mutations into the chromosome of streptococcus pneumoniae. *Mol. Biotechnol.* 26, 81–86. doi: 10.1385/MB:26:1:81

Kolenbrander, P. E. (2000). Oral microbial communities: biofilms, interactions, and genetic systems. *Annu. Rev. Microbiol.* 54, 413–437. doi: 10.1146/annurev.micro.54.1.413

Lavelle, E. C., and Ward, R. W. (2022). Mucosal vaccines - fortifying the frontiers. *Nat. Rev. Immunol.* 22, 236–250. doi: 10.1038/s41577-021-00583-2

Livak, K. J., and Schmittgen, T. D. (2001). Analysis of relative gene expression data using real-time quantitative PCR and the 2−ΔΔCT method. *Methods (San Diego Calif.)* 25, 402–408. doi: 10.1006/meth.2001.1262

Manso, A. S., Chai, M. H., Atack, J. M., Furi, L., De Ste Croix, M., Haigh, R., et al. (2014). A random six-phase switch regulates pneumococcal virulence via global epigenetic changes. *Nat. Commun.* 5, 5055–5055. doi: 10.1038/ncomms6055

Matsuo, T., Suzuki, H., Hashiguchi, M., and Izumori, K. (2002). D-psicose is a rare sugar that provides no energy to growing rats. *J. Nutr. Sci. Vitaminol (Tokyo)* 48, 77–80. doi: 10.3177/jnsv.48.77

Mclean, K. T., Tikhomirova, A., Brazel, E. B., Legendre, S., Haasbroek, G., Minhas, V., et al. (2020). Site-specific mutations of GalR affect galactose metabolism in streptococcus pneumoniae. *J. Bacteriology* 203, e00180-20. doi: 10.1128/JB.00180-20

Miller, M. B., and Bassler, B. L. (2001). Quorum sensing in bacteria. *Annu. Rev. Microbiol.* 55, 165–199. doi: 10.1146/annurev.micro.55.1.165

Minhas, V., Harvey, R. M., Mcallister, L. J., Seemann, T., Syme, A. E., Baines, S. L., et al. (2019). Capacity to utilize raffinose dictates pneumococcal disease phenotype. *mBio* 10, e02596–e02518. doi: 10.1128/mBio.02596-18

Nahar, N., Tram, G., Jen, F. E.-C., Phillips, Z. N., Weinert, L. A., Bossé, J. T., et al. (2023). Actinobacillus pleuropneumoniae encodes multiple phase-variable DNA methyltransferases that control distinct phasevarions. *Nucleic Acids Res* 51 (7), 3240–3260. doi: 10.1093/nar/gkad091

Paixão, L., Caldas, J., Kloosterman, T. G., Kuipers, O. P., Vinga, S., and Neves, A. R. (2015). Transcriptional and metabolic effects of glucose on streptococcus pneumoniae sugar metabolism. *Front. Microbiol.* 6. doi: 10.3389/fmicb.2015.01041

Phillips, Z. N., Husna, A. U., Jennings, M. P., Seib, K. L., and Atack, J. M. (2019). Phasevarions of bacterial pathogens - phase-variable epigenetic regulators evolving from restriction-modification systems. *Microbiol. (Reading)* 165, 917–928. doi: 10.1099/mic.0.000805

Seib, K. L., Jen, F. E., Tan, A., Scott, A. L., Kumar, R., Power, P. M., et al. (2015). Specificity of the ModA11, ModA12 and ModD1 epigenetic regulator N(6)-adenine DNA methyltransferases of neisseria meningitidis. *Nucleic Acids Res.* 43, 4150–4162. doi: 10.1093/nar/gkv219

Seib, K. L., Peak, I. R., and Jennings, M. P. (2002). Phase variable restriction-modification systems in moraxella catarrhalis. *FEMS Immunol. Med. Microbiol.* 32, 159–165. doi: 10.1111/j.1574-695X.2002.tb00548.x

Seib, K. L., Pigozzi, E., Muzzi, A., Gawthorne, J. A., Delany, I., Jennings, M. P., et al. (2011). A novel epigenetic regulator associated with the hypervirulent neisseria meningitidis clonal complex 41/44. *FASEB J.* 25, 3622–3633. doi: 10.1096/fj.11-183590

Seib, K. L., Srikhanta, Y. N., Atack, J. M., and Jennings, M. P. (2020). Epigenetic regulation of virulence and immunoevasion by phase-variable restriction-modification systems in bacterial pathogens. *Annu. Rev. Microbiol.* 74, 655–671. doi: 10.1146/annurev-micro-090817-062346

Srikhanta, Y. N., Dowideit, S. J., Edwards, J. L., Falsetta, M. L., Wu, H. J., Harrison, O. B., et al. (2009). Phasevarions mediate random switching of gene expression in pathogenic neisseria. *PloS Pathog.* 5, e1000400. doi: 10.1371/journal.ppat.1000400

Srikhanta, Y. N., Gorrell, R. J., Steen, J. A., Gawthorne, J. A., Kwok, T., Grimmond, S. M., et al. (2011). Phasevarion mediated epigenetic gene regulation in helicobacter pylori. *PloS One* 6, e27569. doi: 10.1371/journal.pone.0027569

Srikhanta, Y. N., Maguire, T. L., Stacey, K. J., Grimmond, S. M., and Jennings, M. P. (2005). The phasevarion: a genetic system controlling coordinated, random switching of expression of multiple genes. *Proc. Natl. Acad. Sci. U.S.A.* 102, 5547–5551. doi: 10.1073/pnas.0501169102

Stroeher, U. H., Paton, A. W., Ogunniyi, A. D., and Paton, J. C. (2003). Mutation of luxS of streptococcus pneumoniae affects virulence in a mouse model. *Infect. Immun.* 71, 3206–3212. doi: 10.1128/iai.71.6.3206-3212.2003

Tan, A., Hill, D. M. C., Harrison, O. B., Srikhanta, Y. N., Jennings, M. P., Maiden, M. C. J., et al. (2016). Distribution of the type III DNA methyltransferases modA, modB and modD among neisseria meningitidis genotypes: implications for gene regulation and virulence. *Sci. Rep.* 6, 21015. doi: 10.1038/srep21015

Tikhomirova, A., Brazel, E. B., Mclean, K. T., Agnew, H. N., Paton, J. C., and Trappetti, C. (2022). The role of luxS in the middle ear streptococcus pneumoniae isolate 947. *Pathog. (Basel)* 11, 216. doi: 10.3390/pathogens11020216

Trappetti, C., Mcallister, L. J., Chen, A., Wang, H., Paton, A. W., Oggioni, M. R., et al. (2017). Autoinducer 2 signaling via the phosphotransferase FruA drives galactose utilization by streptococcus pneumoniae, resulting in hypervirulence. *mBio* 8, e02269–e02216. doi: 10.1128/mBio.02269-16

Trappetti, C., Ogunniyi, A. D., Oggioni, M. R., and Paton, J. C. (2011a). Extracellular matrix formation enhances the ability of streptococcus pneumoniae to cause invasive disease. *PloS One* 6, e19844–e19844. doi: 10.1371/journal.pone.0019844

Trappetti, C., Potter, A. J., Paton, A. W., Oggioni, M. R., and Paton, J. C. (2011b). LuxS mediates iron-dependent biofilm formation, competence, and fratricide in streptococcus pneumoniae. *Infection Immun.* 79, 4550–4558. doi: 10.1128/IAI.05644-11

Trappetti, C., van der Maten, E., Amin, Z., Potter, A. J., Chen, A. Y., Van Mourik, P. M., et al. (2013). Site of isolation determines biofilm formation and virulence phenotypes of streptococcus pneumoniae serotype 3 clinical isolates. *Infection Immun.* 81, 505–513. doi: 10.1128/IAI.01033-12

Trimble, A., Connor, V., Robinson, R. E., Mclenaghan, D., Hancock, C. A., Wang, D., et al. (2020). Pneumococcal colonisation is an asymptomatic event in healthy adults using an experimental human colonisation model. *PloS One* 15. doi: 10.1371/journal.pone.0229558

Vendeville, A., Winzer, K., Heurlier, K., Tang, C. M., and Hardie, K. R. (2005). Making 'sense' of metabolism: autoinducer-2, LUXS and pathogenic bacteria. *Nat. Rev. Microbiol.* 3, 383–396. doi: 10.1038/nrmicro1146

Vidal, J. E., Ludewick, H. P., Kunkel, R. M., Zähner, D., and Klugman, K. P. (2011). The LuxS-dependent quorum-sensing system regulates early biofilm formation by streptococcus pneumoniae strain D39. *Infect. Immun.* 79, 4050–4060. doi: 10.1128/iai.05186-11

Von Bodman, S. B., Willey, J. M., and Diggle, S. P. (2008). Cell-cell communication in bacteria: united we stand. *J. Bacteriology* 190, 4377–4391. doi: 10.1128/JB.00486-08

3.4 Supplementary material

frontiers

Supplementary Material

Uncovering the link between the SpnIII restriction modification system and LuxS in *Streptococcus pneumoniae* meningitis isolates.

Hannah N Agnew[1], John M Atack[2 3], Ann RD Fernando[1], Sophie N Waters[1], Mark van der Linden[3], Erin Smith[5], Andrew D. Abell[5], Erin B Brazel[1], James C Paton[1*], Claudia Trappetti[1*]

*** Correspondence:** claudia.trappetti@adelaide.edu.au, james.paton@adelaide.edu.au

1 Supplementary Data

Synthesis of AI-2 (DPD)

Starting materials were obtained from commercial sources and used without further purification unless otherwise stated. Thin layer chromatography (TLC) was performed on Merck aluminium sheets with silica gel 60 F_{254} silica plates. The compounds were visualised with an Oliphant (6W 254 nm tube) UV lamp, vanillin stain and/or potassium permanganate stain. Flash chromatography was carried out using Merck Kiselgel 60 (230-400 mesh). All yields are reported as isolated yields as judged to homogenous by TLC and NMR spectroscopy. NMR spectra were recorded using either an Agilent DD2 console 500 MHz or a Varian Inova 600 MHz spectrometer. NMR spectra were reference to their respective solvents: chloroform-*d* ($CDCl_3$, ^1H δ 7.26 ppm, ^{13}C δ 49.3 ppm); water-d_2 (D_2O, ^1H 4.65 ppm)

Dimethyl amine (10 mL, 33vol% in ethanol) was added to (-)-methyl (S)-2,2-dimethyl-1,3-dioxalane-4-carboxylate (0.49 mL, 3.38 mmol) at 0°C and stirred for 3 hours before being placed in the fridge (5 °C) for 3 days. The volatile compounds were evaporated, and the residue was subjected to flash chromatography. Elution with 1:1 EtOAC in hexanes produced *N*,*N*-dimethyl (S)-α,β-isopropylideneglyceramide as an oil (0.449 g, 77%).

^1H NMR (500 MHz, $CDCl_3$) δ 4.69 (t, J = 6.6 Hz, 1H), 4.38 (dd, J = 8.4, 6.5 Hz, 1H), 4.14 (dd, J = 8.5, 6.8 Hz, 1H), 3.12 (s, 3H), 2.97 (s, 3H), 1.42 (d, J = 1.4 Hz, 6H) ppm.

N,*N*-dimethyl (S)-α,β-isopropylideneglyceramide (0.440 g, 2.54 mmol) was dissolved in anhydrous ether (10 mL) under nitrogen and cooled to 0°C. Isopropenylmagnesium bromide (5.33 mL, 2.67 mmol, 0.5M in THF) was added slowly. The resulting mixture was stirred for 10 min before sulfuric acid solution (1M) was added dropwise until the precipitate redissolved. The aqueous layer was extracted with ether (x3) and the combined organic extracts were neutralised over solid sodium carbonate, dried over anhydrous magnesium sulfate, filtered and concentrated under reduced pressure. The residue was subjected to flash chromatography. Elution with 20% EtOAC in hexanes afforded (S)-4-methacryloyl-2,2-dimethyl-1,3-dioxolane as an oil (0.166 g, 38%).

^1H NMR (500 MHz, $CDCl_3$) δ 6.04 (d, J = 1.2 Hz, 1H), 5.92 (d, J = 1.5 Hz, 1H), 5.07 (dd, J = 7.3, 6.1 Hz, 1H), 4.23 (dd, J = 8.5, 7.3 Hz, 1H), 4.10 (dd, J = 6.4, 5.9 Hz, 1H), 1.91 (s, 1H), 1.44 (s, 2H), 1.43 (s, 3H).

(S)-4-methacryloyl-2,2-dimethyl-1,3-dioxolane (0.05 g, 0.24 mmol) was dissolved in THF (1mL) and water (1 mL) and cooled to 0°C. TFA (1 mL) was added dropwise and the resulting mixture was stirred for 1.5 hrs. The volatiles were concentrated under reduced pressure. The residue was subjected to flash chromatography. Elution with 5% MeOH in DCM afforded (S)-1,2-dihydroxy-4-methyl-4-penten-3-one as a colourless liquid (0.015 g, 41%).

1H NMR (500 MHz, $CDCl_3$) δ 5.96 (d, J = 1.5 Hz, 1H), 5.95 (s, 1H), 4.91 (m, 1H), 3.95 (m, 1H), 3.71 (dd, J = 11.6, 4.8 Hz, 1H), 3.01 (s, 2H), 1.95 (s, 3H).

(S)-1,2-dihydroxy-4-methyl-4-penten-3-one (15 mg, 0.12 mmol) was dissolved in MeOH (10 mL) and cooled in an acetone-dry ice bath (-78 °C). Ozone was bubbled through the solution until it turned blue (approx. 2 min). Oxygen gas was then bubbled through until the ozone was removed and dimethyl sulphide was added. The mixture was allowed to come to room temperature and stirred overnight.

The bulk of the material was added water (3 mL) and concentrated to remove the volatiles. Diluted with 1M potassium phosphate buffer to give pH 7.3 and final concentration 5 mM product in 0.5M potassium phosphate buffer.

Supplementary Table 1: Phenotype microarray results for 60B, 60CSF, *luxS* mutants and isolates recovered from murine noses 24 h post-infection in Biolog PM1 plate. Catabolism was measured through a colorless tetrazolium dye being reduced by NADH produced during catabolism. +, metabolism occurred; -, no metabolism occurred. Metabolism was determined by calculating the change in OD_{590} from the initial (0 h) to final (24 h) measurements. These values were then compared with the change in the negative value and an arbitrary value based on the change in the negative control was used to determine if catabolism occurred. Carbon sources in which there were no differences in metabolism between the WT, mutant or strains recovered from mice are not shown.

Carbon source	**60B**	**60CSF**	**60BΔluxS**	**60CSFΔluxS**	**60B (mouse)**	**60CSF (mouse)**
L-Fucose	-	-	+	+	+	+
D-Psicose	+	+	-	-	-	-

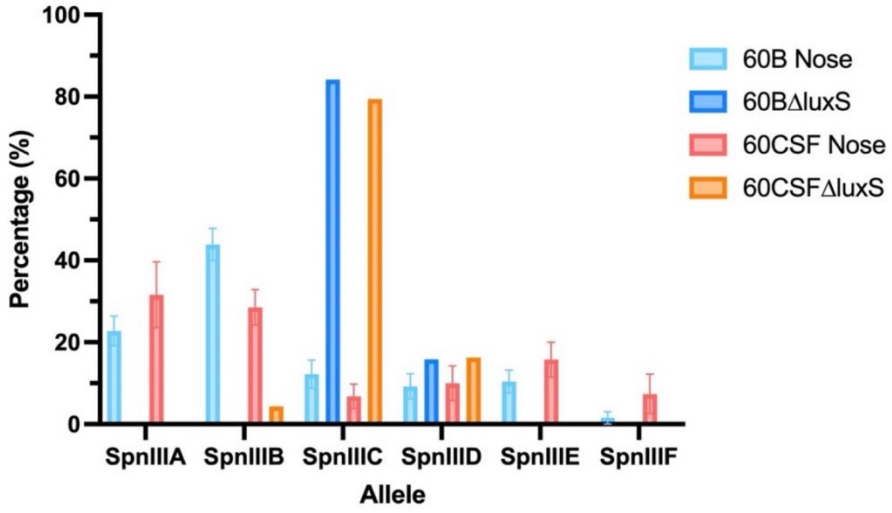

Supplementary Figure 1: *spnIII* allele frequencies of *luxS* mutants, and 60B and 60CSF recovered post intranasal murine infection. Mice were intranasally challenged with 10^8 CFU *S. pneumoniae* serotype 15C ST8711 blood isolate (60B) or CSF isolate (60CSF). At 24 h, mice from each group were humanely euthanized and pneumococci in the nasal tissue were harvested. *spnIII* allele quantification was performed on DNA extracted from colonies grown from nasopharynx samples, in addition to 60BΔluxS and 60CSFΔluxS colonies grown on BA plates overnight at 37°C with 5% CO_2. Allele percentages are displayed for WT strains recovered from the nose of mice (Figure 1) and *luxS* mutants from frozen stock.

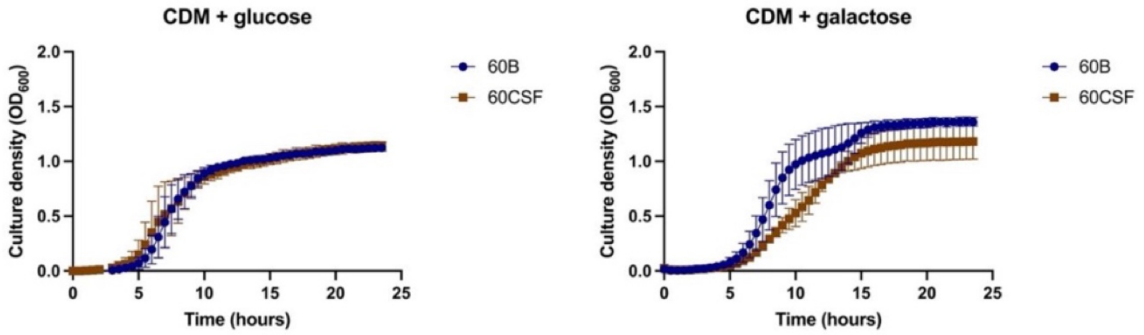

Supplementary Figure 2: Growth of 60B and 60CSF in CDM + glucose and CDM + galactose. Isolates were grown in 200 µL CDM supplemented with 0.5% glucose (CDM + glucose) or 0.5% galactose (CDM + galactose). OD_{600} was measured every 30 min for 24 h. Data are mean OD_{600} ± standard error mean (SEM) from two independent assays, each performed in triplicate. Significance of differences in final OD and mid-exponential phase OD between strains was determined using two-tailed Student's *t* test.

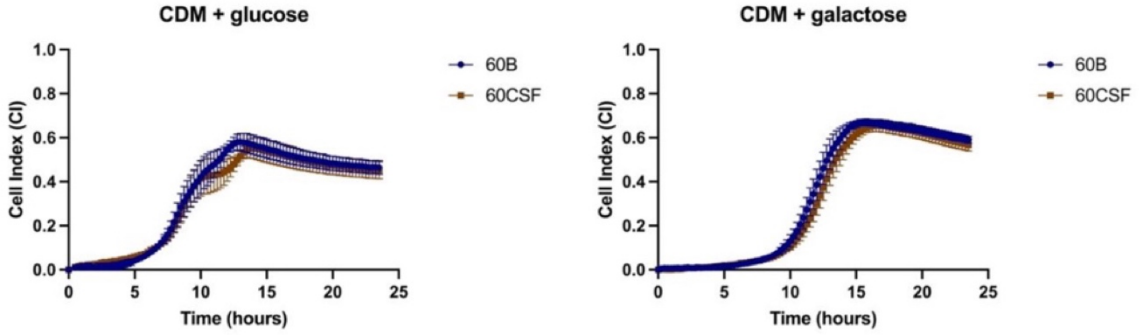

Supplementary Figure 3: Biofilm formation of 60B and 60CSF in CDM + glucose and CDM + galactose. Bacteria were cultured overnight on BA plates before being diluted to a final OD_{600} of 0.05 in CDM + 0.5% glucose or CDM + 0.5% galactose. 200 µL of each bacterial strain in each culture medium was placed into wells of a xCELLigence E-plate, with the plate being placed in the cradles of the RTCA-DP platform and incubated at 37°C with 5% CO_2. Biofilm formation was determined by measuring cell index (CI) every 15 min over 24 h using real-time cell analysis (RTCA) xCELLigence technology. Data are mean CI ± standard error mean (SEM) from three independent assays, each performed in triplicate.

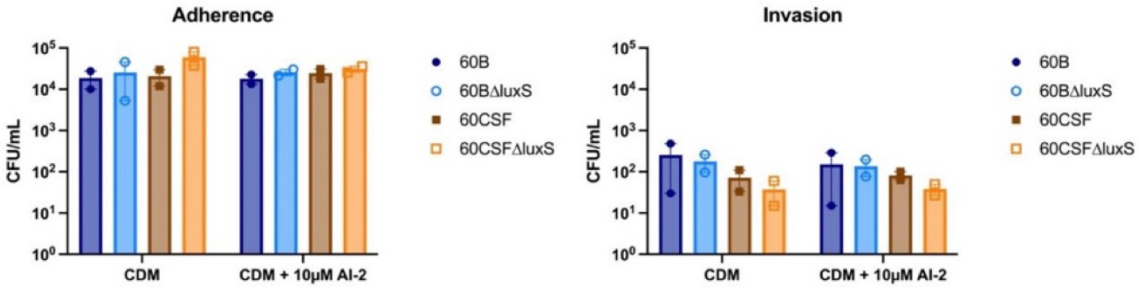

Supplementary Figure 4: Adherence and invasion of 60B, 60CSF, 60BΔluxS and 60CSFΔluxS strains to Detroit 562 cells. Strains at OD_{600} 0.2 were inoculated onto monolayers of Detroit 562 cells in CDM ± 10µM AI-2, and incubated for 2 h before being tested for adherent and invasive bacteria (see Materials and Methods). Data are mean adherent or invasive bacteria ± standard error mean (SEM) from two independent assays, each performed in triplicate. Statistical analysis was performed using two-tailed Student's *t* test. No significant differences were detected between the adherence and invasion of the strains in different conditions.

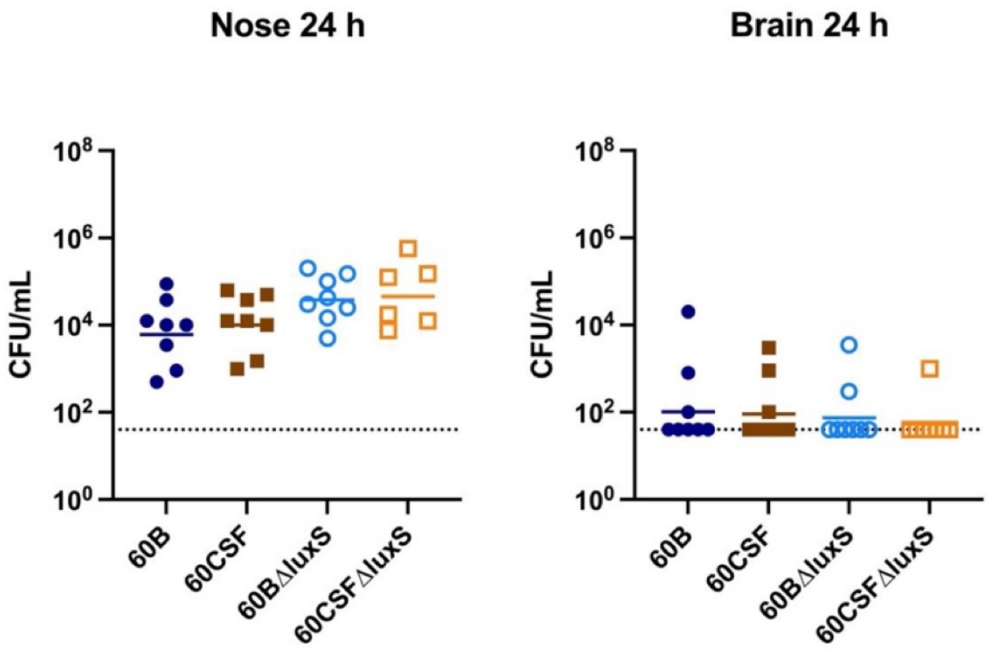

Supplementary Figure 5: Murine brain and nose bacterial burden post-infection with 60B, 60CSF, 60BΔluxS and 60CSFΔluxS strains. Groups of 8 mice were infected intranasally with 10^8 CFU of the indicated strain. At 24 h, mice from each group were humanely euthanized and pneumococci in the brain, ear, lungs and nasal tissue were enumerated. Viable bacterial counts are displayed for each mouse in the brain and nose (ears and lungs are in manuscript); horizontal bars indicate the geometric mean (GM) CFU for each group; the dotted line indicates the detection threshold. No significant differences in bacterial load between groups were detected.

Chapter 4: Final Discussion

Streptococcus pneumoniae poses a global health threat, causing significant morbidity and mortality each year. Despite extensive research, the mechanisms governing its transition from colonization to disease, along with the specific diseases it causes, remain unclear. The bacterium's extensive genomic diversity, with over 100 capsular serotypes, 12,000 sequence types, and 30% of the genome varying among clonal lineages, complicates the issue (Donati et al., 2010; Cremers et al., 2019; Ganaie et al., 2021).

To address these challenges, researchers have begun to focus on using clinical isolates from a range of carriage and disease instances in humans (Silva et al., 2006; Hall-Stoodley et al., 2008; Croucher et al., 2013; Trappetti et al., 2013; Amin et al., 2015; Hartmann et al., 2018; Minhas et al., 2019; Minhas et al., 2020; Tikhomirova et al., 2022). The choice between laboratory-adapted and clinical isolates is crucial, with clinical isolates offering unique insights into the bacterium's lifestyle and disease progression. To circumvent the genomic disparity still present between pneumococcal clinical isolates, recent studies have begun to explore closely related (same serotype and sequence type) isolates from different types of disease or anatomical niches within a single patient (Trappetti et al., 2013; Amin et al., 2015; Minhas et al., 2019; Tikhomirova et al., 2022). Employing closely related isolates provides an opportunity to explore various factors, including biofilm formation capacity, carbohydrate metabolism profiles, and antibiotic sensitivity, that are relevant in a disease context. Subsequent research conducted using murine infection models can help elucidate the role of these factors in the pathogenic process (Trappetti et al., 2013; Amin et al., 2015; Minhas et al., 2019).

This thesis has used closely related clinical isolates of *Streptococcus pneumoniae* taken at the same time from the blood and cerebrospinal fluid (CSF) of a single paediatric meningitis patient provided through a collaboration with the German National Reference Center for Streptococci (Aachen). Initial characterisation of the collection of isolates (Appendix C) revealed that the serotype 15C, sequence type 8711 blood and CSF isolates obtained from a single paediatric meningitis patient, displayed differences in carbohydrate metabolism. These differences may have influenced host adaptation and disease type. Consequently, it was hypothesised that these isolates could possess distinct molecular variations that emerged during disease progression, leading to a change in lifestyle and ultimately impacting differential niche adaptation. As a result, phenotypic, genetic and epigenetic characteristics were investigated in both *in vitro* and *in vivo* settings to uncover the factors influencing disease progression.

In Chapter 2 of this thesis, an investigation was conducted to discern the unique phenotypic characteristics of the blood and CSF isolates, referred to as 60B and 60CSF, respectively. Analysis of carbohydrate metabolism revealed that 60CSF metabolised the carbon sources raffinose and melibiose, while 60B did not. The ability to metabolise different carbohydrates is crucial for niche adaptation and disease progression, as demonstrated in a recent study by Im et al. (2022). This study found that carbohydrate availability in different anatomical sites influenced pneumococcal physiology and virulence, promoting site-specific fitness. Specifically, when the pneumococcal strain TIGR4 was cultured in chemically defined media (CDM) containing carbohydrates (galactose and sialic acid), mimicking the nasopharyngeal environment, the pneumococci exhibited decreased metabolic activity and a slower growth rate. This environment induced a mixed acid fermentation pathway with a pronounced production of hydrogen peroxide. Additionally, these cells were found to be in a state of carbon-catabolite de-repression compared to cells cultured in CDM with carbohydrates (glucose and sialic acid), which mimic the conditions in the blood. Furthermore, alterations in gene expression, primarily centred around carbohydrate metabolism, included critical virulence factors such as capsule and surface adhesins. This study exemplified how site-specific carbohydrate availability can significantly impact the physiology, virulence, and overall fitness of pneumococci (Im et al., 2022). Moreover, the ability to metabolise specific carbohydrate sources has been shown to influence disease outcome (Paixão et al., 2015; Hatcher et al., 2016; McLean et al., 2020). For instance, one study found that the administration of free sialic acid prior to intranasal challenge led to an increase in bacterial counts within the central nervous system of mice. This phenomenon is likely facilitated by the spread of bacteria from the nasopharynx through the olfactory neurons (Hatcher et al., 2016). Preventing the metabolism of galactose has also been found to prevent nasopharyngeal colonisation, as well as ear and lung infections in a murine model (McLean et al., 2020), resulting in increased survival times in intranasally infected mice (Paixão et al., 2015). Importantly, past research in closely related blood and ear isolates has suggested a role of raffinose metabolism in tissue tropism (Minhas et al., 2019), indicating that this metabolic difference may have driven the differential niche adaption in the human patient.

To delve deeper, we studied strain growth in a chemically defined medium (CDM) with the clinically relevant carbon sources: glucose, raffinose, melibiose, galactose, and lactose. Glucose is the primary carbon source available in the blood (Güemes et al., 2016), whilst galactose is the primary carbon source in the upper respiratory tract, after cleavage from N-linked glycoconjugates present on host epithelial cells, and necessary for colonisation (Paixão et al., 2015). Importantly, both galactose and lactose have been shown to be essential for successful establishment of lung infections (Hava and Camilli, 2002), whilst the ability to metabolise raffinose has influenced niche

adaptation in a murine model (Minhas et al., 2019).Growth in glucose was similar for both strains, indicating no significant defects. In CDM with lactose and galactose, both 60B and 60CSF grew similarly, though slower than in glucose. Surprisingly, neither strain could grow with melibiose as the sole carbon source, differing from previous findings with a lab-adapted strain (D39, serotype 2), possibly due to varying media and sugar concentrations (Bidossi et al., 2012). It should be noted that melibiose is an alpha-galactoside commonly derived from raffinose, and subsequently is imported and metabolised through the same pathway as raffinose (Rosenow et al., 1999).

Despite being unable to grow in CDM with melibiose, 60CSF displayed the ability to grow when raffinose was the sole carbon source, whilst 60B was unable to grow. This discovery suggests that even though these strains originated from the same patient and caused similar diseases, variations in their metabolic profiles might have played a role in how the disease progressed and adapted within the host's specific environment. Intriguingly, our results contrast with earlier research that showed blood isolates were better at raffinose metabolism compared to ear isolates (Minhas et al., 2019). Here, the closely related ear isolate, 101E, of 60B/60CSF could metabolise and grow with raffinose (Appendix C). In the study by Minhas et al. (2019), the differential raffinose metabolism was attributed to a SNP in either *rafR* (for serotype 14 ST15 isolates) or *rafK* (for serotype 3 ST180 isolates), neither of which are present in the clinical isolates investigated in this thesis. The disparity between the two studies may be due to a variety of reasons, including the isolates being different serotypes and STs. Furthermore, the isolates in this study were obtained from patients with either meningitis or otitis media, whilst the blood isolates in Minhas et al. (2019) study were from cases of sepsis, which may have had different environmental conditions to cause raffinose metabolism. This uncertainty underscores the importance of using clinical isolates to investigate factors affecting tissue tropism, as multiple factors seem to influence disease outcomes. Indeed, in a study investigating vitamins metabolism by clinical pneumococcal strains, it was found that the ability to metabolise riboflavin resulted in increased clearance by the mucosal-associated invariant T (MAIT) cells of the human immune system. Importantly, this finding was associated with specific ST groups within serotype 19F strains, and expression of riboflavin metabolism genes was also dependent on the levels of riboflavin in the environment, subsequently impacting immune response and disease outcome (Hartmann et al., 2018). This underscores the variability in metabolism within pneumococcal strains, highlighting the intricate interplay between bacterial metabolism, host immunity, and the potential impact on disease dynamics.

Sequencing the genes responsible for raffinose metabolism, including *aga, rafR, rafE, rafF, rafG*, and *rafK*, revealed identical sequences in both 60B and 60CSF. However, an important finding was

an early stop codon in the *aga* gene, relative to the published D39 and TIGR4 sequences (Tettelin et al., 2001; Lanie et al., 2007), resulting in a truncated Aga protein that would lack the C-terminal region harbouring the catalytic and active sites, suggesting this protein would function poorly if at all.

Strikingly, despite the shared early stop codon in *aga*, 60CSF could metabolise raffinose and grow, whereas 60B could not. Whole genome sequencing performed on the Illumina revealed no genetic variations in the raffinose locus or other loci between the two strains. However, further analysis unveiled fragments of an alternative alpha-galactosidase gene, GH36, in both 60B and 60CSF, which showed no similarity in sequence to the *aga* gene at the *raf* locus.

Whilst the sequencing results from Illumina revealed 60B and 60CSF had different fragments of the gene, indicating potential differences in the functionality, Sanger sequencing of this alternative alpha-galactosidase in both strains revealed no differences (Appendix D), indicating it was likely not responsible for the metabolic difference. The observed different fragments of the alternative alpha-galactosidase were likely due to using the Illumina sequencing platform, which generates short reads ideal for SNP analysis but are less ideal for larger DNA modifications due to the large number of gaps (Nakamura et al., 2011).

Deletions of the *aga* gene were introduced in both strains to validate that the observed differences were indeed due to the presence of *aga* in the *raf* locus. Growth experiments demonstrated that neither strain could thrive solely on raffinose (Appendix E), providing confirmation of the essential role played by the *aga*-encoded alpha-galactosidase in raffinose metabolism (Rosenow et al., 1999). However, the mechanism by which 60CSF could metabolise raffinose despite the early stop codon in *aga* remained unclear, especially as the truncated protein was predicted to lack the C-terminal region that harbors the catalytic and active sites, implying that this protein would lack functionality. Further long-read sequencing using the Nanopore platform (Appendix H) and genome analysis suggested that 60CSF might have multiple copies of *aga*, potentially one without the early stop codon, thus enabling raffinose metabolism. Unfortunately, due to being unable to successfully generate a complete genome of 60CSF, this is still uncertain and requires further investigation.

Analysing the gene expression levels of *rafR*, *aga*, *rafK*, and *rafG* mRNA, essential components of the RafR-regulated transcriptional units, through qRT-PCR unveiled notable distinctions between the strains. Unexpectedly, *rafR* expression was absent in both strains. However, the expression level of *rafG,* encoding a cognate permease of the ABC transporter, remained consistent in both, suggesting the functionality of the raffinose ABC transporter in both strains. However, *aga* and *rafK* expression was significantly higher in 60CSF compared to 60B. The reduced *rafK* expression in

60B, in comparison to 60CSF, may limit raffinose import into the cell, as RafK is crucial for energizing the ABC transporter (Marion et al., 2011a). Consequently, this may explain why 60B cannot metabolise and grow with raffinose, as it lacks the necessary RafK function for efficient raffinose import. Furthermore, previous work has found that pneumococci lacking RafK showed a significant reduction in expression of *aga* and *rafEFG* (Tyx et al., 2011). This suggests that the diminished expression of *aga* in strain 60B could be attributed to a lower level of RafK.

Notably, the transcriptional activator of the *raf* operon, RafR, was undetectable in both 60B and 60CSF. *rafR* and *rafS* are co-transcribed, and they regulate the raffinose-dependent stimulation of a second promoter controlling *aga* expression (Rosenow et al., 1999). This suggests that the operon's regulation is highly influenced by cellular raffinose levels. Therefore, the decreased transcription of raffinose uptake genes in 60B might be due to an excess accumulation of raffinose, possibly stemming from a lack of alpha-galactosidase activity. This surplus raffinose may interact with the regulatory protein, RafR, leading to the repression of these genes in 60B when compared to 60CSF. Alternatively, 60B may be lacking functional dihydrolipoamide dehydrogenase (DLDH) which has been demonstrated to have a role in raffinose metabolism (Smith et al., 2002; Tyx et al., 2011). Specifically, it has been shown that pneumococci lacking DLDH have reduced ability to metabolise alpha-galactosides, such as raffinose and stachyose (Smith et al., 2002). The nanopore sequencing (Appendix H) indicates that 60B does encode DLDH, however, further studies will need to be conducted to determine if the DLDH is functional, which could be driving the differences in raffinose metabolism observed between these two clinical isolates.

In an effort to understand the impact of raffinose metabolism on disease tropism in closely-related pneumococcal isolates, as previously observed (Minhas et al., 2019; Minhas et al., 2020), we conducted *in vivo* experiments using an intranasal murine infection model with strains 60B and 60CSF, and bacterial counts were assessed in the blood, brain, ears, lungs, and nose of mice. Surprisingly, neither strains were detected in the blood at 24 h. Subsequent studies, based on exploring the transition of pneumococci from the nasopharynx to the brain (Audshasai et al., 2022), were carried out in which groups of 6 to 8 mice were intranasally infected with either 60B or 60CSF and bacteria enumerated in the nasopharynx, lungs, blood, ears and brain at different time points (5 min, 5 hour, 10 hour and 24 hour) post-infection (Appendix F). Here, both strains were detected in the blood at 5 h post-infection but not at 24 h post-infection, indicating they may be unable to survive for long in this niche (Appendix F). Both strains were present at similar levels after in the brain and lungs at 24 h. However, in the nose at 24 h, mice infected with 60B had a higher bacterial burden compared to those infected with 60CSF. Notably, 60B was not detected in the ears of any

mice at 24 hours, whereas 60CSF was found in over 85% of the mice. This suggested that 60B either couldn't migrate to or survive in the ear following intranasal challenge. However, the results of the time course experiment indicated that 60B was present in the ears up to 10 hours post-infection but became undetectable at 24 hours, signifying its inability to thrive in the ears of mice (Appendix F). This finding aligns with prior research showing that regardless of serotype and sequence type, pneumococci isolated from the blood displayed lower bacterial burdens in the ears compared to those from other isolation sites (Trappetti et al., 2013; Amin et al., 2015; Minhas et al., 2019).

In a previous study by Minhas et al. (2019), increased raffinose metabolism was linked to fewer bacteria in the ears of infected mice, with the defect attributed to SNPs in *rafR* or *rafK*. However, in this investigation, utilising isolates derived from the same patient exhibiting significantly reduced genetic disparities and no detected SNPs in genes related to raffinose uptake and metabolism, it suggests that raffinose metabolism alone is unlikely to be the singular factor accountable for the observed niche adaptation in mice for strains 60B and 60CSF. To further validate this theory, a series of mutants employing gene-swap mutations, where genes from the *raf* operon are interchanged between 60B and 60CSF, could be employed to ascertain whether the observed *in vivo* and metabolic variances switch between strains, similar to prior studies (Minhas et al., 2019).

In order to investigate if other factors, such as capsule – the major virulence factor (Austrian, 1981; Ganaie et al., 2021), were potentially contributing to the observed *in vivo* differences between strains 60B and 60CSF, a series of *in vitro* tests were conducted. Previously it has been shown that the ability to metabolise various carbohydrates, such as galactose and uracil, can influence capsule production (Carvalho et al., 2011; Trappetti et al., 2017; Carvalho et al., 2018). Furthermore, it has been observed that as pneumococci transition from colonisation to host cell invasion during infection progression, they exhibit a substantial reduction in capsular polysaccharide (CPS) thickness, a phenomenon documented in studies like Hammerschmidt et al. (2005). Additionally, there are notable alterations in the expression of various virulence determinants, allowing pneumococci to adapt to the diverse host environments encountered throughout this process, as demonstrated in studies such as Orihuela et al. (2004) and Ogunniyi et al. (2012).

Therefore, it may have been possible that the ability to metabolise raffinose had a previously unknown impact on capsule production, resulting in the *in vivo* differences. However, it was found that there were no significant differences between strains in their capsule abundance and adherence capability, all of which have previously been demonstrated to have major impacts on

virulence (MacLeod and Kraus, 1950; Rosenow et al., 1997; Stoodley et al., 2004; Hammerschmidt et al., 2005). The ability to form biofilm also influences virulence, with biofilm-dispersed pneumococci displaying a remarkable capacity for colonising the nasopharynx at significantly higher levels in murine infection models compared to pneumococci cultured in broth (Trappetti et al., 2011b). Moreover, these dispersed bacteria exhibited an enhanced ability to disseminate to the middle ear and lungs, as documented in previous studies (Marks et al., 2013). Therefore, it may have been possible that the *in vivo* results were due to 60CSF being capable of forming biofilm, with pneumococci dispersing to the ears whilst 60B could not form biofilm. However, it was found that both 60B and 60CSF formed comparable levels of biofilm, indicating that this was not the cause of the *in vivo* differences observed.

In summary, the findings of Chapter 2 indicate that the observed *in vivo* differences between 60B and 60CSF were not associated with variations in capsule, adherence, or biofilm formation. While the differential ability to metabolise raffinose might contribute to the observed niche adaptation, this finding does not align with results from previous studies in blood and ear isolates of serotype 3 ST180 and serotype 14 ST15. In those studies, the blood isolates displayed the ability to metabolise raffinose (Minhas et al., 2019). Moreover, the absence of detectable SNPs or genetic differences in the genomes of 60B and 60CSF implies that the differences in niche adaptation are attributable to other unknown factors. To explore the possibility of epigenetic changes driving the observed *in vivo* distinctions, Chapter 3 investigates the *spnIII* Type I restriction-modification (RM) system in 60B and 60CSF (Agnew et al., 2023).

As previously discussed in Chapter 1, the *spnIII* Type I RM system can generate six distinct methyltransferase specificities (A-F), through recombination, with each specificity targeting a unique DNA sequence, thus governing different phasevarions. This can result in a single culture of pneumococci containing a mixture of six distinct cellular subtypes, with the cellular subtypes displaying phenotypic variations that favour either carriage or invasive disease. This system serves as a pivotal contingency mechanism enabling pneumococcal adaptation to dynamic environmental changes, particularly those encountered during the transition from asymptomatic colonisation to invasive pneumococcal disease. Evidently, the SpnD39III system emerges as a central regulatory mechanism that governs the fitness of the pneumococcus in various host niches (Manso et al., 2014).

Since the observed *in vivo* differences between 60B and 60CSF could not be attributed to genomic variations, the distribution of *spnIII* alleles in these strains was assessed using pneumococcal DNA

obtained from the nasopharynx of intranasally infected mice, as well as the inoculum used for the challenge.

It is noteworthy that the inoculum of 60B used to challenge the mice was primarily composed of *spnIIIB*, while the inoculum of 60CSF was mostly *spnIIIA*. Interestingly, the bacteria recovered from the nasopharynx of the infected mice showed no significant changes in *spnIII* allele proportions. 60B still predominantly displayed *spnIIIB*, and whilst 60CSF exhibited a similar proportion of both *spnIIIA* and *spnIIIB*, with a slight increase in *spnIIIB* compared to the inoculum. This suggests a slight shift in allele proportions during nasopharynx colonisation for 60CSF. Interestingly, it was previously demonstrated in a murine infection model that SpnD39IIIB-locked strains, only expressing *spnIIIB*, were able to colonise the nasopharynx to a greater extent than the other SpnD39III-locked variants (Manso et al., 2014). However, a fascinating study using a pneumococcal strain of serotype 6B (BHN418) investigated the shift of *spnIII* alleles during nasopharyngeal colonisation of humans found slightly different results (De Ste Croix et al., 2020). Here healthy volunteers were inoculated with 80000 CFU in 100 µl saline per nostril, and nasal wash samples were collected pre-inoculation and post-inoculation (days 2, 7, 14, and 21). Interestingly, in this study it was found that the bacteria obtained from human carriage were predominantly *spnIIID*, indicating that this phenotype is better suited to adherence in the human nasopharynx or is more able to avoid detection by the immune system. Importantly, the results of the human carriage study were not the same as what they found in their murine intranasal infection study, wherein *spnIIIB* and *spnIIIA* were the dominant alleles 7-days post-infection (De Ste Croix et al., 2020). Together, the results of the studies by Manso et al. and De Ste Croix et al., indicate that although *spnIIIB* may not be required for nasopharyngeal colonisation in humans, this *spnIII* variant is likely important in murine nasopharyngeal colonisation. It is crucial to emphasise that the human colonisation study utilised a serotype 6B clinical isolate (De Ste Croix et al., 2020), as opposed to a laboratory-adapted strain, again underscoring the significance of examining clinical isolates and exploring potential distinctions from extensively studied pneumococcal strains. Moreover, the disparate outcomes observed in the *in vivo* studies using distinct models (Manso et al., 2014; De Ste Croix et al., 2020) underscore the limitations associated with using mice as a sole source of information to infer the behaviour of pathogens in humans.

Thus, with the implication that *spnIIIB* aids in murine nasopharyngeal colonisation, the slight increase of *spnIIIB* in 60CSF may have contributed to the bacteria's survival in this niche.

The *spnIIIB* allele has also been linked to the LuxS/AI-2 quorum-sensing system (Section 1.8.2) with SpnD39IIIB-locked strains exhibiting significant downregulation of the *luxS* gene compared to

wildtype D39 and other SpnD39III-locked variants (Manso et al., 2014). Given the higher proportion of *spnIIIB* in the original 60B inoculum compared to 60CSF, *luxS* expression was measured, finding a significant downregulation of the *luxS* gene in 60B relative to 60CSF. As mentioned in Section 1.8.2, luxS encodes the metabolic enzyme S-ribosyl-homocysteine lyase, which converts S-ribosyl-homocysteine to homocysteine, an integral part of the activated methyl cycle. During this conversion, LuxS also generates the precursor to AI-2, called 4,5-dihydroxy-2,3-pentanedione (DPD), as a by-product, which is essential for the LuxS/AI-2 quorum-sensing system (Schauder et al., 2001; Winzer et al., 2003; Yadav et al., 2018). Hence, LuxS can regulate critical aspects of carbohydrate metabolism in pneumococci with the ability to metabolise various carbon sources being essential for successful nasopharyngeal colonisation and subsequent disease progression (Minhas et al., 2019; McLean et al., 2020). Comparison of the carbohydrate metabolic profiles of 60B and 60CSF, obtained from the nasopharynx of mice infected with the original 60B and 60CSF inoculums (Chapter 2)(Agnew et al., 2022), revealed that the strains recovered from the nasopharynx were now capable of metabolising L-fucose but unable to metabolise D-psicose. This suggests that during nasopharyngeal colonisation, 60B and 60CSF may have adjusted their carbohydrate metabolism to enhance their survival in this environment. Similar adaptations have been observed in the pneumococcal strain TIGR4 when grown in media mimicking the nasopharyngeal environment compared to when grown in media mimicking the blood (Im et al., 2022).

There are multiple examples of quorum sensing systems in pneumococci that have been shown to be critical for carbohydrate metabolism and adaptation to the host (Motib et al., 2019; Shlla et al., 2021). Furthermore, it has also been demonstrated in the TprA/PhrA quorum sensing system that sugar availability was able to regulate the expression of TprA, which in turn controls the expression of nine operons for galactose and mannose metabolism (Motib et al., 2019).

To further investigate whether the downregulation of the *luxS* gene contributed to the observed differences between 60B and 60CSF, *luxS* deletion mutants for both strains were generated, referred to as 60BΔ*luxS* and 60CSFΔ*luxS*. Interestingly, following carbohydrate metabolism analyses, it was found that both mutants exhibited metabolic profiles similar to those of 60B and 60CSF recovered from the nasopharynx of infected mice, rather than resembling the profiles of the original inoculum. These findings further support the theory that 60B and 60CSF undergo alterations within the nasal environment of mice, in which an increase of the *spnIIIB* allele to aid colonisation occurs, coupled with a decrease in *luxS* expression, thus resulting in similar metabolic profiles.

Importantly, the similar carbohydrate metabolic profiles of 60B and 60CSF recovered from the murine nasopharynx and the *luxS* mutants supports the notion of a connection between LuxS and the *spnIIIB* allele, as previously implicated (Manso et al., 2014). Further evidence of the link between *spnIIIB* and LuxS was uncovered by quantifying *spnIII* alleles in the 60BΔ*luxS* and 60CSFΔ*luxS* mutants. This analysis revealed a significant impact of *luxS* deletion on the proportions of *spnIII* alleles, with both 60BΔ*luxS* and 60CSFΔ*luxS* primarily containing *spnIIIC*, with a smaller proportion of *spnIIID* and little to no *spnIIIA* and *spnIIIB*. Unfortunately, little research has been conducted on *spnIIIC* and *spnIIID* (Manso et al., 2014), therefore a future avenue of research would be to gain a better understanding of the roles these alleles have in pneumococcal pathogenesis. Potentially, *in vivo* dual RNA sequencing using locked *spnIIIC* and *spnIIID* variants of 60B and 60CSF may reveal the interactions taking place between the pneumococci and host during disease in an intranasal murine infection model, as previously described (Minhas et al., 2020).

For the first time, these results indicate that in addition to the *spnIII* locus influencing *luxS* expression, LuxS is able to influence the switching of *spnIII* alleles. The exact nature of this unknown connection between the *spnIII* RM I system and *luxS* calls for further investigation to elucidate its precise nature and function. This unknown link is similar to what has previously been observed between the LuxS/AI-2 QS system and competence (CSP/Com) QS system in the laboratory strain D39 (Trappetti et al., 2011c) (Appendix B). Specifically, the deletion of *luxS* in D39 resulted in the downregulation of essential competence genes, including *ciaR*, *comD*, *comX*, *comW*, *cglA* and *dltA* (Trappetti et al., 2011c; Yadav et al., 2018). The CSP/Com QS system has been demonstrated to have multiple roles in pneumococcal virulence, such as aiding biofilm formation, and importantly genetic transformability, DNA uptake, recombination, production of bacteriocins, and fratricide (Håvarstein et al., 2006; Oggioni et al., 2006; Trappetti et al., 2011a; Martin et al., 2013; Vidal et al., 2013). Recently it has also been uncovered that activation of competence is important for adherence to the host (Minhas et al., 2023). This mechanism is facilitated through the action of the fratricin choline-binding protein D (CbpD). CbpD plays a pivotal role in exposing key virulence factors, PspA and PspC, on the cell surface (Rosenow et al., 1997; Iovino et al., 2017; Park et al., 2021a). Specifically, CbpD is predicted to cleave peptidoglycan, resulting in the shedding of the capsule and exposing PspA and PspC for binding, as proposed in Minhas et al. (2023). This theory finds support in previous studies that have demonstrated a reduced amount of capsule promotes adherence and colonization by exposing adhesive molecules (Hammerschmidt et al., 2005). Here, using wildtype D39 and D39 with *luxS* deleted we found that

deletion of *luxS* resulted in poorer adherence and invasion of Detroit 562 nasopharyngeal cells under certain conditions (Appendix B). Importantly, the addition of CSP-1 (100 ng/µL) drastically enhanced both the adhesion and invasion capabilities of D39 and complemented the defects in D39Δ*luxS*, supporting the findings of Minhas et al. (2023) for the role of complementation activation, through administration of CSP-1, in being essential for adherence.

Further studies into the link between the competence and LuxS/AI-2 QS systems using D39 mutants with deletion of either *luxS*, *comD* (encoding the CSP histidine kinase receptor) or *comE* (encoding the response regulator) revealed that *comE* may be able to indirectly regulate the LuxS/AI-2 QS system through an unknown mechanism (Appendix B). Specifically, it was found that the addition of exogenous CSP-1 produced a unique growth phenotype and increased AI-2 production in wildtype D39, that was not present in both the *luxS* and *comE* deletion mutants, implying that *comE* may be able to regulate AI-2 production (Appendix B).

In addition to potential regulation of the LuxS/AI-2 QS system by the competence QS system, fatty acids may also affect these QS systems in *Streptococcus pneumoniae*. Studies conducted within a range of different bacterial species, both Gram-negative and Gram-positive have indicated that fatty acids can affect quorum sensing systems (Soni et al., 2008; Nicol et al., 2018; Park et al., 2021b). In *S. pneumoniae*, it has been found that *briC*, encoding the biofilm regulator induced by competence, is co-transcribed alongside the genes within the fab gene cluster and its expression regulates the composition of membrane fatty acids in *S. pneumoniae*. Strains in which *briC* is knocked out show decreased *fabT* expression, leading to a noticeable shift in the composition of molecular species of membrane phospholipids. This indicates that BriC plays a role in regulating the FASII process in pneumococci, either directly or indirectly, through its influence on the transcription of the FabT regulon, importantly indicating there is a link between fatty acids and the competence QS system (Aggarwal et al., 2021). Although the link between the competence QS system and fatty acids has been identified, the effect of fatty acids on other QS systems, such as the LuxS/AI-2 QS system. Therefore, we have performed a preliminary investigated into the effect of fatty acids on the LuxS/AI-2 QS system in 60CSF and its respective *luxS* deletion strain. Preliminary results found that when grown in CDM with glucose as the sole carbon source, the addition of stearic acid (18:0) at a concentration of 62.5 µM resulted in impaired growth for both 60CSF and 60CSFΔ*luxS* (Appendix G). Strikingly, the addition of AI-2 (10 µM) restored the growth defect caused by the addition of the fatty acid, indicating that AI-2 may be able to inhibit the mechanism by which the fatty acid caused growth defects. In addition to impairing growth of both 60CSF and 60CSFΔ*luxS*, the supplementation of stearic acid impacts expression of genes within

the FakA/B system, which acts to assimilate exogenous fatty acids into the pneumococcal membrane (Parsons et al., 2014), and those involved in the LuxS/AI-2 QS system (Appendix G). Specifically, it was found that in 60CSF, the addition of both stearic acid and AI-2 appeared to result in increased *fruA*, *fakB1*, *fakB2* and *fakB3* expression. The expression of *fakB1*, *fakB2* and *fakB3* was also increased in 60CSF∆*luxS* with the addition of both AI-2 and stearic acid, although not to the extent as what was seen for 60CSF. In 60CSF the expression of *luxS* also appeared to have slightly increased with supplementation of AI-2 and stearic acid. The upregulation of the *fakB* genes when both strains were supplemented with stearic acid is not entirely unexpected as *fakB* genes encodes the fatty acid binding proteins, that are essential for the incorporation of external fatty acids into the cell membrane (Parsons et al., 2014). Importantly, detection of exogenous AI-2 has been shown to rely on FruA, a fructose-specific phosphoenolpyruvate-phosphotransferase system that exhibits high conservation among Gram-positive pathogens (Trappetti et al., 2017). The upregulation of *fruA* by 60CSF when both AI-2 and stearic acid is present has not been observed before and indicates that there may interplay occurring between the fatty acid uptake system and the predicted AI-2 receptor, FruA. Furthermore, the potential upregulation of *luxS* in the presence of both stearic acid and AI-2 further supports the hypothesis of a link between fatty acids and the LuxS/AI-2 QS system.

Past research has highlighted the connection between galactose metabolism and the LuxS/AI-2 QS system (Trappetti et al., 2017; Yadav et al., 2018; Tikhomirova et al., 2022)(see Appendix A). Using CDM with galactose as the primary carbon source it was found that 60B∆*luxS* displayed slower growth compared to 60B, while 60CSF∆*luxS* exhibited faster growth compared to 60CSF. These results suggest that the LuxS/AI-2 QS system has distinct roles in these two isolates. Earlier research conducted on the clinical ear isolate 947 (serotype 14 ST15) revealed distinctions in the effects of the LuxS/AI-2 QS system compared to those observed in the laboratory-adapted strain D39, suggesting a strain-specific role for LuxS/AI-2 (Trappetti et al., 2011c; Trappetti et al., 2017; Tikhomirova et al., 2022). To validate this theory, additional exploration involving strains of various serotypes and sequence types is necessary.

We examined the role of LuxS in the quorum-sensing system by introducing exogenous AI-2. Previous studies on D39∆*luxS* indicated that the addition of 10 µM AI-2 could restore growth, which was negatively impacted by the deletion of *luxS* (Trappetti et al., 2017). In contrast, serotype 14 blood and ear isolates displayed AI-2-dependent growth reduction in a dose-dependent manner (Tikhomirova et al., 2022)(see Appendix A).

Our investigation revealed that, in CDM with galactose, the addition of AI-2 disrupted the growth of wildtype 60CSF and 60B, consistent with observations in serotype 14 blood and ear isolates (Tikhomirova et al., 2022). However, in the case of 60BΔ*luxS*, the addition of 10 μM AI-2 improved growth in galactose-containing media, similar to previous findings with D39Δ*luxS* (Trappetti et al., 2017).

Biofilm formation has been shown to be impacted by the LuxS/AI-2 QS system (Trappetti et al., 2011c; Vidal et al., 2011; Vidal et al., 2013; Yadav et al., 2018). In CDM with glucose, 60BΔ*luxS* formed biofilm more quickly than the wildtype 60B, whilst 60CSFΔ*luxS* displayed delayed biofilm formation compared to wildtype 60CSF. Of note, the addition of AI-2 to glucose-containing media enhanced biofilm formation in wildtype 60B and 60CSF but had no effect on the *luxS* mutants. In CDM with galactose, both *luxS* mutants exhibited delayed biofilm formation compared to their wildtype counterparts (60B and 60CSF), with 60CSFΔ*luxS* eventually forming more biofilm than 60CSF. Again, the introduction of AI-2 increased biofilm formation in wildtype 60B and 60CSF but minimally affected biofilm formation in the *luxS* mutants. These results contrast with previous observations in D39 *luxS* deletion mutants has reduced biofilm, with the supplementation of AI-2 restoring biofilm production (Vidal et al., 2011; Trappetti et al., 2017) These findings suggest that in 60B and 60CSF, LuxS likely plays a metabolic role rather than a quorum-sensing role, which is a departure from what was observed in D39 (Vidal et al., 2011; Trappetti et al., 2017; Yadav et al., 2018) but more similar to what was observed in the serotype 14 ear isolate 947 (Tikhomirova et al., 2022). However, there are also differences to the study with strain 947, which found that *luxS* had an effect on adherence to epithelial cells, wherein the *luxS* mutant had reduced adherence (Tikhomirova et al., 2022). Notably, a difference in adherence was not observed with the 60BΔ*luxS* and 60CSFΔ*luxS* strains, regardless of AI-2 presence. Instead, these results aligned with observations from a D39Δ*luxS* mutant, which showed no differences in adherence to lung or larynx-derived cell lines (Stroeher et al., 2003). Importantly, it has previously been theorised that LuxS signalling in *S. pneumoniae* is not dependent upon high cell density, thus is not mediated by a quorum-sensing mechanism (Joyce et al., 2004), which is likely what is being observed in 60B and 60CSF. Together, these results underscore the strain-specific roles of LuxS.

Due to the established role of LuxS in the pathogenesis of D39 (Stroeher et al., 2003; Joyce et al., 2004; Trappetti et al., 2017; Yadav et al., 2018) and middle ear strain 947 (Tikhomirova et al., 2022), an intranasal murine infection model was used to assess the 60B and 60CSF *luxS* deletion mutants *in vivo*. As seen in Chapter 2 (Agnew et al., 2022), 60B was unable to survive in the middle

ear, whilst 60CSF thrived. Remarkably, 60BΔ*luxS* exhibited significantly higher bacterial burdens in the ears of infected mice compared to both 60B ($P < 0.0001$) and 60CSF ($P < 0.05$), similar to what was seen for the serotype 14 ST15 middle ear isolate 947 *luxS* deletion mutant (Tikhomirova et al., 2022). While the number of 60CSFΔ*luxS* and 60CSF pneumococci in the ears showed no significant difference, the lungs of infected mice had a significantly higher abundance of 60CSFΔ*luxS* ($P < 0.05$).

The increased bacterial burden of 60BΔ*luxS* in the murine ear compared to wildtype 60B, suggests, that for 60B, functional LuxS hampers survival in the ear up to 24 h (Appendix F). Previous studies with a D39 *luxS* deletion mutant found that *luxS* is required for persistence in the murine nasopharynx (Joyce et al., 2004; Trappetti et al., 2017). Therefore, it could be that in wildtype 60B, functional LuxS may act to facilitate adherence to the nasopharynx for 60B, whilst interfering with survival in other host niches, such as the ear. In contrast, the absence of LuxS in 60CSFΔ*luxS* contributed to its persistence in the murine lung, differing from observations in D39 *luxS* deletion mutants (Trappetti et al., 2017), indicating distinct roles for LuxS in the disease progression of these two clinical isolates.

The findings in Chapter 3 suggest that the distinct pathogenic profiles observed in Chapter 2 are likely influenced by multiple factors, potentially involving both *luxS* and the *spnIII* restriction-modification I system. Moreover, the results presented in Chapter 3 provide further evidence of an unidentified connection between *luxS* and the *spnIII* locus. This connection demands further investigation to uncover the precise underlying mechanism and its impact on disease progression.

This PhD project employed clinical pneumococcal isolates from a single paediatric meningitis patient to investigate factors affecting disease progression within the human body. The use of serotype 15C ST8711 strains from the blood and cerebrospinal fluid, derived from the same patient and instance of disease, minimised the impact of genomic diversity. This allowed for a detailed exploration of pneumococcal factors influencing disease progression within an individual patient.

Initial *in vitro* analysis revealed significant differences in carbohydrate metabolism between the strains, unrelated to genetic disparities. Subsequent *in vivo* investigations indicated the strains had distinct survivability in different anatomical niches of mice, potentially linked to the observed carbohydrate metabolism distinctions.

Further exploration into potential epigenetic factors unveiled the possible involvement of the *spnIII* restriction-modification I system in these two isolates. Additionally, a connection between the *spnIII*

locus and *luxS* in these clinical isolates was identified, suggesting for the first time that they may mutually influence the other and in turn influence the disease progression within a murine model. Notably, rather than its role in quorum sensing, LuxS appears to mainly have a metabolic role in these isolates, which may contribute to the observed differences in carbohydrate metabolism. However, further studies are needed to confirm that it is the role of LuxS in the activated-methyl cycle that is affecting these clinical isolates.

While not all the mechanisms governing disease progression and niche adaptation in these isolates have been fully elucidated, this research represents a significant leap in our comprehension of the strain-specific roles within *Streptococcus pneumoniae*. As the importance of using clinical isolates, as opposed to laboratory adapted strains, in traditional laboratory settings has been well demonstrated, combining these methods in combination with novel human infection challenges, may allow us to delve even more into a range of novel factors that affect disease progression. As an example, Minhas et al. (2019, 2020) examined clinical isolates identified as serotype 3; a serotype commonly linked to numerous instances of pneumococcal disease. Another research team has recently focused on creating a human infection challenge model specific to serotype 3 (Robinson et al., 2022). Potentially, these challenge models may become more widely utilised and enable us to fully elucidate how the factors identified in traditional laboratory settings influence pneumococcal disease in humans, with the subsequent promise for novel drug design and potential vaccine candidates.

Appendices

Appendix A: Published article (middle author)

pathogens

MDPI

Article

The Role of *luxS* in the Middle Ear *Streptococcus pneumoniae* Isolate 947

Alexandra Tikhomirova, Erin B. Brazel, Kimberley T. McLean, Hannah N. Agnew, James C. Paton and Claudia Trappetti *

Research Centre for Infectious Diseases, Department of Molecular and Biomedical Science, University of Adelaide, Adelaide, SA 5005, Australia; alexandra.tikhomirova@adelaide.edu.au (A.T.); erin.brazel@adelaide.edu.au (E.B.B.); kimberley.t.mclean@adelaide.edu.au (K.T.M.); hannah.agnew@adelaide.edu.au (H.N.A.); james.paton@adelaide.edu.au (J.C.P.)
* Correspondence: claudia.trappetti@adelaide.edu.au

Abstract: The LuxS protein, encoded by *luxS*, is required for the production of autoinducer 2 (AI-2) in *Streptococcus pneumoniae*. The AI-2 molecule serves as a quorum sensing signal, and thus regulates cellular processes such as carbohydrate utilisation and biofilm formation, as well as impacting virulence. The role of *luxS* in *S. pneumoniae* biology and lifestyle has been predominantly assessed in the laboratory strain D39. However, as biofilm formation, which is regulated by *luxS*, is critical for the ability of *S. pneumoniae* to cause otitis media, we investigated the role of *luxS* in a middle ear isolate, strain 947. Our results identified *luxS* to have a role in prevention of *S. pneumoniae* transition from colonisation of the nasopharynx to the ear, and in facilitating adherence to host epithelial cells.

Keywords: *Streptococcus pneumoniae*; quorum sensing; biofilms; otitis media

Citation: Tikhomirova, A.; Brazel, E.B.; McLean, K.T.; Agnew, H.N.; Paton, J.C.; Trappetti, C. The Role of *luxS* in the Middle Ear *Streptococcus pneumoniae* Isolate 947. *Pathogens* **2022**, *11*, 216. https://doi.org/10.3390/pathogens11020216

Academic Editors: Bindu Nanduri and Ed Swiatlo

Received: 18 December 2021
Accepted: 1 February 2022
Published: 7 February 2022

1. Introduction

Streptococcus pneumoniae colonizes the nasopharynx of up to 97% of infants [1], and frequently this colonization is asymptomatic [2]. However, *S. pneumoniae* can transition from this niche to cause a variety of diseases, including pneumonia upon transit to the lungs, sepsis once in the blood, meningitis upon transit to the brain and otitis media (OM) in the middle ear [3,4]. Persistence of *S. pneumoniae* within these niches relies on its ability to colonize varied host environments. Pertinent to *S. pneumoniae* persistence on mucosal surfaces, such as in the nasopharynx and middle ear, is its ability to form a biofilm community [5,6]. Biofilms exhibit a highly sophisticated structure whereby bacteria can exchange metabolic signals and communicate via a series of small peptide and diffusible autoinducer (AI) molecules. These molecules specifically induce changes in gene expression in target cells in a density-dependent fashion to help the establishment and maintenance of a biofilm. Such interactions are grouped under the general term quorum sensing (QS) systems, or more neutrally as cell–cell signalling systems [7].

In *S. pneumoniae*, *luxS*, encoding an s-ribosylhomocysteine lyase (LuxS), is responsible for producing the autoinducer-2 quorum sensing signal [8]. The AI-2 molecule is secreted into the extracellular environment where it is sensed by nearby bacteria and modulates their behaviour. Furthermore, AI-2 plays an important role in biofilm establishment [8]. In the laboratory strain D39, exposure to AI-2 molecule induces biofilm formation, while the deletion of the *luxS* gene results in a reduction in biofilm formation [8]. Interestingly, AI-2 can also increase the virulence of *S. pneumoniae* by shifting metabolic flux towards the catabolism of the sugar galactose, concomitantly increasing capsule production and transit from the nasopharynx to the lungs and the blood [9]. A previous study from our laboratory identified the AI-2 uptake system in Gram-positive bacteria [10]. In particular, we found that the fructose-specific phosphotransferase system (PTS) component FruA is the receptor for the universal QS signaling molecule AI-2 and elucidated the mechanism

whereby pneumococci increase the production of capsular polysaccharide and virulence in response to the AI-2 molecule.

Importantly, *luxS* expression has also been shown to be directly related to biofilm formation in clinical isolates [11]. A total of 25 serotype 3 isolates from distinct patients (12 from blood and 13 from ears) were sequence typed (ST) and assessed for biofilm formation and virulence phenotype. All 12 of the blood isolates formed more robust biofilms at pH 7.4. Conversely, all 13 of the ear isolates formed more robust biofilms at pH 6.8. Significantly, pH 7.4 and pH 6.8 correspond to the physiological pH of the blood and middle ear cavity, respectively. Importantly, biofilm formation paralleled *luxS* expression and genetic competence, and the level of *luxS* expression in blood isolates (in conditions optimal for these strains) was higher than *luxS* expression in the ear isolates in optimal conditions for biofilm formation of those strains, indicating that the key role of *luxS* in biofilm formation of isolates from distinct anatomical niches may differ [11].

Interestingly, in other bacterial species, *luxS* was shown to have strain-specific functions. In *Haemophilus influenzae*, *luxS* was found to have distinct roles in pathogenesis in isolates obtained from different niches. Strain 86-028NP, which was isolated from the nasopharynx of an otitis media patient, showed reduced biofilm formation and persistence in vivo when *luxS* was deleted [12]. In contrast, isolate R3157, isolated from the middle ear of an otitis media patient, showed no reduction in biofilm formation when *luxS* was deleted; moreover, it showed a hypervirulent phenotype in a chinchilla model of otitis media [13].

While a role for *luxS* has been shown in biofilm formation in both *S. pneumoniae* laboratory strain D39 and clinical isolates, an analysis of *luxS* in the pathogenesis of a middle ear isolate has not yet been performed, despite biofilm playing a role in the middle ear pathology. In this study, we aimed to assess a role of *luxS* in the biofilm formation and pathogenesis of the middle ear isolate 947, which we have previously characterized in detail [14].

2. Results

2.1. The Otitis Media Isolate 947 Displays Differences in Expression of Quorum Sensing Associated Genes Compared to the Blood Isolate 4559

We have previously shown that *S. pneumoniae* clinical isolates, which are closely related genomically and belong to the same serotype and multi locus sequence type (MLST), may display distinct virulence phenotypes in mice, in accordance with their original site of isolation in humans (blood versus ear) as well as different capacities to utilize carbon sources [14,15]. Importantly, strains isolated from patients with otitis media are more able to colonize the nasopharynx and utilize galactose as a carbon source, compared to the invasive clinical isolates [14]. Interestingly, we have shown that this capacity is linked to the LuxS/AI-2 quorum sensing system whereby AI-2 signaling via FruA allows the bacterium to catabolise galactose as a carbon source and upregulates the Leloir pathway [10].

To investigate this relationship further, we performed a gene expression analysis on Serotype 14 ST15 blood isolate 4559 and ear isolate 947, for which we have performed a genomic and phenotypic analysis in a previous publication, showing that the distinction in the virulence phenotype is driven by the inability of 947 to catabolise raffinose [14]. Both 4559 and 947 strains were grown to the same OD_{600} (0.2) in chemically defined media with glucose (Glc) as the sole carbon source (CDM + Glc), then washed and resuspended in chemically defined media with raffinose (Raf) as the carbon source (CDM + Raf) and chemically defined media with galactose (Gal) as the carbon source (CDM + Gal), and incubated for a further 30 min [14].

In CDM + Raf, expression levels of *luxS* and *fruA* were significantly greater in the blood isolate than in the ear isolate. However, in CDM + Gal *luxS* and *fruA* expression were significantly greater in the ear isolate (Figure 1). These results showed that *luxS* and *fruA* expression were induced by the presence of extracellular galactose in the ear isolate to a

greater extent than in the blood isolate. Thus, we further investigated the impact of *luxS* mutation in the ear isolate 947.

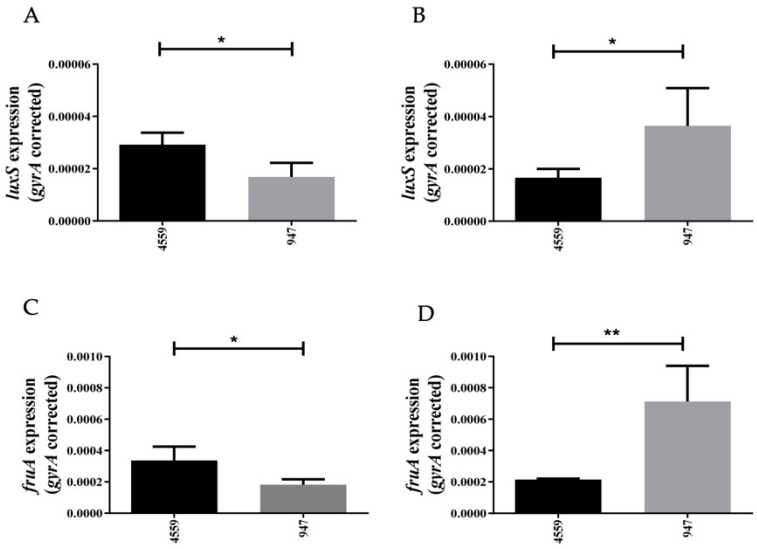

Figure 1. Relative expression of *luxS* (**A**,**B**) and *fruA* (**C**,**D**) in clinical isolates 947 and 4559 grown in CDM + Raf (**A**,**C**) and CDM + Gal (**B**,**D**) was quantitated by qRT-PCR with *gyrA* mRNA as an internal standard. Data are total expression relative to *gyrA* mRNA (mean ± the standard deviation of three independent experiments). *, $p < 0.05$; **, $p < 0.01$ (Student's unpaired *t* test).

2.2. Exogenous AI-2 Has Different Effects on the Blood and Ear Isolates

In the human upper respiratory tract, the principal sugar available for *S. pneumoniae* for use as a carbon source is galactose [16]. We have previously shown that supplementation of 10 µM AI-2 partially restored the growth defect of D39 *luxS*- in galactose media [10].

We therefore compared the effect of exogenous AI-2 on blood and ear isolates in galactose media. In CDM + Gal, there was a significant increase in the generation time of the blood isolate compared to the ear isolate, but a similar final cell density was observed (Figure 2). Interestingly, supplementation with 10 µM AI-2 increased the final cell density of the blood isolate, but had the opposite effect on the ear isolate, where the final cell density was significantly reduced in presence of AI-2 (Figure 2). Thus, previous observations obtained with the invasive D39 strain [10] are consistent with the role of *luxS* in the invasive blood strain 4559, but opposite effects were found in the ear isolate 947. These results suggest a strain-specific role for *luxS* in *S. pneumoniae*.

To confirm that the reduced growth of the otitis media isolate 947 in the presence of AI-2 was a dose-dependent phenomenon, we constructed a *luxS*- mutant and assessed the ability of these strains to grow in the presence of different concentrations of AI-2 (Figure 3). In CDM + Gal, there was a marked increase in the generation time and a reduction in the final cell density of the *luxS*- strain compared to the 947 wild type (WT) parent strain. To distinguish between true QS effects mediated by AI-2 from the indirect consequences of *luxS* disruption on the activated methyl cycle, we examined the capacity of various concentrations of exogenous AI-2 to complement the growth defect of *luxS*-. Supplementation with 10 µM AI-2 partially restored growth, but supplementation with lower (4 µM) AI-2 concentrations had no impact whatsoever and higher concentrations (20 or 100 µM) decreased the growth of *luxS*- strain. Interestingly, in 947 WT, the effect of 4 µM AI-2 had no effect on growth, but 10 µM inhibited growth, thereby confirming a dose-dependent effect previously observed in the D39 strain [10].

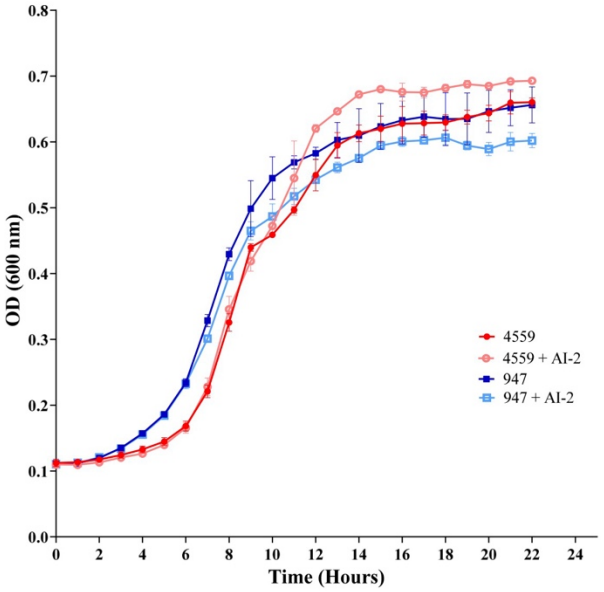

Figure 2. Relative growth of the clinical isolates 947 and 4995, with and without the addition of exogenous 10 µM AI-2 in CDM + Gal over a 24 h period.

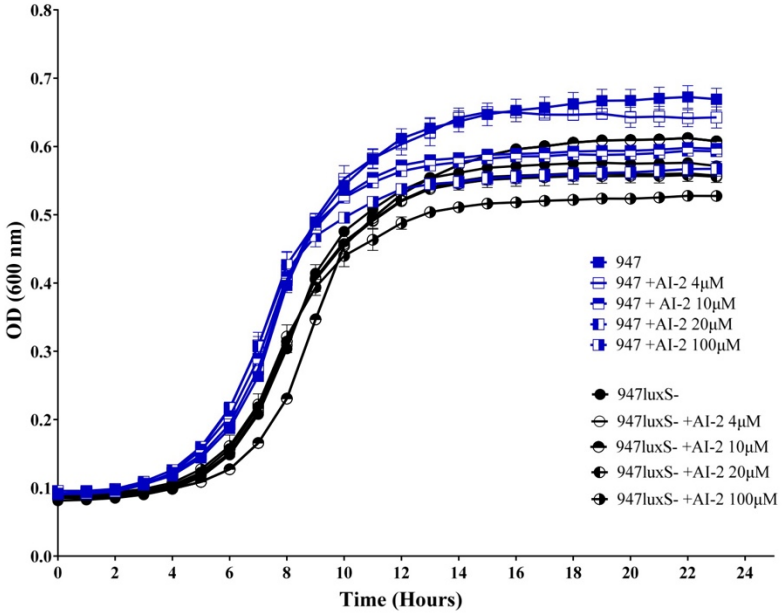

Figure 3. Impact of AI-2 on bacterial growth. 947 and 947 *luxS*- were cultured in CDM + Gal supplemented with 0, 4, 10, 20 or 100 µM and growth was monitored by measuring the OD_{600}. Data are mean values of triplicate cultures.

2.3. luxS Is Critical for Adherence of 947 to Epithelial Cells, but Does Not Play a Role in In Vitro Biofilm Formation

To further investigate the role of AI-2 in the otitis media isolate 947, we assessed the ability of the 947 WT, *luxS*- and complemented strains (comp strain) to adhere to the human nasopharyngeal Detroit 562 cell line. The *luxS*- strain had a significantly reduced ability to adhere to the Detroit cells in comparison to both the WT and complemented strain (Figure 4), indicating that *luxS* is potentially important for adherence to the host cell surface.

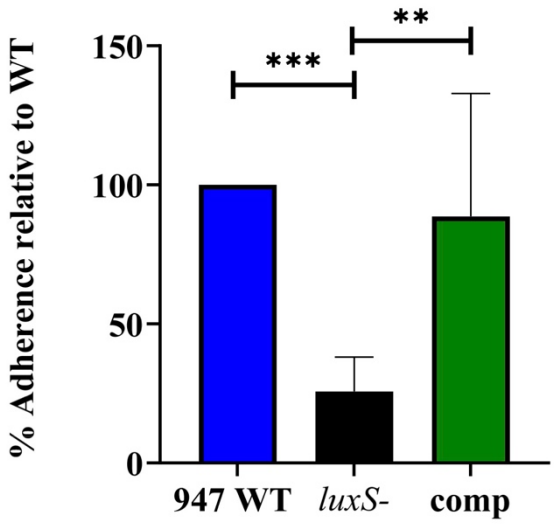

Figure 4. Adherence of the *luxS*- (black) and complemented (green) strain to Detroit 562 cells, presented as a percentage of the adherence of 947 WT (blue). **, $p < 0.01$; ***, $p < 0.001$.

As *luxS* has been shown to play a significant role in biofilm formation in the D39 strain [8], we assessed the capacity of the WT, *luxS*- mutant and complemented 947 strains to form a biofilm in vitro. For this assay we used the xCelligence (Agilent Technologies, Santa Clara, CA, USA) biofilm formation system. This new technology is a real-time cellular biosensor, which uses gold microelectrodes fused to the bottom of the surface of a microtiter plate to measure the electric potential across these electrodes. The presence of adherent bacteria at the electrode/solution interface impedes the electron flow. As shown in Figure 5, all three strains showed comparable biofilm formation in glucose and galactose media (Figure 5A,B, respectively), suggesting a different role for *luxS* in this otitis media isolate compared to the laboratory D39 strain.

2.4. luxS Does Not Influence Capsule Production, but Reduces the Capacity of the S. pneumoniae Middle Ear Isolate 947 to Cause Invasive Disease

We have previously shown that *luxS* has a specific role in *S. pneumoniae D39* pathogenesis [12,13]. Therefore, we assessed the infection profile of the 947 wild-type strain, its *luxS* mutant, and its complemented strain, in our intranasal murine challenge model [17].

Prior to murine challenge, the capsule was quantified using the FITC dextran exclusion assay, as previously described [18]. No significant differences were observed between the amount of capsule produced by the WT, *luxS*- or complemented strains (Figure 6).

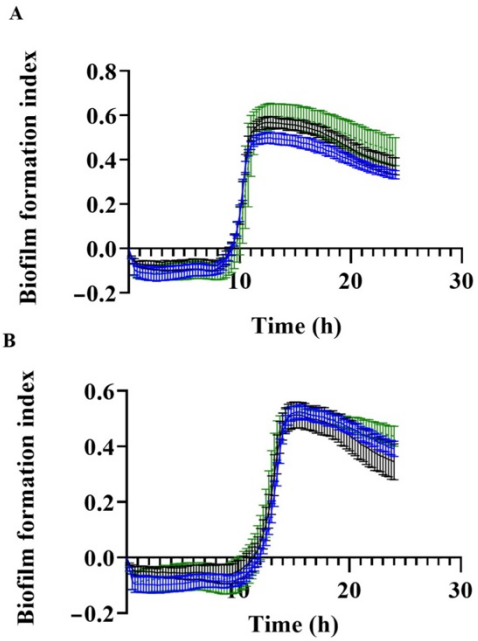

Figure 5. Biofilm formation index of 947 WT (blue), *luxS*- mutant (black), and complemented strain (green) over 24 h in (**A**) CDM + Glc and (**B**) CDM + Gal.

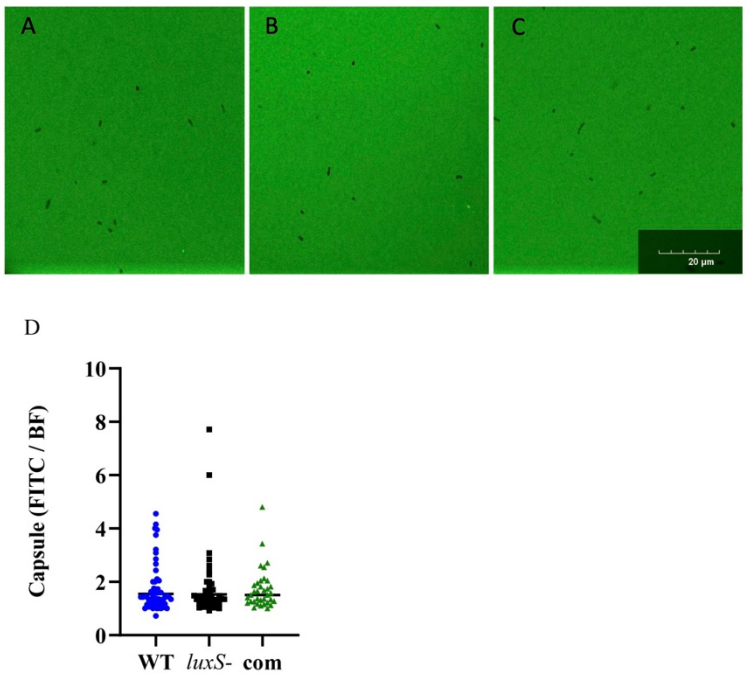

Figure 6. Capsule sizes of strains 947 WT, *luxS*- and complemented strains. (**A**–**C**): FITC-dextran exclusion images of 947 WT(**A**), *luxS*- (**B**) and complemented strains (**C**). All images are to the same

scale, taken using a 100X objective, and the scale bar indicates 20 µm. Capsule production by the 947 WT (blue circles), *luxS*- (black squares) and complemented (green triangle) strains, represented as the ratio of FITC to Bright Field (FITC/BF) image areas (**D**).

Groups of Swiss mice were challenged with 10^8 CFU of each strain, and bacterial loads were quantitated in various tissues 24 h post challenge (Figure 7). No significant differences in bacterial numbers in the nasopharynx were observed between the *luxS*- strain and WT-challenged mice. However, the *luxS* mutant was better able to persist in the nasopharynx of infected mice than the complemented strain, with a significantly higher geometric mean (GM) bacterial load ($p < 0.05$) (Figure 7). In the ear compartment, the bacterial loads of the *luxS* mutant were significantly greater than for mice challenged with either the WT or the complemented strains ($p < 0.01$) (Figure 7). A similar trend was also seen in the brain (Figure 7), although this was not statistically significant. Bacterial loads of all three strains in the lungs were comparable.

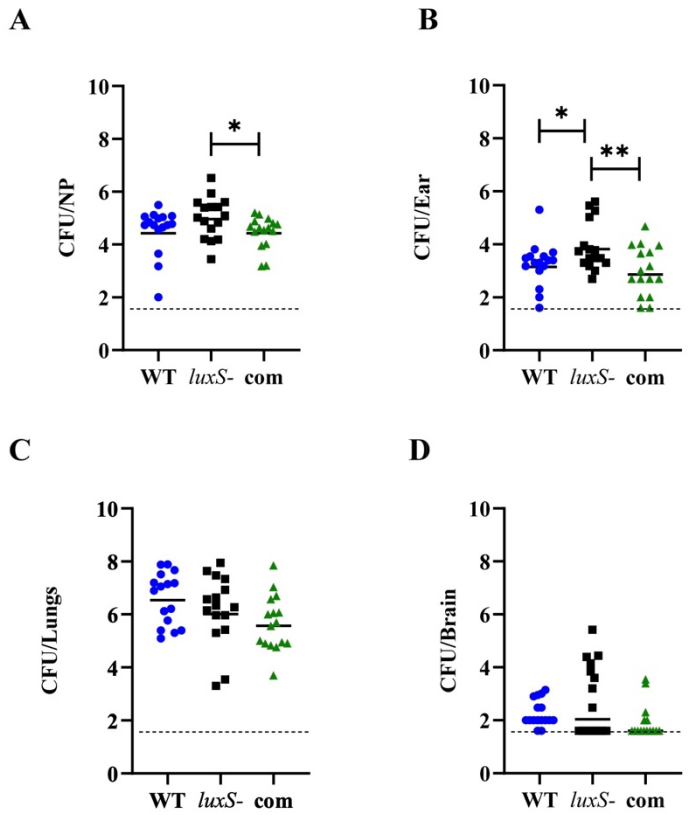

Figure 7. Virulence phenotypes of the 947 WT (blue circles), *luxS*- (black squares) and complemented (com, green triangles) strains at 24 h. Groups of eight mice were infected intranasally with 1×10^8 CFU of the respective strain and at 24 h, mice were euthanized and numbers of pneumococci in the (**A**) Nasopharynx, (**B**) Ear, (**C**) Lungs and (**D**) Brain were quantitated (see Materials and Methods). Viable counts (total CFU per tissue) are shown for each mouse at each site; horizontal bars indicate the geometric mean (GM) for each group, and broken lines indicate the limit of detection. Statistically significant differences in the GM bacterial loads between groups are indicated by asterisks (* $p < 0.05$, ** $p < 0.01$).

3. Discussion

The LuxS/AI-2 quorum sensing system has been shown to be central to biofilm formation and virulence in multiple bacterial species, including *S. pneumoniae*. In *S. pneumoniae* D39, a *luxS* mutant had an equivalent ability to colonize the murine nasopharynx compared to the WT, but had a reduced capacity to transit to the blood or the lungs [9]. Furthermore, *luxS* has also been demonstrated to be central to the biofilm formation of D39 *in vitro* [8], and adherence to human respiratory epithelial cells [19].

We previously compared and characterized the genomic and transcriptomic profiles of the *S. pneumoniae* blood isolate strain 4559 and the middle ear isolate strain 947 [14], which displayed very distinct *in vitro* and in vivo phenotypes. Interestingly, the ear isolate had a greater capacity to cause OM in mice relative to the blood isolate. OM has traditionally been viewed as a biofilm-mediated disease and thus connected to the LuxS/AI-2 Quorum sensing system. However, direct studies on ear isolates are missing and most of the research on *luxS*-mediated QS has been performed on invasive isolates such as D39. In this context, we endeavored to assess the role of *luxS* in the ear isolate 947.

Interestingly, we demonstrated the genes involved in AI-2-mediated QS, *luxS* and *fruA*, to have higher expression in the middle ear isolate 947, in comparison to the blood isolate 4559, indicating the potential importance of QS in this strain (Figure 1). The addition of exogenous AI-2 reduced the growth of 947 in galactose media, but enhanced the growth of 4559 (Figure 2). This suggested potential dose-dependent effects of AI-2 in strains with an initially different expression of QS-associated genes, as well as indicating strain-specificity effects of *luxS* in these clinical isolates (Figures 2 and 3). Remarkably, the concentration of the signaling molecule AI-2 required to complement the growth defect of the *luxS*- mutant in the 947 otitis media strain (Figure 3) is the same of that required to enhance the virulence strain D39 [10].

To further understand the role of *luxS* in the middle ear isolate 947, which displayed a higher expression of QS-associated genes, we assessed the ability of the 947 WT, its *luxS* mutant (*luxS-)* and complemented strains to adhere to human epithelial cells, to form a biofilm, and to cause disease in our murine model.

We have shown that the 947 *luxS*- mutant had a significantly reduced ability to adhere to human respiratory epithelial cells (Figure 4), but did not have attenuated biofilm formation in vitro (Figure 5), suggesting that adherence and potential downstream biofilm formation in this strain may be affected in vivo.

Interestingly, while *luxS* did not influence capsule production (Figure 6), it did impact the infection profile in our murine model (Figure 7). The 947 *luxS*- strain displayed an enhanced transit to the ear, a trend towards increased nasopharyngeal colonization and increased transit to the brain (Figure 7). An increased transit of the *luxS*- strain to the ear and brain in vivo, together with the reduced adherence to epithelial cells, suggests that functional *luxS* may act to facilitate an adherent lifestyle in vivo and to prevent transit to other host niches, characteristic of localized or systemic invasive diseases such as meningitis or otitis media. These results suggested an opposite role for *luxS* in the infection profile of the non-invasive strain 947 in comparison to the invasive isolate D39.

Our results have shown that the role of *luxS* in *S. pneumoniae* is not universal across strains, but rather it is strain-specific, and may be related to the genomic background of the isolate as well as its niche of isolation. Furthermore, 947 had a distinct expression of *luxS*-mediated QS genes compared to the blood isolate 4559, and a distinct impact on infection profile compared to the blood isolate D39. As 947 is a middle ear (OM) isolate, the role of *luxS* in this strain appears to involve the facilitation of adherence and limitation of spread to more invasive sites, whereas in D39, a laboratory strain originally isolated from the blood, *luxS* appears to drive transition to invasive disease. These results imply a need for a re-examination of the role of *luxS* in pathogenesis in a strain-specific manner, which may help to understand the pathogenesis of these strains, and define the role of *luxS* in these processes.

4. Materials and Methods

4.1. Bacterial Strains and Culture Conditions

The *Streptococcus pneumoniae* serotype 14 ST15 middle ear isolate 947 and blood isolate 4559, were used for initial gene expression experiments. The middle ear isolate 947 was the background used to create the following strains explored in this study: the 947 strains harbouring a mutation in *rpsL* (referred to as WT), the *luxS*- knockout 947 *rpsL* strain (referred to as *luxS*-), and the complemented 947 *rpsL* strain with wild-type *luxS* re-inserted into the *luxS*- strain (referred to as com), were used for this study. The transformation methods used previously for making mutants using the Janus cassette method were used to obtain all mutants used in this study [14]. All bacterial strains were cultured overnight on Columbia agar, supplemented with 5% horse blood, with or without 40 µg/mL gentamicin. Cells were routinely grown in serum broth for murine experiments, or in a chemically defined medium (CDM). CDM is comprised of SILAC RPMI 1640 Flex Media, no glucose, no phenol red (Sigma), supplemented with amino acids, vitamins, choline, and catalase as described previously [20], with either 0.5% glucose (CDM + Glc), 0.5% raffinose (CDM + Raf), or 0.5% galactose (CDM + Gal).

4.2. qRT-PCR Gene Expression Analyses

S. pneumoniae 4559 and 947, were grown to the same OD_{600} (0.2) in CDM + Glc, then washed and resuspended in CDM + Raf and CDM + Gal and incubated for a further 30 min. RNA was then extracted, and levels of *fruA* and *luxS* mRNA were then measured relative to gyrase mRNA by quantitative real-time reverse transcription-PCR (qRT-PCR) [15]. Primers used for qRT-PCR are listed in Table 1.

Table 1. Primers used in this study.

Primer	Sequence (5′–3′)
gyrA-RT-R	ACCTGATTTCCCCATGCAA
gyrA-RT-F	ACTGGTATCGCGGTTGGGAT
luxS-RT-F	CCCTATGTTCGCTTGATTGGGG
luxS-RT-R	AGTCAATCATGCCGTCAATGCG
fruA-RT-F	TCAATCGTCCAGTTGCTGAC
fruA-RT-R	TTTGTACAAGGCACCACCAA
luxS Janus down	CATTATCCATTAAAAATCAAACGGCTTTCGACAATAACTTCTTTTG
luxS Janus forw	GGAAAGGGGCCAGGTCTCTGCCTTTGAACGTCATGTGATTTAA
luxS forw	CAAATCAATGGCATCAAATCT
luxS down	TGATAAGGTGACAGACTTC
Janus forw	AGACCTGGGCCCCTTTCC
Janus down	CCGTTTGATTTTTAATGGATA

4.3. Construction of Mutants

The 947 *luxS*- and complemented strains were constructed using allelic exchange mutagenesis utilizing the Janus cassette, as previously described [17]. This was performed in a 3-step procedure. First, the endogenous *rpsL* in strain 947 (conferring streptomycin sensitivity) was replaced with *rpsL1* allele (which confers streptomycin resistance), by direct transformation. Subsequently, the Janus cassette (harbouring a kanamycin resistant marker and a dominant, counter-selective, *rpsL*+ marker) was used to replace the endogenous *luxS* by transformation of a linear PCR product comprising the Janus cassette flanked by 1-kb sequences 5′ and 3′ of *luxS*. Successful transformants were selected for kanamycin resistance and streptomycin sensitivity. Mutants were confirmed by PCR and Sanger sequencing using the primers listed in Table 1 (AGRF, Adelaide, Australia).

To complement the *luxS*- strain, a PCR product harbouring the *luxS* gene amplified from the WT 947, and 1 kb 5′ and 3′ of *luxS*, was transformed into the *luxS*- strain. Successful transformants were selected for streptomycin resistance and kanamycin sensitivity. The presence of the wild-type *luxS* was verified by PCR.

4.4. Assessment of Biofilm Formation

Biofilm formation was measured using the real time cell analyzer xCELLigence (Agilent Technologies, USA), as described previously for *Streptococcus mutans* [21]. This equipment allows for the detection of variations in the impedance signal, due to bacterial attachment and biofilm formation on the gold-microelectrodes present at the bottom of the E-plates (Agilent Technologies, USA). An initial baseline impedance reading of 150 µL of blank media for the sample wells, or 200 µL of media for the controls wells, was taken prior to bacterial cultures being added to wells. Bacteria were initially grown overnight on Columbia blood agar. Bacterial cells were resuspended in CDM+Glc to OD_{600} of 0.2. Fifty µL of bacterial cell suspension was added to the wells of the E-plate for a $\frac{1}{4}$ dilution. The xCELLigence system harbouring the bacterial cell cultures was incubated at 37 °C for the duration of the experiment. Biofilm formation was monitored over 24 h by recording the impedance signal at 15 min intervals.

4.5. Assessment of Capsule Production

Capsule thickness was assessed using the FITC-dextran exclusion assay previously described [18] and FITC-dextran of 2000 kDa (Sigma, St. Louis, MO, USA). Bacteria were cultured overnight on blood agar, and resuspended in a chemically defined medium (Silac) to an OD 0.7. Then, 80 µL of bacterial cell suspension was added to 20 µL of FITC dextran (10 mg/mL), 10 µL of the resulting suspension was then pipetted onto a microscope slide and a coverslip was applied firmly. Each strain was prepared twice on different days. The slides were viewed using a Olympus FV3000 Laser Scanning microscope with a 60× objective. The mean area of the FITC and Bright Field (BF) of 40–60 colonies of each strain was determined. Images were analysed using Zen 3.5 Software. Statistical analyses were performed using two-tailed Student's *t* test; *p* values of <0.05 were deemed statistically significant.

4.6. Murine Infection Model

Animal experiments were approved by the University of Adelaide Animal Ethics Committee (approval number S-2016-183). Groups of 16 female, outbred, 4–6 week old CD1 Swiss mice were anaesthetized and intranasally challenged with 1×10^8 CFU of the 947 WT, *luxS*- or complemented strains in 50 µL, as described previously. Nasopharyngeal, ear, lung, blood and brain tissue samples were collected 24 h post-infection. Tissue samples were homogenized in 1 mL of PBS, serially diluted and plated onto Columbia blood agar supplemented with 10 µg/mL gentamicin for viable cell enumeration [17]. Gentamicin supplementation specifically allowed for the detection of *S. pneumoniae*, preventing the interference of murine flora in CFU determination. Statistical analyses were performed using two-tailed Student's *t* test; *p* values of <0.05 were deemed statistically significant.

4.7. Adherence Assays

Adherence assays were carried out using the Detroit 562 human nasopharyngeal cell line. Cells were grown in Dulbecco's modified Eagle's medium (DMEM), supplemented with 10% fetal calf serum and 1% penicillin and streptomycin, at 37 °C, in 5% CO_2. The day prior to the inoculation of *S. pneumoniae* to the tissue cultures, wells of the 24-well tissue culture trays were seeded with the Detroit cells (2×10^5 cells per well) in DMEM with 10% FCS. Bacterial cells were resuspended in CDM+Glc at a final OD_{600} of 0.2. 500 µL of bacterial suspension was added to the washed Detroit cells. Concurrently, each bacterial suspension was added in the same volumes to empty wells, to serve as a control. After incubation for 2 h at 37 °C, wells were washed three times with PBS. Following this, cells were detached from the plate by treatment with 100 µL of 0.25% trypsin-0.02% EDTA, and 400 µL of Triton-x100. Samples were serially diluted and spot plated onto Columbia blood agar to enumerate the adherent bacteria. Assays were conducted in triplicate, and with three independent experiments. Data are presented as percentage of adherence relative

to the wild-type. Statistical analyses were performed using two-tailed Student's *t* test; *p* values of <0.05 were deemed statistically significant.

Author Contributions: Conceptualization, A.T. and C.T.; methodology, A.T., E.B.B., K.T.M., H.N.A., C.T.; software, A.T. and C.T.; validation A.T., E.B.B., K.T.M., H.N.A., C.T.; formal analysis, A.T.; investigation, A.T., E.B.B., K.T.M., H.N.A., J.C.P., C.T.; resources, J.C.P. and C.T.; data curation, C.T. writing—original draft preparation, A.T.; writing—review and editing, J.C.P., A.T. and C.T.; visualization, A.T.; supervision, C.T.; project administration, C.T.; funding acquisition, J.C.P. and C.T. All authors have read and agreed to the published version of the manuscript.

Funding: This work was supported by the Australian Research Council (ARC) Discovery Project 351 DP190102980 to C.T. and J.C.P., National Health and Medical Research Council (NHMRC) Program 352 Grant 1071659 to J.C.P., and NHMRC Investigator Grant 1174876 to J.C.P.

Institutional Review Board Statement: Animal experiments were approved by the University of Adelaide Animal Ethics Committee (approval number S-2016–183).

Acknowledgments: We would like to acknowledge Peter S Zilm for access and assistance with the xCelligence (Agilent Technologies, USA) biofilm formation system.

Conflicts of Interest: The authors declare no conflict of interest.

References

1. Chaguza, C.; Senghore, M.; Bojang, E.; Gladstone, R.A.; Lo, S.W.; Tientcheu, P.-E.; Bancroft, R.E.; Worwui, A.; Foster-Nyarko, E.; Ceesay, F. Within-host microevolution of *Streptococcus pneumoniae* is rapid and adaptive during natural colonisation. *Nat. Commun.* **2020**, *11*, 3442. [CrossRef] [PubMed]
2. Bogaert, D.; van Belkum, A.; Sluijter, M.; Luijendijk, A.; de Groot, R.; Rümke, H.; Verbrugh, H.; Hermans, P. Colonisation by *Streptococcus pneumoniae* and *Staphylococcus aureus* in healthy children. *Lancet* **2004**, *363*, 1871–1872. [CrossRef]
3. O'brien, K.L.; Wolfson, L.J.; Watt, J.P.; Henkle, E.; Deloria-Knoll, M.; McCall, N.; Lee, E.; Mulholland, K.; Levine, O.S.; Cherian, T. Burden of disease caused by *Streptococcus pneumoniae* in children younger than 5 years: Global estimates. *Lancet* **2009**, *374*, 893–902. [CrossRef]
4. Bergenfelz, C.; Hakansson, A.P. *Streptococcus pneumoniae* otitis media pathogenesis and how it informs our understanding of vaccine strategies. *Curr. Otorhinolaryngol. Rep.* **2017**, *5*, 115–124. [CrossRef] [PubMed]
5. Hall-Stoodley, L.; Hu, F.Z.; Gieseke, A.; Nistico, L.; Nguyen, D.; Hayes, J.; Forbes, M.; Greenberg, D.P.; Dice, B.; Burrows, A.; et al. Direct detection of bacterial biofilms on the middle-ear mucosa of children with chronic otitis media. *JAMA* **2006**, *296*, 202–211. [CrossRef] [PubMed]
6. Chao, Y.; Marks, L.R.; Pettigrew, M.M.; Hakansson, A.P. *Streptococcus pneumoniae* biofilm formation and dispersion during colonization and disease. *Front. Cell. Infect. Microbiol.* **2015**, *4*, 194. [CrossRef]
7. Mukherjee, S.; Bassler, B.L. Bacterial quorum sensing in complex and dynamically changing environments. *Nat. Rev. Microbiol.* **2019**, *17*, 371–382. [CrossRef]
8. Trappetti, C.; Potter, A.J.; Paton, A.W.; Oggioni, M.R.; Paton, J.C. LuxS mediates iron-dependent biofilm formation, competence, and fratricide in *Streptococcus pneumoniae*. *Infect. Immun.* **2011**, *79*, 4550–4558. [CrossRef]
9. Stroeher, U.H.; Paton, A.W.; Ogunniyi, A.D.; Paton, J.C. Mutation of *luxS* of *Streptococcus pneumoniae* affects virulence in a mouse model. *Infect. Immun.* **2003**, *71*, 3206–3212. [CrossRef]
10. Trappetti, C.; McAllister, L.J.; Chen, A.; Wang, H.; Paton, A.W.; Oggioni, M.R.; McDevitt, C.A.; Paton, J.C.J.M. Autoinducer 2 signaling via the phosphotransferase FruA drives galactose utilization by Streptococcus pneumoniae, resulting in hypervirulence. *mBio* **2017**, *8*, e02269-16. [CrossRef]
11. Trappetti, C.; van der Maten, E.; Amin, Z.; Potter, A.J.; Chen, A.Y.; van Mourik, P.M.; Lawrence, A.J.; Paton, A.W.; Paton, J.C. Site of isolation determines biofilm formation and virulence phenotypes of *Streptococcus pneumoniae* serotype 3 clinical isolates. *Infect. Immun.* **2013**, *81*, 505–513. [CrossRef] [PubMed]
12. Armbruster, C.E.; Hong, W.; Pang, B.; Dew, K.E.; Juneau, R.A.; Byrd, M.S.; Love, C.F.; Kock, N.D.; Swords, W.E. LuxS promotes biofilm maturation and persistence of nontypeable *Haemophilus influenzae* in vivo via modulation of lipooligosaccharides on the bacterial surface. *Infect. Immun.* **2009**, *77*, 4081–4091. [CrossRef] [PubMed]
13. Daines, D.A.; Bothwell, M.; Furrer, J.; Unrath, W.; Nelson, K.; Jarisch, J.; Melrose, N.; Greiner, L.; Apicella, M.; Smith, A.L. *Haemophilus influenzae luxS* mutants form a biofilm and have increased virulence. *Microb. Pathog.* **2005**, *39*, 87–96. [CrossRef] [PubMed]
14. Minhas, V.; Harvey, R.M.; McAllister, L.J.; Seemann, T.; Syme, A.E.; Baines, S.L.; Paton, J.C.; Trappetti, C. Capacity to utilize raffinose dictates pneumococcal disease phenotype. *mBio* **2019**, *10*, e02596-18. [CrossRef]
15. Minhas, V.; Aprianto, R.; McAllister, L.J.; Wang, H.; David, S.C.; McLean, K.T.; Comerford, I.; McColl, S.R.; Paton, J.C.; Veening, J.-W.; et al. In vivo dual RNA-seq reveals that neutrophil recruitment underlies differential tissue tropism of *Streptococcus pneumoniae*. *Commun. Biol.* **2020**, *3*, 293. [CrossRef]

16. Paixão, L.; Oliveira, J.; Veríssimo, A.; Vinga, S.; Lourenço, E.C.; Ventura, M.R.; Kjos, M.; Veening, J.-W.; Fernandes, V.E.; Andrew, P.W.; et al. Host glycan sugar-specific pathways in *Streptococcus pneumoniae*: Galactose as a key sugar in colonisation and infection. *PLoS ONE* **2015**, *10*, e0121042. [CrossRef]
17. Tikhomirova, A.; Trappetti, C.; Paton, J.C.; Watson-Haigh, N.; Wabnitz, D.; Jervis-Bardy, J.; Jardeleza, C.; Kidd, S.P. A single nucleotide polymorphism in an IgA1 protease gene determines *Streptococcus pneumoniae* adaptation to the middle ear during otitis media. *Pathog. Dis.* **2021**, *79*, ftaa077. [CrossRef]
18. Hamaguchi, S.; Zafar, M.A.; Cammer, M.; Weiser, J.N. Capsule prolongs survival of *Streptococcus pneumoniae* during starvation. *Infect. Immun.* **2018**, *86*, e00802-17. [CrossRef]
19. Vidal, J.E.; Howery, K.E.; Ludewick, H.P.; Nava, P.; Klugman, K.P. Quorum-Sensing Systems LuxS/Autoinducer 2 and Com regulate *Streptococcus pneumoniae* biofilms in a bioreactor with living cultures of human respiratory cells. *Infect. Immun.* **2013**, *81*, 1341–1353. [CrossRef]
20. Kloosterman, T.G.; Bijlsma, J.J.; Kok, J.; Kuipers, O.P. To have neighbour's fare: Extending the molecular toolbox for *Streptococcus pneumoniae*. *Microbiology* **2006**, *152*, 351–359. [CrossRef]
21. Abrantes, P.M.; Africa, C.W.J. Measuring *Streptococcus mutans*, *Streptococcus sanguinis* and *Candida albicans* biofilm formation using a real-time impedance-based system. *J. Microbiol. Methods* **2020**, *169*, 105815. [CrossRef] [PubMed]

Appendix B: Manuscript in preparation (first author)

Statement of Authorship

Title of Paper	Unravelling the Synergy of Competence Genes and the LuxS/AI-2 Quorum Sensing System in *Streptococcus pneumoniae*
Publication Status	☑ Unpublished and Unsubmitted work written in manuscript style
Publication Details	NA

Principal Author

Name of Principal Author (Candidate)	Hannah N. Agnew		
Contribution to the Paper	Designed and performed experiments, performed analysis on and interpreted data, and wrote the manuscript.		
Overall percentage (%)	50%		
Certification:	This paper reports on original research I conducted during the period of my Higher Degree by Research candidature and is not subject to any obligations or contractual agreements with a third party that would constrain its inclusion in this thesis. I am the primary author of this paper.		
Signature		Date	10/11/2023

Co-Author Contributions

By signing the Statement of Authorship, each author certifies that:

i. the candidate's stated contribution to the publication is accurate (as detailed above);
ii. permission is granted for the candidate in include the publication in the thesis; and
iii. the sum of all co-author contributions is equal to 100% less the candidate's stated contribution.

Name of Co-Author	Layla Mahdi		
Contribution to the Paper	Performed experiments.		
Signature		Date	08/11/2023

Name of Co-Author	Sophie N. Waters
Contribution to the Paper	Performed experiments.

Signature		Date	08/11/2023

Name of Co-Author	James C. Paton
Contribution to the Paper	Supervised development of work, provision of laboratory and materials.
Signature	Date 8/11/2023

Name of Co-Author	Claudia Trappetti
Contribution to the Paper	Designed and performed experiments, performed analysis on and interpreted data, and aided in writing the manuscript.
Signature	Date 9/11/2023

Unravelling the Synergy of Competence Genes and the LuxS/AI-2 Quorum Sensing System in *Streptococcus pneumoniae*

Hannah N Agnew[1], Layla Mahdi[2], Sophie N Waters[1], James C Paton[1] and Claudia Trappetti[1]

[1] Research Centre for Infectious Diseases, Department of Molecular and Biomedical Science, University of Adelaide, South Australia, Australia,

[2] School of Pharmacy and Medical Science, University of South Australia, South Australia, Australia

Keywords: *Streptococcus pneumoniae*, virulence, quorum sensing, LuxS/AI-2, competence.

Abstract

Streptococcus pneumoniae, the pneumococcus, is a major cause of morbidity and mortality each year, causing over 1 million deaths. Despite being a part of the normal nasopharyngeal flora in humans, it can switch to invasive pathogen through unknown mechanisms. Essential to disease progression is colonisation of the nasopharynx, which often includes the formation of biofilms on host mucosal surfaces. Pneumococci employ different types of quorum sensing (QS) systems to adhere on host mucosal surfaces, including the competence QS, which is modulated by the competence stimulating peptide (CSP), and the LuxS/Autoinducer-2 (AI-2) QS system. In this work we have investigated the regulatory link between the competence and LuxS/AI-2 QS systems in *S. pneumoniae* in the well characterised laboratory strain, D39. Growth analyses revealed a distinctive growth phenotype in wildtype D39 when synthetic CSP-1 was introduced into acidic pH media. However, this phenotype was absent in the *luxS* and *comE* mutant strains, suggesting that both genes are crucial for this unique growth phenotype, which appears to be conditional upon specific CSP-1 and pH conditions for wildtype D39. Strikingly, our study has also unveiled that AI-2 production is not solely under the control of LuxS. It can also be indirectly regulated by ComE. This discovery adds a layer of complexity to the interplay between these two QS systems in *S. pneumoniae*, shedding light on the intricate mechanisms governing biofilm formation in this pathogenic bacterium.

1. Introduction

During the early stages of childhood, *Streptococcus pneumoniae* establishes colonisation on the mucosal surfaces within the human nasopharynx (Bidossi et al., 2012). In this hospitable environment, these bacteria can persist for months asymptomatically, but they also possess the potential to disseminate to other regions of the body, through mechanisms that have not been well established, giving rise to a spectrum of diseases. These infections can manifest as invasive diseases, including meningitis, sepsis, and pneumonia in the brain, blood and lungs, respectively. Additionally, pneumococci can be responsible for non-invasive conditions such as sinusitis and otitis media, in the sinuses and middle ear, respectively.

Following colonisation, pneumococci possess the ability to assemble intricately structured and ever-changing multicellular communities, referred to as biofilms, on the epithelial surface of the nasopharynx. This ability to form biofilms on host mucosal surfaces plays a pivotal role in the development of both sinusitis in the sinuses, and otitis media in the middle ear. These biofilms serve as a defence mechanism, allowing pneumococci to elude the host's immune defences and the effects of antibiotics (Stoodley et al., 2004; Chao et al., 2014).

Within these biofilms bacteria are able to organise themselves into complex structured communities, engaging in intricate interactions that are facilitated by the release of small extracellular molecules. This bacterial communication is achieved through a process known as quorum sensing (QS), where bacteria secrete and detect specific extracellular chemical signalling molecules, known as autoinducers, in a dose-dependent manner. In both Gram-positive and Gram-negative bacteria, the most prevalent QS system is the LuxS/Autoinducer-2 (AI-2) system (Miller and Bassler, 2001). In the LuxS/AI-2 QS system, AI-2 is synthesised as a by-product of the conversion of S-ribosyl-homocysteine to homocysteine by the enzyme S-ribosylhomocysteine lyase (LuxS), an essential reaction in the activated methyl cycle (Winzer et al., 2003).

In *S. pneumoniae*, the *luxS* gene is present in both invasive and carriage strains. LuxS/AI-2 signalling exerts a profound influence on various genes associated with critical cellular processes and virulence factors, including biofilm formation (Vidal et al., 2013; Trappetti et al., 2017; Yadav et al., 2018). In the well-studied laboratory strain D39, deletion of *luxS* resulted in defective biofilm formation (Trappetti et al., 2011c) and reduced capacity to cause invasive disease in a murine intranasal infection model (Stroeher et al., 2003). Furthermore, these investigations have unveiled multiple alterations in gene expression within *luxS* mutant strains (Trappetti et al., 2017; Yadav et al., 2018). These findings underscore the pivotal role of LuxS/AI-2 signalling in the regulation of virulence and biofilm formation in S. pneumoniae.

Another extensively documented Quorum Sensing (QS) system is the CSP/Com QS system, which holds significant importance for most streptococcal species, as it is vital for their ability to genetically transform DNA. Competence, a state of genetic transformability, is triggered by the competence stimulating peptide (CSP), a 41-amino acid polypeptide. This CSP is initially synthesised as a propeptide and subsequently exported and processed by a dedicated ABC transporter called the *comCDE* operon (Stock et al., 2000; Vidal et al., 2013).

Within this system, *comD* encodes the CSP histidine kinase receptor, whilst *comE* encodes the response regulator. The secreted CSP in the extracellular milieu is detected by the ComDE two-component signalling system, setting in motion the expression of early competence genes. ComE takes the lead by activating transcription of its own operon, comCDE. This, in turn, induces the transcription of *comAB*, responsible for CSP secretion, and the alternative sigma factor ComX (Peterson et al., 2004). ComX, then triggers the expression of late competence genes, which are essential for DNA uptake, recombination, production of bacteriocins, and cell wall lysis (Håvarstein et al., 2006; Martin et al., 2013). This last phenomenon is commonly referred to as 'fratricide,' a process wherein cell wall lysins can kill and release DNA from non-competent sibling cells sharing the same ecological niche (Steinmoen et al., 2002). The Com QS system, through this intricate cascade of events, is integral to the acquisition and sharing of genetic material among streptococcal species.

There is accumulating evidence pointing towards the integration of the LuxS/AI-2 QS system into the regulatory network governing both competence and cell autolysis (Romao et al., 2006; Trappetti et al., 2011c; Vidal et al., 2011; Yadav et al., 2018). In the current study we have investigated the potential interplay between the LuxS/AI-2 and competence QS mechanisms within the *Streptococcus pneumoniae* laboratory strain D39.

2. Materials and methods

2.1 Bacterial strains and growth conditions

The *S. pneumoniae* strains used in this study are listed in Table 1. Bacterial strains were routinely grown in a casein-based semisynthetic liquid media (C+Y) or on Columbia agar plates supplemented with 5% (vol/vol) horse blood (BA plates) at 37° with 5% CO_2. BA plates were supplemented with 0.2 µg/ml erythromycin and 200 µg/ml spectinomycin for selection of mutant strains. Bacterial stocks were prepared from mid-log-phase cultures and stored at -80°C in 10% glycerol for use in growth assays.

Table 1. *S. pneumonia* strains used in this study.

Strain name	Serotype	Origin	Notes
D39	2 (capsular)	NCTC7466	Reference strain
D39Δ*luxS*	2	Trappetti et al., 2011	
D39Δ*comE*	2	This study	
D39Δ*comD*	2	This study	

2.2 Construction of mutant strains

The mutant strains, D39Δ*comE* and D39Δ*comD*, were generated in *S. pneumonia* wildtype D39 using splicing by overlap extension in which *comD* or *comE* was deleted and replaced by a spectinomycin antibiotic resistance cassette. Linear DNA containing the antibiotic resistance cassette was generated by overlap extension PCR as described previously (Iannelli and Pozzi, 2004) using primers listed in Table 2.

Table 2. Primers used in this study.

Primer	Sequence (5'-3')	Source or reference
16S F	GGTGAGTAACGCGTAGGTAA	Trappetti et al., 2011
16S R	GGTGAGTAACGCGTAGGTAA	Trappetti et al., 2011
luxS RT F	CCCTATGTTCGCTTGATTGGGG	Trappetti et al., 2011
luxS RT R	AGTCAATCATGCCGTCAATGCG	Trappetti et al., 2011
comD RTF	AAGGCATGCTCTGCTTACAT	Trappetti et al., 2011

comD RT R	CCTGAAGGAGTCATCGTCAT	Trappetti et al., 2011
comX RT F	CCAAGGGACTGTGTATAAGTG	This study
comX RT R	CTACGCTTCTGACTTTCCTGC	This study
comE 1 up	CATAAAGTTCAAATGGAG	This study
comE 2 down	TATGTATTCATATATATCCTCCTCAAATTCCCTCTTAAATCT	This study
comE 4 down	CGTTCCAGCTTCTATACTCAC	This study
comE 3 up	AAATAACAGATTGAAGAAGGTATAATTGACAATTAGCAAGAAAT	This study
comD 1 up	GATGGTATCGCAGAGTATTC	This study
comD 2 down	TATGTATTCATATATATCCTCCTCTACTCTTTCCCCTTATTTC	This study
comD 3 up	AAATAACAGATTGAAGAAGGATAAGAAGATGTTATTGAACATCAAG	This study
comD 4 down	CCCTTGACCAACGGACCTTC	This study

2.3 Growth assays

Stocks of pneumococci were diluted 10-fold into fresh C+Y medium (pH 7.4 or 6.8) to a starting optical density at 600nm (OD_{600}) of 0.04 and incubated at 37°C with 5% CO_2 to an OD_{600} of 0.4. These cultures underwent a 10-fold diluted again in the same C+Y media as the preculture or in C+Y medium supplemented with 50, 100 or 500 ng/µl CSP-1 or CSP-2 (Chiron Technologies, Australia). Bacterial strains were then inoculated into a final volume of 200µl in a 96-well microtiter plate or 12 ml in 20 mL tubes. The plate and tubes were incubated at 37°C with 5% CO_2 for 24 h, with OD_{600} recorded for the plate every 30 min using a Spectramax spectrophotometer (Molecular Devices). Assays were conducted triplicate with at least two repeated independent experiments.

2.4 Adherence and Invasion assays

Adherence and invasion assays were carried out using the Detroit 562 human pharyngeal cell line as previously described (Trappetti et al., 2011b; Amin et al., 2015). Detroit 562 human pharyngeal cells were grown in Dulbecco's modified Eagle's medium (DMEM) supplemented with 10% foetal calf serum (FCS), 100 U/mL penicillin and 100 µg/mL streptomycin at 37°C in 5% CO_2. Wells of 24-well tissue culture trays were seeded with Detroit cells in DMEM with 10% FCS as previously described (Trappetti et al., 2011b) and left to grow overnight. Cells were inoculated with 500 µL of each bacterial suspension grown overnight on BA plates and resuspended in C+Y at pH 6.8 or pH 7.4 with or without CSP-1 (100 ng/µL) at a final OD_{600} of 0.2. The same volume of each bacterial strain was added to empty wells as a control. Adherence assays were conducted after incubation of the bacteria with the Detroit cells for 2 h at 37°C. The wells were washed 3 times with PBS, the cells were detached from the plate by treatment with 100 µL 0.25% trypsin-0.02% EDTA and 400 µL of 0.1% Triton X-100 (Sigma), and samples were plated on BA plates to determine the number of adherent bacteria. Invasion assays were carried out essentially as described above. After the post-adherence washing step, cultures were incubated for 1 h in fresh media supplemented with 200 µg/mL gentamicin and 10 µg/mL penicillin to kill extracellular bacteria. Monolayers were again washed, lysed, serially diluted, and plated on BA, as described above. The assays were conducted in triplicate with at least two repeated independent experiments. Statistical analysis was carried out using a two-tailed Student's t-test; P values < 0.05 were considered statistically significant. Data collected are presented as mean adherent or invasive bacteria ± standard error mean (SEM) in CFU/mL. The controls were used to monitor bacterial growth during the 2 h incubation period, ensuring strains grew at similar rates.

2.5 AI-2 activity assay

Relative levels of AI-2 in cell-free culture fluids of *S. pneumoniae* strains were measured using the *Vibrio harveyi* bioluminescence assay as described previously (Bassler et al., 1993; Bassler et al., 1997). The *V. harveyi* strains were grown in Autoinducer Bioassay (AB) medium containing 0.3M NaCl, 0.05M MgSO4, 10ml of 1M KPi, 1ml of 0.1M L-arginine and 0.2% Casamino acids (Difco, MI) per 100 ml of water. The pH was brought to 7.5 using NaOH and the medium filter-sterilised, before adding 2ml of sterile 50% glycerol. Briefly, *V. harveyi* BB170 (-l*uxN*) reporter strain and BB152 AI-2 producing strain were incubated in 10ml AB medium for 16 h at 30°C with shaking (200rpm) before centrifuging 1ml of the *V. harveyi* BB152 culture at 12600 rpm for 3 min. The

supernatant containing AI-2 was filter-sterilised with 0.45 µm membrane filters and stored at -20°C. To examine the influence of CSP-1 on the LuxS expression and AI-2 production in the different pneumococcal strains, the strains were incubated as described in **Section 2.2** using 1 mL of culture. Cell free culture fluids were prepared as described above for the *V. harveyi* BB152 culture. The *V. harveyi* BB170 was diluted 1:5000 in AB medium. The supernatants were assessed for AI-2 activity at 10% (v/v), using the *V. harveyi* reporter strain incubated at 30°C with shaking (Bassler et al., 1993; Turovskiy and Chikindas, 2006). Bioluminescence measurements were taken after 4, 5 and 6 h of growth using the Glomax luminometer (Promega). After 4 hours growth OD_{600} was measured using the Spectramax spectrophotometer (Molecular Devices).

2.6 RNA extraction and qRT-PCR

Pneumococcal strains were grown in C+Y medium (pH 7.4 or 6.8) with or without CSP-1 (100 µg/ml) to an OD_{600} of 0.1 or 0.4 for the early and late exponential phases of the first growth peak and early- (16 h) and late-exponential (20 h) phase of the second growth curve. 1 mL of cell cultures were aliquoted into 2 ml of RNAprotect bacteria reagent (QIAGEN) and incubated for 5 min at room temperature (RT). Bacterial cultures were pelleted by centrifugation at 4500 rpm for 15 minutes at 4°C. Cell pellets were stored at -80°C or used directly for RNA extraction. The pellet was resuspended in 300µl of pre-warmed (65°C) acid-chloroform-isoamyl alcohol (125:24:1 Ambion), transferred to a 1.5 mL Eppendorf tube and incubated for 5 min at 65°C. 300µl of pre-warmed NAES-buffer (50mM sodium acetate pH 5.1, 10mM EDTA, 1% SDS) was added and the mix was vortexed before being incubated for 5 min at 65°C. The samples were placed on ice for 1 min before being centrifuged at 16000rpm for 1 min. The supernatant was transferred to a new tube and sodium acetate added to a final concentration of 300mM. The RNA was precipitated with 2 volumes of ethanol at -80°C for 2h or overnight. Samples were centrifuged 16000rpm at 4°C for 30 min and the pellet resuspended in 700µl of 70% ethanol before being centrifuged at 16000rpm for a further 15 min at 4°C. The pellet was dried and resuspended in 50 µl nuclease free water. DNase treatment was performed using 6µl DNase RQ1 (Promega,10U/µl), 6µl 10x DNase-buffer RQ1(Promega) and incubating for 30 min at 37°C and blocked for 10 min at 65°C. PCR was performed using the 16S primers to test for DNA contamination. The amount of RNA was quantified using the Nanodrop 1000 Spectrophotometer.

Real-time PCR was performed using the Invitrogen superscript III Platinum SYBR Green one-step qRT-PCR kit (Invitrogen). The specific primers used for the various genes are listed in **Table 2** and were used at a final concentration of 200µM per reaction. The 16S primers, specific for 16S rRNA, was used as an internal control. Amplification was performed by using the Roche LC480 real-time

cycler. The relative gene expression was analysed by using the comparative critical threshold ($2^{-\Delta\Delta CT}$) method (Livak and Schmittgen, 2001).

3. Results

3.1 Wildtype *S. pneumoniae* strain D39 displays different growth phenotypes in presence/absence of synthetic CSP-1 at different pH levels.

In *Streptococcus pneumoniae*, the competence-stimulating peptide (CSP) is a small signalling molecule that induces competence for genetic transformation. CSP is secreted by pneumococcal cells and acts as an autoinducer, triggering the expression of genes necessary for the uptake and integration of exogenous DNA. The efficiency of pneumococcal transformation can be influenced by the concentration of CSP in the environment. Different concentrations of CSP can have varying effects on the induction of competence and subsequent transformation, but the effect of CSP on growth has not been fully studied. To examine this effect wildtype D39 was grown in a semisynthetic media, C+Y, in the presence or absence of different concentrations (50, 100 or 500 ng/µL) of synthetic CSP-1. At the lowest concentration of 50 ng/µL of CSP-1, the growth of D39 in this condition was comparable to growth without CSP-1 being present (Figure 1). However, upon increasing the concentration to 100 ng/µL of CSP-1, a second growth peak appeared at approximately 16 h, reaching an OD_{600} of approximately 0.7. Upon further increasing the concentration of CSP-1 to 500 ng/µL, the second growth peak appeared at approximately 13 h, however the OD_{600} was lower than what was present for CSP-1 at 100 ng/µL, only reaching 0.6 (Figure 1). In *S. pneumoniae*, natural transformation is a crucial mechanism for genetic exchange and adaptation. During competence, pneumococci are capable of taking up exogenous DNA from their environment, integrating it into their genome, and acquiring new genetic traits. The pH of the environment can influence the transformation process, but the exact mechanism of how pH affects pneumococcal transformation is a complex area of study. To assess if different pH conditions had an impact on the observed growth phenotype D39 was grown in C+Y with a pH of 6.8 (mimicking the ear cavity) or 7.4 (mimicking the blood environment) supplemented with 100 ng/µL of CSP-1, as this was the concentration that had the largest impact on growth. In Figure 2, it can be seen that in C+Y at pH 6.8 with or without CSP-1, D39 begins growing earlier than in C+Y at pH 7.4. Additionally, the addition of CSP-1 to C+Y at pH 6.8 still results in a second growth peak (as seen in Figure 1), however when CSP-1 is added to C+Y pH 7.4, no second growth peak is observed (Figure 2). Furthermore, when other concentrations (50 or 500 ng/µL) of CSP-1 was supplemented to C+Y pH 7.4, no second growth peak appeared (data not shown). Furthermore, when CSP-2 was

used, this second growth peak was absent in all conditions (data not shown), suggesting this phenomenon is pherotype-specific.

Together these results suggest that the second growth peak requires CSP-1 at a concentration of at least 100 ng/µL and is sensitive to the pH of the C+Y medium. Importantly, it has been shown that the expression of *luxS* is directly associated with biofilm formation in clinical isolates under varying pH conditions (Trappetti et al., 2011c).

3.2 Addition of CSP-1 enhances adherence and invasion capabilities of D39 and complements D39Δ*luxS* adherence and invasion defects

Recently, it has been found that activation of competence, via addition of CSP-1, is critical for host adherence by increasing the surface exposure of several choline-binding proteins (CBPs) (Minhas et al., 2023). Furthermore, the LuxS/AI-2 QS system has previously been shown to be necessary in adherence to epithelial cells (Tikhomirova et al., 2022). Therefore, to investigate the effect of the interplay between the LuxS/AI-2 QS system and competence system on adherence and invasion, D39 and D39Δ*luxS* strains were used. The *in vitro* adherence and invasion of each strain to Detroit 562 pharyngeal cells was investigated in C+Y at either pH 6.8 or pH 7.4 with or without the addition of CSP-1 (100 ng/µL). In Figure 3A, that in C+Y at pH 6.8 without CSP-1 D39Δ*luxS* was significantly less adherent than D39. Furthermore, in C+Y at pH 7.4 without CSP-1, D39Δ*luxS* was also significantly less invasive than wildtype D39 (Figure 3B). Importantly, for both D39 and D39Δ*luxS* in C+Y at both pH 6.8 and pH 6.4, the addition of CSP-1 resulted in enhanced adhesion and invasion (Figure 3). Together these results demonstrate that *luxS* is required for adhesion at pH 6.8 and invasion at pH 7.4 and that the addition of CSP-1, activating competence, complements the defects observed in D39Δ*luxS* and enhances the adhesion and invasive capabilities of wildtype D39.

3.3 Mutant strains D39Δ*luxS* and D39Δ*comE* display different growth to wildtype D39 in the presence of CSP-1

Based on the results presented, we began further exploration of the connection between the CSP/Com and LuxS/AI-2 QS systems. A series of deletion mutants were created in D39, specifically deleting either *comD* or *comE,* in addition to the *luxS* deletion mutant. The effect of these mutations on growth was then determined by growing the strains in C+Y at different pH levels (6.8 or 7.4) with or without CSP-1 supplementation. The *luxS* deletion mutant, D39Δ*luxS*, showed similar growth to D39 initially in C+Y (pH 6.8) without CSP-1 present, however when wildtype D39 entered stationary phase, D39Δ*luxS* continued to grow, albeit at a slower rate than the initial

exponential phase, reaching a final OD_{600} of 0.6 compared to wildtype D39 at OD_{600} of 0.4. The addition of CSP-1 (100 ng/µL) to C+Y (pH 6.8) still caused D39 to form a secondary growth curve, reaching OD_{600} 0.8, whilst D39Δ*luxS* had no second growth curve, reaching an OD_{600} of 0.7 (Figure 4A). When grown in C+Y (pH 7.8) with or without CSP-1 supplementation, D39Δ*luxS* began growing earlier than wildtype D39, however both reached a similar final OD_{600} of 0.4, which was lower than what was observed in C+Y at pH 6.8 (Figure 4B). As seen previously in Figure 1, supplementation with CSP-1 in C+Y at pH 7.4 had no effect on D39 growth, a result that was mirrored by D39Δ*luxS* (Figure 4B). Taken together, these results indicate that D39Δ*luxS* grew slightly better than wildtype D39 in C+Y at both pH 6.8 and 7.4, with the supplementation of CSP-1 having little effect on growth of D39Δ*luxS*.

The *comD* deletion mutant showed an earlier growth than wildtype D39 in C+Y at pH 6.8 with or without CSP-1 supplementation (Figure 5A). Furthermore, similar to D39 when CSP-1 was present, a second growth curve began at approximately 20 h. Interestingly, even when CSP-1 was not present, a second growth curve began, indicating that the phenotype was not dependent on exogenous CSP-1 (Figure 5A). In C+Y at pH 7.8, regardless of CSP-1 supplementation, D39Δ*comD* began growing slightly earlier than wildtype D39, however both reached similar OD_{600} with no second growth curve present (Figure 5B).

Interestingly, the D39Δ*comE* strain began growth earlier than D39 in C+Y at pH 6.8 and 7.4, reaching a similar OD_{600} of approximately 0.4 in both conditions (Figure 5). At either pH level, the addition of exogenous CSP-1 had no discernible effect on growth, indicating that the second growth curve observed in the presence of CSP-1 in C+Y (pH 6.8) for wildtype D39 and D39Δ*comD* is dependent on *comE* being present.

3.4 CSP-1 supplementation increases *luxS* and competence gene expression in strain D39 growing in C+Y medium at pH 6.8 and 7.4.

To investigate the molecular mechanism causing the second growth peak in D39 in C+Y (pH 6.8) when supplemented with CSP-1, the gene expression of *luxS* and competence genes, *comD* and *comX*, was measured for D39 grown under various conditions. D39 strain was grown to OD_{600} 0.1 (early exponential phase) or 0.4 (late exponential phase) in C+Y pH 6.8 or 7.4 with or without CSP-1 (100 ng/µL) supplementation (Figure5). Here it was found that during early exponential phase, *comD* was expressed at extremely low levels, and whilst *luxS* had higher expression, neither pH level nor supplementation of CSP-1 had a discernible effect on gene expression (Figure 6A). Strikingly, the expression of *comX* was drastically increased with the addition of CSP-1 at both pH 6.8 and 7.4 (Figure 6A).

In the later exponential phase, *comD* continued to exhibit low expression levels under all tested conditions (Figure 6B). The expression pattern of *comX* remained consistent with what was observed in the early exponential phase: the addition of CSP-1 increased expression in D39 grown in C+Y at both pH 6.8 and 7.4 (Figure 6B). Notably, there were significant changes in *luxS* expression compared to the early exponential phase (Figure 6A). As depicted in Figure 6B, there was no substantial difference in *luxS* expression when grown in C+Y media at pH 6.8, regardless of the presence of CSP-1. However, in C+Y pH 7.4, *luxS* expression was relatively low compared to that in C+Y pH 6.8 and the addition of CSP-1 drastically elevated luxS expression (Figure 6B).
The expression levels of the genes *luxS*, *comD*, and *comX* were assessed following the cultivation of D39 in C+Y medium (pH 6.8) with or without CSP-1 for 16 and 20 hours. This analysis aimed to understand the alterations occurring during the second growth peak, as illustrated in Figure 1. In Figure 7, it can be observed that *luxS* expression was similar at 16 h with or without CSP-1 supplementation. After 20 h in C+Y (pH 6.8) with no CSP-1 supplementation, there was greater *luxS* expression compared to at 16 h (Figure 7). Additionally, at 20 hours, CSP-1 supplementation led to a substantial increase in *luxS* expression in C+Y (pH 6.8) (Figure 7), and while both *comD* and *comX* expression levels were highest with CSP-1 supplementation at 16 hours, the increase was less pronounced at 20 hours (Figure 8).
These findings shed light on the dynamic gene expression patterns of *luxS*, *comD*, and *comX* in different growth phases and under varying environmental conditions, providing valuable insights into the regulatory mechanisms at play.

3.5 Autoinducer 2 production is influenced by LuxS and ComE

To investigate whether the change in *luxS* expression observed during late exponential phase of the second growth peak in C+Y (pH 6.8) with CSP-1 supplementation resulted in more AI-2 production, the AI-2 released by D39 was quantified. Similar to the qRT-PCR assay, samples were obtained at 16 and 20 h, during the second growth peak, from D39 grown in C+Y (pH 6.8) with or without CSP-1 (100 ng/µL) supplementation. As shown in Figure 9, D39 cultured for 16 hours exhibited consistent AI-2 levels, irrespective of CSP-1 supplementation, aligning with the *luxS* expression data illustrated in Figure 7. At the 20-hour mark without CSP-1 supplementation, AI-2 activity remained comparable to that observed at 16 hours (Figure 9). However, the introduction of CSP-1 led to a notable rise in AI-2 levels (Figure 9), echoing the *luxS* expression trends depicted in Figure 7.
To further elucidate the link between the two QS systems, the AI-2 activity was also measured for wildtype D39, D39Δ*comE* and D39Δ*luxS* during the first growth peak at early (OD_{600} 0.1)

exponential and, for D39 only, late (OD_{600} 0.4) exponential phase when grown in C+Y (pH 6.8 or 7.4) with or without CSP-1 (100 ng/µL) supplementation. For D39Δ*luxS* and D39Δ*comE* strains cultivated to OD_{600} 0.1, minimal AI-2 was detected following growth in C+Y medium at both pH 6.8 and 7.4, regardless of the presence of CSP-1 (Figure 10). Intriguingly, when D39 was grown to OD_{600} 0.1 in C+Y medium at pH 7.4 with or without CSP-1, there was a substantial increase in AI-2 levels compared to growth in C+Y medium at pH 6.8, irrespective of CSP-1 supplementation (Figure 10). At OD_{600} 0.4, D39 cultured under all conditions exhibited comparable AI-2 levels, indicating that the addition of CSP-1 at this stage had minimal effects (Figure 10). Importantly, these results are not reflective of what was observed for *luxS* expression at these time points, wherein *luxS* expression at OD_{600} 0.1 was relatively low and only higher at OD_{600} 0.4 (Figure 6).
Collectively, these findings confirm the anticipated necessity of LuxS for AI-2 production. The deletion of LuxS in D39 resulted in significantly reduced AI-2 activity, aligning with expectations. Intriguingly, the results also suggest a potential role for ComE in AI-2 regulation. Deleting *comE* from D39 led to remarkably low AI-2 levels in the mutant strain compared to wildtype D39 grown under identical conditions.

4. Discussion

Streptococcus pneumoniae employs two distinct quorum sensing (QS) systems for biofilm formation. The first QS system centres around a 17-amino-acid peptide known as the competence-stimulating peptide (CSP), which is secreted by *S. pneumoniae.* In the CSP/Com system, CSP is detected by the histidine kinase, ComD, which initiates a cascade of molecular events. The phosphate group is transferred to the response regulator protein, ComE, resulting in the activation of genes that play a crucial role in the regulation of genetic competence (Martin et al., 2013).
The second QS system relies on the universal Autoinducer-2 (AI-2) signalling molecule. The *luxS* gene encodes S-ribosylhomocysteine lyase, an enzyme responsible for generating the quorum sensing molecule AI-2 as a by-product within the activated methyl cycle. Notably, studies have revealed that a pneumococcal *luxS* mutant strain displays impairments in biofilm formation and a reduced capacity to cause invasive diseases when compared to wild-type pneumococci (Stroeher et al., 2003; Trappetti et al., 2011c; Yadav et al., 2018). Previously it has been observed that in a D39 *luxS* deletion mutant, the competence genes *comD, comX, comW, cglA* and *dltA* were all directly related to *luxS* expression. Specifically, when *luxS* was deleted, expression was severely downregulated, whilst overexpression of *luxS* resulted in upregulation of competence gene expression. Furthermore, the *luxS* deletion mutant displayed decreased genetic competence, as measured by transformation frequency (Trappetti et al., 2011c). Based on these findings, it was

proposed that *luxS* may be a central regulator for competence. Therefore, we present compelling evidence that further establishes a regulatory connection between the competence and LuxS/AI-2 QS systems.

In this investigation, we explored the *in vitro* growth patterns of four different *S. pneumoniae* strains: the wildtype D39, along with mutants lacking *luxS*, *comE*, and *comD* genes. We observed their growth responses upon the addition of synthetic CSP-1 at varying pH levels (7.4, resembling the blood environment, and 6.8, resembling the ear cavity). Remarkably, wildtype D39 exhibited a distinct second growth peak approximately 16 hours after entering the stationary phase, notably in C+Y medium at pH 6.8, when exposed to synthetic CSP-1. Interestingly, this growth phenomenon did not occur in the *luxS* and *comE* mutant strains, even under the same conditions. Surprisingly, the *comD* mutant displayed a second growth peak without the addition of synthetic CSP-1. Previous studies have identified two forms of the histidine kinase ComD, ComD-1 and ComD-2, differing in 12 amino acid positions and specific for CSP-1 and CSP-2, respectively (Håvarstein, 2003; Johnsborg et al., 2004). Consequently, supplementation with CSP-2 under identical conditions did not induce the secondary growth phase within 24 hours, indicating the pherotype-specific nature of this second growth phenomenon, likely involving ComD-1.

Our findings strongly suggest the critical role of the *luxS* and *comE* genes in facilitating this unique second growth phenomenon, which appears to be specific to CSP-1 within the D39 strains. Furthermore, we found that the pH of the growth medium significantly influenced the occurrence of this secondary growth phase. Specifically, strains cultured in medium with a pH of 6.8 exhibited the second growth peak, while those grown in medium with a pH of 7.4 did not exhibit this behaviour. Additionally, the initiation of the second growth peak correlated with the concentration of exogenously added synthetic CSP-1; higher CSP-1 concentrations led to an earlier onset of the secondary growth phase.

These differences in growth suggest that despite ComD being required for internalising CSP, it is ComE that is having an impact on growth. Previous work has found that ComE can be phosphorylated by the serine-threonine kinase (StkP) under acidic conditions independent of ComD, resulting in the regulation of 104 genes involved in different cellular processes, such as oxidative stress tolerance (Piñas et al., 2018). This suggests that ComE may be a global regulator of multiple genes, as it participates in both histidine kinase dependent and independent stress regulatory systems. As the results in the current study observed the second growth phenotype at the more acidic pH level 6.8, it could be that ComE is being phosphorylated by StkP, thus resulting

in differential gene regulation than if it had been phosphorylated by ComD, leading to differences in growth phenotype.

To determine the molecular bases underpinnings of how *luxS* impacted this second growth phenomenon, we employed qRT-PCR to delve into the relative gene expression patterns of *luxS* and the competence genes, *comD* and *comX*. The supplementation of CSP-1 resulted in a notable augmentation in the gene expression of *luxS* and both competence genes, *comD* and *comX*, during both growth phases regardless of pH level. During the early exponential phase of the first growth peak, addition of CSP-1 increased expression of *comD* and *comX,* however it had no discernible effects on *luxS* expression. However, at late exponential phase of the first growth phase, addition of CSP-1 in C+Y media at pH 7.4 resulted in significantly more *luxS* expression than in other conditions, whilst similar results were observed for *comD* and *comX* as in early exponential phase. For the second growth peak, the genes related to competence in strain D39 exhibited the highest expression levels after 16 hours of growth in C+Y medium at pH 6.8 supplemented with CSP-1. It should be noted that addition of CSP-1 at either time point did result in significantly higher gene expression of *comD* and *comX* than when CSP-1 was absent from the media. Notably, *luxS* gene expression reached its zenith after 20 hours of growth in the presence of CSP-1.
The gene expression changes displayed during both growth peaks indicate that *comD* and *comX* are upregulated at early exponential phase when CSP-1 is present, whilst *luxS* is upregulated in the presence of CSP-1 at late exponential phase when the strains are beginning to enter stationary phase. The upregulation of *luxS* at late exponential phase, when pneumococci are transitioning to stationary phase, indicates that the bacteria may be beginning to enter a biofilm-forming lifestyle, which requires the LuxS/AI-2 QS system (Trappetti et al., 2011c; Trappetti et al., 2017; Yadav et al., 2018).

Our study delved into the roles played by the LuxS/AI-2 Quorum Sensing system and competence in the capacity of D39 to adhere to and invade epithelial cells. While earlier research with D39 didn't highlight the criticality of *luxS* in adhering to lung or larynx-derived cell lines (Stroeher et al., 2003), a study involving the clinical middle ear isolate 947 (Serotype 14 ST15) indicated the importance of *luxS* in adherence to pharyngeal cells (Tikhomirova et al., 2022). Notably, recent findings suggest that activating competence through CSP-1 supplementation enhances host adherence (Minhas et al., 2023). In our investigation, we observed that under C+Y conditions at pH 6.8, D39Δ*luxS* exhibited lower adherence to Detroit 562 pharyngeal cells compared to wildtype D39, in contrast to prior research (Stroeher et al., 2003). The disparity in results might be attributed to

varying environmental conditions experienced by the strains. Furthermore, at in C+Y at pH 7.4 wildtype D39 demonstrated a greater ability to invade pharyngeal cells than D39Δ*luxS*. Importantly, it was found that for C+Y at both pH 6.8 and pH 7.4, the addition of CSP-1 significantly enhanced the ability of wildtype D39 to adhere to and invade Detroit 562 cells. Similarly, supplementation with CSP-1 restored the D39Δ*luxS* strain's capacity to adhere to and invade the pharyngeal cells. Furthermore, at pH 7.4 in C+Y, wildtype D39 displayed a superior ability to invade pharyngeal cells compared to D39Δ*luxS*. Crucially, the addition of CSP-1 significantly improved the adherence and invasion capabilities of both wildtype D39 and D39Δ*luxS* under C+Y conditions at both pH 6.8 and 7.4. This supplementation effectively restored the adherence and invasion potential of the D39Δ*luxS* strain. Previous work with a D39 *luxS* deletion strain found that deletion of *luxS* results in less capsule production and reduced colonisation of the nasopharynx in an intranasal infection model (Trappetti et al., 2017), similar to the results seen here where the *luxS* deletion strain showed less adherence to nasopharyngeal cells. Although it has previously been found that reduced capsule facilitates adhesion and consequent colonisation through the exposure of surface virulence factors (Hammerschmidt et al., 2005), the reduced amount of capsule in D39Δ*luxS* may not be enough to enhance adhesion and there may be other factors at work that prevent successful adherence.

Minhas et al.'s study (2023) revealed that the activation of competence is pivotal for host adherence and subsequent invasion, primarily through the action of the fratricin choline-binding protein D (CbpD). CbpD facilitates the exposure of key virulence factors, PspA and PspC, on the cell surface (Rosenow et al., 1997; Iovino et al., 2017; Park et al., 2021a). Specifically, CbpD is predicted to cleave peptidoglycan resulting in shedding of the capsule and exposing PspA and PspC for binding (Minhas et al., 2023), with previous studies supporting this theory as reduced amount of capsule has been found to promote adherence and colonisation, due to the exposure of adhesive molecules (Hammerschmidt et al., 2005).

Therefore, it is plausible that the addition of CSP-1 triggers competence in both D39 and D39Δ*luxS*, resulting in the exposure of PspA and PspC due to capsule shedding via CbpD activity. This, in turn, facilitates adherence to and invasion of Detroit 562 pharyngeal cells, as previously demonstrated (Minhas et al., 2023). It appears that the adherence and invasion shortcomings resulting from the *luxS* deletion can be compensated for by the activation of competence, leading to the exposure of critical virulence factors, PspA and PspC, which are essential for binding to and invading epithelial cells (Iovino et al., 2017; Park et al., 2021a; Minhas et al., 2023).

While LuxS is classically recognized for its involvement in AI-2 production, our current study sheds new light on the complex interplay of components. Specifically, we propose that ComE indirectly influences AI-2 production. Our evidence for this interaction was further substantiated through a bioluminescence assay employing the *Vibrio harveyii* BB170 reporter strain, which allowed us to quantify AI-2 secretion by *S. pneumoniae* into the surrounding media. Our findings revealed intriguing patterns in AI-2 concentrations. During the early exponential phase, a notably high AI-2 concentration was detected in the first growth peak of D39 incubated in medium at pH 7.4, regardless of the supplementation of CSP-1. However, a significant AI-2 concentration was also measured during the second growth peak, occurring after 20 hours, when D39 was cultivated in medium at pH 6.8 with CSP-1 supplementation. This observed pattern in AI-2 concentration corresponds to the gene expression data for the *luxS* gene, as mentioned earlier, highlighting the complex dynamics of AI-2 production in this context. Notably, in the *comE* deletion mutant, minimal AI-2 was detected, suggesting that *comE* has a role in the regulation of AI-2 production.

Previous studies have highlighted that acidic stress triggers LytA-mediated autolysis, a process regulated by a CSP-independent ComE pathway, which is instead phosphorylated by StkP (Piñas et al., 2018). This suggests that ComE has the capacity to sense acidic stress, while the two-component system CiaRH operates through a ComE-independent pathway to protect cells from the consequences of activated acidic stress-induced lysis (ASIL). Notably, CiaRH null mutants exhibit *comE* derepression and CSP-dependent autolysis induction under alkaline pH conditions (Piñas et al., 2008). This scenario opens up the possibility that the observed peak may indeed be attributed to autolysis. Our experimental results support this notion. Specifically, the *comE* mutant did not display this second peak after 24 hours of growth in medium at pH 6.8, even in the presence of exogenously added synthetic CSP-1. Conversely, the *comD* mutant exhibited the second peak, irrespective of CSP presence.

Based on our observations, it is reasonable to postulate that LuxS is either directly or indirectly dependent on CSP-1 and ComE, as both the *luxS* and *comE* mutants exhibited comparable phenotypes. Consequently, it is likely that both LuxS and ComE play integral roles in autolysis, and the initial concentration of CSP-1 at the beginning of growth appears to influence the timing of autolysis onset during the stationary phase.

In this study, we have delved deeper into the intricate interplay between the LuxS/AI-2 quorum sensing system and the CSP/Com quorum sensing system in *Streptococcus pneumoniae,* shedding light on their profound influences on growth and gene expression dynamics. While our

findings provide valuable insights, the complexity of this interaction warrants further investigation. Additional studies are imperative to unravel this intricate connection and to gain a comprehensive understanding of its implications on disease progression. Such insights hold the promise of identifying novel therapeutic targets with the potential to transform the management of related conditions.

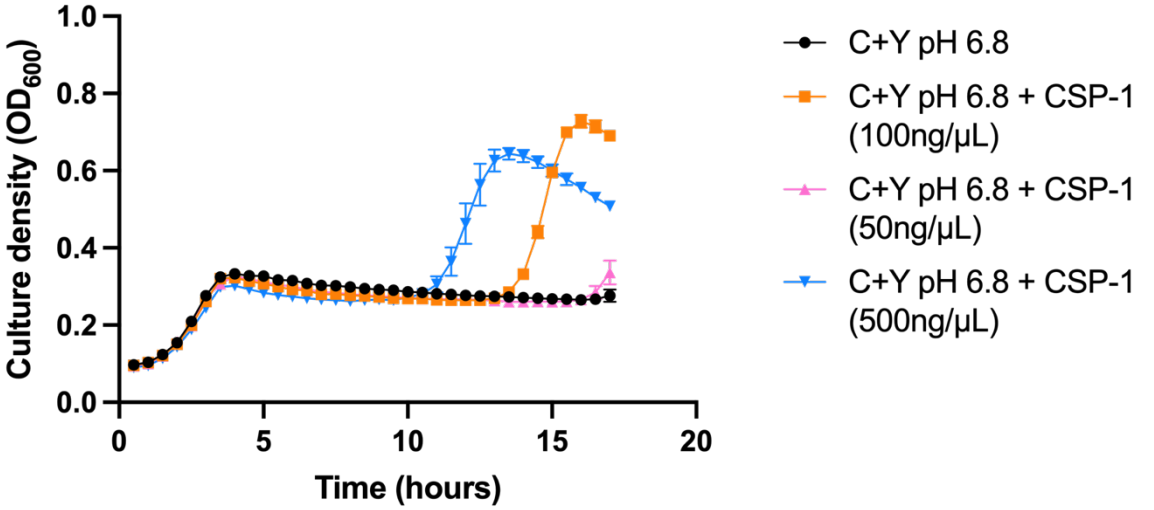

Figure 1: Growth of D39 in C+Y at pH 6.8 with CSP-1 at different concentrations. The strain D39 was incubated in C+Y medium (pH 6.8) with or without CSP-1 at concentrations of 50, 100 or 500 ng/µL. for 24 hours. OD_{600} was measured every 30 min for 24 h. Data are mean OD_{600} ± standard error mean (SEM) from a single representative assay performed in triplicate; assay was performed three independent times.

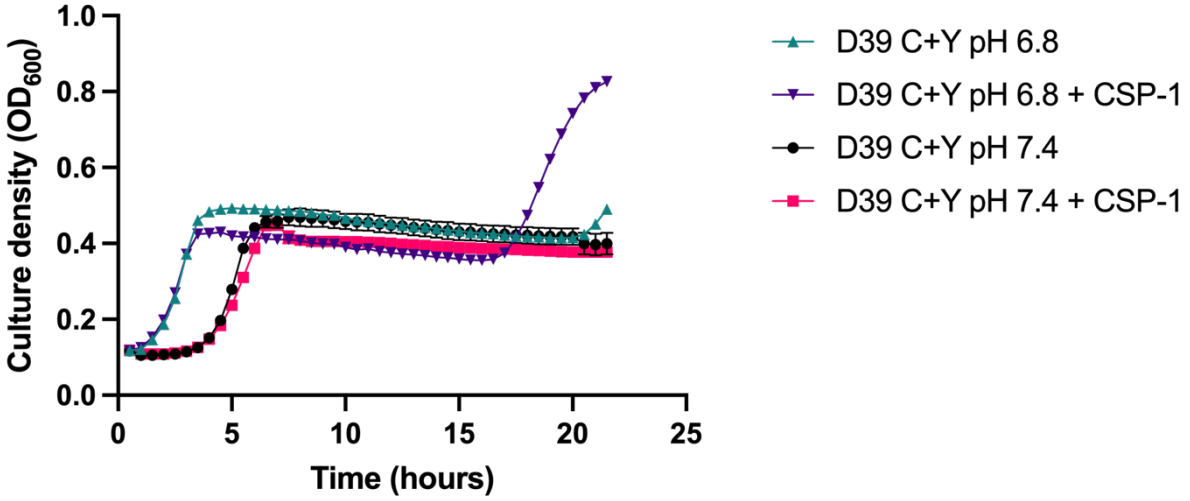

Figure 2: Growth of D39 in C+Y at pH 6.8 or 7.4 with or without CSP-1. The strain D39 was grown in 200µL C+Y medium (pH 6.8 or 7.4) in the presence or absence of CSP-1 (100 ng/µL). OD_{600} was measured every 30 min for 24 h. Data are mean OD_{600} ± standard error mean (SEM) from a single representative assay performed in triplicate; assay was performed three independent times.

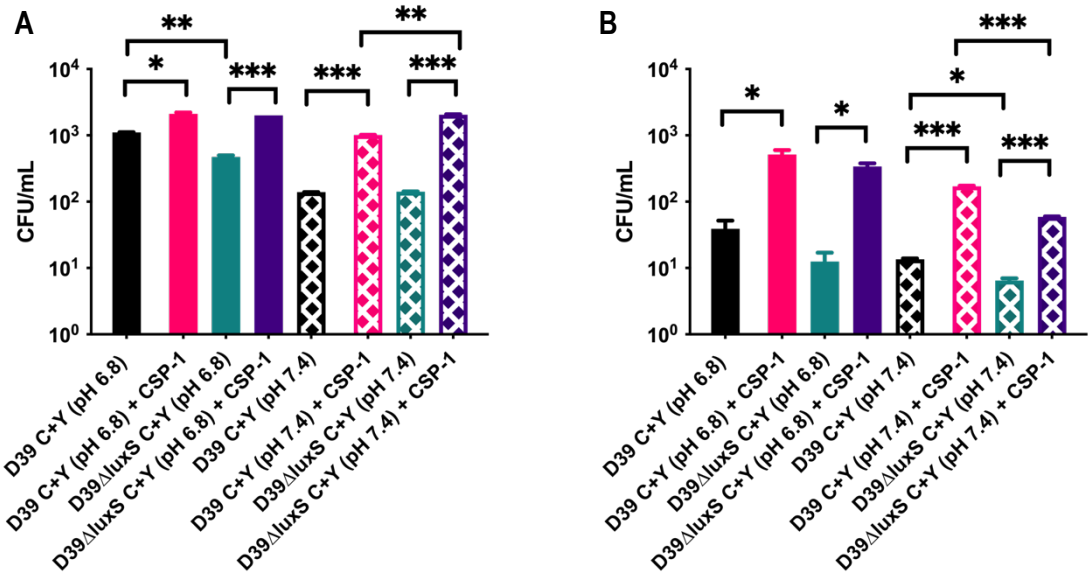

Figure 3: Adherence to and invasion of Detroit 562 pharyngeal cells by D39 and D39Δ*luxS* in different conditions. *S. pneumoniae* strains D39 and D39Δ*luxS* at OD_{600} 0.2 were inoculated onto monolayers of Detroit 562 cells in C+Y at pH 6.8 or pH 7.4 with or without CSP-1 (100 ng/µL) and incubated for 2 h before testing for adherent bacteria (A). Invasion assays were carried out similarly, after the post-adherence washing step, cultures were incubated for 1 h in fresh media supplemented with 200 µg/mL gentamicin and 10 µg/mL penicillin to kill extracellular bacteria, before the number of invasive bacteria were determined (B), as described in Materials and Methods. Data are mean adherent or invasive bacteria ± standard error mean (SEM) in CFU/mL from two independent assays, each performed in triplicate. Statistical analysis was performed using two-tailed Student's *t* test; **P* < 0.0332, ***P* < 0.0021, ****P* < 0.0003, non-significant data is not shown.

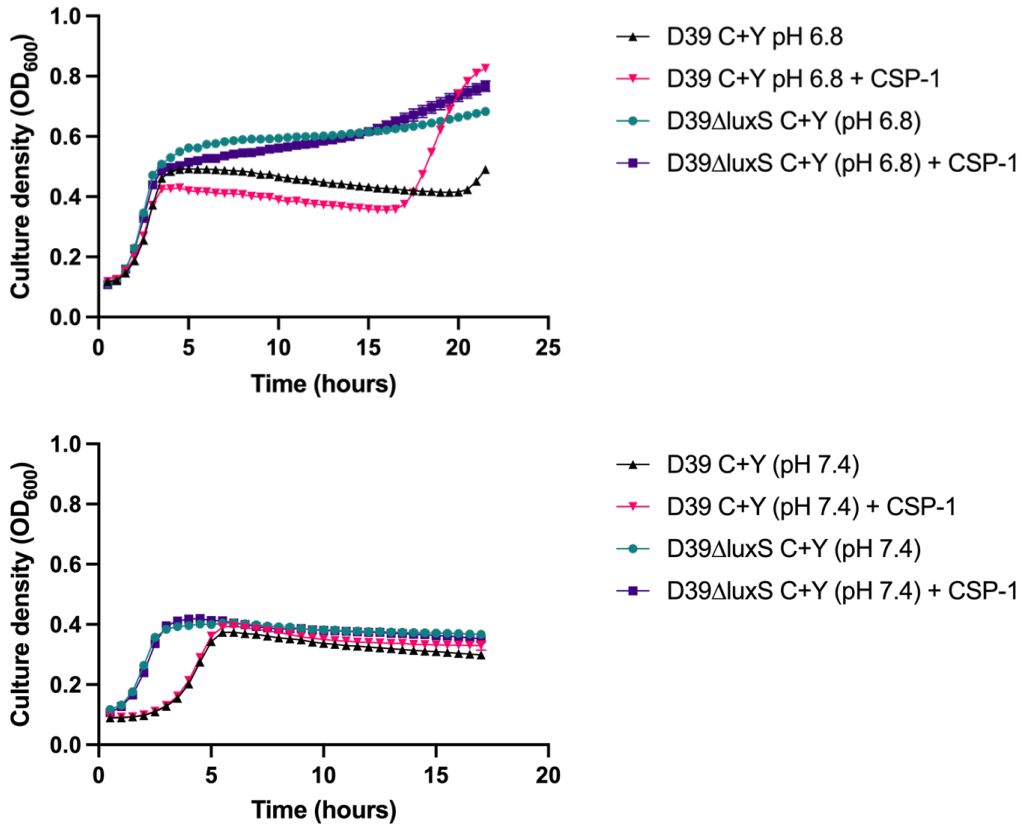

Figure 4: Growth of wildtype D39 and D39Δ*luxS* in C+Y (pH 6.8 or 7.4) with or without CSP-1. Wildtype D39 and D39Δ*luxS* were grown in C+Y medium at pH 6.8 (A) or 7.4 (B) in the presence or absence of CSP-1 (100 ng/µL) for 24 hours, with OD_{600} being recorded every 30 min. Data are mean OD_{600} ± standard error mean (SEM) from a single representative assay performed in triplicate; assay was performed three independent times.

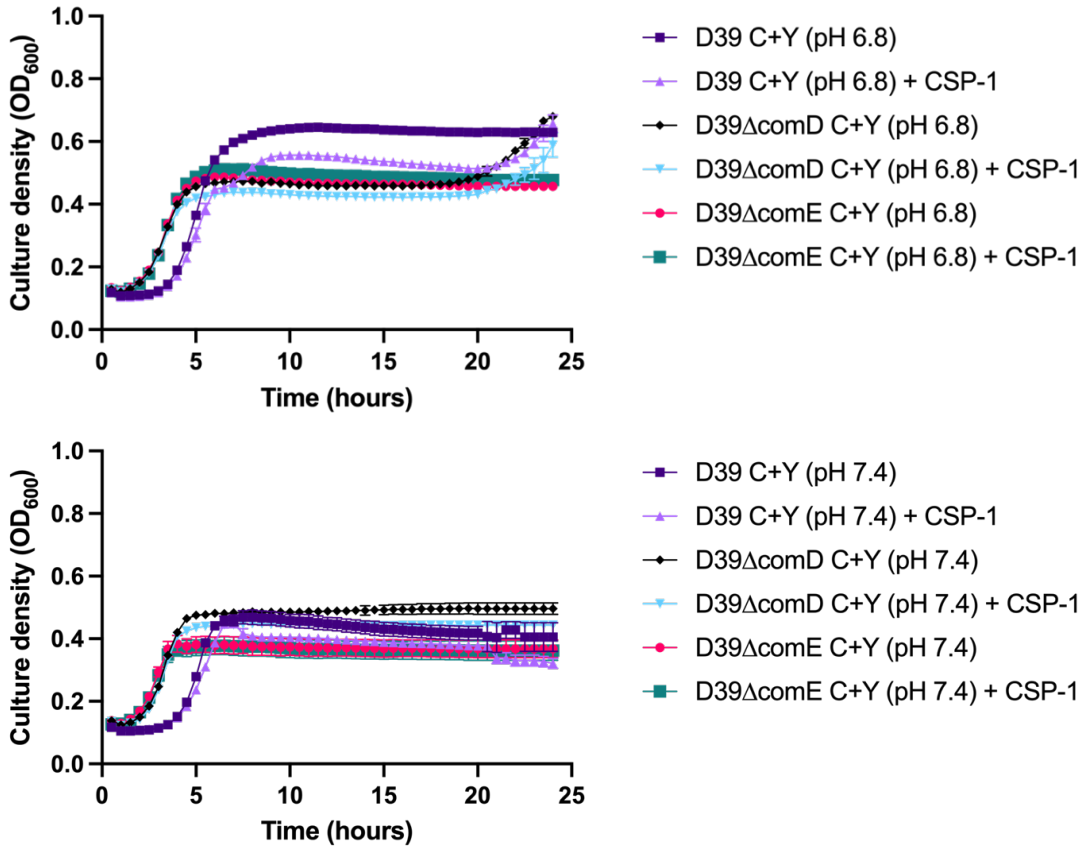

Figure 5: Growth of wildtype D39, D39Δ*comD* and D39Δ*comE* in C+Y (pH 6.8 or 7.4) with or without CSP-1. Wildtype D39, D39Δ*comD* and D39Δ*comE* were grown in C+Y medium at pH 6.8 (A) or 7.4 (B) in the presence or absence of CSP-1 (100 ng/µL) for 24 hours, with OD_{600} being recorded every 30 min. Data are mean OD_{600} ± standard error mean (SEM) from a single representative assay performed in triplicate; assay was performed three independent times.

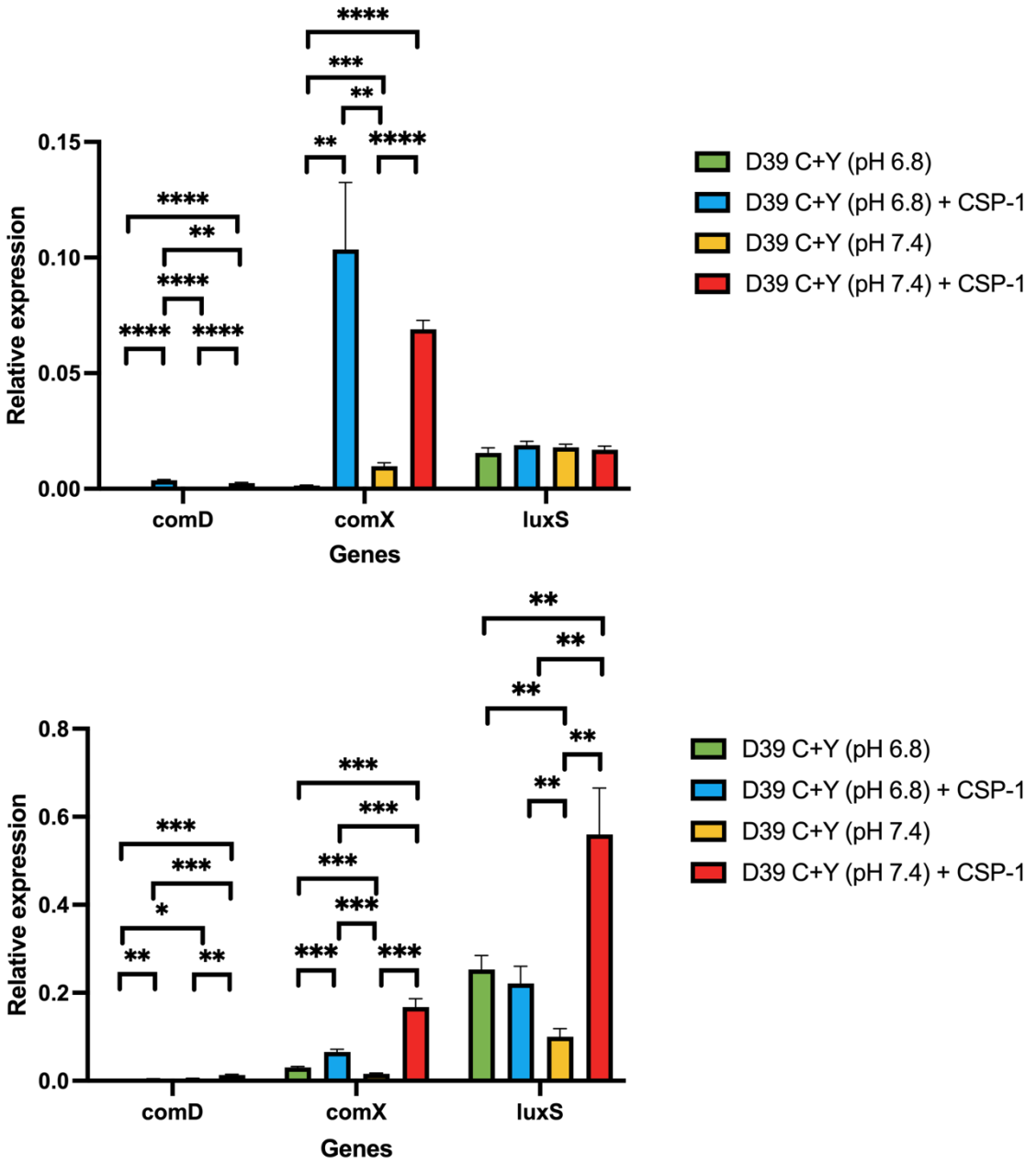

Figure 6: Expression of *luxS* and competence genes, *comD* and *comX*, at early (OD 0.1) and late (OD 0.4) exponential growth stages of D39 in C+Y pH 6.8 or 7.4 with or without CSP-1 supplementation. The relative gene expression by D39 grown in C+Y medium pH 6.8 or 7.4 in the presence or absence of CSP-1 (100 ng/µL), was quantified by qRT-PCR using 16S rRNA as an internal control, as described in Material and Methods. **A** represents the relative gene expression of D39 grown to an OD_{600} of 0.1 (early exponential phase in first growth curve), whilst **B** represents the gene expression of D39 grown to an OD_{600} of 0.4 (late exponential phase in first growth curve). Data presented are the mean ± standard deviation (SD) from assay conducted in triplicate. Significance of differences in gene expression was determined using two-tailed Student's *t* test; **P* < 0.0332, ***P* < 0.0021, ****P* < 0.0003, *****P* < 0.0001, non-significant data is not shown.

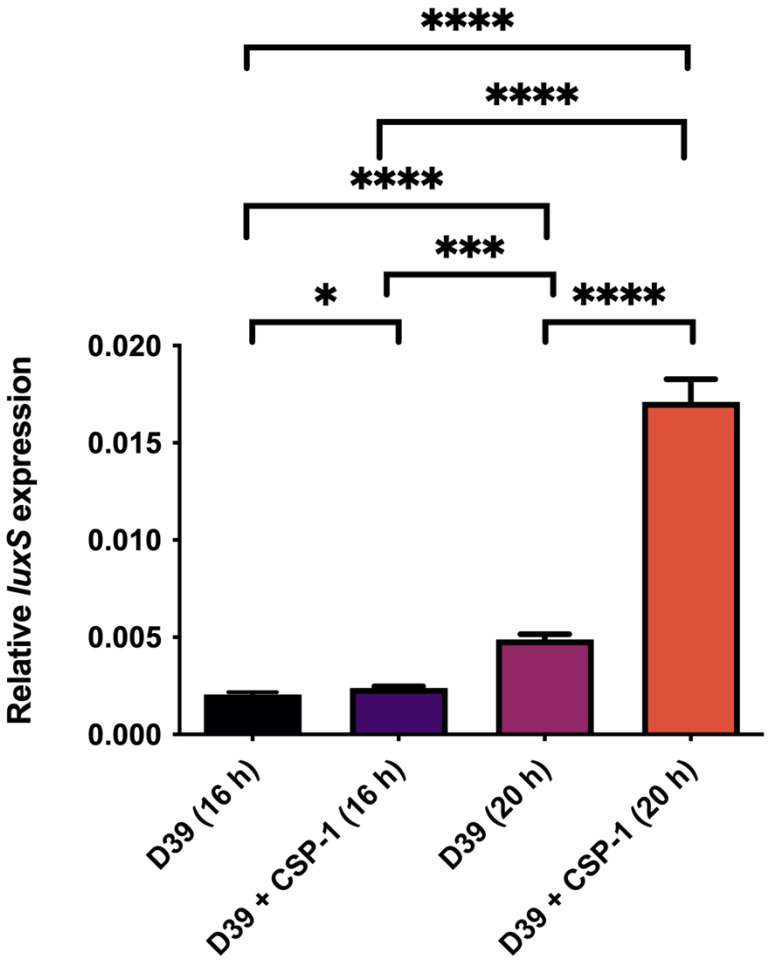

Figure 7: Expression of *luxS* at early (16 h) and late (20 h) exponential growth stages of the second growth peak in D39 grown in C+Y pH 6.8 with or without CSP-1 supplementation. The relative *luxS* gene expression by D39 grown in C+Y (pH 6.8) in presence or absence of CSP-1 (100 ng/µL), was quantified by qRT-PCR using 16S rRNA as an internal control, as described in Material and Methods. Data presented are the mean ± standard deviation (SD) from assay conducted in triplicate. Significance of differences in gene expression was determined using two-tailed Student's *t* test; **P* < 0.0332, ****P* < 0.0003, *****P* < 0.0001.

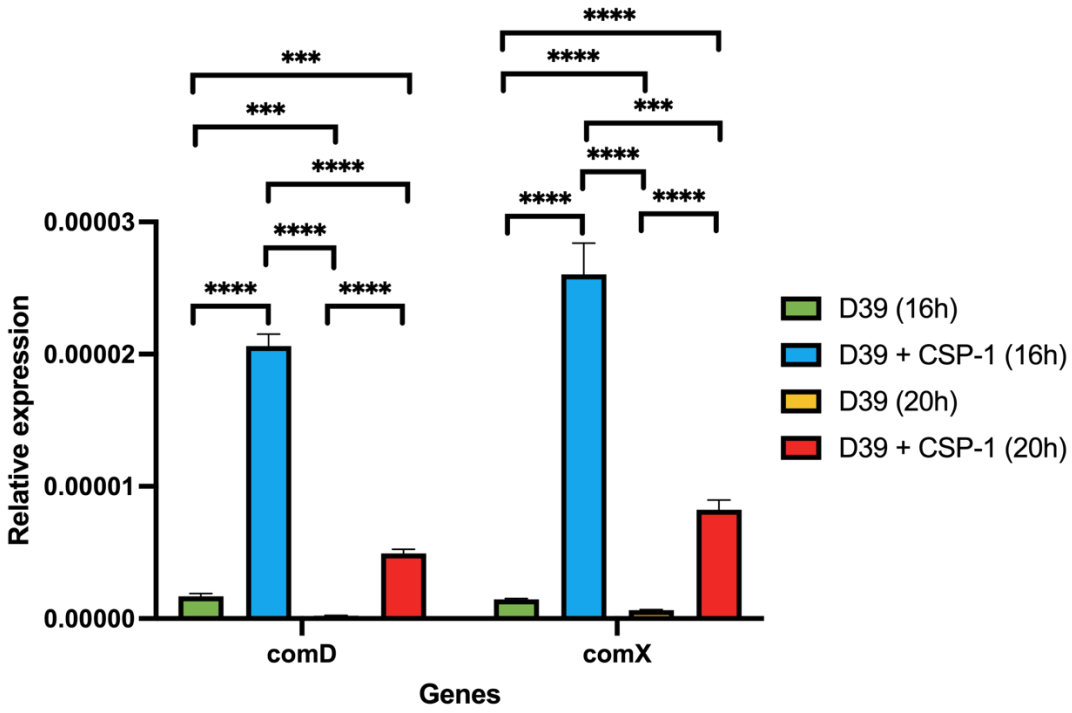

Figure 8: Expression of competence genes, *comD* and *comX,* at early (16 h) and late (20 h) exponential growth stages of the second growth peak in D39 grown in C+Y pH 6.8 with or without CSP-1 supplementation. The relative expression of *comD* and *comX* by D39 grown in C+Y medium (pH 6.8) in the presence or absence of CSP-1 (100 ng/µL), was quantified by qRT-PCR using 16S rRNA as an internal control, as described in Material and Methods. Data presented are the mean ± standard deviation (SD) from assay conducted in triplicate. Significance of differences in gene expression was determined using two-tailed Student's *t* test; ***$P < 0.0003$, ****$P < 0.0001$.

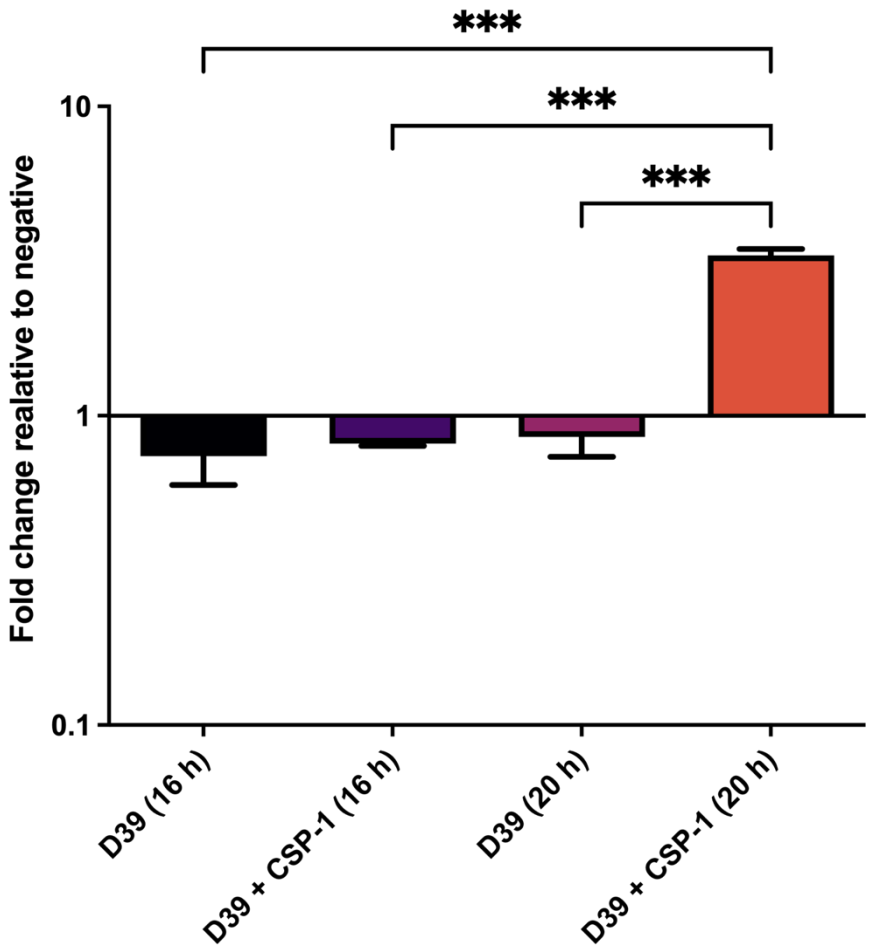

Figure 9: Measurements of autoinducer-2 (AI-2) in D39 at early (16 h) and late (20 h) exponential phase of the second growth peak. Wildtype D39 was grown in C+Y medium (pH 6.8) with or without CSP-1 (100 ng/µL). Supernatant was taken after 16 and 20 hours of growth to measure AI-2 levels as described in Materials and Methods. The AI-2 measurements were calculated using the fold change relative to the negative control (AB medium). Data is representative of a single assay; two independent assays were performed, each in duplicate. Statistical analysis was performed using one-way ANOVA; ***$P < 0.0002$.

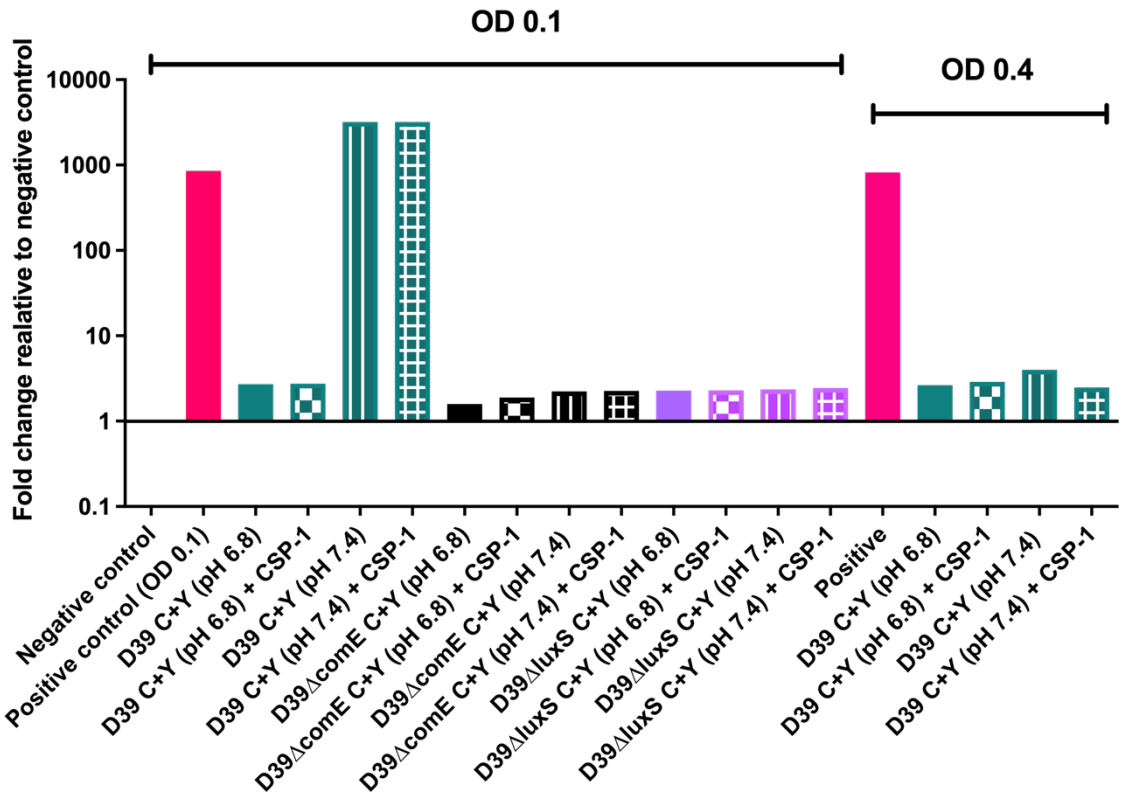

Figure 10: Measurements of autoinducer-2 (AI-2) in D39, D39ΔcomE and D39ΔluxS during early (OD_{600} 0.1) and late (OD_{600} 0.4) exponential phase of the first growth peak. The strains were grown in C+Y medium (pH 6.8 or 7.4) in the presence or absence of CSP-1 (100 ng/µL). Supernatant was taken at early exponential phase (OD_{600} = 0.1) and late exponential phase (OD_{600} = 0.4) to measure AI-2 levels as described in Materials and Methods. The AI-2 measurements were calculated using the fold change relative to the negative control (AB medium). Data is representative of a single assay with two independent assays having been performed.

Appendix C: Data from initial screening of multiple closely related clinical isolates

Table 1: Clinical isolates with matching serotypes and STs initially characterised.

Clinical isolates supplied by the German National Reference Centre for Streptococci were initially characterised based on serotype. After grouping isolates on serotype MLST was performed primarily on ear and blood isolates, representative of each disease type – otitis media and meningitis respectively. MLST analysis was conducted as described in Chapter 2. Briefly, the *aroE*, *gdh*, *gki*, *recP*, *spi*, *xpt* and *ddl* genes of the strains were PCR amplified and purified using the QiaQuick Purification Kit (Qiagen). Purified PCR samples were Sanger sequenced by the Australian Genome Research Facility (AGRF) as described previously (Enright and Spratt, 1998). The sequence types (ST) of the pneumococci strains were determined by using the MLST database (https://pubmlst.org/) to find matching allelic profiles.

Isolate pair ID	Serotype	ST	Material	Diagnosis
54	19A	199	Blood	Meningitis
54	19A	199	CSF	Meningitis
3	19A	199	Ear	Otitis media
3	19A	199	Nasopharynx	Otitis media
7	19A	199	Ear	Otitis media
7	19A	199	Nasopharynx	Otitis media
29	19A	199	Ear	Otitis media
29	19A	199	Nasopharynx	Otitis media
17	19F	179	Blood	Meningitis
17	19F	179	CSF	Meningitis
25	19F	179	Blood	Meningitis
25	19F	179	CSF	Meningitis
54	19F	179	Ear	Otitis media
54	19F	179	Nasopharynx	Otitis media
68	19F	179	Ear	Otitis media
68	19F	179	Nasopharynx	Otitis media
89	19F	179	Ear	Otitis media
89	19F	179	Nasopharynx	Otitis media
22	19F	654	Blood	Meningitis
22	19F	654	CSF	Meningitis

59	19F	654	Ear	Otitis media
59	19F	654	Nasopharynx	Otitis media
6	15C	1262	Blood	Meningitis
6	15C	1262	CSF	Meningitis
15	15C	1262	Blood	Meningitis
15	15C	1262	CSF	Meningitis
103	15C	1262	Ear	Otitis media
103	15C	1262	Nasopharynx	Otitis media
60	15C	8711	Blood	Meningitis
60	15C	8711	CSF	Meningitis
101	15C	8711	Ear	Otitis media
101	15C	8711	Nasopharynx	Otitis media

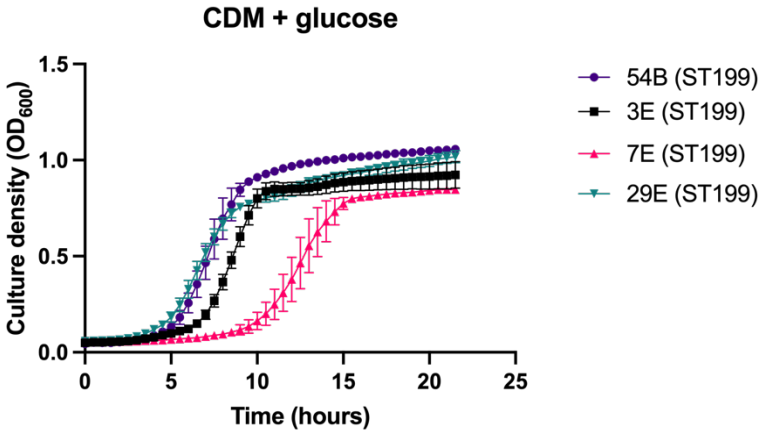

Figure 1: Growth of serotype 19A ST199 blood and ear isolates in glucose.

S. pneumoniae serotype 19A ST199 blood isolate (54B) and ear isolates (3E, 7E, 29E) were grown in 200µL CDM supplemented with 0.5% glucose (CDM + glucose). OD_{600} was measured every 30 min for 24 h. Data are mean OD_{600} ± standard error mean (SEM) from three independent assays, each performed in triplicate.

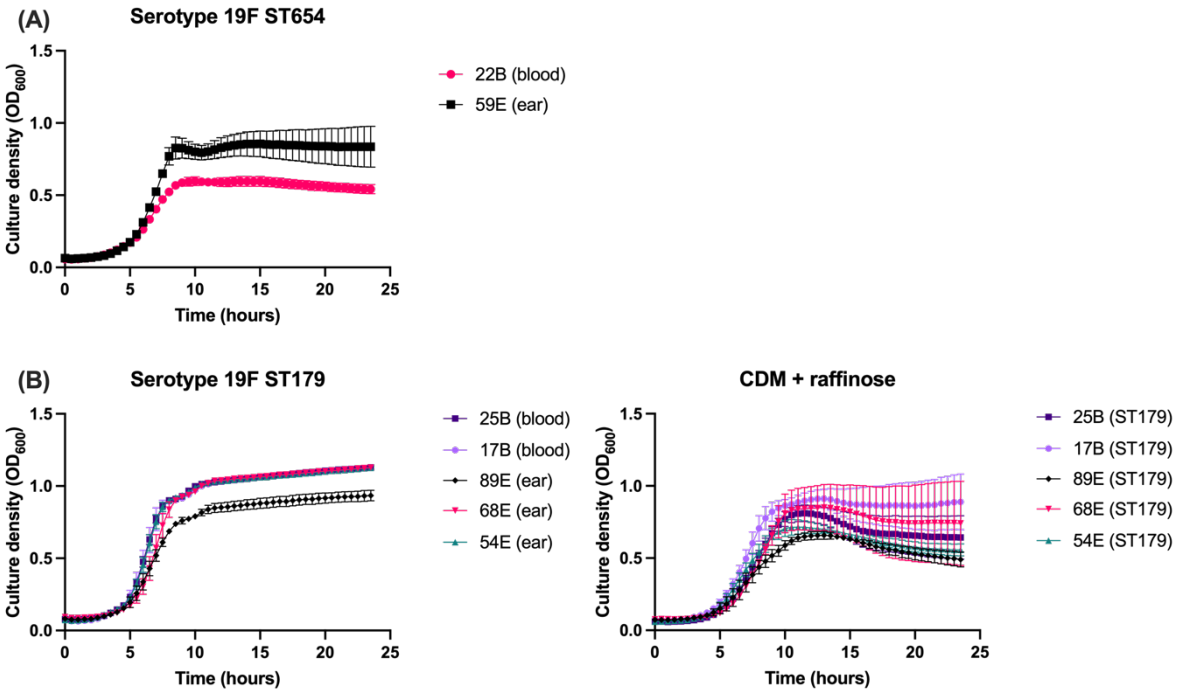

Figure 2: Growth of serotype 19F ST654 blood and ear isolates in glucose, and ST179 blood and ear isolates in glucose and raffinose.

S. pneumoniae serotype 19F ST654 blood isolate (22B) and ear isolate (59E), (A), and ST179 blood isolates (25B, 17B) and ear isolates (89E, 68E, 54E), (B), were grown in CDM supplemented with 0.5% glucose (CDM + glucose) or 0.5% raffinose (CDM + raffinose). OD_{600} was measured every 30 min for 24 h. Data are mean OD_{600} ± standard error mean (SEM) from three independent assays, each performed in triplicate.

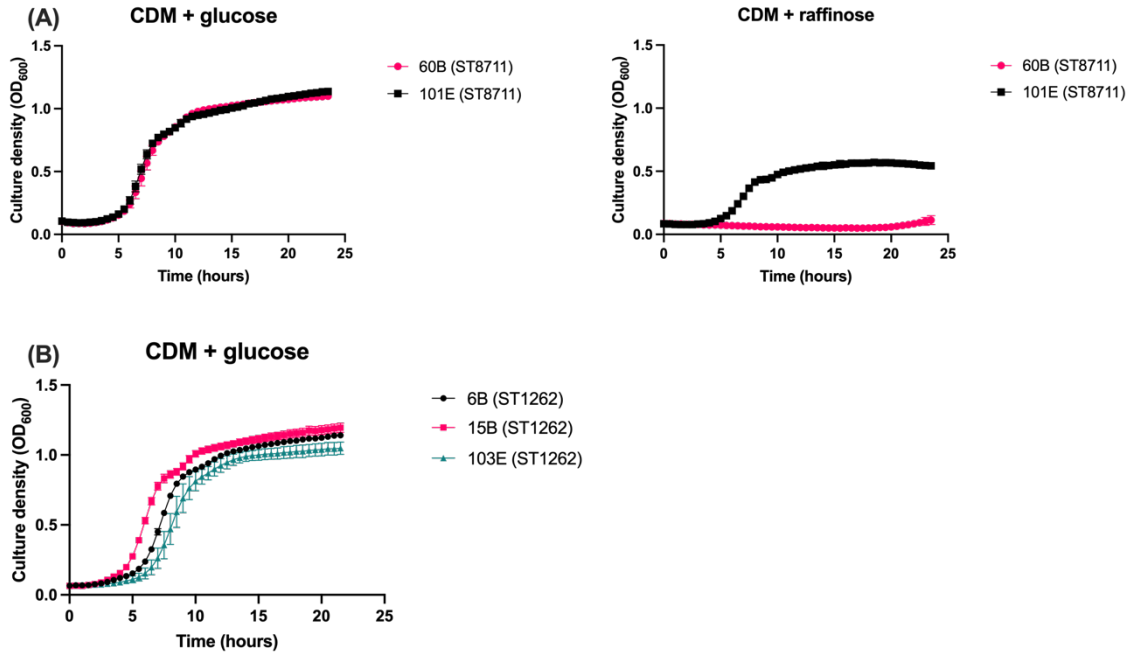

Figure 3: Growth of serotype 15C ST8711 blood and ear isolates in glucose and raffinose, and ST1262 blood and ear isolates in glucose.

S. pneumoniae serotype 15C ST8711 blood isolate (60B) and ear isolate (101E), (A), ST1262 blood isolates (6B, 15B) and ear isolate (103E), (B), were grown in CDM supplemented with 0.5% glucose (CDM + glucose) or 0.5% raffinose (CDM + raffinose). OD_{600} was measured every 30 min for 24 h. Data are mean OD_{600} ± standard error mean (SEM) from three independent assays, each performed in triplicate.

Table 2: Phenotype microarray results for serotype 19F ST179 blood (17B & 25B) and ear (54E & 68E) isolates in Biolog PM1 plate.

Catabolism was measured through a colourless tetrazolium dye being reduced by NADH produced during catabolism. +, metabolism occurred; -, no metabolism occurred. Metabolism was determined by calculating the change in OD_{600} from the initial to final measurements. These values were then compared with the change in the negative control and an arbitrary value based on the change in negative control was used to determine if metabolism occurred. Carbon sources which no strain metabolised are not shown. Bold font indicates carbon sources that were differentially metabolised by the strains.

Carbon source	**17B**	**25B**	**54E**	**68E**
L-Arabinose	+	+	+	+

N-Acetyl-D-Glucosamine	+	+	+	+
D-Galactose	+	+	+	+
D-Trehalose	+	+	+	+
D-Mannose	+	+	+	+
D-Sorbitol	**+**	**+**	**+**	**-**
Glycerol	+	+	+	+
L-Fucose	**+**	**+**	**+**	**-**
D-Glucuronic Acid	**+**	**-**	**-**	**-**
D-Xylose	+	+	+	+
L-Lactic Acid	**+**	**+**	**+**	**-**
D-Mannitol	**+**	**+**	**+**	**-**
D-Glucose-6-Phosphate	**-**	**+**	**+**	**-**
D-Ribose	+	+	+	+
Tween 20	**+**	**+**	**-**	**-**
L-Rhamnose	+	+	+	+
D-Fructose	+	+	+	+
Acetic Acid	+	+	+	+
α-D-Glucose	+	+	+	+
Maltose	+	+	+	+
D-Melibiose	+	+	+	+
α-Methyl-D-Galactoside	**+**	**+**	**+**	**-**
α-D-Lactose	+	+	+	+
Lactulose	+	+	+	+
Sucrose	+	+	+	+
D-Glucose-1-Phosphate	**-**	**+**	**-**	**-**
D-Fructose-6-Phosphate	**+**	**+**	**-**	**-**
β-Methyl-D- Glucoside	+	+	+	+
Maltotriose	+	+	+	+
Adenosine	**+**	**+**	**-**	**-**
D-Cellobiose	+	+	+	+
Acetoacetic Acid	**+**	**+**	**+**	**-**
N-Acetyl-β-D-Mannosamine	+	+	+	+

Methyl Pyruvate	**-**	**-**	**+**	**-**
D-Psicose	+	+	+	+
L-Lyxose	+	+	+	+
Pyruvic Acid	**+**	**-**	**-**	**-**

Table 3: Phenotype microarray results for serotype 15C ST8711 blood (60B), CSF (60CSF), ear (101E) and nasopharynx (101N) isolates in Biolog PM1 plate.

Catabolism was measured through a colourless tetrazolium dye being reduced by NADH produced during catabolism. +, metabolism occurred; -, no metabolism occurred. Metabolism was determined by calculating the change in OD_{600} from the initial to final measurements. These values were then compared with the change in the negative control and an arbitrary value based on the change in negative control was used to determine if metabolism occurred. Carbon sources which neither strain metabolised are not shown. Bold font indicates carbon sources that were differentially metabolised by the strains.

Carbon source	**60B**	**60CSF**	**101E**	**101N**
L-Arabinose	**+**	**+**	**+**	**-**
N-Acetyl-D-Glucosamine	+	+	+	+
D-Galactose	+	+	+	+
D-Trehalose	**+**	**+**	**+**	**-**
D-Mannose	+	+	+	+
Glycerol	+	+	+	-
L-Fucose	**-**	**-**	**+**	**-**
D-Xylose	**+**	**+**	**+**	**-**
D-Ribose	**+**	**+**	**+**	**-**
L-Rhamnose	**-**	**-**	**+**	**-**
D-Fructose	+	+	+	+
α-D-Glucose	+	+	+	+
Maltose	+	+	+	+
D-Melibiose	**-**	**+**	**+**	**-**

α-D-Lactose	+	+	+	+
Lactulose	**+**	**+**	**+**	**-**
Sucrose	+	+	+	+
Uridine	**-**	**-**	**+**	**-**
β-Methyl-D- Glucoside	+	+	+	+
Maltotriose	+	+	+	+
Adenosine	**-**	**-**	**+**	**-**
D-Cellobiose	**-**	**+**	**+**	**-**
Acetoacetic Acid	**-**	**-**	**+**	**-**
N-Acetyl-β-D-Mannosamine	+	+	+	+
D-Psicose	**+**	**+**	**+**	**-**
L-Lyxose	+	+	+	+

Table 4: Phenotype microarray results for serotype 15C ST8711 blood (60B) and CSF (60CSF) isolates in Biolog PM2a plate.

Catabolism was measured through a colourless tetrazolium dye being reduced by NADH produced during catabolism. +, metabolism occurred; -, no metabolism occurred. Metabolism was determined by calculating the change in OD_{600} from the initial to final measurements. These values were then compared with the change in the negative control and an arbitrary value based on the change in negative control was used to determine if metabolism occurred. Carbon sources which neither strain metabolized are not shown. Bold font indicates carbon sources that were differentially metabolized by the strains.

CARBON SOURCE	**60B**	**60CSF**
Chondroitin sulfate c	**-**	**+**
Dextrin	+	+
Inulin	+	+
Pectin	+	+
N-Acetyl-D-Galactosamine	+	+
N-Acetyl Neuraminic Acid	+	+
D-Arabinose	**-**	**+**
2-Deoxy-DRibose	**-**	**+**

3-0-β-D-Galactopyranosyl-D-Arabinose	**-**	**+**
Palatinose	+	+
D-Raffinose	**-**	**+**
Salicin	+	+
D-Tagatose	**-**	**+**
Turanose	**-**	**+**
D-Glucosamine	+	+
5-Keto-D-Gluconic Acid	+	+
Dihydroxy Acetone	**-**	**+**

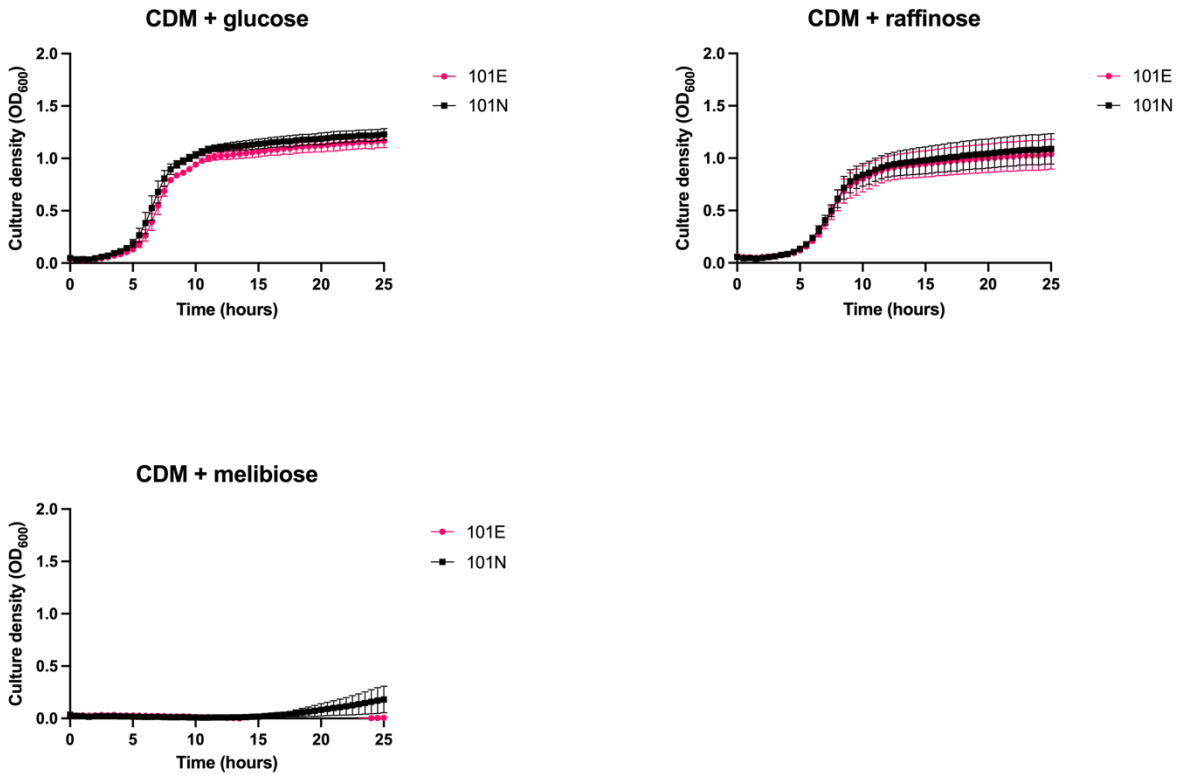

Figure 4: Growth of serotype 15C ST8711 ear (101E) and nasopharynx (101N) isolates in different carbon sources.

S. pneumoniae serotype 15C ST8711 ear isolate (101E) and nasopharyngeal isolate (101N) were grown in CDM supplemented with 0.5% glucose (CDM + glucose), 0.5% raffinose (CDM + raffinose) or 0.5% melibiose (CDM + melibiose). OD_{600} was measured every 30 min for 24 h. Data

are mean OD_{600} ± standard error mean (SEM) from three independent assays, each performed in triplicate.

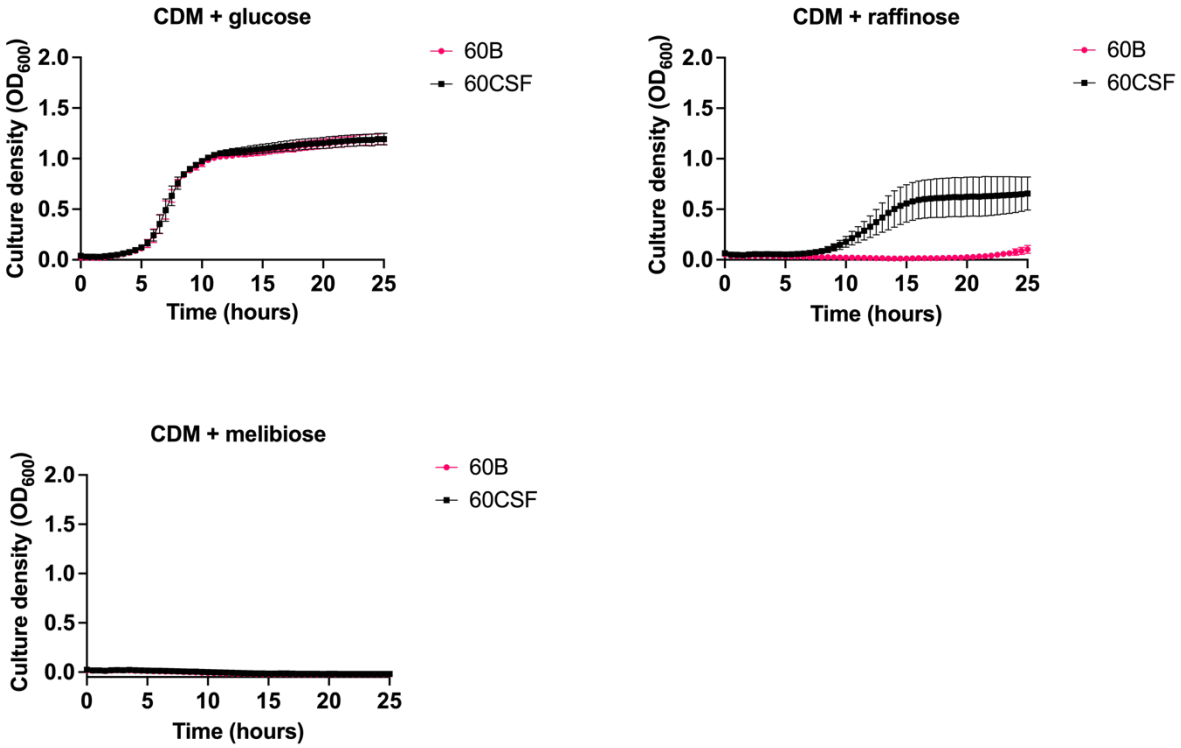

Figure 5: Growth of serotype 15C ST8711 blood (60B) and CSF (60CSF) isolates in different carbon sources.

S. pneumoniae serotype 15C ST8711 blood isolate (60B) and CSF isolate (60CSF) were grown in CDM supplemented with 0.5% glucose (CDM + glucose), 0.5% raffinose (CDM + raffinose) or 0.5% melibiose (CDM + melibiose). OD_{600} was measured every 30 min for 24 h. Data are mean OD_{600} ± standard error mean (SEM) from three independent assays, each performed in triplicate.

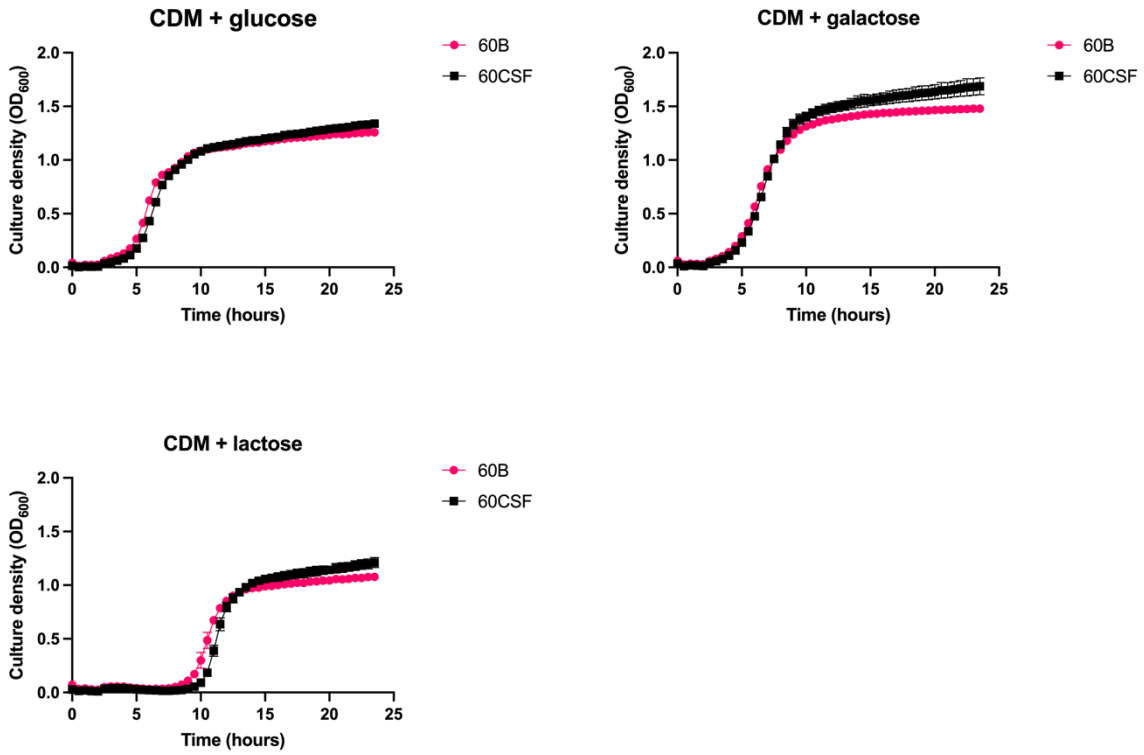

Figure 6: Growth of serotype 15C ST8711 blood (60B) and CSF (60CSF) isolates in different carbon sources.

S. pneumoniae serotype 15C ST8711 blood isolate (60B) and CSF isolate (60CSF) were grown in CDM supplemented with 0.5% glucose (CDM + glucose), 0.5% galactose (CDM + galactose) or 0.5% lactose (CDM + galactose). OD_{600} was measured every 30 min for 24 h. Data are mean OD_{600} ± standard error mean (SEM) from a representative assay that was performed in triplicate.

Appendix D: Sequence of alternative alpha-galactosidase in 60B and 60CSF

Alignment of Sanger sequences of alternative alpha-galactosidase in 60B and 60CSF.

Primers were designed using the published genomes of D39 and TIGR4 as reference (Tettelin et al., 2001; Lanie et al., 2007). The alternative alpha-galactosidase gene (*alt-aga*) was PCR amplified and purified using the QiaQuick Purification Kit (Qiagen). Purified PCR samples were Sanger sequenced by the Australian Genome Research Facility (AGRF). The sequences were initially aligned to the sequence of *alt-aga* in D39 (data not shown) to confirm the sequence was correct before comparing the sequence between 60B and 60CSF.

```
60B_alt-aga         ATGACGATTTATATTAATAAGGACGAGACCGTTTTTCATTTGGCAATGAAAGATAGTAGT   60
60CSF_alt-aga       ATGACGATTTATATTAATAAGGACGAGACCGTTTTTCATTTGGCAATGAAAGATAGTAGT   60
                    ************************************************************

60B_alt-aga         TATATTTTTAGAATTTTAGAAAATGGGGAACTTCAACATCTACATTTTGGGAAAAGGATT   120
60CSF_alt-aga       TATATTTTTAGAATTTTAGAAAATGGGGAACTTCAACATCTACATTTTGGGAAAAGGATT   120
                    ************************************************************

60B_alt-aga         CATGTCAAGGAAAATTATAACCAATTGATGGCCTATGAAAAAAGAGGATTTGAAGTATCT   180
60CSF_alt-aga       CATGTCAAGGAAAATTATAACCAATTGATGGCCTATGAAAAAAGAGGATTTGAAGTATCT   180
                    ************************************************************

60B_alt-aga         TTTTCTGAAGAATTTGAGGATATTCAACAGTCTATGATACAAAATGAATATTCTTCATAT   240
60CSF_alt-aga       TTTTCTGAAGAATTTGAGGATATTCAACAGTCTATGATACAAAATGAATATTCTTCATAT   240
                    ************************************************************

60B_alt-aga         GGGAAAGGAGATTTTCGGCATCCAGCCTTTCAAGTTCAAGGAATGAATGGTAGTAGGATA   300
60CSF_alt-aga       GGGAAAGGAGATTTTCGGCATCCAGCCTTTCAAGTTCAAGGAATGAATGGTAGTAGGATA   300
                    ************************************************************

60B_alt-aga         ACGACACTAAAATATCAAGGTTTTGAACTTGAAAAAGGGAAAAATCGTCTTAACTCTCTA   360
60CSF_alt-aga       ACGACACTAAAATATCAAGGTTTTGAACTTGAAAAAGGGAAAAATCGTCTTAACTCTCTA   360
                    ************************************************************

60B_alt-aga         CCTTCAACATTTGATGATATTGGTCAGTGTGCGGAAACATTAACGATTATTTTAACAGAT   420
60CSF_alt-aga       CCTTCAACATTTGATGATATTGGTCAGTGTGCGGAAACATTAACGATTATTTTAACAGAT   420
                    ************************************************************

60B_alt-aga         TCCATATTAGATTTAACTGTTAGACTAAATTACACAATTTTTCCGGAATACAATGTCTTA   480
60CSF_alt-aga       TCCATATTAGATTTAACTGTTAGACTAAATTACACAATTTTTCCGGAATACAATGTCTTA   480
                    ************************************************************

60B_alt-aga         GTTAGAAATACGGAATTTTTAAATAATAGCAATAATAAGTTGACTCTTTTGAAAGCAATG   540
60CSF_alt-aga       GTTAGAAATACGGAATTTTTAAATAATAGCAATAATAAGTTGACTCTTTTGAAAGCAATG   540
                    ************************************************************

60B_alt-aga         AGCTTACAGCTAGATCTACCTGATAGTCAATATGACTTTATTCAATTTTCTGGAGCATGG   600
60CSF_alt-aga       AGCTTACAGCTAGATCTACCTGATAGTCAATATGACTTTATTCAATTTTCTGGAGCATGG   600
                    ************************************************************
```

```
60B_alt-aga         CTGAGGGAACGTCAGTTATATAGAACTTCGCTTAGACCAGGTATTCAAGCAATAGATAGC  660
60CSF_alt-aga       CTGAGGGAACGTCAGTTATATAGAACTTCGCTTAGACCAGGTATTCAAGCAATAGATAGC  660
                    ************************************************************

60B_alt-aga         TTGAGATACTCATCAAGTCCTCAGCAAAATCCTTTCTTTATGCTATCAAGGAGGGAAACT  720
60CSF_alt-aga       TTGAGATACTCATCAAGTCCTCAGCAAAATCCTTTCTTTATGCTATCAAGGAGGGAAACT  720
                    ************************************************************

60B_alt-aga         ACAGAGCATAGTGGTGAGGTTTATGGTTTTAACTTTATCTATTCTGGAAATTTTCAAAAT  780
60CSF_alt-aga       ACAGAGCATAGTGGTGAGGTTTATGGTTTTAACTTTATCTATTCTGGAAATTTTCAAAAT  780
                    ************************************************************

60B_alt-aga         ATGATTGAAGTTGACCATTTTGACACCGCTAGAGTAACGGTAGGAATAAATCCAGTAGAA  840
60CSF_alt-aga       ATGATTGAAGTTGACCATTTTGACACCGCTAGAGTAACGGTAGGAATAAATCCAGTAGAA  840
                    ************************************************************

60B_alt-aga         TTTCGTTTTTTATTAAATCCTGCCGAAAGTTTTGTGACACCAGAAGCAATTGTGATCTAT  900
60CSF_alt-aga       TTTCGTTTTTTATTAAATCCTGCCGAAAGTTTTGTGACACCAGAAGCAATTGTGATCTAT  900
                    ************************************************************

60B_alt-aga         TCTGATCAAGGGATGAATCAGATGAGCCAACAACTATCAGATTTTTATCGACATCATTTA  960
60CSF_alt-aga       TCTGATCAAGGGATGAATCAGATGAGCCAACAACTATCAGATTTTTATCGACATCATTTA  960
                    ************************************************************

60B_alt-aga         GTTAATCCTAATTTTTCTCAAGCTAGTCGTCCTATAATACTCAATAGTTGGGAAACATTT  1020
60CSF_alt-aga       GTTAATCCTAATTTTTCTCAAGCTAGTCGTCCTATAATACTCAATAGTTGGGAAACATTT  1020
                    ************************************************************

60B_alt-aga         TATTTTGACTTGAGTACAGAAAAAATTTTAGATTTAGCAAAGGCTGCTAAAGATTTAGGG  1080
60CSF_alt-aga       TATTTTGACTTGAGTACAGAAAAAATTTTAGATTTAGCAAAGGCTGCTAAAGATTTAGGG  1080
                    ************************************************************

60B_alt-aga         ATAGAATTATTTGTACTGGATGATGGTTGGTTTGGTCATAGGAAAGATGACAAAAGTTCT  1140
60CSF_alt-aga       ATAGAATTATTTGTACTGGATGATGGTTGGTTTGGTCATAGGAAAGATGACAAAAGTTCT  1140
                    ************************************************************

60B_alt-aga         CTGGGTGATTGGGTAACAGATAGAAGTCGCCTTCCTGAAGGTATTGGATTTCTTGCAGAT  1200
60CSF_alt-aga       CTGGGTGATTGGGTAACAGATAGAAGTCGCCTTCCTGAAGGTATTGGATTTCTTGCAGAT  1200
                    ************************************************************

60B_alt-aga         GAAATTCACAAAATAGGTTTACAATTTGGTTTGTGGTTTGAGCCTGAAATGATTTCTATT  1260
60CSF_alt-aga       GAAATTCACAAAATAGGTTTACAATTTGGTTTGTGGTTTGAGCCTGAAATGATTTCTATT  1260
                    ************************************************************

60B_alt-aga         GATAGTGATTTGTACAAGAATCATGCCGATTGGACTATCCATTTGTTAGACAGAGAGAAG  1320
60CSF_alt-aga       GATAGTGATTTGTACAAGAATCATGCCGATTGGACTATCCATTTGTTAGACAGAGAGAAG  1320
                    ************************************************************

60B_alt-aga         TCAGTAGGAAGAAATCAATATGTGTTGGATTTGACGAGACAGGAAGTTGTTGATTATCTT  1380
60CSF_alt-aga       TCAGTAGGAAGAAATCAATATGTGTTGGATTTGACGAGACAGGAAGTTGTTGATTATCTT  1380
                    ************************************************************

60B_alt-aga         TTTGATTCTATTTCTAAAATCATAATCAAAACAAATCTGGATTATATCAAATGGGATATG  1440
60CSF_alt-aga       TTTGATTCTATTTCTAAAATCATAATCAAAACAAATCTGGATTATATCAAATGGGATATG  1440
                    ************************************************************
```

```
60B_alt-aga       AATCGTCATATAACAGATATTTATAGTATTGAACTTGATTCTGAACAGCAGATGGAATTT  1500
60CSF_alt-aga     AATCGTCATATAACAGATATTTATAGTATTGAACTTGATTCTGAACAGCAGATGGAATTT  1500
                  ************************************************************

60B_alt-aga       GGTCATCGATATATCTTAGGTCTTTATCAGTTATTAGATCGTTTAATAACTAAGTTCCCT  1560
60CSF_alt-aga     GGTCATCGATATATCTTAGGTCTTTATCAGTTATTAGATCGTTTAATAACTAAGTTCCCT  1560
                  ************************************************************

60B_alt-aga       TCAGTTCTATTTGAATCTTGTTCTTCAGGTGGTGGACGTTTTGATTTAGGACTTATGTAT  1620
60CSF_alt-aga     TCAGTTCTATTTGAATCTTGTTCTTCAGGTGGTGGACGTTTTGATTTAGGACTTATGTAT  1620
                  ************************************************************

60B_alt-aga       TATGCACCGCAAGCGTGGACGAGTGATGATACGGACCCGATAGAAAGATTGAAAATTCAG  1680
60CSF_alt-aga     TATGCACCGCAAGCGTGGACGAGTGATGATACGGACCCGATAGAAAGATTGAAAATTCAG  1680
                  ************************************************************

60B_alt-aga       CATGGAACTTCTTATGGATATTCTCCATCAATGATGACAGCCCATGTTTCTATTTCTCCA  1740
60CSF_alt-aga     CATGGAACTTCTTATGGATATTCTCCATCAATGATGACAGCCCATGTTTCTATTTCTCCA  1740
                  ************************************************************

60B_alt-aga       AATGAACAAAGTGGAAGACAAACGAGTTTGGACACTAGGACAAATGTAGCTTATTTTAGT  1800
60CSF_alt-aga     AATGAACAAAGTGGAAGACAAACGAGTTTGGACACTAGGACAAATGTAGCTTATTTTAGT  1800
                  ************************************************************

60B_alt-aga       TCTTTCGGTTATGAATTAGATGTTACGAGATTGTCGGTAGAAGAAAAAGAACAAGTGAGA  1860
60CSF_alt-aga     TCTTTCGGTTATGAATTAGATGTTACGAGATTGTCGGTAGAAGAAAAAGAACAAGTGAGA  1860
                  ************************************************************

60B_alt-aga       GAACAAATTCAGTTTTATAAAAAATATCGTTCATTGCTTCAATATGGGGATTTCTATAGG  1920
60CSF_alt-aga     GAACAAATTCAGTTTTATAAAAAATATCGTTCATTGCTTCAATATGGGGATTTCTATAGG  1920
                  ************************************************************

60B_alt-aga       ATAAACAGTCCTTTTAGTTGTGATTCTGCTAGTTGGCAAGTTGTTTCAAAAGATAAATGC  1980
60CSF_alt-aga     ATAAACAGTCCTTTTAGTTGTGATTCTGCTAGTTGGCAAGTTGTTTCAAAAGATAAATGC  1980
                  ************************************************************

60B_alt-aga       CAATCGATTTTATTGTATGCTCAATTGAATAGTAAGTTGAATCCAGGTTATACAAGAGTT  2040
60CSF_alt-aga     CAATCGATTTTATTGTATGCTCAATTGAATAGTAAGTTGAATCCAGGTTATACAAGAGTT  2040
                  ************************************************************

60B_alt-aga       TATTTTAGTGGTTTAGATAAAGATAAATGCTATTCCGTCTCTGGATTTGATGAGTTCTTT  2100
60CSF_alt-aga     TATTTTAGTGGTTTAGATAAAGATAAATGCTATTCCGTCTCTGGATTTGATGAGTTCTTT  2100
                  ************************************************************

60B_alt-aga       TATGGAGATGAATTAATGAATGCTGGAATAAAAGTAAGTTTAAGTAATTTAGCACTTTGT  2160
60CSF_alt-aga     TATGGAGATGAATTAATGAATGCTGGAATAAAAGTAAGTTTAAGTAATTTAGCACTTTGT  2160
                  ************************************************************

60B_alt-aga       GTTCCAGAATATCTTACAAAATTATTTGTTATTGAAGAAGTTGTATGTAAATATTGA     2217
60CSF_alt-aga     GTTCCAGAATATCTTACAAAATTATTTGTTATTGAAGAAGTTGTATGTAAATATTGA     2217
                  ********************************************************
```

Appendix E: Growth of *aga* deletion 60B and 60CSF mutants

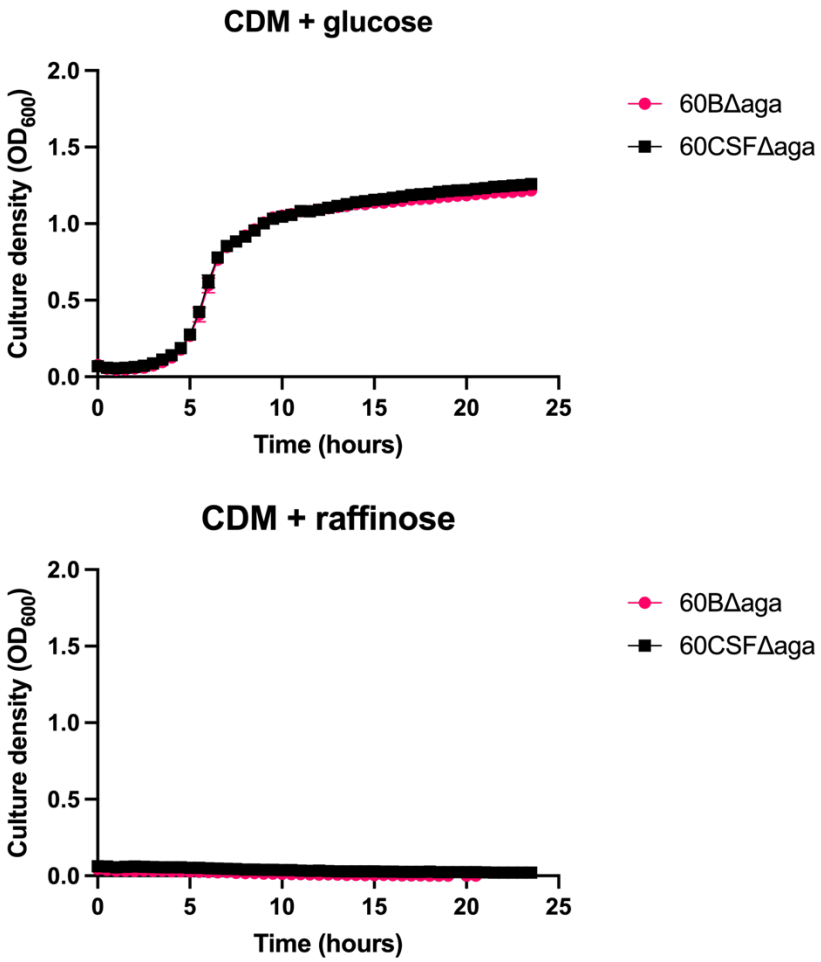

Figure 7: Growth of serotype 15C ST8711 *aga* deletion mutants in blood (60BΔ*aga*) and CSF (60CSFΔ*aga*) isolates in different carbon sources.

S. pneumoniae aga deletion mutants in blood isolate (60BΔ*aga*) and CSF isolate (60CSFΔ*aga*) were grown in CDM supplemented with 0.5% glucose (CDM + glucose) or 0.5% raffinose (CDM + raffinose). OD_{600} was measured every 30 min for 24 h. Data are mean OD_{600} ± standard error mean (SEM) from one representative assay performed in triplicate. Four independent assays were performed on separate days.

Appendix F: Murine intranasal infection time-course experiment

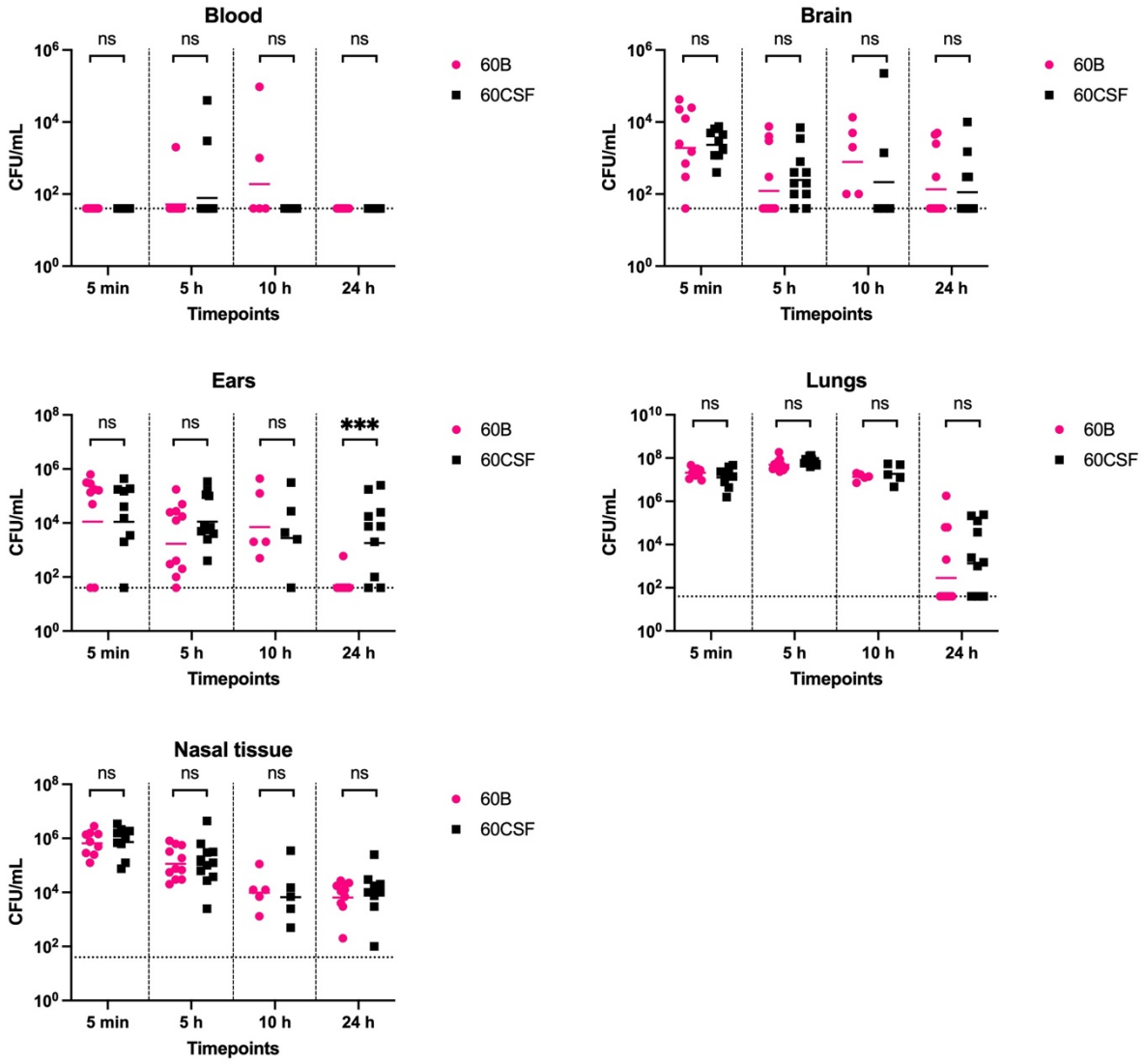

Figure 8: Bacterial burden in different anatomical niches of mice over time post intranasal infection with 60B and 60CSF.

In two separate experiments groups of 8 mice (some passed during challenge) were intranasally infected with 10^8 CFU of the indicated strain. At 5 min, 5 h, 10 h and 24 h post challenge, mice from each group were humanely euthanised and pneumococci in the blood, brain, ears, lungs and nose were enumerated. Viable bacterial counts are displayed for each mouse in each niche for all timepoints; horizontal bars indicate the geometric mean (GM) CFU for each group; the dotted line indicates the detection threshold. Note different scales of y-axis. Significance of differences in bacterial load between groups was determined using two-tailed Student's t test; ***P < 0.0002. ns, not significant.

Appendix G: Effect of stearic acid on the LuxS/AI-2 QS system in 60CSF

To investigate the potential link between fatty acids and the LuxS/AI-2 QS system, growth assays were performed on 60CSF and 60CSF∆*luxS* with both autoinducer-2 and fatty acids (16:0, 18:0 and 18:1) supplementation in a chemically defined media with glucose. Here it was found that only stearic acid (18:0) at a concentration of 62.5 µM interfered with growth (Figure 9), whilst neither palmitic acid (16:0) and oleic acid (18:1) had any effect on growth (data not shown). The addition of stearic acid led to a decrease in bacterial growth, but the addition of AI-2 (10 µM) rescued the growth (Figure 9).

Gene expression analysis (3 biological replicates in 3 days) on the influence of stearic acid found that *fakB1*, *fakB2*, and *fakB3* showed upregulation when both stearic acid and AI-2 were added together to the culture (Figure 10). Furthermore, although not statistically significant, expression of *fruA* and *luxS* in 60CSF appears to be slightly more upregulated when both stearic acid and AI-2 were added together (Figure 10).

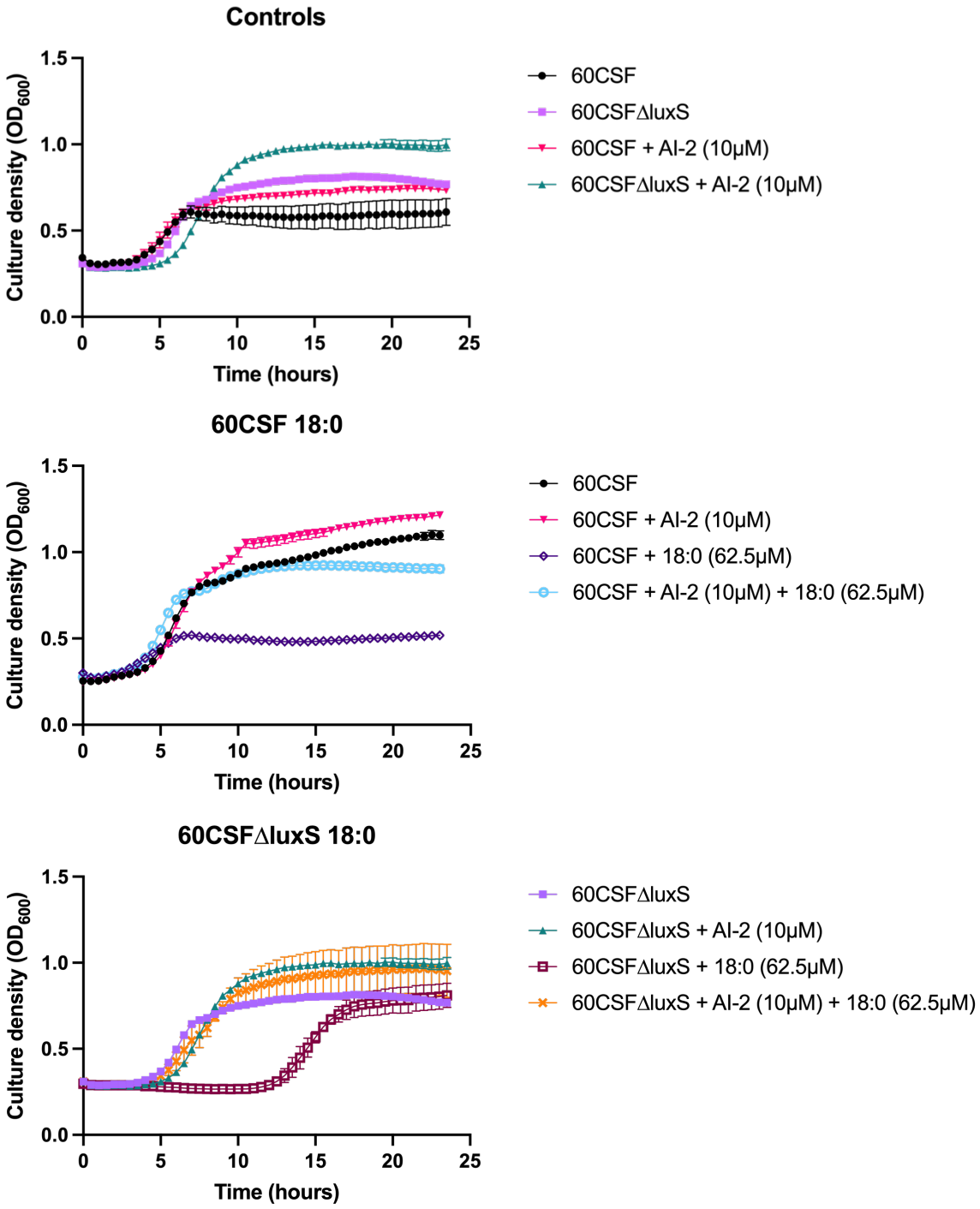

Figure 9: Impact of stearic acid (18:0) on the growth of 60CSF and 60CSFΔ*luxS*.

S. pneumoniae strains 60CSF and 60CSFΔ*luxS* were grown in 200 µL CDM supplemented with 0.5% glucose ± 10 µM AI-2 ± 62.5 µM stearic acid (18:0). OD_{600} was measured every 30 min for 24 h. Data are mean OD_{600} ± standard error mean (SEM) from one representative assay performed in triplicate. Five independent assays were performed on separate days.

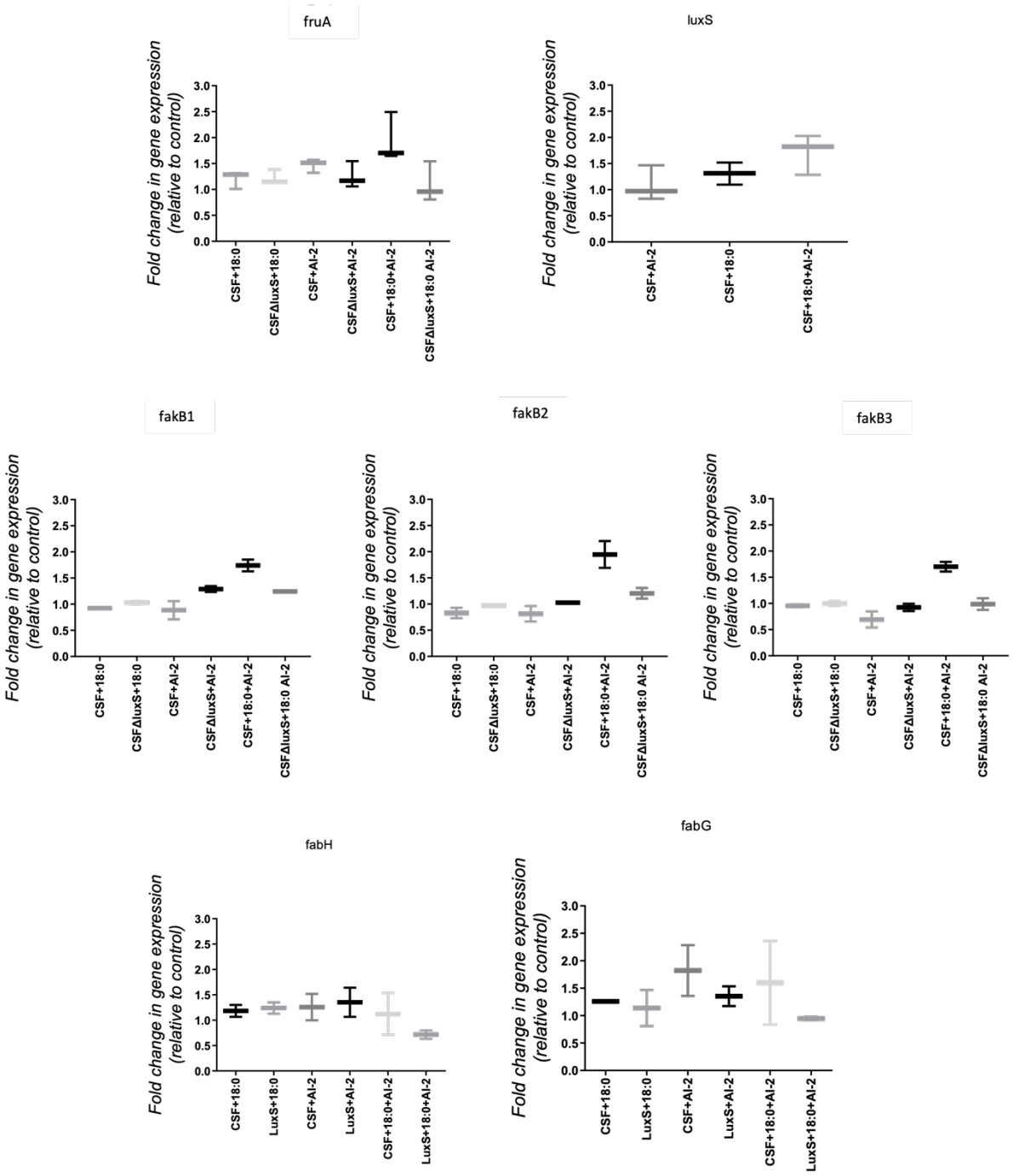

Figure 10: Effect of stearic acid (18:0) on expression of genes involved in the LuxS/AI-2 quorum sensing system and the FakA/B fatty acid uptake system.

S. pneumoniae strains 60CSF (denoted CSF) and 60CSFΔ*luxS* (denoted LuxS) were resuspended to OD_{600} 0.2 in CDM supplemented with 0.5% glucose ± 10 µM AI-2 ± 62.5 µM stearic acid (18:0) and incubated at 37°C for 30 min. RNA was then extracted, and levels of *fruA, luxS*, *fakB1, fakB2, fakB3, fabH*, and *fabG* mRNA were analysed by qRT-PCR using *gyrA* rRNA as an internal control (similar to as in Chapter 2's Materials and Methods). Data are fold change in expression relative to *gyrA* mRNA (mean ± the standard deviation of three independent experiments).

Appendix H: 60B and 60CSF genome sequences accession

Illumina sequencing data can be found in online repositories. The name of the repository and accession number can be found here:

NCBI; Bioproject ID: PRJNA803929; BioSample: SAMN25690480; Sample name: 60B.

NCBI; Bioproject ID: PRJNA803929; BioSample: SAMN25690481; Sample name: 60CSF.

Nanopore sequencing data can be found in online repositories. The name of the repository and accession number can be found here:

NCBI; Bioproject ID: PRJNA803929; BioSample: SAMN37954648; Sample name: 60B genome assembly.

NCBI; Bioproject ID: PRJNA803929; BioSample: SAMN37954649; Sample name: 60CSF genome assembly.

References

Aanensen, D. M., Mavroidi, A., Bentley, S. D., Reeves, P. R., & Spratt, B. G. (2007). Predicted functions and linkage specificities of the products of the *Streptococcus pneumoniae* capsular biosynthetic loci. *Journal of Bacteriology*, 189(21), 7856-7876. doi:10.1128/jb.00837-07

Abeyta, M., Hardy, G. G., & Yother, J. (2003). Genetic alteration of capsule type but not PspA type affects accessibility of surface-bound complement and surface antigens of *Streptococcus pneumoniae*. *Infection and Immunity*, 71(1), 218-225. doi:10.1128/IAI.71.1.218-225.2003

Afshar, D., Rafiee, F., Kheirandish, M., Ohadian-Moghadam, S., & Azarsa, M. (2020). Autolysin (LytA) recombinant protein: A potential target for developing vaccines against pneumococcal infections. *Clinical and Experimental Vaccine Research (Seoul)*, 9(2), 76-80. doi:10.7774/cevr.2020.9.2.76

Aggarwal, S. D., Eutsey, R., West-Roberts, J., Domenech, A., Xu, W., Abdullah, I. T., Mitchell, A. P., Veening, J.-W., Yesilkaya, H., & Hiller, N. L. (2018). Function of BriC peptide in the pneumococcal competence and virulence portfolio. *PLoS Pathogens*, 14(10), e1007328-e1007328. doi:10.1371/journal.ppat.1007328

Aggarwal, S. D., Yesilkaya, H., Dawid, S., & Hiller, N. L. (2020). The pneumococcal social network. *PLoS Pathogens*, 16(10), e1008931-e1008931. doi:10.1371/journal.ppat.1008931

Aggarwal, S. D., Gullett, J. M., Fedder, T., Safi, J. P. F., Rock, C. O., & Hiller, N. L. (2021). Competence-associated peptide BriC alters fatty acid biosynthesis in *Streptococcus pneumoniae*. *mSphere*, 6(3), e0014521. doi:10.1128/mSphere.00145-21

Agnew, H. N., Brazel, E. B., Tikhomirova, A., van der Linden, M., McLean, K. T., Paton, J. C., & Trappetti, C. (2022). *Streptococcus pneumoniae* strains isolated from a single pediatric patient display distinct phenotypes. *Frontiers in Cellular and Infection Microbiology*, 12, 866259-866259. doi:10.3389/fcimb.2022.866259

Agnew, H. N., Atack, J. M., Fernando, A. R. D., Waters, S. N., van der Linden, M., Smith, E., Abell, A. D., Brazel, E. B., Paton, J. C., & Trappetti, C. (2023). Uncovering the link between the SpnIII restriction modification system and LuxS in *Streptococcus pneumoniae* meningitis isolates. *Frontiers in Cellular and Infection Microbiology*, 13. doi:10.3389/fcimb.2023.1177857

Al-Bayati, F. A. Y., Kahya, H. F. H., Damianou, A., Shafeeq, S., Kuipers, O. P., Andrew, P. W., & Yesilkaya, H. (2017). Pneumococcal galactose catabolism is controlled by multiple regulators acting on pyruvate formate lyase. *Scientific Reports*, 7(1), 43587. doi:10.1038/srep43587

Alexander, J. E., Lock, R. A., Peeters, C. C. A. M., Poolman, J. T., Andrew, P. W., Mitchell, T. J., Hansman, D., & Paton, J. C. (1994). Immunization of mice with pneumolysin toxoid confers a significant degree of protection against at least nine serotypes of *Streptococcus pneumoniae*. *Infection and Immunity*, 62(12), 5683-5688. doi:10.1128/IAI.62.12.5683-5688.1994

Alexander, J. E., Berry, A. M., Paton, J. C., Rubins, J. B., Andrew, P. W., & Mitchell, T. J. (1998). Amino acid changes affecting the activity of pneumolysin alter the behaviour of pneumococci in pneumonia. *Microbial Pathogenesis*, 24(3), 167-174. doi:10.1006/mpat.1997.0185

Alioing, G., Granadel, C., Morrison, D. A., & Claverys, J. P. (1996). Competence pheromone, oligopeptide permease, and induction of competence in *Streptococcus pneumoniae*. *Molecular Microbiology*, 21(3), 471-478. doi:10.1111/j.1365-2958.1996.tb02556.x

Allan, R. N., Skipp, P., Jefferies, J., Clarke, S. C., Faust, S. N., Hall-Stoodley, L., & Webb, J. (2014). Pronounced metabolic changes in adaptation to biofilm growth by *Streptococcus pneumoniae*. *PloS One,* 9(9), e107015. doi:10.1371/journal.pone.0107015

Allegrucci, M., & Sauer, K. (2008). Formation of *Streptococcus pneumoniae* non-phase-variable colony variants is due to increased mutation frequency present under biofilm growth conditions. *Journal of Bacteriology*, 190(19), 6330-6339. doi:10.1128/jb.00707-08

Amin, Z., Harvey, R. M., Wang, H., Hughes, C. E., Paton, A. W., Paton, J. C., & Trappetti, C. (2015). Isolation site influences virulence phenotype of serotype 14 *Streptococcus pneumoniae* strains belonging to multilocus sequence type 15. *Infection and Immunity*, 83(12), 4781-4790. doi:10.1128/IAI.01081-15

Amin-Chowdhury, Z., Aiano, F., Mensah, A., Sheppard, C. L., Litt, D., Fry, N. K., Andrews, N., Ramsay, M. E., & Ladhani, S. N. (2020). Impact of the coronavirus disease 2019 (COVID-19) pandemic on invasive pneumococcal disease and risk of pneumococcal coinfection with severe acute respiratory syndrome coronavirus 2 (SARS-CoV-2): Prospective national cohort study, England. *Clinical Infectious Diseases,* 72(5), e65-e75. doi:10.1093/cid/ciaa1728

André, G. O., Politano, W. R., Mirza, S., Converso, T. R., Ferraz, L. F. C., Leite, L. C. C., & Darrieux, M. (2015). Combined effects of lactoferrin and lysozyme on *Streptococcus pneumoniae* killing. *Microbial Pathogenesis,* 89, 7-17. doi:10.1016/j.micpath.2015.08.008

Antunes, M. B., & Cohen, N. A. (2007). Mucociliary clearance – a critical upper airway host defense mechanism and methods of assessment. *Current Opinion in Allergy and Clinical Immunology*, 7(1), 5-10. doi:10.1097/ACI.0b013e3280114eef

Asmat, T. M., Agarwal, V., Saleh, M., & Hammerschmidt, S. (2014). Endocytosis of *Streptococcus pneumoniae* via the polymeric immunoglobulin receptor of epithelial cells relies on clathrin and caveolin dependent mechanisms. *International Journal of Medical Microbiology*, 304(8), 1233-1246. doi:10.1016/j.ijmm.2014.10.001

Attaiech, L., Olivier, A., Mortier-Barrière, I., Soulet, A.-L., Granadel, C., Martin, B., Polard, P., & Claverys, J.-P. (2011). Role of the single-stranded DNA-binding protein SsbB in pneumococcal transformation: Maintenance of a reservoir for genetic plasticity. *PLoS Genetics*, 7(6), e1002156-e1002156. doi:10.1371/journal.pgen.1002156

Attali, C., Durmort, C., Vernet, T., & Di Guilmi, A. M. (2008). The interaction of *Streptococcus pneumoniae* with plasmin mediates transmigration across endothelial and epithelial monolayers by intercellular junction cleavage. *Infection and Immunity*, 76(11), 5350-5356. doi:10.1128/IAI.00184-08

Audshasai, T., Coles, J. A., Panagiotou, S., Khandaker, S., Scales, H. E., Kjos, M., Baltazar, M., Vignau, J., Brewer, J. M., Kadioglu, A., & Yang, M. (2022). *Streptococcus pneumoniae* rapidly translocate from the nasopharynx through the cribriform plate to invade the outer meninges. *mBio*, 13(4), e0102422. doi:10.1128/mbio.01024-22

Australian Institute of Health and Welfare (2019). *Vaccine-preventable diseases*. Retrieved from https://www.aihw.gov.au/reports/immunisation/vaccine-preventable-diseases

Austrian, R., Douglas, R. M., Schiffman, G., Coetzee, A. M., Koornhof, H. J., Hayden-Smith, S., & Reid, R. D. (1976). Prevention of pneumococcal pneumonia by vaccination. *Transactions of the Association of American Physicians*, 89, 184-194.

Austrian, R. (1981). Some observations on the pneumococcus and on the current status of pneumococcal disease and its prevention. *Reviews of Infectious Diseases*, 3(Supplement_1), S1-S17. doi:10.1093/clinids/3.Supplement_1.S1

Avadhanula, V., Rodriguez, C. A., Devincenzo, J. P., Wang, Y., Webby, R. J., Ulett, G. C., & Adderson, E. E. (2006). Respiratory viruses augment the adhesion of bacterial pathogens to respiratory epithelium in a viral species- and cell type-dependent manner. *Journal of Virology*, 80(4), 1629-1636. doi:10.1128/JVI.80.4.1629-1636.2006

Ayoubi, P., Kilic, A. O., & Vijayakumar, M. N. (1991). Tn5253, the pneumococcal omega (cat tet) BM6001 element, is a composite structure of two conjugative transposons, Tn5251 and Tn5252. *Journal of Bacteriology*, 173(5), 1617-1622. doi:10.1128/jb.173.5.1617-1622.1991

Azarpazhooh, A., Lawrence, H. P., & Shah, P. S. (2016). Xylitol for preventing acute otitis media in children up to 12 years of age. *Cochrane database of systematic reviews*, (8). doi:10.1002/14651858.CD007095.pub3

Baba, H., Kawamura, I., Kohda, C., Nomura, T., Ito, Y., Kimoto, T., Watanabe, I., Ichiyama, S., & Mitsuyama, M. (2002). Induction of gamma interferon and nitric oxide by truncated pneumolysin that lacks pore-forming activity. *Infection and Immunity*, 70(1), 107-113. doi:10.1128/IAI.70.1.107-113.2002

Babb, R., Chen, A., Hirst, T. R., Kara, E. E., McColl, S. R., Ogunniyi, A. D., Paton, J. C., & Alsharifi, M. (2016). Intranasal vaccination with γ-irradiated *Streptococcus pneumoniae* whole-cell vaccine provides serotype-independent protection mediated by b-cells and innate IL-17 responses. *Clinical science (1979)*, 130(9), 697-710. doi:10.1042/CS20150699

Babb, R., Chen, A., Ogunniyi, A. D., Hirst, T. R., Kara, E. E., McColl, S. R., Alsharifi, M., & Paton, J. C. (2017). Enhanced protective responses to a serotype-independent pneumococcal vaccine when combined with an inactivated influenza vaccine. *Clinical science (1979)*, 131(2), 169-180. doi:10.1042/CS20160475

Badgujar, D. C., Anil, A., Green, A. E., Surve, M. V., Madhavan, S., Beckett, A., Prior, I. A., Godsora, B. K., Patil, S. B., More, P. K., Sarkar, S. G., Mitchell, A., Banerjee, R., Phale, P. S., Mitchell, T. J., Neill, D. R., Bhaumik, P., & Banerjee, A. (2020). Structural insights into loss of function of a pore forming toxin and its role in pneumococcal adaptation to an intracellular lifestyle. *PLoS Pathogens*, 16(11), e1009016. doi: 10.1371/journal.ppat.1009016

Balemans, W., Lounis, N., Gilissen, R., Guillemont, J., Simmen, K., Andries, K., Koul, A., Brinster, S., Lamberet, G., Staels, B., Trieu-Cuot, P., Gruss, A., & Poyart, C. (2010). Essentiality of FASII pathway for *Staphylococcus aureus*. *Nature*, 463, E3. doi: 10.1038/nature08667

Barakat, R., Abou El-Ela, N. E., Sharaf, S., El Sagheer, O., Selim, S., Tallima, H., Bruins, M. J., Hadley, K. B., & El Ridi, R. (2015). Efficacy and safety of arachidonic acid for treatment of school-age children in *Schistosoma mansoni* high-endemicity regions. *The American Journal of Tropical Medicine and Hygiene*, 92(4), 797-804. doi:10.4269/ajtmh.14-0675

Bassler, B. L., Wright, M., Showalter, R. E., & Silverman, M. R. (1993). Intercellular signalling in *Vibrio harveyi*: Sequence and function of genes regulating expression of luminescence. *Molecular Microbiology*, 9(4), 773-786. doi:10.1111/j.1365-2958.1993.tb01737.x

Bassler, B. L., Greenberg, E. P., & Stevens, A. M. (1997). Cross-species induction of luminescence in the quorum-sensing bacterium *Vibrio harveyi*. *Journal of Bacteriology*, 179(12), 4043-4045. doi:10.1128/jb.179.12.4043-4045.1997

Belanger, A. E., Clague, M. J., Glass, J. I., & Leblanc, D. J. (2004). Pyruvate oxidase is a determinant of Avery's rough morphology. *Journal of Bacteriology*, 186(24), 8164-8171. doi:10.1128/jb.186.24.8164-8171.2004

Bergmann, S., & Hammerschmidt, S. (2006). Versatility of pneumococcal surface proteins. *Microbiology (Society for General Microbiology)*, 152(2), 295-303. doi:10.1099/mic.0.28610-0

Berry, A. M., Yother, J., Briles, D. E., Hansman, D., & Paton, J. C. (1989). Reduced virulence of a defined pneumolysin-negative mutant of *Streptococcus pneumoniae*. Infection and Immunology, 57(7), 2037-2042. doi:10.1128/iai.57.7.2037-2042.1989

Berry, A. M., Alexander, J. E., Mitchell, T. J., Andrew, P. W., Hansman, D., & Paton, J. C. (1995). Effect of defined point mutations in the pneumolysin gene on the virulence of *Streptococcus pneumoniae*. *Infection and Immunology*, 63(5), 1969-1974. doi:10.1128/iai.63.5.1969-1974.1995

Berry, A. M., Lock, R. A., & Paton, J. C. (1996). Cloning and characterization of *nanB*, a second *Streptococcus pneumoniae* neuraminidase gene, and purification of the NanB enzyme from recombinant *Escherichia coli*. *Journal of Bacteriology*, 178(16), 4854-4860. doi:10.1128/jb.178.16.4854-4860.1996

Berry, A. M., & Paton, J. C. (1996). Sequence heterogeneity of PsaA, a 37-kilodalton putative adhesin essential for virulence of *Streptococcus pneumoniae*. *Infection and Immunity*, 64(12), 5255-5262. doi:10.1128/iai.64.12.5255-5262.1996

Berry, A. M., & Paton, J. C. (2000). Additive attenuation of virulence of *Streptococcus pneumoniae* by mutation of the genes encoding pneumolysin and other putative pneumococcal virulence proteins. *Infection and Immunity*, 68(1), 133-140. doi:10.1128/IAI.68.1.133-140.2000

Bertani, G., & Weigle, J. J. (1953). Host controlled variation in bacterial viruses. *Journal of Bacteriology*, 65(2), 113-121. doi:10.1128/JB.65.2.113-121.1953

Bidossi, A., Mulas, L., Decorosi, F., Colomba, L., Ricci, S., Pozzi, G., Deutscher, J., Viti, C., & Oggioni, M. R. (2012). A functional genomics approach to establish the complement of carbohydrate transporters in *Streptococcus pneumoniae*. *PloS One*, 7(3), e33320-e33320. doi:10.1371/journal.pone.0033320

Blanchette-Cain, K., Hinojosa, C. A., Akula Suresh Babu, R., Lizcano, A., Gonzalez-Juarbe, N., Munoz-Almagro, C., Sanchez, C. J., Bergman, M. A., & Orihuela, C. J. (2013). *Streptococcus pneumoniae* biofilm formation is strain dependent, multifactorial, and associated with reduced invasiveness and immunoreactivity during colonization. *mBio*, 4(5), e00745-e00713. doi:10.1128/mBio.00745-13

Bogaert, D., de Groot, R., & Hermans, P. W. M. (2004). *Streptococcus pneumoniae* colonisation: The key to pneumococcal disease. *The Lancet Infectious Diseases*, 4(3), 144-154. doi:10.1016/S1473-3099(04)00938-7

Boulnois, G. J., Paton, J. C., Mitchell, T. J., & Andrew, P. W. (1991). Structure and function of pneumolysin, the multifunctional, thiol-activated toxin of *Streptococcus pneumoniae*. *Molecular Microbiology*, 5(11), 2611-2616. doi:10.1111/j.1365-2958.1991.tb01969.x

Boyer, H. W., & Roulland-dussoix, D. (1969). A complementation analysis of the restriction and modification of DNA in *Escherichia coli*. *Journal of Molecular Biology*, 41(3), 459-472. doi:10.1016/0022-2836(69)90288-5

Brixner, D. I. (2005). Improving acute otitis media outcomes through proper antibiotic use and adherence. The American Journal of Managed Care, 11(6), S202-S210.

Brook, I. (2013). Acute sinusitis in children. *The Pediatric Clinics of North America*, 60(2), 409-424. doi:10.1016/j.pcl.2012.12.002

Brooks, L. R. K., & Mias, G. I. (2018). *Streptococcus pneumoniae's* virulence and host immunity: Aging, diagnostics, and prevention. *Frontiers in Immunology*, 9, 1366-1366. doi:10.3389/fimmu.2018.01366

Brouwer, M. C., Tunkel, A. R., & van de Beek, D. (2010). Epidemiology, diagnosis, and antimicrobial treatment of acute bacterial meningitis. *Clinical Microbiology Reviews*, 23(3), 467-492. doi:10.1128/CMR.00070-09

Brown, A. O., Mann, B., Gao, G., Hankins, J. S., Humann, J., Giardina, J., Faverio, P., Restrepo, M. I., Halade, G. V., Mortensen, E. M., Lindsey, M. L., Hanes, M., Happel, K. I., Nelson, S., Bagby, G. J., Lorent, J. A., Cardinal, P., Granados, R., Esteban, A., LeSaux, C. J., Tuomanen, E. I., & Orihuela, C. J. (2014). *Streptococcus pneumoniae* translocates into the myocardium and forms unique microlesions that disrupt cardiac function. *PLoS Pathogens*, 10(9), e1004383-e1004383. doi:10.1371/journal.ppat.1004383

Brown, J. S., Gilliland, S. M., Ruiz-Albert, J., & Holden, D. W. (2002). Characterization of Pit, a *Streptococcus pneumoniae* iron uptake ABC transporter. *Infection and Immunology*, 70(8), 4389-4398. doi:10.1128/iai.70.8.4389-4398.2002

Brueggemann, A. B., Harrold, C. L., Rezaei Javan, R., van Tonder, A. J., McDonnell, A. J., & Edwards, B. A. (2017). Pneumococcal prophages are diverse, but not without structure or history. *Scientific Reports*, 7(1), 42976-42976. doi:10.1038/srep42976

Brueggemann, A. B., Jansen van Rensburg, M. J., Shaw, D., McCarthy, N. D., Jolley, K. A., Maiden, M. C. J., van der Linden, M. P. G., Amin-Chowdhury, Z., Bennett, D. E., Borrow, R., Brandileone, M.-C. C., Broughton, K., Campbell, R., Cao, B., Casanova, C., Choi, E. H., Chu, Y.

W., Clark, S. A., Claus, H., Coelho, J., Corcoran, M., Cottrell, S., Cunney, R. J., Dalby, T., Davies, H., de Gouveia, L., Deghmane, A.-E., Demczuk, W., Desmet, S., Drew, R. J., du Plessis, M., Erlendsdottir, H., Fry, N. K., Fuursted, K., Gray, S. J., Henriques-Normark, B., Hale, T., Hilty, M., Hoffmann, S., Humphreys, H., Ip, M., Jacobsson, S., Johnston, J., Kozakova, J., Kristinsson, K. G., Krizova, P., Kuch, A., Ladhani, S. N., Lâm, T.-T., Lebedova, V., Lindholm, L., Litt, D. J., Martin, I., Martiny, D., Mattheus, W., McElligott, M., Meehan, M., Meiring, S., Mölling, P., Morfeldt, E., Morgan, J., Mulhall, R. M., Muñoz-Almagro, C., Murdoch, D. R., Murphy, J., Musilek, M., Mzabi, A., Perez-Argüello, A., Perrin, M., Perry, M., Redin, A., Roberts, R., Roberts, M., Rokney, A., Ron, M., Scott, K. J., Sheppard, C. L., Siira, L., Skoczyńska, A., Sloan, M., Slotved, H.-C., Smith, A. J., Song, J. Y., Taha, M.-K., Toropainen, M., Tsang, D., Vainio, A., van Sorge, N. M., Varon, E., Vlach, J., Vogel, U., Vohrnova, S., von Gottberg, A., Zanella, R. C., & Zhou, F. (2021). Changes in the incidence of invasive disease due to *Streptococcus pneumoniae*, *Haemophilus influenzae*, and *Neisseria meningitidis* during the COVID-19 pandemic in 26 countries and territories in the invasive respiratory infection surveillance initiative: A prospective analysis of surveillance data. *The Lancet Digital Health*, 3(6), e360-e370. doi:10.1016/S2589-7500(21)00077-7

Bruinsma, N., Kristinsson, K. G., Bronzwaer, S., Schrijnemakers, P., Degener, J., Tiemersma, E., Hryniewicz, W., Monen, J., & Grundmann, H. (2004). Trends of penicillin and erythromycin resistance among invasive *Streptococcus pneumoniae* in Europe. *Journal of Antimicrobial Chemotherapy*, 54(6), 1045-1050. doi:10.1093/jac/dkh458

Bryant, K. A., Block, S. L., Baker, S. A., Gruber, W. C., & Scott, D. A. (2010). Safety and immunogenicity of a 13-valent pneumococcal conjugate vaccine. *Pediatrics*, 125(5), 866-875. doi:10.1542/peds.2009-1405

Buckwalter, C. M., & King, S. J. (2012). Pneumococcal carbohydrate transport: Food for thought. *Trends in Microbiology (Regular ed.)*, 20(11), 517-522. doi:10.1016/j.tim.2012.08.008

Burrus, V., Pavlovic, G., Decaris, B., & Guédon, G. (2002). Conjugative transposons: The tip of the iceberg. *Molecular Microbiology*, 46(3), 601-610. doi:10.1046/j.1365-2958.2002.03191.x

Canvin, J. R., Marvin, A. P., Sivakumaran, M., Paton, J. C., Boulnois, G. J., Andrew, P. W., & Mitchell, T. J. (1995). The role of pneumolysin and autolysin in the pathology of pneumonia and septicemia in mice infected with a type 2 pneumococcus. *Journal of Infectious Diseases*, 172(1), 119-123. doi:10.1093/infdis/172.1.119

Caroff, M., & Perry, M. B. (1984). The specific capsular polysaccharide of *Streptococcus pneumoniae* type 15A. Canadian Journal of Biochemistry and Cell Biology, 62(2-3), 151-161. doi:10.1139/o84-022%M 6426760

Cartee, R. T., Forsee, W. T., & Yother, J. (2005). Initiation and synthesis of the *Streptococcus pneumoniae* type 3 capsule on a phosphatidylglycerol membrane anchor. *Journal of Bacteriology*, 187(13), 4470-4479. doi:10.1128/jb.187.13.4470-4479.2005

Carvalho, S. M., Kloosterman, T. G., Kuipers, O. P., & Neves, A. R. (2011). CcpA ensures optimal metabolic fitness of *Streptococcus pneumoniae*. *PloS One*, 6(10), e26707-e26707. doi:10.1371/journal.pone.0026707

Carvalho, S. M., Farshchi Andisi, V., Gradstedt, H., Neef, J., Kuipers, O. P., Neves, A. R., & Bijlsma, J. J. (2013). Pyruvate oxidase influences the sugar utilization pattern and capsule production in *Streptococcus pneumoniae*. *PloS One*, 8(7), e68277. doi:10.1371/journal.pone.0068277

Carvalho, S. M., Kloosterman, T. G., Manzoor, I., Caldas, J., Vinga, S., Martinussen, J., Saraiva, L. M., Kuipers, O. P., & Neves, A. R. (2018). Interplay between capsule expression and uracil metabolism in *Streptococcus pneumoniae* D39. *Frontiers in Microbiology*, 9, 321. doi:10.3389/fmicb.2018.00321

Chai, M. H., Weiland, F., Harvey, R. M., Hoffmann, P., Ogunniyi, A. D., & Paton, J. C. (2017). Proteomic comparisons of opaque and transparent variants of *Streptococcus pneumoniae* by two dimensional-differential gel electrophoresis. *Scientific Reports*, 7(1), 2453. doi:10.1038/s41598-017-02465-x

Chancey, S. T., Agrawal, S., Schroeder, M. R., Farley, M. M., Tettelin, H., & Stephens, D. S. (2015). Composite mobile genetic elements disseminating macrolide resistance in *Streptococcus pneumoniae*. Frontiers in Microbiology, 6(26). doi:10.3389/fmicb.2015.00026

Chao, Y., Marks, L. R., Pettigrew, M. M., & Hakansson, A. P. (2014). *Streptococcus pneumoniae* biofilm formation and dispersion during colonization and disease. *Frontiers in Cellular and Infection Microbiology*, 4(194). doi:10.3389/fcimb.2014.00194

Chen, A., Mann, B., Gao, G., Heath, R., King, J., Maissoneuve, J., Alderson, M., Tate, A., Hollingshead, S. K., Tweten, R. K., Briles, D. E., Tuomanen, E. I., & Paton, J. C. (2015). Multivalent pneumococcal protein vaccines comprising pneumolysoid with epitopes/fragments of CbpA and/or PspA elicit strong and broad protection. *Clinical and Vaccine Immunology*, 22(10), 1079-1089. doi:10.1128/CVI.00293-15

Chen, S., Paterson, G. K., Tong, H. H., Mitchell, T. J., & DeMaria, T. F. (2005). Sortase a contributes to pneumococcal nasopharyngeal colonization in the chinchilla model. *FEMS Microbiology Letters*, 253(1), 151-154. doi:10.1016/j.femsle.2005.09.052

Cheng, W., Li, Q., Jiang, Y.-L., Zhou, C.-Z., & Chen, Y. (2013). Structures of *Streptococcus pneumoniae* PiaA and its complex with ferrichrome reveal insights into the substrate binding and release of high affinity iron transporters. *PloS One*, 8(8), e71451-e71451. doi:10.1371/journal.pone.0071451

Cherazard, R., Epstein, M., Doan, T.-L., Salim, T., Bharti, S., & Smith, M. A. (2017). Antimicrobial resistant *Streptococcus pneumoniae*: Prevalence, mechanisms, and clinical implications. *American Journal of Therapeutics*, 24(3), e361-e369. doi:10.1097/MJT.0000000000000551

Chiba, N., Morozumi, M., Shouji, M., Wajima, T., Iwata, S., & Ubukata, K. (2014). Changes in capsule and drug resistance of pneumococci after introduction of PCV7, Japan, 2010-2013. *Emerging Infectious Disease*, 20(7), 1132-1139. doi:10.3201/eid2007.131485

Cho, H., Jönsson, H., Campbell, K., Melke, P., Williams, J. W., Jedynak, B., Stevens, A. M., Groisman, A., & Levchenko, A. (2007). Self-organization in high-density bacterial colonies: Efficient crowd control. *PLoS Biology*, 5(11), e302-e302. doi:10.1371/journal.pbio.0050302

Cillóniz, C., Ewig, S., Menéndez, R., Ferrer, M., Polverino, E., Reyes, S., Gabarrús, A., Marcos, M. A., Cordoba, J., Mensa, J., & Torres, A. (2012). Bacterial co-infection with H1N1 infection in patients admitted with community acquired pneumonia. *The Journal of Infection*, 65(3), 223-230. doi:10.1016/j.jinf.2012.04.009

Claverys, J.-P., & Håvarstein, L. S. (2002). Extracellular-peptide control of competence for genetic transformation in *Streptococcus pneumoniae*. *Frontiers in Bioscience-Landmark*, 7(4), 1798-1814. doi:10.2741/claverys

Claverys, J.-P., Prudhomme, M., & Martin, B. (2006). Induction of competence regulons as a general response to stress in gram-positive bacteria. *Annual Review of Microbiology*, 60(1), 451-475. doi:10.1146/annurev.micro.60.080805.142139

Claverys, J.-P., & Håvarstein, L. S. (2007). Cannibalism and fratricide: Mechanisms and raisons d'être. *Nature Reviews Microbiology*, 5(3), 219-229. doi:10.1038/nrmicro1613

Cohen, R., Bingen, E., Varon, E., de La Rocque, F., Brahimi, N., Levy, C., Boucherat, M., Langue, J., & Geslin, P. (1997). Change in nasopharyngeal carriage of *Streptococcus pneumoniae* resulting from antibiotic therapy for acute otitis media in children. *The Pediatric Infectious Disease Journal*, 16(6), 555-560. doi:10.1097/00006454-199706000-00004

Comis, S. D., Osborne, M. P., Stephen, J., Tarlow, M. J., Hayward, T. L., Mitchell, T. J., Andrew, P. W., & Boulnois, G. J. (1993). Cytotoxic effects on hair cells of guinea pig cochlea produced by pneumolysin, the thiol activated toxin of *Streptococcus pneumoniae*. *Acta Oto-Laryngologica*, 113(1-2), 152-159. doi:10.3109/00016489309135784

Corbett, A. J., Eckle, S. B., Birkinshaw, R. W., Liu, L., Patel, O., Mahony, J., Chen, Z., Reantragoon, R., Meehan, B., Cao, H., Williamson, N. A., Strugnell, R. A., Van Sinderen, D., Mak, J. Y., Fairlie, D. P., Kjer-Nielsen, L., Rossjohn, J., & McCluskey, J. (2014). T-cell activation by transitory neo-antigens derived from distinct microbial pathways. *Nature*, 509(7500), 361-365. doi:10.1038/nature13160

Corcoran, M., Mereckiene, J., Murchan, S., McElligott, M., 'Flanagan, D., Cotter, S., Cunney, R., & Humphreys, H. (2019). Is it time to review the vaccination strategy to protect adults against invasive pneumococcal disease? *Irish Medical Journal*, 112(3), 894-894.

Costerton, J. W., Stewart, P. S., & Greenberg, E. P. (1999). Bacterial biofilms: A common cause of persistent infections. *Science*, 284(5418), 1318-1322. doi:10.1126/science.284.5418.1318

Craig, A., Mai, J., Cai, S., & Jeyaseelan, S. (2009). Neutrophil recruitment to the lungs during bacterial pneumonia. *Infection and Immunity*, 77(2), 568-575. doi:10.1128/IAI.00832-08

Cremers, A. J., Zomer, A. L., Gritzfeld, J. F., Ferwerda, G., van Hijum, S. A., Ferreira, D. M., Shak, J. R., Klugman, K. P., Boekhorst, J., Timmerman, H. M., de Jonge, M. I., Gordon, S. B., & Hermans, P. W. (2014). The adult nasopharyngeal microbiome as a determinant of pneumococcal acquisition. *Microbiome*, 2(1), 44. doi:10.1186/2049-2618-2-44

Cremers, A. J. H., Mobegi, F. M., Gaast-de Jongh, C. E. v. d., Weert, M. v., Opzeeland, F. J. v., Vehkala, M., Meis, J. F., Hijum, S. A. F. T. v., Ferwerda, G., & Jonge, M. I. d. (2019). The

contribution of genetic variation of *Streptococcus pneumoniae* to the clinical manifestation of invasive pneumococcal disease. Clinical Infectious Diseases, 68(1), 61-69. doi:10.1093/cid/ciy417

Croucher, N. J., Walker, D., Romero, P., Lennard, N., Paterson, G. K., Bason, N. C., Mitchell, A. M., Quail, M. A., Andrew, P. W., Parkhill, J., Bentley, S. D., & Mitchell, T. J. (2009). Role of conjugative elements in the evolution of the multidrug-resistant pandemic clone *Streptococcus pneumoniae*^{Spain23F} ST81. *Journal of Bacteriology*, 191(5), 1480-1489. doi:10.1128/JB.01343-08

Croucher, N. J., Finkelstein, J. A., Pelton, S. I., Mitchell, P. K., Lee, G. M., Parkhill, J., Bentley, S. D., Hanage, W. P., & Lipsitch, M. (2013). Population genomics of post-vaccine changes in pneumococcal epidemiology. *Nature Genetics*, 45(6), 656-663. doi:10.1038/ng.2625

Cundell, D. R., Gerard, N. P., Gerard, C., Idanpaan-Heikkila, I., & Tuomanen, E. I. (1995). *Streptococcus pneumoniae* anchor to activated human cells by the receptor for platelet-activating factor. *Nature*, 377(6548), 435-438. doi:10.1038/377435a0

Dabernat, H., Geslin, P., Megraud, F., Bégué, P., Boulesteix, J., Dubreuil, C., De La Roque, F., Trinh, A., & Scheimberg, A. (1998). Effects of cefixime or co-amoxiclav treatment on nasopharyngeal carriage of *Streptococcus pneumoniae* and *Haemophilus influenzae* in children with acute otitis media. *Journal of Antimicrobial Chemotherapy*, 41(2), 253-258. doi:10.1093/jac/41.2.253

Dagan, R. (2009). Impact of pneumococcal conjugate vaccine on infections caused by antibiotic-resistant *Streptococcus pneumoniae*. *Clinical Microbiology and Infection*, 15(s3), 16-20. doi:10.1111/j.1469-0691.2009.02726.x

Dagan, R. O. N., Leibovitz, E., Greenberg, D., Yagupsky, P., Fliss, D. M., & Leiberman, A. (1998). Dynamics of pneumococcal nasopharyngeal colonization during the first days of antibiotic treatment in pediatric patients. The Pediatric Infectious Disease Journal, 17(10), 880-885. doi:10.1097/00006454-199810000-00006

Daniels, C. C., Rogers, P. D., & Shelton, C. M. (2016). A review of pneumococcal vaccines: Current polysaccharide vaccine recommendations and future protein antigens. *The Journal of Pediatric Pharmacology and Therapeutics*, 21(1), 27-35. doi:10.5863/1551-6776-21.1.27

Danishyar, A., & Ashurst, J. (2023). Acute otitis media. *Treasure Island (FL): StatPearls Publishing.* Retrieved from https://www.ncbi.nlm.nih.gov/books/NBK470332/

Dave, S., Carmicle, S., Hammerschmidt, S., Pangburn, M. K., & McDaniel, L. S. (2004). Dual roles of PspC, a surface protein of *Streptococcus pneumoniae*, in binding human secretory IgA and factor H. *The Journal of Immunology,* 173(1), 471-477. doi:10.4049/jimmunol.173.1.471

David, S. C., Laan, Z., Minhas, V., Chen, A. Y., Davies, J., Hirst, T. R., McColl, S. R., Alsharifi, M., & Paton, J. C. (2019). Enhanced safety and immunogenicity of a pneumococcal surface antigen a mutant whole-cell inactivated pneumococcal vaccine. *Immunology and Cell Biology*, 97(8), 726-739. doi:10.1111/imcb.12257

David, S. C., Brazel, E. B., Singleton, E. V., Minhas, V., Laan, Z., Scougall, C., Chen, A. Y., Wang, H., Gates, C. J., McLean, K. T., Brown, J. S., Ercoli, G., Higgins, R. A., Licciardi, P. V., Mulholland, K., Davies, J. B., Hirst, T. R., Paton, J. C., & Alsharifi, M. (2022). A nonadjuvanted whole-inactivated

pneumococcal vaccine induces multiserotype opsonophagocytic responses mediated by noncapsule-specific antibodies. *mBio*, 13(5), e02367-02322. doi:10.1128/mbio.02367-22

Davis, K. M., Akinbi, H. T., Standish, A. J., & Weiser, J. N. (2008). Resistance to mucosal lysozyme compensates for the fitness deficit of peptidoglycan modifications by *Streptococcus pneumoniae*. *PLoS Pathogens*, 4(12), e1000241-e1000241. doi:10.1371/journal.ppat.1000241

Dawid, S., Roche, A. M., & Weiser, J. N. (2007). Blp bacteriocins of *Streptococcus pneumoniae* mediate intraspecies competition both *in vitro* and *in vivo*. *Infection and Immunity*, 75(1), 443-451. doi:10.1128/IAI.01775-05

Dawid, S., Sebert, M. E., & Weiser, J. N. (2009). Bacteriocin activity of *Streptococcus pneumoniae* is controlled by the serine protease HtrA via posttranscriptional regulation. *Journal of Bacteriology*, 191(5), 1509-1518. doi:10.1128/JB.01213-08

de la Fuente-Núñez, C., Reffuveille, F., Fernández, L., & Hancock, R. E. W. (2013). Bacterial biofilm development as a multicellular adaptation: Antibiotic resistance and new therapeutic strategies. *Current Opinion in Microbiology*, 16(5), 580-589. doi:10.1016/j.mib.2013.06.013

de Saizieu, A., Gardès, C., Flint, N., Wagner, C., Kamber, M., Mitchell, T. J., Keck, W., Amrein, K. E., & Lange, R. (2000). Microarray-based identification of a novel *Streptococcus pneumoniae* regulon controlled by an autoinduced peptide. *Journal of Bacteriology*, 182(17), 4696-4703. doi:10.1128/JB.182.17.4696-4703.2000

De Ste Croix, M., Mitsi, E., Morozov, A., Glenn, S., Andrew, P. W., Ferreira, D. M., & Oggioni, M. R. (2020). Phase variation in pneumococcal populations during carriage in the human nasopharynx. *Nature Scientific Reports*, 10(1), 1803. doi:10.1038/s41598-020-58684-2

de Vries, S. P. W., van Hijum, S. A. F. T., Schueler, W., Riesbeck, K., Hays, J. P., Hermans, P. W. M., & Bootsma, H. J. (2010). Genome analysis of *Moraxella catarrhalis* strain BBH18, [corrected] a human respiratory tract pathogen. *Journal of Bacteriology*, 192(14), 3574-3583. doi:10.1128/JB.00121-10

DeBardeleben, H. K., Lysenko, E. S., Dalia, A. B., & Weiser, J. N. (2014). Tolerance of a phage element by *Streptococcus pneumoniae* leads to a fitness defect during colonization. *Journal of Bacteriology*, 196(14), 2670-2680. doi:10.1128/JB.01556-14

Desbois, A. P., & Smith, V. J. (2010). Antibacterial free fatty acids: Activities, mechanisms of action and biotechnological potential. *Applied Microbiology and Biotechnology*, 85(6), 1629-1642. doi:10.1007/s00253-009-2355-3

Deutscher, J., Herro, R., Bourand, A., Mijakovic, I., & Poncet, S. (2005). P-Ser-HPr—a link between carbon metabolism and the virulence of some pathogenic bacteria. *Biochimica et Biophysica Acta (BBA) - Proteins and Proteomics*, 1754(1), 118-125. doi:10.1016/j.bbapap.2005.07.029

Dintilhac, A., Alloing, G., Granadel, C., & Claverys, J. P. (1997). Competence and virulence of *Streptococcus pneumoniae*: Adc and PsaA mutants exhibit a requirement for Zn and Mn resulting from inactivation of putative ABC metal permeases. *Molecular Microbiology*, 25(4), 727-739. doi:10.1046/j.1365-2958.1997.5111879.x

Dockrell, D. H., & Brown, J. S. (2016). Chapter 21 - *Streptococcus pneumoniae* interactions with macrophages and mechanisms of immune evasion. In (pp. 401-422): *Elsevier Inc*.

Domenech, A., Slager, J., & Veening, J.-W. (2018). Antibiotic-induced cell chaining triggers pneumococcal competence by reshaping quorum sensing to autocrine-like signaling. *Cell Reports*, 25(9), 2390-2400.e2393. doi:10.1016/j.celrep.2018.11.007

Donati, C., Hiller, N. L., Tettelin, H., Muzzi, A., Croucher, N. J., Angiuoli, S. V., Oggioni, M., Dunning Hotopp, J. C., Hu, F. Z., Riley, D. R., Covacci, A., Mitchell, T. J., Bentley, S. D., Kilian, M., Ehrlich, G. D., Rappuoli, R., Moxon, E. R., & Masignani, V. (2010). Structure and dynamics of the pan-genome of *Streptococcus pneumoniae* and closely related species. *Genome Biology*, 11(10), R107-R107. doi:10.1186/gb-2010-11-10-r107

Donlan, R. M., & Costerton, J. W. (2002). Biofilms: Survival mechanisms of clinically relevant microorganisms. *Clinical Microbiology Reviews*, 15(2), 167-148. doi:10.1128/CMR.15.2.167-193.2002

Egan, J. B., & Morse, M. L. (1966). Carbohydrate transport in *Staphylococcus aureus*: III. Studies of the transport process. *Biochimica et Biophysica Acta. Biophysics including Photosynthesis*, 112(1), 63-73. doi:10.1016/S0926-6585(96)90009-6

Ehrlich, G. D., Hu, F. Z., Shen, K., Stoodley, P., & Post, J. C. (2005). Bacterial plurality as a general mechanism driving persistence in chronic infections. *Clinical Orthopaedics and Related Research*, 437, 20-24. doi:10.1097/00003086-200508000-00005

El Moujaber, G., Osman, M., Rafei, R., Dabboussi, F., & Hamze, M. (2017). Molecular mechanisms and epidemiology of resistance in *Streptococcus pneumoniae* in the Middle East region. *Journal of Medical Microbiology*, 66(7), 847-858. doi:10.1099/jmm.0.000503

Eldholm, V., Johnsborg, O., Haugen, K., Ohnstad, H. S., & Håvarstein, L. S. (2009). Fratricide in *Streptococcus pneumoniae*: Contributions and role of the cell wall hydrolases CbpD, LytA and LytC. *Microbiology (Society for General Microbiology)*, 155(7), 2223-2234. doi:10.1099/mic.0.026328-0

Eldholm, V., Johnsborg, O., Straume, D., Ohnstad, H. S., Berg, K. H., Hermoso, J. A., & Håvarstein, L. S. (2010). Pneumococcal CbpD is a murein hydrolase that requires a dual cell envelope binding specificity to kill target cells during fratricide: The pneumococcal murein hydrolase CbpD. *Molecular Microbiology*, 76(4), 905-917. doi:10.1111/j.1365-2958.2010.07143.x

Ells, R., Kock, J. L. F., Van Wyk, P. W. J., Botes, P. J., & Pohl, C. H. (2009). Arachidonic acid increases antifungal susceptibility of *Candida albicans* and *Candida dubliniensis*. *Journal of Antimicrobial Chemotherapy*, 63(1), 124-128. doi:10.1093/jac/dkn446

Enright, M. C., & Spratt, B. G. (1998). A multilocus sequence typing scheme for *Streptococcus pneumoniae*: Identification of clones associated with serious invasive disease. *Microbiology (Society for General Microbiology)*, 144(11), 3049-3060. doi:10.1099/00221287-144-11-3049

Essink, B., Sabharwal, C., Cannon, K., Frenck, R., Lal, H., Xu, X., Sundaraiyer, V., Peng, Y., Moyer, L., Pride, M. W., Scully, I. L., Jansen, K. U., Gruber, W. C., Scott, D. A., & Watson, W. (2021). Pivotal phase 3 randomized clinical trial of the safety, tolerability, and immunogenicity of 20-valent

pneumococcal conjugate vaccine in adults aged ≥18 years. *Clinical Infectious Diseases*, 75(3), 390-398. doi:10.1093/cid/ciab990

Falloon, J., & Gallin, J. I. (1986). Neutrophil granules in health and disease. *Journal of Allergy and Clinical Immunology*, 77(5), 653-662. doi:10.1016/0091-6749(86)90404-5

Fasching, C. E., Grossman, T., Corthésy, B., Plaut, A. G., Weiser, J. N., & Janoff, E. N. (2007). Impact of the molecular form of immunoglobulin a on functional activity in defense against *Streptococcus pneumoniae*. *Infection and Immunology*, 75(4), 1801-1810. doi:10.1128/iai.01758-06

Feldman, C., Munro, N. C., Jeffery, P. K., Mitchell, T. J., Andrew, P. W., Boulnois, G. J., Guerreiro, D., Rohde, J. A. L., Todd, H. C., Cole, P. J., & Wilson, R. (1991). Pneumolysin induces the salient histologic features of pneumococcal infection in the rat lung in vivo. *American Journal of Respiratory Cell and Molecular Biology*, 5(5), 416-423. doi:10.1165/ajrcmb/5.5.416

Feldman, C., Read, R., Rutman, A., Jeffery, P. K., Brain, A., Lund, V., Mitchell, T. J., Andrew, P. W., Boulnois, G. J., & Todd, H. C. (1992). The interaction of *Streptococcus pneumoniae* with intact human respiratory mucosa *in vitro*. *The European Respiratory Journal*, 5(5), 576-583. doi:10.1183/09031936.93.05050576

Ferreira, D. M., Neill, D. R., Wright, A. D., Collins, A. M., Goldblatt, D., Kadioglu, A., Gordon, S. B., Bangert, M., Gritzfeld, J. F., Green, N., Wright, A. K. A., Pennington, S. H., Moreno, L. B., Moreno, A. T., & Miyaji, E. N. (2013). Controlled human infection and rechallenge with *Streptococcus pneumoniae* reveals the protective efficacy of carriage in healthy adults. *American Journal of Respiratory and Critical Care Medicine*, 187(8), 855-864. doi:10.1164/rccm.201212-2277OC

Fine, M. J., Smith, M. A., Carson, C. A., Meffe, F., Sankey, S. S., Weissfeld, L. A., Detsky, A. S., & Kapoor, W. N. (1994). Efficacy of pneumococcal vaccination in adults: A meta-analysis of randomized controlled trials. *Archives of Internal Medicine*, 154(23), 2666-2677. doi:10.1001/archinte.1994.00420230051007

Fleming, E., Lazinski, D. W., & Camilli, A. (2015). Carbon catabolite repression by seryl phosphorylated HPr is essential to *Streptococcus pneumoniae* in carbohydrate-rich environments. *Molecular Microbiology*, 97(2), 360-380. doi:10.1111/mmi.13033

Forrest, J. M. S., McIntyre, P. B., & Burgess, M. A. (2000). Pneumococcal disease in Australia [summary of the pneumococcal disease in Australia: Epidemiology, surveillance and immunisation workshop, Royal Alexandra Hospital for Children (1999: Sydney)]. *Communicable Diseases Intelligence*, 24(4), 89-92. Retrieved from https://search.informit.org/doi/10.3316/ielapa.200009737

Franchi, L., Warner, N., Viani, K., & Nuñez, G. (2009). Function of NOD-like receptors in microbial recognition and host defense. *Immunological Reviews*, 227(1), 106-128. doi:10.1111/j.1600-065X.2008.00734.x

Ganaie, F., Maruhn, K., Li, C., Porambo, R. J., Elverdal, P. L., Abeygunwardana, C., Linden, M. v. d., Duus, J. Ø., Sheppard, C. L., & Nahm, M. H. (2021). Structural, genetic, and serological elucidation of *Streptococcus pneumoniae* serogroup 24 serotypes: Discovery of a new serotype,

24C, with a variable capsule structure. *Journal of Clinical Microbiology*, 59(7). doi:10.1128/jcm.00540-21

Ganzle, M. G. (2015). Lactic metabolism revisited: Metabolism of lactic acid bacteria in food fermentations and food spoilage. *Current Opinion in Food Science*, 2, 106-117. doi:10.1016/j.cofs.2015.03.001

Garcia-Rodriguez, J. A., & Fresnadillo Martinez, M. J. (2002). Dynamics of nasopharyngeal colonization by potential respiratory pathogens. Journal of Antimicrobial Chemotherapy, 50(suppl-3), 59-74. doi:10.1093/jac/dkf506

Gardiner, E. E., & Andrews, R. K. (2012). Neutrophil extracellular traps (NETs) and infection-related vascular dysfunction. *Blood Reviews*, 26(6), 255-259. doi:10.1016/j.blre.2012.09.001

Geno, K. A., Gilbert, G. L., Song, J. Y., Skovsted, I. C., Klugman, K. P., Jones, C., Konradsen, H. B., & Nahm, M. H. (2015). Pneumococcal capsules and their types: Past, present, and future. *Clinical Microbiology Reviews*, 28(3), 871-899. doi:10.1128/CMR.00024-15

Ghaffar, F., Barton, T., Lozano, J., Muniz, L. S., Hicks, P., Gan, V., Ahmad, N., & McCracken, G. H. (2004). Effect of the 7-valent pneumococcal conjugate vaccine on nasopharyngeal colonization by *Streptococcus pneumoniae* in the first 2 years of life. *Clinical Infectious Diseases*, 39(7), 930-938. doi:10.1086/423379

Gladstone, R. A., Jefferies, J. M., Tocheva, A. S., Beard, K. R., Garley, D., Chong, W. W., Bentley, S. D., Faust, S. N., & Clarke, S. C. (2015). Five winters of pneumococcal serotype replacement in UK carriage following PCV introduction. *Vaccine*, 33(17), 2015-2021. doi:10.1016/j.vaccine.2015.03.012

Gladstone, R. A., Devine, V., Jones, J., Cleary, D., Jefferies, J. M., Bentley, S. D., Faust, S. N., & Clarke, S. C. (2017). Pre-vaccine serotype composition within a lineage signposts its serotype replacement - a carriage study over 7 years following pneumococcal conjugate vaccine use in the UK. *Microbial Genomics*, 3(6), e000119-e000119. doi:10.1099/mgen.0.000119

Gold, M. C., Eid, T., Smyk-Pearson, S., Eberling, Y., Swarbrick, G. M., Langley, S. M., Streeter, P. R., Lewinsohn, D. A., & Lewinsohn, D. M. (2013). Human thymic MR1-restricted MAIT cells are innate pathogen-reactive effectors that adapt following thymic egress. *Mucosal Immunology*, 6(1), 35-44. doi:10.1038/mi.2012.45

Gray, B. M., Converse, G. M., III, & Dillon, H. C., Jr. (1980). Epidemiologic studies of *Streptococcus pneumoniae* in infants: Acquisition, carriage, and infection during the first 24 months of life. *The Journal of Infectious Diseases*, 142(6), 923-933. doi:10.1093/infdis/142.6.923

Gray, B. M., Turner, M. E., & Dillon, H. C., JR. (1982). Epidemiologic studies of *Streptococcus pneumoniae* in infants: The effects of season and age on pneumococcal acquisition and carriage in the first 24 months of life. *American Journal of Epidemiology*, 116(4), 692-703. doi:10.1093/oxfordjournals.aje.a113452

Grebe, K. M., Takeda, K., Hickman, H. D., Bailey, A. M., Embry, A. C., Bennink, J. R., & Yewdell, J. W. (2010). Cutting edge: Sympathetic nervous system increases proinflammatory cytokines and

exacerbates Influenza A Virus pathogenesis. *The Journal of Immunology*, 184(5), 2736-2736. doi:10.4049/jimmunol.1090003

Grivea, I. N., Panagiotou, M., Tsantouli, A. G., & Syrogiannopoulos, G. A. (2008). Impact of heptavalent pneumococcal conjugate vaccine on nasopharyngeal carriage of penicillin-resistant *Streptococcus pneumoniae* among day-care center attendees in central Greece. *The Pediatric Infectious Disease Journal*, 27(6), 519-525. doi:10.1097/INF.0b013e318168d28a

Güemes, M., Rahman, S. A., & Hussain, K. (2016). What is a normal blood glucose? *Archives of Disease in Childhood*, 101(6), 569-574. doi:10.1136/archdischild-2015-308336

Guiral, S., Mitchell, T. J., Martin, B., Claverys, J.-P., & Losick, R. M. (2005). Competence-programmed predation of noncompetent cells in the human pathogen *Streptococcus pneumoniae*: Genetic requirements. *Proceedings of the National Academy of Sciences - PNAS*, 102(24), 8710-8715. doi:10.1073/pnas.0500879102

Gwaltney, J. M., Sande, M. A., Austrian, R., & Owen Hendley, J. (1975). Spread of *Streptococcus pneumoniae* in families. II. Relation of transfer of S. pneumoniae to incidence of colds and serum antibody. *The Journal of Infectious Diseases*, 132(1), 62-68. doi:10.1093/infdis/132.1.62

Hall-Stoodley, L., Nistico, L., Sambanthamoorthy, K., Dice, B., Nguyen, D., Mershon, W. J., Johnson, C., Hu, F. Z., Stoodley, P., Ehrlich, G. D., & Post, J. C. (2008). Characterization of biofilm matrix, degradation by DNase treatment and evidence of capsule downregulation in *Streptococcus pneumoniae* clinical isolates. *BMC Microbiology*, 8, 173. doi:10.1186/1471-2180-8-173

Hamaguchi, S., Zafar, M. A., Cammer, M., & Weiser, J. N. (2018). Capsule prolongs survival of *Streptococcus pneumoniae* during starvation. *Infection and Immunity*, 86(3). doi:10.1128/IAI.00802-17

Hammerschmidt, S., Tillig, M. P., Wolff, S., Vaerman, J. P., & Chhatwal, G. S. (2000). Species-specific binding of human secretory component to SpsA protein of *Streptococcus pneumoniae* via a hexapeptide motif. *Molecular microbiology*, 36(3), 726-736. doi:10.1046/j.1365-2958.2000.01897.x

Hammerschmidt, S., Wolff, S., Hocke, A., Rosseau, S., Muůller, E., & Rohde, M. (2005). Illustration of pneumococcal polysaccharide capsule during adherence and invasion of epithelial cells. *Infection and Immunity*, 73(8), 4653-4667. doi:10.1128/IAI.73.8.4653-4667.2005

Hammitt, L. L., Bruden, D. L., Butler, J. C., Baggett, H. C., Hurlburt, D. A., Reasonover, A., & Hennessy, T. W. (2006). Indirect effect of conjugate vaccine on adult carriage of *Streptococcus pneumoniae*: An explanation of trends in invasive pneumococcal disease. *The Journal of Infectious Diseases*, 193(11), 1487-1494. doi:10.1086/503805

Han, S. B., Kim, J. H., Kang, J. H., Ma, S. H., Kim, C. S., Kim, K. H., Kim, H. M., & Choi, Y. Y. (2017). Recent epidemiology of *Streptococcus pneumoniae* in nasopharynxes of Korean children with acute otitis media. *Journal of Infection and Chemotherapy*, 23(3), 136-141. doi:10.1016/j.jiac.2016.10.006

Hansman, D., & Bullen, M. M. (1967). A resistant pneumococcus. *The Lancet (British edition)*, 290(7509), 264-265. doi:10.1016/S0140-6736(67)92346-X

Hao, L., Kuttel, M. M., Ravenscroft, N., Thompson, A., Prasad, A. K., Gangolli, S., Tan, C., Cooper, D., Watson, W., Liberator, P., Pride, M. W., Jansen, K. U., Anderson, A. S., & Scully, I. L. (2022). *Streptococcus pneumoniae* serotype 15B polysaccharide conjugate elicits a cross-functional immune response against serotype 15C but not 15A. *Vaccine*, 40(33), 4872-4880. doi:10.1016/j.vaccine.2022.06.041

Harboe, Z. B., Thomsen, R. W., Riis, A., Valentiner-Branth, P., Christensen, J. J., Lambertsen, L., Krogfelt, K. A., Konradsen, H. B., & Benfield, T. L. (2009). Pneumococcal serotypes and mortality following invasive pneumococcal disease: A population-based cohort study. *PLoS Medicine*, 6(5), e1000081-e1000081. doi:10.1371/journal.pmed.1000081

Harris, R., & Harper, E. (2015). Glycolytic pathway. In (Vol. 8, pp. 241-249) *eLS*. Chichester, UK: John Wiley & Sons, Ltd. doi:10.1002/9780470015902.a0000619.pub3

Hartmann, N., McMurtrey, C., Sorensen, M. L., Huber, M. E., Kurapova, R., Coleman, F. T., Mizgerd, J. P., Hildebrand, W., Kronenberg, M., Lewinsohn, D. M., & Harriff, M. J. (2018). Riboflavin metabolism variation among clinical isolates of *Streptococcus pneumoniae* results in differential activation of mucosal-associated invariant t cells. *American Journal of Respiratory Cell and Molecular Biology*, 58(6), 767-776. doi:10.1165/rcmb.2017-0290OC

Harvey, R. M., Stroeher, U. H., Ogunniyi, A. D., Smith-Vaughan, H. C., Leach, A. J., & Paton, J. C. (2011). A variable region within the genome of *Streptococcus pneumoniae* contributes to strain-strain variation in virulence. *PloS One*, 6(5), e19650-e19650. doi:10.1371/journal.pone.0019650

Hatcher, B. L., Hale, J. Y., & Briles, D. E. (2016). Free sialic acid acts as a signal that promotes *Streptococcus pneumoniae* invasion of nasal tissue and nonhematogenous invasion of the central nervous system. *Infection and Immunity*, 84(9), 2607-2615. doi:10.1128/IAI.01514-15

Hathaway, L. J., Brugger, S. D., Morand, B., Bangert, M., Rotzetter, J. U., Hauser, C., Graber, W. A., Gore, S., Kadioglu, A., & Mühlemann, K. (2012). Capsule type of *Streptococcus pneumoniae* determines growth phenotype. *PLoS Pathogens*, 8(3), e1002574. doi:10.1371/journal.ppat.1002574

Hava, D. L., & Camilli, A. (2002). Large-scale identification of serotype 4 *Streptococcus pneumoniae* virulence factors. *Molecular Microbiology*, 45(5), 1389-1406.

Håvarstein, L. S., Coomaraswamy, G., & Morrison, D. A. (1995). An unmodified heptadecapeptide pheromone induces competence for genetic transformation in *Streptococcus pneumoniae*. *Proceedings of the National Academy of Sciences - PNAS*, 92(24), 11140-11144. doi:10.1073/pnas.92.24.11140

Håvarstein, L. S. (2003). Chapter 16 - intercellular communication in gram-positive bacteria depends on peptide pheromones and their histidine kinase receptors. In *Histidine Kinases in Signal Transduction* (pp. 341-363). M. Inouye & R. Dutta (Eds.), San Diego: Academic Press.

Håvarstein, L. S., Martin, B., Johnsborg, O., Granadel, C., & Claverys, J.-P. (2006). New insights into the pneumococcal fratricide: Relationship to clumping and identification of a novel immunity factor. *Molecular Microbiology*, 59(4), 1297-1037. doi:10.1111/j.1365-2958.2005.05021.x

Heilmann, C. (1990). Human B and T lymphocyte responses to vaccination with pneumococcal polysaccharides. Copenhagen: *Munksgaard*

Henckaerts, L., Desmet, S., Schalck, N., Lagrou, K., Verhaegen, J., Peetermans, W. E., & Flamaing, J. (2021). The impact of childhood 13-valent pneumococcal conjugate vaccination on overall invasive pneumococcal disease, including the oldest old. *Acta Clinica Belgica*, 76(4), 272-279. doi:10.1080/17843286.2020.1721131

Hergott, C. B., Roche, A. M., Naidu, N. A., Mesaros, C., Blair, I. A., & Weiser, J. N. (2015). Bacterial exploitation of phosphorylcholine mimicry suppresses inflammation to promote airway infection. *The Journal of Clinical Investigation*, 125(10), 3878-3890. doi:10.1172/JCI81888

Hiller, N. L., Janto, B., Hogg, J. S., Boissy, R., Yu, S., Powell, E., Keefe, R., Ehrlich, N. E., Shen, K., Hayes, J., Barbadora, K., Klimke, W., Dernovoy, D., Tatusova, T., Parkhill, J., Bentley, S. D., Post, J. C., Ehrlich, G. D., & Hu, F. Z. (2007). Comparative genomic analyses of seventeen *Streptococcus pneumoniae* strains: Insights into the pneumococcal supragenome. *Journal of Bacteriology*, 189(22), 8186-8195. doi:10.1128/JB.00690-07

Hirst, R. A., Kadioglu, A., O'Callaghan, C., & Andrew, P. W. (2004). The role of pneumolysin in pneumococcal pneumonia and meningitis. *Clinical and Experimental Immunology*, 138(2), 195-201. doi:10.1111/j.1365-2249.2004.02611.x

Hiss, P. H. (1905). A contribution to the physiological differentiation of pneumococcus and *Streptococcus*, and to methods of staining capsules. *The Journal of Experimental Medicine*, 6(4-6), 317-345. doi:10.1084/jem.6.4-6.317

Ho, P. L., Chiu, S. S., Law, P. Y., Chan, E. L., Lai, E. L., & Chow, K. H. (2015). Increase in the nasopharyngeal carriage of non-vaccine serogroup 15 *Streptococcus pneumoniae* after introduction of children pneumococcal conjugate vaccination in Hong Kong. *Diagnostic Microbiology and Infectious Disease*, 81(2), 145-148. doi:10.1016/j.diagmicrobio.2014.11.006

Hoe, E., Anderson, J., Nathanielsz, J., Toh, Z. Q., Marimla, R., Balloch, A., & Licciardi, P. V. (2017). The contrasting roles of Th17 immunity in human health and disease. *Microbiology and Immunology*, 61(2), 49-56. doi:10.1111/1348-0421.12471

Hollingshead, S. K., Becker, R., & Briles, D. E. (2000). Diversity of PspA: Mosaic genes and evidence for past recombination in *Streptococcus pneumoniae*. *Infection and Immunity*, 68(10), 5889-5900. doi:10.1128/IAI.68.10.5889-5900.2000

Holmes, A. R., McNab, R., Millsap, K. W., Rohde, M., Hammerschmidt, S., Mawdsley, J. L., & Jenkinson, H. F. (2001). The *pavA* gene of *Streptococcus pneumoniae* encodes a fibronectin-binding protein that is essential for virulence. *Molecular Microbiology*, 41(6), 1395-1408. doi:10.1046/j.1365-2958.2001.02610.x

Hoskins, J., Alborn, J. W. E., Arnold, J., Blaszczak, L. C., Burgett, S., DeHoff, B. S., Estrem, S. T., Fritz, L., Fu, D. J., Fuller, W., Geringer, C., Gilmour, R., Glass, J. S., Khoja, H., Kraft, A. R., Lagace, R. E., LeBlanc, D. J., Lee, L. N., Lefkowitz, E. J., Lu, J., Matsushima, P., McAhren, S. M., McHenney, M., McLeaster, K., Mundy, C. W., Nicas, T. I., Norris, F. H., O'Gara, M., Peery, R. B., Robertson, G. T., Rockey, P., Sun, P. M., Winkler, M. E., Yang, Y., Young-Bellido, M., Zhao, G., Zook, C. A., Baltz, R. H., Jaskunas, S. R., Rosteck, J. P. R., Skatrud, P. L., & Glass, J. I. (2001).

Genome of the bacterium *Streptococcus pneumoniae* strain R6. *Journal of Bacteriology*, 183(19), 5709-5717. doi:10.1128/JB.183.19.5709-5717.2001

Hosseini, S. M., Poorolajal, J., Karami, M., & Ameri, P. (2015). Prevalence of nasopharyngeal carriage of *Streptococcus pneumonia* in Iran: A meta-analysis. *Journal of Research in Health Sciences*, 15(3), 141-146.

Howard, L. V., & Gooder, H. (1974). Specificity of the autolysin of *Streptococcus* (diplococcus) *pneumoniae*. *Journal of Bacteriology*, 117(2), 796-804. doi:10.1128/JB.117.2.796-804.1974

Hsieh, Y.-C., Lin, T.-L., Lin, C.-M., & Wang, J.-T. (2015). Identification of PbIB mediating galactose-specific adhesion in a successful *Streptococcus pneumoniae* clone. *Scientific Reports*, 5(1), 12265-12265. doi:10.1038/srep12265

Hubacek, J., & Glover, S. W. (1970). Complementation analysis of temperature-sensitive host specificity mutations in *Escherichia coli. Journal of Molecular Biology*, 50(1), 111-127. doi:10.1016/0022-2836(70)90108-7

Hurley, D., Griffin, C., Young, M., Scott, D. A., Pride, M. W., Scully, I. L., Ginis, J., Severs, J., Jansen, K. U., Gruber, W. C., & Watson, W. (2021). Safety, tolerability, and immunogenicity of a 20-valent pneumococcal conjugate vaccine (PCV20) in adults 60 to 64 years of age. *Clinical Infectious Diseases*, 73(7), e1489-e1497. doi:10.1093/cid/ciaa1045

Hyams, C., Camberlein, E., Cohen, J. M., Bax, K., & Brown, J. S. (2010). *Streptococcus pneumoniae* capsule inhibits complement activity and neutrophil phagocytosis by multiple mechanisms. *Infection and Immunity*, 78(2), 704-715. doi:10.1128/IAI.00881-09

Iannelli, F., Oggioni, M. R., & Pozzi, G. (2002). Allelic variation in the highly polymorphic locus *pspC* of *Streptococcus pneumoniae*. *Gene*, 284(1-2), 63-71. doi:10.1016/S0378-1119(01)00896-4

Iannelli, F., & Pozzi, G. (2004). Method for introducing specific and unmarked mutations into the chromosome of *Streptococcus pneumoniae*. *Molecular Biotechnology*, 26(1), 81-86. doi:10.1385/MB:26:1:81

Ibrahim, Y. M., Kerr, A. R., McCluskey, J., & Mitchell, T. J. (2004). Control of virulence by the two-component system CiaR/H is mediated via HtrA, a major virulence factor of *Streptococcus pneumoniae*. *Journal of Bacteriology*, 186(16), 5258-5266. doi:10.1128/JB.186.16.5258-5266.2004

Im, H., Kruckow, K. L., D'Mello, A., Ganaie, F., Martinez, E., Luck, J. N., Cichos, K. H., Riegler, A. N., Song, X., Ghanem, E., Saad, J. S., Nahm, M. H., Tettelin, H., & Orihuela, C. J. (2022). Anatomical site-specific carbohydrate availability impacts *Streptococcus pneumoniae* virulence and fitness during colonization and disease. *Infection and Immunology*, 90(1), e0045121. doi:10.1128/iai.00451-21

Iovino, F., Engelen-Lee, J.-Y., Brouwer, M., van de Beek, D., van der Ende, A., Valls Seron, M., Mellroth, P., Muschiol, S., Bergstrand, J., Widengren, J., & Henriques-Normark, B. (2017). pIgR and PECAM-1 bind to pneumococcal adhesins RrgA and PspC mediating bacterial brain invasion. *The Journal of Experimental Medicine*, 214(6), 1619-1630. doi:10.1084/jem.20161668

Iroh Tam, P.-Y., Thielen, B. K., Obaro, S. K., Brearley, A. M., Kaizer, A. M., Chu, H., & Janoff, E. N. (2017). Childhood pneumococcal disease in Africa – a systematic review and meta-analysis of incidence, serotype distribution, and antimicrobial susceptibility. *Vaccine*, 35(15), 1817-1827. doi:10.1016/j.vaccine.2017.02.045

Iyer, R., Baliga, N. S., & Camilli, A. (2005). Catabolite control protein A (CcpA) contributes to virulence and regulation of sugar metabolism in *Streptococcus pneumoniae*. *Journal of Bacteriology*, 187(24), 8340-8349. doi:10.1128/JB.187.24.8340-8349.2005

Iyer, R., & Camilli, A. (2007). Sucrose metabolism contributes to *in vivo* fitness of *Streptococcus pneumoniae*. *Molecular Microbiology*, 66(1), 1-13. doi:10.1111/j.1365-2958.2007.05878.x

Janapatla, R. P., Su, L. H., Chen, H. H., Chang, H. J., Tsai, T. C., Chen, P. Y., Chen, C. L., & Chiu, C. H. (2017). Epidemiology of culture-confirmed infections of *Streptococcus pneumoniae* (2012-2015) and nasopharyngeal carriage in children and households in Taiwan (2014-2015). *Journal of Medical Microbiology*, 66(6), 729-736. doi:10.1099/jmm.0.000488

Janoff, E. N., Rubins, J. B., Fasching, C., Charboneau, D., Rahkola, J. T., Plaut, A. G., & Weiser, J. N. (2014). Pneumococcal IgA1 protease subverts specific protection by human IgA1. *Mucosal Immunology*, 7(2), 249-256. doi:10.1038/mi.2013.41

Janulczyk, R., Iannelli, F., Sjöholm, A. G., Pozzi, G., & Björck, L. (2000). Hic, a novel surface protein of *Streptococcus pneumoniae* that interferes with complement function. *The Journal of Biological Chemistry*, 275(47), 37257-37263. doi:10.1074/jbc.M004572200

Jedrzejas, M. J. (2001a). Pneumococcal virulence factors: Structure and function. *Microbiology and Molecular Biology Reviews,* 65(2), 187-207. doi:10.1128/MMBR.65.2.187-207.2001

Jedrzejas, M. J., Lamani, E., & Becker, R. S. (2001b). Characterization of selected strains of pneumococcal surface protein A. *The Journal of Biological Chemistry*, 276(35), 33121-33128. doi:10.1074/jbc.M103304200

Jensch, I., Gámez, G., Rothe, M., Ebert, S., Fulde, M., Somplatzki, D., Bergmann, S., Petruschka, L., Rohde, M., Nau, R., & Hammerschmidt, S. (2010). PavB is a surface-exposed adhesin of *Streptococcus pneumoniae* contributing to nasopharyngeal colonization and airways infections. *Molecular Microbiology*, 77(1), 22-43. doi:10.1111/j.1365-2958.2010.07189.x

Jerga, A., & Rock, C. O. (2009). Acyl-acyl carrier protein regulates transcription of fatty acid biosynthetic genes via the FabT repressor in *Streptococcus pneumoniae*. *The Journal of Biological Chemistry*, 284(23), 15364-15368. doi:10.1074/jbc.C109.002410

Johnsborg, O., Godager, L. H., & Nes, I. F. (2004). Identification of a region involved in the pheromone receptor function of the histidine kinase PlnB. *Archives of Microbiology*, 182(6), 450-457. doi:10.1007/s00203-004-0728-7

Johnsborg, O., Eldholm, V., Bjørnstad, M. L., & Håvarstein, L. S. (2008). Predatory mechanism dramatically increases the efficiency of lateral gene transfer in *Streptococcus pneumoniae* and related commensal species. *Molecular Microbiology*, 69(1), 245-253. doi:10.1111/j.1365-2958.2008.06288.x

Johnson, S. E., Dykes, J. K., Jue, D. L., Sampson, J. S., Carlone, G. M., & Ades, E. W. (2002). Inhibition of pneumococcal carriage in mice by subcutaneous immunization with peptides from the common surface protein pneumococcal surface adhesin A. *The Journal of Infectious Diseases*, 185(4), 489-496. doi:10.1086/338928

Johnston, C., Martin, B., Fichant, G., Polard, P., & Claverys, J.-P. (2014). Bacterial transformation: Distribution, shared mechanisms and divergent control. *Nature Reviews Microbiology*, 12(3), 181-196. doi:10.1038/nrmicro3199

Jones, C., & Lemercinier, X. (2005). Full NMR assignment and revised structure for the capsular polysaccharide from *Streptococcus pneumoniae* type 15B. *Carbohydrate Research*, 340(3), 403-409. doi:10.1016/j.carres.2004.12.009

Jones, R. N., Sader, H. S., Mendes, R. E., & Flamm, R. K. (2013). Update on antimicrobial susceptibility trends among *Streptococcus pneumoniae* in the United States: Report of ceftaroline activity from the sentry antimicrobial surveillance program (1998–2011). *Diagnostic Microbiology and Infectious Disease*, 75(1), 107-109. doi:10.1016/j.diagmicrobio.2012.08.024

Jounblat, R., Kadioglu, A., Mitchell, T. J., & Andrew, P. W. (2003). Pneumococcal behavior and host responses during bronchopneumonia are affected differently by the cytolytic and complement-activating activities of pneumolysin. *Infection and Immunology*, 71(4), 1813-1819. doi:10.1128/iai.71.4.1813-1819.2003

Joyce, E. A., Kawale, A., Censini, S., Kim, C. C., Covacci, A., & Falkow, S. (2004). LuxS is required for persistent pneumococcal carriage and expression of virulence and biosynthesis genes. *Infection and Immunology*, 72(5), 2964-2975. doi:10.1128/iai.72.5.2964-2975.2004

Kadioglu, A., Coward, W., Colston, M. J., Hewitt, C. R. A., & Andrew, P. W. (2004). CD4-T-lymphocyte interactions with pneumolysin and pneumococci suggest a crucial protective role in the host response to pneumococcal infection. *Infection and Immunity*, 72(5), 2689-2697. doi:10.1128/IAI.72.5.2689-2697.2004

Kadioglu, A., Weiser, J. N., Paton, J. C., & Andrew, P. W. (2008). The role of *Streptococcus pneumoniae* virulence factors in host respiratory colonization and disease. *Nature Reviews Microbiology*, 6(4), 288-301. doi:10.1038/nrmicro1871

Kahya, H. F., Andrew, P. W., & Yesilkaya, H. (2017). Deacetylation of sialic acid by esterases potentiates pneumococcal neuraminidase activity for mucin utilization, colonization and virulence. *PLoS Pathogens*, 13(3), e1006263-e1006263. doi:10.1371/journal.ppat.1006263

Kandasamy, R., Voysey, M., Collins, S., Berbers, G., Robinson, H., Noel, I., Hughes, H., Ndimah, S., Gould, K., Fry, N., Sheppard, C., Ladhani, S., Snape, M. D., Hinds, J., & Pollard, A. J. (2020). Persistent circulation of vaccine serotypes and serotype replacement after 5 years of infant immunization with 13-valent pneumococcal conjugate vaccine in the United Kingdom. *The Journal of Infectious Diseases*, 221(8), 1361-1370. doi:10.1093/infdis/jiz178

Kandler, O. (1983). Carbohydrate metabolism in lactic acid bacteria. *Antonie van Leeuwenhoek*, 49(3), 209-224. doi:10.1007/BF00399499

Kaplan, S. L., Barson, W. J., Lin, P. L., Romero, J. R., Bradley, J. S., Tan, T. Q., Hoffman, J. A., Givner, L. B., & Mason, E. O., Jr. (2013). Early trends for invasive pneumococcal infections in children after the introduction of the 13-valent pneumococcal conjugate vaccine. *The Pediatric Infectious Disease Journal*, 32(3), 203-207. doi:10.1097/INF.0b013e318275614b

Karmakar, M., Katsnelson, M., Malak, H. A., Greene, N. G., Howell, S. J., Hise, A. G., Camilli, A., Kadioglu, A., Dubyak, G. R., & Pearlman, E. (2015). Neutrophil IL-1β processing induced by pneumolysin is mediated by the NLRP3/ASC inflammasome and caspase-1 activation and is dependent on K^+ efflux. *The Journal of Immunology*, 194(4), 1763-1775. doi:10.4049/jimmunol.1401624

Kaur, A., Capalash, N., & Sharma, P. (2018). Quorum sensing in thermophiles: Prevalence of autoinducer-2 system. *BMC Microbiology*, 18(1), 62. doi:10.1186/s12866-018-1204-x

Kausmally, L., Johnsborg, O., Lunde, M., Knutsen, E., & Havarstein, L. S. (2005). Choline-binding protein D (CbpD) in *Streptococcus pneumoniae* is essential for competence-induced cell lysis. *Journal of Bacteriology*, 187(13), 4338-4345. doi:10.1128/JB.187.13.4338-4345.2005

Kawaguchiya, M., Urushibara, N., Aung, M. S., Morimoto, S., Ito, M., Kudo, K., Sumi, A., & Kobayashi, N. (2016). Emerging non-PCV serotypes of noninvasive *Streptococcus pneumoniae* with macrolide resistance genes in northern Japan. *New Microbes and New Infections*, 9, 66-72. doi:10.1016/j.nmni.2015.11.001

Kc, R., Shukla, S. D., Walters, E. H., apos, & Toole, R. F. (2017). Temporal upregulation of host surface receptors provides a window of opportunity for bacterial adhesion and disease. *Microbiology*, 163(4), 421-430. doi:10.1099/mic.0.000434

Keller, L. E., Robinson, D. A., & McDaniel, L. S. (2016). Nonencapsulated *Streptococcus pneumoniae*: Emergence and pathogenesis. *mBio*, 7(2), e01792-e01792. doi:10.1128/mBio.01792-15

Kharat, A. S., & Tomasz, A. (2003). Inactivation of the *srtA* gene affects localization of surface proteins and decreases adhesion of *Streptococcus pneumoniae* to human pharyngeal cells *in vitro*. *Infection and Immunity*, 71(5), 2758-2765. doi:10.1128/IAI.71.5.2758-2765.2003

Kilian, M., Poulsen, K., Blomqvist, T., Håvarstein, L. S., Bek-Thomsen, M., Tettelin, H., & Sørensen, U. B. S. (2008). Evolution of *Streptococcus pneumoniae* and its close commensal relatives. *PloS One*, 3(7), e2683-e2683. doi:10.1371/journal.pone.0002683

Kim, J. O., & Weiser, J. N. (1998). Association of intrastrain phase variation in quantity of capsular polysaccharide and teichoic acid with the virulence of *Streptococcus pneumoniae*. *The Journal of Infectious Diseases*, 177(2), 368-377. doi:10.1086/514205

King, S. J., Hippe, K. R., Gould, J. M., Bae, D., Peterson, S., Cline, R. T., Fasching, C., Janoff, E. N., & Weiser, J. N. (2004). Phase variable desialylation of host proteins that bind to *Streptococcus pneumoniae in vivo* and protect the airway. *Molecular Microbiology*, 54(1), 159-171. doi:10.1111/j.1365-2958.2004.04252.x

King, S. J. (2010). Pneumococcal modification of host sugars: A major contributor to colonization of the human airway? *Molecular Oral Microbiology*, 25(1), 15-24. doi:10.1111/j.2041-1014.2009.00564.x

Kirkham, L.-A. S., Jefferies, J. M. C., Kerr, A. R., Jing, Y., Clarke, S. C., Smith, A., & Mitchell, T. J. (2006). Identification of invasive serotype 1 pneumococcal isolates that express nonhemolytic pneumolysin. *Journal of Clinical Microbiology*, 44(1), 151-159. doi:10.1128/JCM.44.1.151-159.2006

Kjer-Nielsen, L., Patel, O., Corbett, A. J., Le Nours, J., Meehan, B., Liu, L., Bhati, M., Chen, Z., Kostenko, L., Reantragoon, R., Williamson, N. A., Purcell, A. W., Dudek, N. L., McConville, M. J., O'Hair, R. A., Khairallah, G. N., Godfrey, D. I., Fairlie, D. P., Rossjohn, J., & McCluskey, J. (2012). MR1 presents microbial vitamin B metabolites to MAIT cells. *Nature*, 491(7426), 717-723. doi:10.1038/nature11605

Knutsen, E., Ween, O., & Havarstein, L. S. (2004). Two separate quorum-sensing systems upregulate transcription of the same ABC transporter in *Streptococcus pneumoniae. Journal of Bacteriology*, 186(10), 3078-3085. doi:10.1128/JB.186.10.3078-3085.2004

Kohn, A., Gitelman, J., & Inbar, M. (1980). Unsaturated free fatty acids inactivate animal enveloped viruses. *Archives of Virology*, 66(4), 301-307. doi:10.1007/BF01320626

Kolaczkowska, E., & Kubes, P. (2013). Neutrophil recruitment and function in health and inflammation. *Nature Reviews Immunology*, 13(3), 159-175. doi:10.1038/nri3399

Kohler, S., Voß, F., Gómez Mejia, A., Brown, J. S., & Hammerschmidt, S. (2016). Pneumococcal lipoproteins involved in bacterial fitness, virulence, and immune evasion. *FEBS letters*, 590(21), 3820-3839. doi: 10.1002/1873-3468.12352

Kono, M., Zafar, M. A., Zuniga, M., Roche, A. M., Hamaguchi, S., & Weiser, J. N. (2016). Single cell bottlenecks in the pathogenesis of *Streptococcus pneumoniae*. *PLoS Pathogens*, 12(10), e1005887-e1005887. doi:10.1371/journal.ppat.1005887

Koppe, U., Suttorp, N., & Opitz, B. (2012). Recognition of *Streptococcus pneumoniae* by the innate immune system: Innate immune recognition of *Streptococcus pneumoniae*. *Cellular Microbiology*, 14(4), 460-466. doi:10.1111/j.1462-5822.2011.01746.x

Kowalko, J. E., & Sebert, M. E. (2008). The *Streptococcus pneumoniae* competence regulatory system influences respiratory tract colonization. *Infection and Immunity*, 76(7), 3131-3140. doi:10.1128/IAI.01696-07

Kraal, G., van der Laan, L. J. W., Elomaa, O., & Tryggvason, K. (2000). The macrophage receptor MARCO. Microbes and Infection, 2(3), 313-316. doi:10.1016/S1286-4579(00)00296-3

Langford, B. J., So, M., Raybardhan, S., Leung, V., Westwood, D., MacFadden, D. R., Soucy, J.-P. R., & Daneman, N. (2020). Bacterial co-infection and secondary infection in patients with COVID-19: A living rapid review and meta-analysis. *Clinical Microbiology and Infection*, 26(12), 1622-1629. doi:10.1016/j.cmi.2020.07.016

Lanie, J. A., Ng, W. L., Kazmierczak, K. M., Andrzejewski, T. M., Davidsen, T. M., Wayne, K. J., Tettelin, H., Glass, J. I., & Winkler, M. E. (2007). Genome sequence of Avery's virulent serotype 2 strain D39 of *Streptococcus pneumoniae* and comparison with that of unencapsulated laboratory strain R6. *Journal of Bacteriology*, 189(1), 38-51. doi:10.1128/jb.01148-06

Lau, G. W., Haataja, S., Lonetto, M., Kensit, S. E., Marra, A., Bryant, A. P., McDevitt, D., Morrison, D. A., & Holden, D. W. (2001). A functional genomic analysis of type 3 *Streptococcus pneumoniae* virulence. *Molecular Microbiology*, 40(3), 555-571. doi:10.1046/j.1365-2958.2001.02335.x

Lavelle, E. C., & Ward, R. W. (2022). Mucosal vaccines - fortifying the frontiers. *Nature Reviews Immunology*, 22(4), 236-250. doi:10.1038/s41577-021-00583-2

Lawrence, M. C., Pilling, P. A., Epa, V. C., Berry, A. M., Ogunniyi, A. D., & Paton, J. C. (1998). The crystal structure of pneumococcal surface antigen PsaA reveals a metal-binding site and a novel structure for a putative ABC-type binding protein. *Structure*, 6(12), 1553-1561. doi:10.1016/S0969-2126(98)00153-1

Lee, M. S., & Morrison, D. A. (1999). Identification of a new regulator in *Streptococcus pneumoniae* linking quorum sensing to competence for genetic transformation. *Journal of Bacteriology*, 181(16), 5004-5016. doi:10.1128/jb.181.16.5004-5016.1999

Leighton, M. P., Kelly, D. J., Williamson, M. P., & Shaw, J. G. (2001). An NMR and enzyme study of the carbon metabolism of *Neisseria meningitidis. Microbiology (Society for General Microbiology)*, 147(6), 1473-1482. doi:10.1099/00221287-147-6-1473

Lewis, K. (2008). Multidrug tolerance of biofilms and persister cells. *Bacterial Biofilms*, 107-131. doi:10.1007/978-3-540-75418-3_6

Li, C., Andersen, K. B., Elverdal, P. L., Skovsted, I. C., Duus, J. Ø., & Kjeldsen, C. (2021). Full NMR assignment, revised structure and biosynthetic analysis for the capsular polysaccharide from *Streptococcus pneumoniae* serotype 15F. *Carbohydrate Research*, 508, 108418. doi:10.1016/j.carres.2021.108418

Li, J., Li, J.-W., Feng, Z., Wang, J., An, H., Liu, Y., Wang, Y., Wang, K., Zhang, X., Miao, Z., Liang, W., Sebra, R., Wang, G., Wang, W.-C., & Zhang, J.-R. (2016). Epigenetic switch driven by DNA inversions dictates phase variation in *Streptococcus pneumoniae*. *PLoS Pathogens*, 12(7), e1005762. doi:10.1371/journal.ppat.1005762

Li, J.-W., Li, J., Wang, J., Li, C., & Zhang, J.-R. (2019). Molecular mechanisms of *hsdS* inversions in the *cod* locus of *Streptococcus pneumoniae. Journal of Bacteriology*, 201(6), 10.1128/jb.00581-00518. doi:10.1128/jb.00581-18

Li, Y., Thompson, C. M., Trzciński, K., & Lipsitch, M. (2013). Within-host selection is limited by an effective population of *Streptococcus pneumoniae* during nasopharyngeal colonization. *Infection and Immunology*, 81(12), 4534-4543. doi:10.1128/iai.00527-13

Lindén, A., Laan, M., & Anderson, G. P. (2005). Neutrophils, interleukin-17A and lung disease. *European Respiratory Journal*, 25(1), 159-172. doi:10.1183/09031936.04.00032904

Lipsitch, M., O'Neill, K., Cordy, D., Bugalter, B., Trzcinski, K., Thompson, C. M., Goldstein, R., Pelton, S., Huot, H., Bouchet, V., Reid, R., Santosham, M., & O'Brien, K. L. (2007). Strain characteristics of *Streptococcus pne*umoniae carriage and invasive disease isolates during a cluster-randomized clinical trial of the 7-valent pneumococcal conjugate vaccine. *The Journal of Infectious Diseases*, 196(8), 1221-1227. doi:10.1086/521831

Livak, K. J., & Schmittgen, T. D. (2001). Analysis of relative gene expression data using real-time quantitative PCR and the $2^{-\Delta\Delta ct}$ method. *Methods*, 25(4), 402-408. doi:10.1006/meth.2001.1262

Lock, R. A., Qing Yang, Z., Berry, A. M., & Paton, J. C. (1996). Sequence variation in the *Streptococcus pneumoniae* pneumolysin gene affecting haemolytic activity and electrophoretic mobility of the toxin. *Microbial Pathogenesis*, 21(2), 71-83. doi:10.1006/mpat.1996.0044

Lock, R. A., Paton, J. C., & Hansman, D. (1988). Comparative efficacy of pneumococcal neuraminidase and pneumolysin as immunogens protective against *Streptococcus pneumoniae. Microbial Pathogenesis*, 5(6), 461-467. doi:10.1016/0882-4010(88)90007-1

Loeffler, J. M., & Fischetti, V. A. (2006). Lysogeny of *Streptococcus pneumoniae* with MM1 phage: Improved adherence and other phenotypic changes. *Infection and Immunity*, 74(8), 4486-4495. doi:10.1128/IAI.00020-06

Loenen, W. A., Dryden, D. T., Raleigh, E. A., Wilson, G. G., & Murray, N. E. (2014). Highlights of the DNA cutters: A short history of the restriction enzymes. *Nucleic Acids Research*, 42(1), 3-19. doi:10.1093/nar/gkt990

Long, J. P., Tong, H. H., Shannon, P. A., & Demaria, T. F. (2003). Differential expression of cytokine genes and inducible nitric oxide synthase induced by opacity phenotype variants of *Streptococcus pneumoniae* during acute otitis media in the rat. *Infection and Immunity*, 71(10), 5531-5540. doi:10.1128/IAI.71.10.5531-5540.2003

Long, J. P., Tong, H. H., & DeMaria, T. F. (2004). Immunization with native or recombinant *Streptococcus pneumoniae* neuraminidase affords protection in the chinchilla otitis media model. *Infection and Immunity*, 72(7), 4309-4313. doi:10.1128/iai.72.7.4309-4313.2004

Loo, C. Y., Corliss, D. A., & Ganeshkumar, N. (2000). *Streptococcus gordonii* biofilm formation: Identification of genes that code for biofilm phenotypes. *Journal of Bacteriology*, 182(5), 1374-1382. doi:10.1128/JB.182.5.1374-1382.2000

Loughran, A. J., Orihuela, C. J., & Tuomanen, E. I. (2019). *Streptococcus pneumoniae*: Invasion and inflammation. *Microbiology Spectrum*, 7(2). doi:10.1128/microbiolspec.GPP3-0004-2018

Lu, Y.-J., Leite, L., Gonçalves, V. M., Dias, W. d. O., Liberman, C., Fratelli, F., Alderson, M., Tate, A., Maisonneuve, J.-F., Robertson, G., Graca, R., Sayeed, S., Thompson, C. M., Anderson, P., & Malley, R. (2010). GMP-grade pneumococcal whole-cell vaccine injected subcutaneously protects mice from nasopharyngeal colonization and fatal aspiration-sepsis. *Vaccine*, 28(47), 7468-7475. doi:10.1016/j.vaccine.2010.09.031

Luria, S. E., & Human, M. L. (1952). A nonhereditary, host-induced variation of bacterial viruses. *Journal of Bacteriology*, 64(4), 557-569. doi:10.1128/JB.64.4.557-569.1952

Lynch, J. P., & Zhanel, G. G. (2009). *Streptococcus pneumoniae*: Does antimicrobial resistance matter? *Seminars in Respiratory and Critical Care Medicine*, 30(2), 210-238. doi:10.1055/s-0029-1202939

Lynch, J. P., & Zhanel, G. G. (2010). *Streptococcus pneumoniae*: Epidemiology and risk factors, evolution of antimicrobial resistance, and impact of vaccines. *Current Opinion in Pulmonary Medicine*, 16(3), 217-225. doi:10.1097/MCP.0b013e3283385653

Macfadyen, L. P., Dorocicz, I. R., Reizer, J., Saier Jr, M. H., & Redfield, R. J. (1996). Regulation of competence development and sugar utilization in *Haemophilus influenzae* Rd by a phosphoenolpyruvate: Fructose phosphotransferase system. *Molecular Microbiology*, 21(5), 941-952. doi:10.1046/j.1365-2958.1996.441420.x

MacLeod, C. M., & Kraus, M. R. (1950). Relation of virulence of pneumococcal strains for mice to the quantity of capsular polysaccharide formed *in vitro*. *The Journal of Experimental Medicine*, 92(1), 1-9. doi:10.1084/jem.92.1.1

Madeddu, G., Fiori, M. L., & Mura, M. S. (2010). Bacterial community-acquired pneumonia in HIV-infected patients. *Current Opinion in Pulmonary Medicine*, 16(3), 201-207. doi:10.1097/MCP.0b013e3283375825

Maestro, B., & Sanz, J. M. (2016). Choline binding proteins from *Streptococcus pneumoniae*: A dual role as enzybiotics and targets for the design of new antimicrobials. *Antibiotics (Basel),* 5(2). doi:10.3390/antibiotics5020021

Mahdi, L. K., Wang, H., Van der Hoek, M. B., Paton, J. C., & Ogunniyi, A. D. (2012). Identification of a novel pneumococcal vaccine antigen preferentially expressed during meningitis in mice. *The Journal of Clinical Investigation*, 122(6), 2208-2220. doi:10.1172/JCI45850

Malley, R., Lipsitch, M., Stack, A., Saladino, R., Fleisher, G., Pelton, S., Thompson, C., Briles, D., & Anderson, P. (2001). Intranasal immunization with killed unencapsulated whole cells prevents colonization and invasive disease by capsulated pneumococci. *Infection and Immunity*, 69(8), 4870-4873. doi:10.1128/IAI.69.8.4870-4873.2001

Malley, R., Henneke, P., Morse, S. C., Cieslewicz, M. J., Lipsitch, M., Thompson, C. M., Kurt-Jones, E., Paton, J. C., Wessels, M. R., & Golenbock, D. T. (2003). Recognition of pneumolysin by Toll-like receptor 4 confers resistance to pneumococcal infection. *Proceedings of the National Academy of Sciences - PNAS*, 100(4), 1966-1971. doi:10.1073/pnas.0435928100

Mamishi, S., Moradkhani, S., Mahmoudi, S., Hosseinpour-Sadeghi, R., & Pourakbari, B. (2014). Penicillin-resistant trend of *Streptococcus pneumoniae* in Asia: A systematic review. Iranian Journal of Microbiology, 6(4), 198-210.

Manco, S., Hernon, F., Yesilkaya, H., Paton, J. C., Andrew, P. W., & Kadioglu, A. (2006). Pneumococcal neuraminidases A and B both have essential roles during infection of the respiratory tract and sepsis. *Infection and Immunity*, 74(7), 4014-4020. doi:10.1128/IAI.01237-05

Mandigers, C. M., Diepersloot, R. J., Dessens, M., Mol, S. J., & van Klingeren, B. (1994). A hospital outbreak of penicillin-resistant pneumococci in the Netherlands. *The European Respiratory Journal*, 7(9), 1635-1639. doi:10.1183/09031936.94.07091635

Manso, A. S., Chai, M. H., Atack, J. M., Furi, L., De Ste Croix, M., Haigh, R., Trappetti, C., Ogunniyi, A. D., Shewell, L. K., Boitano, M., Clark, T. A., Korlach, J., Blades, M., Mirkes, E., Gorban, A. N., Paton, J. C., Jennings, M. P., & Oggioni, M. R. (2014). A random six-phase switch regulates pneumococcal virulence via global epigenetic changes. *Nature Communications*, 5(1), 5055-5055. doi:10.1038/ncomms6055

Marion, C., Aten, A. E., Woodiga, S. A., & King, S. J. (2011a). Identification of an ATPase, MsmK, which energizes multiple carbohydrate ABC transporters in *Streptococcus pneumoniae. Infection and Immunology*, 79(10), 4193-4200. doi:10.1128/iai.05290-11

Marion, C., Burnaugh, A. M., Woodiga, S. A., & King, S. J. (2011b). Sialic acid transport contributes to pneumococcal colonization. *Infection and Immunology*, 79(3), 1262-1269. doi:10.1128/iai.00832-10

Marion, C., Stewart, J. M., Tazi, M. F., Burnaugh, A. M., Linke, C. M., Woodiga, S. A., & King, S. (2012). *Streptococcus pneumoniae* can utilize multiple sources of hyaluronic acid for growth. *Infection and Immunity*, 80(4), 1390-1398. doi:10.1128/IAI.05756-11

Marks, L. R., Parameswaran, G. I., & Hakansson, A. P. (2012a). Pneumococcal interactions with epithelial cells are crucial for optimal biofilm formation and colonization *in vitro* and *in vivo. Infection and Immunity*, 80(8), 2744-2760. doi:10.1128/iai.00488-12

Marks, L. R., Reddinger, R. M., & Hakansson, A. P. (2012b). High levels of genetic recombination during nasopharyngeal carriage and biofilm formation in *Streptococcus pneumoniae. mBio*, 3(5). doi:10.1128/mBio.00200-12

Marks, L. R., Davidson, B. A., Knight, P. R., & Hakansson, A. P. (2013). Interkingdom signaling induces *Streptococcus pneumoniae* biofilm dispersion and transition from asymptomatic colonization to disease. *mBio*, 4(4). doi:10.1128/mBio.00438-13

Marks, L. R., Reddinger, R. M., & Hakansson, A. P. (2014). Biofilm formation enhances fomite survival of *Streptococcus pneumoniae* and *Streptococcus pyogenes. Infection and Immunity*, 82(3), 1141-1146. doi:10.1128/IAI.01310-13

Marra, A., Lawson, S., Asundi, J. S., Brigham, D., & Hromockyj, A. E. (2002). *In vivo* characterization of the *psa* genes from *Streptococcus pneumoniae* in multiple models of infection. *Microbiology (Society for General Microbiology)*, 148(5), 1483-1491. doi:10.1099/00221287-148-5-1483

Martin, B., Soulet, A. L., Mirouze, N., Prudhomme, M., Mortier-Barrière, I., Granadel, C., Noirot-Gros, M. F., Noirot, P., Polard, P., & Claverys, J. P. (2013). ComE/ComE∼P interplay dictates activation or extinction status of pneumococcal x-state (competence). *Molecular Microbiology*, 87(2), 394-411. doi:10.1111/mmi.12104

Mavroidi, A., Aanensen, D. M., Godoy, D., Skovsted, I. C., Kaltoft, M. S., Reeves, P. R., Bentley, S. D., & Spratt, B. G. (2007). Genetic relatedness of the *Streptococcus pneumoniae* capsular biosynthetic loci. *Journal of Bacteriology*, 189(21), 7841-7855. doi:10.1128/jb.00836-07

McAllister, L. J., Tseng, H. J., Ogunniyi, A. D., Jennings, M. P., McEwan, A. G., & Paton, J. C. (2004). Molecular analysis of the *psa* permease complex of *Streptococcus pneumoniae. Molecular Microbiology*, 53(3), 889-901. doi:10.1111/j.1365-2958.2004.04164.x

McCool, T. L., Cate, T. R., Moy, G., & Weiser, J. N. (2002). The immune response to pneumococcal proteins during experimental human carriage. *The Journal of Experimental Medicine*, 195(3), 359-365. doi:10.1084/jem.20011576

McCullers, J. A., & Rehg, J. E. (2002). Lethal synergism between Influenza virus and *Streptococcus pneumoniae*: Characterization of a mouse model and the role of platelet-activating factor receptor. *The Journal of Infectious Diseases*, 186(3), 341-350. doi:10.1086/341462

McDaniel, L. S., Sheffield, J. S., Delucchi, P., & Briles, D. E. (1991). PspA, a surface protein of *Streptococcus pneumoniae*, is capable of eliciting protection against pneumococci of more than one capsular type. *Infection and Immunity*, 59(1), 222-228. doi:10.1128/IAI.59.1.222-228.1991

McKessar, S. J., & Hakenbeck, R. (2007). The two-component regulatory system TCS08 is involved in cellobiose metabolism of *Streptococcus pneumoniae* R6. *Journal of Bacteriology*, 189(4), 1342-1350. doi:10.1128/jb.01170-06

McLean, K. T., Tikhomirova, A., Brazel, E. B., Legendre, S., Haasbroek, G., Minhas, V., Paton, J. C., & Trappetti, C. (2020). Site-specific mutations of *galR* affect galactose metabolism in *Streptococcus pneumoniae. Journal of Bacteriology*, 203(1). doi:10.1128/JB.00180-20

McNeela, E. A., Burke, A., Neill, D. R., Baxter, C., Fernandes, V. E., Ferreira, D., Smeaton, S., El-Rachkidy, R., McLoughlin, R. M., Mori, A., Moran, B., Fitzgerald, K. A., Tschopp, J., Pétrilli, V., Andrew, P. W., Kadioglu, A., & Lavelle, E. C. (2010). Pneumolysin activates the NLRP3 inflammasome and promotes proinflammatory cytokines independently of TLR4. *PLoS Pathogens*, 6(11), e1001191. doi:10.1371/journal.ppat.1001191

Mellroth, P., Daniels, R., Eberhardt, A., Rönnlund, D., Blom, H., Widengren, J., Normark, S., & Henriques-Normark, B. (2012). LytA, major autolysin of *Streptococcus pneumoniae*, requires access to nascent peptidoglycan. *The Journal of Biological Chemistry*, 287(14), 11018-11029. doi:10.1074/jbc.M111.318584

Metcalf, B., Gertz Jr, R., Gladstone, R., Walker, H., Sherwood, L., Jackson, D., Li, Z., Law, C., Hawkins, P., & Chochua, S. (2016). Strain features and distributions in pneumococci from children with invasive disease before and after 13-valent conjugate vaccine implementation in the USA. *Clinical Microbiology and Infection*, 22(1), 60. e69-60. e29.

Mil-Homens, D., Ferreira-Dias, S., & Fialho, A. M. (2016). Fish oils against *Burkholderia* and *Pseudomonas aeruginosa*: *In vitro* efficacy and their therapeutic and prophylactic effects on infected *Galleria mellonella* larvae. *Journal of Applied Microbiology*, 120(6), 1509-1519. doi:10.1111/jam.13145

Miller, M. B., & Bassler, B. L. (2001). Quorum sensing in bacteria. *Annual Review of Microbiology*, 55(1), 165-199. doi:10.1146/annurev.micro.55.1.165

Minhas, V., Harvey, R. M., McAllister, L. J., Seemann, T., Syme, A. E., Baines, S. L., Paton, J. C., Trappetti, C., & McDaniel, L. S. (2019). Capacity to utilize raffinose dictates pneumococcal disease phenotype. *mBio*, 10(1), e02596-02518. doi:10.1128/mBio.02596-18

Minhas, V., Aprianto, R., McAllister, L. J., Wang, H., David, S. C., McLean, K. T., Comerford, I., McColl, S. R., Paton, J. C., Veening, J.-W., & Trappetti, C. (2020). *In vivo* dual RNA-seq reveals that neutrophil recruitment underlies differential tissue tropism of *Streptococcus pneumoniae. Communications Biology*, 3(1), 293-293. doi:10.1038/s42003-020-1018-x

Minhas, V., Domenech, A., Synefiaridou, D., Straume, D., Brendel, M., Cebrero, G., Liu, X., Costa, C., Baldry, M., Sirard, J. C., Perez, C., Gisch, N., Hammerschmidt, S., Håvarstein, L. S., & Veening, J. W. (2023). Competence remodels the pneumococcal cell wall exposing key surface virulence factors that mediate increased host adherence. *PLoS Biology*, 21(1), e3001990. doi:10.1371/journal.pbio.3001990

Mitchell, T. J., Mendez, F., Paton, J. C., Andrew, P. W., & Boulnois, G. J. (1990). Comparison of pneumolysin genes and proteins from *Streptococcus pneumoniae* types 1 and 2. *Nucleic Acids Research*, 18(13), 4010-4010. doi:10.1093/nar/18.13.4010

Mitchell, T. J., Andrew, P. W., Saunders, F. K., Smith, A. N., & Boulnois, G. J. (1991). Complement activation and antibody binding by pneumolysin via a region of the toxin homologous to a human acute-phase protein. *Molecular Microbiology*, 5(8), 1883-1888. doi:10.1111/j.1365-2958.1991.tb00812.x

Mitsi, E., Reiné, J., Urban, B. C., Solórzano, C., Nikolaou, E., Hyder-Wright, A. D., Pojar, S., Howard, A., Hitchins, L., Glynn, S., Farrar, M. C., Liatsikos, K., Collins, A. M., Walker, N. F., Hill, H. C., German, E. L., Cheliotis, K. S., Byrne, R. L., Williams, C. T., Cubas-Atienzar, A. I., Fletcher, T. E., Adams, E. R., Draper, S. J., Pulido, D., Beavon, R., Theilacker, C., Begier, E., Jodar, L., Gessner, B. D., & Ferreira, D. M. (2022). *Streptococcus pneumoniae* colonization associates with impaired adaptive immune responses against SARS-COV-2. *The Journal of Clinical Investigation*, 132(7), e157124. doi:10.1172/JCI157124

Mook-Kanamori, B. B., Geldhoff, M., van der Poll, T., & van de Beek, D. (2011). Pathogenesis and pathophysiology of pneumococcal meningitis. *Clinical Microbiology Reviews*, 24(3), 557-591. doi:10.1128/CMR.00008-11

Morais, V., Texeira, E., & Suarez, N. (2019). Next-generation whole-cell pneumococcal vaccine. *Vaccines*, 7(4), 151. doi:10.3390/vaccines7040151

Moreno-Gámez, S., Sorg, R. A., Domenech, A., Kjos, M., Weissing, F. J., van Doorn, G. S., & Veening, J.-W. (2017). Quorum sensing integrates environmental cues, cell density and cell history to control bacterial competence. *Nature Communications*, 8(1), 854-812. doi:10.1038/s41467-017-00903-y

Morens, D. M., Taubenberger, J. K., & Fauci, A. S. (2008). Predominant role of bacterial pneumonia as a cause of death in pandemic influenza: Implications for pandemic influenza preparedness. *The Journal of Infectious Diseases*, 198(7), 962-970. doi:10.1086/591708

Morris, P. S., Leach, A. J., Silberberg, P., Mellon, G., Wilson, C., Hamilton, E., & Beissbarth, J. (2005). Otitis media in young aboriginal children from remote communities in northern and central Australia: A cross-sectional survey. *BMC Pediatrics*, 5, 27. doi:10.1186/1471-2431-5-27

Motib, A. S., Al-Bayati, F. A. Y., Manzoor, I., Shafeeq, S., Kadam, A., Kuipers, O. P., Hiller, N. L., Andrew, P. W., & Yesilkaya, H. (2019). TprA/PhrA quorum sensing system has a major effect on pneumococcal survival in respiratory tract and blood, and its activity is controlled by CcpA and GlnR. *Frontiers in Cellular and Infection Microbiology*, 9, 326. doi:10.3389/fcimb.2019.00326

Muñoz-Elías, E. J., Marcano, J., & Camilli, A. (2008). Isolation of *Streptococcus pneumoniae* biofilm mutants and their characterization during nasopharyngeal colonization. *Infection and Immunity*, 76(11), 5049-5061. doi:10.1128/iai.00425-08

Murphy, K. P., Travers, P., Walport, M., & Janeway, C. A. (2008). *Janeway's immunobiology* (7th ed. / Kenneth Murphy, Paul Travers, Mark Walport. ed.). New York: Garland Science.

Murray, P. J. (2009). Beyond peptidoglycan for Nod2. *Nature Immunology*, 10(10), 1053-1054. doi:10.1038/ni1009-1053

Musher, D. M. (2003). How contagious are common respiratory tract infections? *The New England Journal of Medicine*, 348(13), 1256-1266. doi:10.1056/NEJMra021771

Nakamura, K., Oshima, T., Morimoto, T., Ikeda, S., Yoshikawa, H., Shiwa, Y., Ishikawa, S., Linak, M. C., Hirai, A., Takahashi, H., Altaf-Ul-Amin, M., Ogasawara, N., & Kanaya, S. (2011). Sequence-specific error profile of Illumina sequencers. *Nucleic Acids Research*, 39(13), e90. doi:10.1093/nar/gkr344

Nakamura, S., Davis, K. M., & Weiser, J. N. (2011). Synergistic stimulation of type I interferons during Influenza virus coinfection promotes *Streptococcus pneumoniae* colonization in mice. *The Journal of Clinical Investigation*, 121(9), 3657-3665. doi:10.1172/JCI57762

Nakano, S., Fujisawa, T., Ito, Y., Chang, B., Suga, S., Noguchi, T., Yamamoto, M., Matsumura, Y., Nagao, M., Takakura, S., Ohnishi, M., Ihara, T., & Ichiyama, S. (2016). Serotypes, antimicrobial susceptibility, and molecular epidemiology of invasive and non-invasive *Streptococcus pneumoniae* isolates in paediatric patients after the introduction of 13-valent conjugate vaccine in a nationwide surveillance study conducted in Japan in 2012-2014. *Vaccine*, 34(1), 67-76. doi:10.1016/j.vaccine.2015.11.015

Nelson, A. L., Roche, A. M., Gould, J. M., Chim, K., Ratner, A. J., & Weiser, J. N. (2007). Capsule enhances pneumococcal colonization by limiting mucus-mediated clearance. *Infection and Immunology*, 75(1), 83-90. doi:10.1128/iai.01475-06

Nguyen, D., Joshi-Datar, A., Lepine, F., Bauerle, E., Olakanmi, O., Beer, K., McKay, G., Siehnel, R., Schafhauser, J., Wang, Y., Britigan, B. E., & Singh, P. K. (2011). Active starvation responses mediate antibiotic tolerance in biofilms and nutrient-limited bacteria. *Science (American Association for the Advancement of Science)*, 334(6058), 982-986. doi:10.1126/science.1211037

Nicol, M., Alexandre, S., Luizet, J. B., Skogman, M., Jouenne, T., Salcedo, S. P., & Dé, E. (2018). Unsaturated fatty acids affect quorum sensing communication system and inhibit motility and

biofilm formation of *Acinetobacter baumannii*. *International Journal of Molecular Sciences*, 19(1). doi:10.3390/ijms19010214

Novick, R. P. (2003). Autoinduction and signal transduction in the regulation of staphylococcal virulence. *Molecular Microbiology*, 48(6), 1429-1449. doi:10.1046/j.1365-2958.2003.03526.x

Novick, R. P., Christie, G. E., & Penadés, J. R. (2010). The phage-related chromosomal islands of gram-positive bacteria. *Nature Reviews Microbiology*, 8(8), 541-551. doi:10.1038/nrmicro2393

Numminen, E., Chewapreecha, C., Turner, C., Goldblatt, D., Nosten, F., Bentley, S. D., Turner, P., & Corander, J. (2015). Climate induces seasonality in pneumococcal transmission. *Scientific Reports*, 5(1), 11344-11344. doi:10.1038/srep11344

O'Connor, T. E., Perry, C. F., & Lannigan, F. J. (2009). Complications of otitis media in indigenous and non-indigenous children. *Medical Journal of Australia*, 191(S9), S60-S64. doi:10.5694/j.1326-5377.2009.tb02929.x

Oggioni, M. R., Iannelli, F., & Pozzi, G. (1999). Characterization of cryptic plasmids pDP1 and pSMB1 of *Streptococcus pneumoniae. Plasmid*, 41(1), 70-72. doi:10.1006/plas.1998.1364

Oggioni, M. R., Trappetti, C., Kadioglu, A., Cassone, M., Iannelli, F., Ricci, S., Andrew, P. W., & Pozzi, G. (2006). Switch from planktonic to sessile life: A major event in pneumococcal pathogenesis. *Molecular Microbiology*, 61(5), 1196-1210. doi:10.1111/j.1365-2958.2006.05310.x

Ogunniyi, A. D., Mahdi, L. K., Trappetti, C., Verhoeven, N., Mermans, D., Van Der Hoek, M. B., Plumptre, C. D., & Paton, J. C. (2012). Identification of genes that contribute to the pathogenesis of invasive pneumococcal disease by in vivo transcriptomic analysis. *Infection and Immunity*, 80(9), 3268-3278. doi:10.1128/IAI.00295-12

Olarte, L., Barson, W. J., Barson, R. M., Lin, P. L., Romero, J. R., Tan, T. Q., Givner, L. B., Bradley, J. S., Hoffman, J. A., & Hultén, K. G. (2015). Impact of the 13-valent pneumococcal conjugate vaccine on pneumococcal meningitis in US children. *Clinical Infectious Diseases*, 61(5), 767-775.

Oligbu, G., Collins, S., Sheppard, C. L., Fry, N. K., Slack, M., Borrow, R., & Ladhani, S. N. (2017). Childhood deaths attributable to invasive pneumococcal disease in England and Wales, 2006–2014. *Clinical Infectious Diseases*, 65(2), 308-314. doi:10.1093/cid/cix310

Oliver, M. B., Basu Roy, A., Kumar, R., Lefkowitz, E. J., & Swords, W. E. (2017). *Streptococcus pneumoniae* TIGR4 phase-locked opacity variants differ in virulence phenotypes. *mSphere*, 2(6). doi:10.1128/mSphere.00386-17

Orihuela, C. J., Radin, J. N., Sublett, J. E., Gao, G., Kaushal, D., & Tuomanen, E. I. (2004). Microarray analysis of pneumococcal gene expression during invasive disease. *Infection and Immunity*, 72(10), 5582-5596. doi:10.1128/IAI.72.10.5582-5596.2004

Orihuela, C. J., Mahdavi, J., Thornton, J., Mann, B., Wooldridge, K. G., Abouseada, N., Oldfield, N. J., Self, T., Ala'Aldeen, D. A. A., & Tuomanen, E. I. (2009). Laminin receptor initiates bacterial contact with the blood brain barrier in experimental meningitis models. *The Journal of Clinical Investigation*, 119(6), 1638-1646. doi:10.1172/JCI36759

Overweg, K., Pericone, C. D., Verhoef, G. G., Weiser, J. N., Meiring, H. D., De Jong, A. P., De Groot, R., & Hermans, P. W. (2000). Differential protein expression in phenotypic variants of *Streptococcus pneumoniae*. *Infection and Immunology*, 68(8), 4604-4610. doi:10.1128/iai.68.8.4604-4610.2000

Paixão, L., Oliveira, J., Veríssimo, A., Vinga, S., Lourenço, E. C., Ventura, M. R., Kjos, M., Veening, J.-W., Fernandes, V. E., Anew, P. W., Yesilkaya, H., & Neves, A. R. (2015). Host glycan sugar-specific pathways in *Streptococcus pneumonia*: Galactose as a key sugar in colonisation and infection. *PloS One*, 10(3), e0121042. doi:10.1371/journal.pone.0121042

Park, S. S., Gonzalez-Juarbe, N., Martínez, E., Hale, J. Y., Lin, Y. H., Huffines, J. T., Kruckow, K. L., Briles, D. E., & Orihuela, C. J. (2021a). *Streptococcus pneumoniae* binds to host lactate dehydrogenase via PspA and PspC to enhance virulence. *mBio*, 12(3). doi:10.1128/mBio.00673-21

Park, T., Im, J., Kim, A. R., Lee, D., Jeong, S., Yun, C.-H., & Han, S. H. (2021b). Short-chain fatty acids inhibit the biofilm formation of *Streptococcus gordonii* through negative regulation of competence-stimulating peptide signaling pathway. *The Journal of Microbiology*, 59(12), 1142-1149. doi:10.1007/s12275-021-1576-8

Parker, A. M., Jackson, N., Awasthi, S., Kim, H., Alwan, T., Wyllie, A. L., Baldwin, A. B., Brennick, N. B., Moehle, E. A., Giannikopoulos, P., Kogut, K., Holland, N., Mora, A. M., Eskenazi, B., Riley, L. W., & Lewnard, J. A. (2022). Association of upper respiratory *Streptococcus pneumoniae* colonization with Severe Acute Respiratory Syndrome Coronavirus 2 infection among adults. *Clinical Infectious Diseases*, 76(7), 1209-1217. doi:10.1093/cid/ciac907

Parker, D., Martin, F. J., Soong, G., Harfenist, B. S., Aguilar, J. L., Ratner, A. J., Fitzgerald, K. A., Schindler, C., & Prince, A. (2011). *Streptococcus pneumoniae* DNA initiates type I interferon signaling in the respiratory tract. *mBio*, 2(3), e00016-e00011. doi:10.1128/mBio.00016-11

Parsons, J. B., Broussard, T. C., Bose, J. L., Rosch, J. W., Jackson, P., Subramanian, C., & Rock, C. O. (2014). Identification of a two-component fatty acid kinase responsible for host fatty acid incorporation by *Staphylococcus aureus. Proceedings of the National Academy of Sciences - PNAS*, 111(29), 10532-10537. doi:10.1073/pnas.1408797111

Parsons, J. B., Frank, M. W., Eleveld, M. J., Schalkwijk, J., Broussard, T. C., Jonge, M. I., & Rock, C. O. (2015). A thioesterase bypasses the requirement for exogenous fatty acids in the *plsX* deletion of *Streptococcus pneumoniae*. *Molecular Microbiology*, 96(1), 28-41. doi:10.1111/mmi.12916

Paterson, G. K., & Mitchell, T. J. (2006a). Innate immunity and the pneumococcus. *Microbiology (Society for General Microbiology)*, 152(2), 285-293. doi:10.1099/mic.0.28551-0

Paterson, G. K., & Mitchell, T. J. (2006b). The role of *Streptococcus pneumoniae* sortase a in colonisation and pathogenesis. *Microbes and Infection*, 8(1), 145-153. doi:10.1016/j.micinf.2005.06.009

Paton, J. C., & Ferrante, A. (1983). Inhibition of human polymorphonuclear leukocyte respiratory burst, bactericidal activity, and migration by pneumolysin. *Infection and Immunity*, 41(3), 1212-1216. doi:10.1128/IAI.41.3.1212-1216.1983

Paton, J. C., Lock, R. A., & Hansman, D. J. (1983). Effect of immunization with pneumolysin on survival time of mice challenged with *Streptococcus pneumoniae. Infection and Immunity*, 40(2), 548-552. doi:10.1128/iai.40.2.548-552.1983

Paton, J. C., Rowan-Kelly, B., & Ferrante, A. (1984). Activation of human complement by the pneumococcal toxin pneumolysin. *Infection and Immunity*, 43(3), 1085-1087. doi:10.1128/IAI.43.3.1085-1087.1984

Paton, J. C., Lock, R. A., Chi-Jen, L. E. E., Li, J. P., Berry, A. M., Mitchell, T. J., Andrew, P. W., Hansman, D., & Boulnois, G. J. (1991). Purification and immunogenicity of genetically obtained pneumolysin toxoids and their conjugation to *Streptococcus pneumoniae* type 19F polysaccharide. *Infection and Immunity*, 59(7), 2297-2304. doi:10.1128/IAI.59.7.2297-2304.1991

Paton, J. C., Andrew, P. W., Boulnois, G. J., & Mitchell, T. J. (1993). Molecular analysis of the pathogenicity of *Streptococcus pneumoniae*: The role of pneumococcal proteins. *Annual Review of Microbiology*, 47, 89-115. doi:10.1146/annurev.mi.47.100193.000513

Pericone, C. D., Bae, D., Shchepetov, M., McCool, T., & Weiser, J. N. (2002). Short-sequence tandem and nontandem DNA repeats and endogenous hydrogen peroxide production contribute to genetic instability of *Streptococcus pneumoniae. Journal of Bacteriology*, 184(16), 4392-4399. doi:10.1128/jb.184.16.4392-4399.2002

Perry, M. B., Bundle, D. R., Daoust, V., & Carlo, D. J. (1982). The specific capsular polysaccharide of *Streptococcus pneumoniae* type 15F. *Molecular Immunology*, 19(2), 235-246. doi:10.1016/0161-5890(82)90336-4

Pessoa, D., Hoti, F., Syrjänen, R., Sá-Leão, R., Kaijalainen, T., Gomes, M. G. M., & Auranen, K. (2013). Comparative analysis of *Streptococcus pneumoniae* transmission in Portuguese and Finnish day-care centres. *BMC Infectious Diseases*, 13(1), 180-180. doi:10.1186/1471-2334-13-180

Peterson, J. T., Stacey, H. L., MacNair, J. E., Li, J., Hartzel, J. S., Sterling, T. M., Benner, P., Tamms, G. M., & Musey, L. K. (2018). Safety and immunogenicity of 15-valent pneumococcal conjugate vaccine compared to 13-valent pneumococcal conjugate vaccine in adults ≥65 years of age previously vaccinated with 23-valent pneumococcal polysaccharide vaccine. *Human Vaccines and Immunotherapeutics*, 15(3), 540-548. doi:10.1080/21645515.2018.1532250

Peterson, S. N., Sung, C. K., Cline, R., Desai, B. V., Snesrud, E. C., Luo, P., Walling, J., Li, H., Mintz, M., Tsegaye, G., Burr, P. C., Do, Y., Ahn, S., Gilbert, J., Fleischmann, R. D., & Morrison, D. A. (2004). Identification of competence pheromone responsive genes in *Streptococcus pneumoniae* by use of DNA microarrays. *Molecular Microbiology*, 51(4), 1051-1070. doi:10.1046/j.1365-2958.2003.03907.x

Pettigrew, M. M., Fennie, K. P., York, M. P., Daniels, J., & Ghaffar, F. (2006). Variation in the presence of neuraminidase genes among *Streptococcus pneumoniae* isolates with identical sequence types. *Infection and Immunity*, 74(6), 3360-3365. doi:10.1128/IAI.01442-05

Philips, B. J., Meguer, J.-X., Redman, J., & Baker, E. H. (2003). Factors determining the appearance of glucose in upper and lower respiratory tract secretions. *Intensive Care Medicine*, 29(12), 2204-2210. doi:10.1007/s00134-003-1961-2

Pichichero, M. E. (2017). Pneumococcal whole-cell and protein-based vaccines: Changing the paradigm. *Expert Review of Vaccines*, 16(12), 1181-1190. doi:10.1080/14760584.2017.1393335

Pimenta, F., Moiane, B., Gertz, R. E., Jr., Chochua, S., Snippes Vagnone, P. M., Lynfield, R., Sigaúque, B., Carvalho, M. D. G., & Beall, B. (2021). New pneumococcal serotype 15D. *Journal of Clinical Microbiology,* 59(5). doi:10.1128/jcm.00329-21

Piñas, G. E., Cortes, P. R., Orio, A. G. A., & Echenique, J. (2008). Acidic stress induces autolysis by a CSP-independent come pathway in *Streptococcus pneumoniae*. *Microbiology*, 154(Pt 5), 1300-1308. doi:10.1099/mic.0.2007/015925-0

Piñas, G. E., Reinoso-Vizcaino, N. M., Yandar Barahona, N. Y., Cortes, P. R., Duran, R., Badapanda, C., Rathore, A., Bichara, D. R., Cian, M. B., Olivero, N. B., Perez, D. R., & Echenique, J. (2018). Crosstalk between the serine/threonine kinase StkP and the response regulator ComE controls the stress response and intracellular survival of *Streptococcus pneumoniae. PLoS Pathogens*, 14(6), e1007118. doi:10.1371/journal.ppat.1007118

Platt, H. L., Greenberg, D., Tapiero, B., Clifford, R. A., Klein, N. P., Hurley, D. C., Shekar, T., Li, J., Hurtado, K., Su, S. C., Nolan, K. M., Acosta, C. J., McFetridge, R. D., Bickham, K., & Musey, L. K. (2020). A phase II trial of safety, tolerability and immunogenicity of V114, a 15-valent pneumococcal conjugate vaccine, compared with 13-valent pneumococcal conjugate vaccine in healthy infants. *The Pediatric Infectious Disease Journal*, 39(8), 763-770. doi:10.1097/inf.0000000000002765

Postma, P. W., Lengeler, J. W., & Jacobson, G. R. (1993). Phosphoenolpyruvate: Carbohydrate phosphotransferase systems of bacteria. *Microbiological Reviews*, 57(3), 543-594. doi:10.1128/mmbr.57.3.543-594.1993

Prudhomme, M., Libante, V., & Claverys, J.-P. (2002). Homologous recombination at the border: Insertion-deletions and the trapping of foreign DNA in *Streptococcus pneumoniae. Proceedings of the National Academy of Sciences - PNAS*, 99(4), 2100-2105. doi:10.1073/pnas.032262999

Prudhomme, M., Attaiech, L., Sanchez, G., Martin, B., & Claverys, J.-P. (2006). Antibiotic stress induces genetic transformability in the human pathogen *Streptococcus pneumoniae. Science (American Association for the Advancement of Science)*, 313(5783), 89-92. doi:10.1126/science.1127912

Puyet, A., Ibáñez, A. M., & Espinosa, M. (1993). Characterization of the *Streptococcus pneumoniae* maltosaccharide regulator MalR, a member of the LacI-GalR family of repressors displaying distinctive genetic features. *Journal of Biological Chemistry*, 268(34), 25402-25408.

Quin, L. R., Carmicle, S., Dave, S., Pangburn, M. K., Evenhuis, J. P., & McDaniel, L. S. (2005). *In vivo* binding of complement regulator factor H by *Streptococcus pneumoniae*. T*he Journal of Infectious Diseases*, 192(11), 1996-2003. doi:10.1086/497605

Quirk, S. J., Haraldsson, G., Erlendsdóttir, H., Hjálmarsdóttir, M., van Tonder, A. J., Hrafnkelsson, B., Sigurdsson, S., Bentley, S. D., Haraldsson, Á., Brueggemann, A. B., & Kristinsson, K. G. (2018). Effect of vaccination on pneumococci isolated from the nasopharynx of healthy children and the middle ear of children with otitis media in Iceland. *Journal of Clinical Microbiology*, 56(12). doi:10.1128/jcm.01046-18

Rabes, A., Suttorp, N., & Opitz, B. (2016). Inflammasomes in pneumococcal infection: Innate immune sensing and bacterial evasion strategies. *Current Topics in Microbiology and Immunology*, 397, 215-227. doi:10.1007/978-3-319-41171-2_11

Rahman, A. H., Taylor, D. K., & Turka, L. A. (2009). The contribution of direct TLR signaling to T cell responses. *Immunologic Research*, 45(1), 25-36. doi:10.1007/s12026-009-8113-x

Ramirez, M., Severina, E., & Tomasz, A. (1999). A high incidence of prophage carriage among natural isolates of *Streptococcus pneumoniae. Journal of Bacteriology*, 181(12), 3618-3625. doi:10.1128/JB.181.12.3618-3625.1999

Ramos-Montañez, S., Tsui, H. C., Wayne, K. J., Morris, J. L., Peters, L. E., Zhang, F., Kazmierczak, K. M., Sham, L. T., & Winkler, M. E. (2008). Polymorphism and regulation of the *spxB* (pyruvate oxidase) virulence factor gene by a CBS-HotDog domain protein (SpxR) in serotype 2 *Streptococcus pneumoniae*. *Molecular Microbiology*, 67(4), 729-746. doi:10.1111/j.1365-2958.2007.06082.x

Ramos-Sevillano, E., Ercoli, G., & Brown, J. S. (2019). Mechanisms of naturally acquired immunity to *Streptococcus pneumoniae. Frontiers in Immunology*, 10, 358-358. doi:10.3389/fimmu.2019.00358

Rayner, C. F. J., Jackson, A. D., Rutman, A., Dewar, A., Mitchell, T. J., Andrew, P. W., Cole, P. J., & Wilson, R. (1995). Interaction of pneumolysin-sufficient and -deficient isogenic variants of *Streptococcus pneumoniae* with human respiratory mucosa. *Infection and Immunity*, 63(2), 442-447. doi:10.1128/iai.63.2.442-447.1995

Regev-Yochay, G., Raz, M., Dagan, R., Porat, N., Shainberg, B., Pinco, E., Keller, N., & Rubinstein, E. (2004). Nasopharyngeal carriage of *Streptococcus pneumoniae* by adults and children in community and family settings. *Clinical Infectious Diseases*, 38(5), 632-639. doi:10.1086/381547

Regev-Yochay, G., Paran, Y., Bishara, J., Oren, I., Chowers, M., Tziba, Y., Istomin, V., Weinberger, M., Miron, D., Temper, V., Rahav, G., & Dagan, R. (2015). Early impact of PCV7/PCV13 sequential introduction to the national pediatric immunization plan, on adult invasive pneumococcal disease: A nationwide surveillance study. *Vaccine*, 33(9), 1135-1142. doi:10.1016/j.vaccine.2015.01.030

Richard, A. L., Siegel, S. J., Erikson, J., & Weiser, J. N. (2014). TLR2 signaling decreases transmission of *Streptococcus pneumoniae* by limiting bacterial shedding in an infant mouse Influenza A co-infection model. *PLoS Pathogens*, 10(8), e1004339. doi:10.1371/journal.ppat.1004339

Richards, L., Ferreira, D. M., Miyaji, E. N., Andrew, P. W., & Kadioglu, A. (2010). The immunising effect of pneumococcal nasopharyngeal colonisation; protection against future colonisation and fatal invasive disease. *Immunobiology*, 215(4), 251-263. doi:10.1016/j.imbio.2009.12.004

Riley, I. D., Andrews, M., Howard, R., Tarr, P. I., Pfeiffer, M., Challands, P., Jennison, G., & Douglas, R. M. (1977). Immunisation with a polyvalent pneumococcal vaccine: Reduction of adult respiratory mortality in a new guinea highlands community. *The Lancet*, 309(8026), 1338-1341. doi:10.1016/S0140-6736(77)92552-1

Ritchie, N. D., Ritchie, R., Bayes, H. K., Mitchell, T. J., & Evans, T. J. (2018). IL-17 can be protective or deleterious in murine pneumococcal pneumonia. *PLoS Pathogens*, 14(5), e1007099. doi:10.1371/journal.ppat.1007099

Robb, M., Hobbs, J. K., Woodiga, S. A., Shapiro-Ward, S., Suits, M. D. L., McGregor, N., Brumer, H., Yesilkaya, H., King, S. J., & Boraston, A. B. (2017). Molecular characterization of N-glycan degradation and transport in *Streptococcus pneumoniae* and its contribution to virulence. *PLoS Pathogens*, 13(1), e1006090-e1006090. doi:10.1371/journal.ppat.1006090

Roberts, R. J., Belfort, M., Bestor, T., Bhagwat, A. S., Bickle, T. A., Bitinaite, J., Blumenthal, R. M., Degtyarev, S. K., Dryden, D. T. F., Dybvig, K., Firman, K., Gromova, E. S., Gumport, R. I., Halford, S. E., Hattman, S., Heitman, J., Hornby, D. P., Janulaitis, A., Jeltsch, A., Josephsen, J., Kiss, A., Klaenhammer, T. R., Kobayashi, I., Kong, H., Krüger, D. H., Lacks, S., Marinus, M. G., Miyahara, M., Morgan, R. D., Murray, N. E., Nagaraja, V., Piekarowicz, A., Pingoud, A., Raleigh, E., Rao, D. N., Reich, N., Repin, V. E., Selker, E. U., Shaw, P. C., Stein, D. C., Stoddard, B. L., Szybalski, W., Trautner, T. A., Van Etten, J. L., Vitor, J. M. B., Wilson, G. G., & Xu, S. y. (2003). A nomenclature for restriction enzymes, DNA methyltransferases, homing endonucleases and their genes. *Nucleic Acids Research*, 31(7), 1805-1812. doi:10.1093/nar/gkg274

Robinson, R. E., Mitsi, E., Nikolaou, E., Pojar, S., Chen, T., Reiné, J., Nyazika, T. K., Court, J., Davies, K., Farrar, M., Gonzalez-Dias, P., Hamilton, J., Hill, H., Hitchins, L., Howard, A., Hyder-Wright, A., Lesosky, M., Liatsikos, K., Matope, A., McLenaghan, D., Myerscough, C., Murphy, A., Solórzano, C., Wang, D., Burhan, H., Gautam, M., Begier, E., Theilacker, C., Beavon, R., Anderson, A. S., Gessner, B. D., Gordon, S. B., Collins, A. M., & Ferreira, D. M. (2022). Human infection challenge with serotype 3 pneumococcus. *American Journal of Respiratory and Critical Care Medicine*, 206(11), 1379-1392. doi:10.1164/rccm.202112-2700OC

Roche, A. M., Richard, A. L., Rahkola, J. T., Janoff, E. N., & Weiser, J. N. (2015). Antibody blocks acquisition of bacterial colonization through agglutination. *Mucosal Immunology*, 8(1), 176-185. doi:10.1038/mi.2014.55

Rodic, A., Blagojevic, B., Zdobnov, E., Djordjevic, M., & Djordjevic, M. (2017). Understanding key features of bacterial restriction-modification systems through quantitative modeling. *BMC Systems Biology*, 11(Suppl 1), 377. doi:10.1186/s12918-016-0377-x

Rodrigues, F., Foster, D., Nicoli, E., Trotter, C., Vipond, B., Muir, P., Goncalves, G., Januario, L., & Finn, A. (2013). Relationships between rhinitis symptoms, respiratory viral infections and nasopharyngeal colonization with *Streptococcus pneumoniae, Haemophilus influenzae* and *Staphylococcus aureus* in children attending daycare. *The Pediatric Infectious Disease Journal*, 32(3), 227-232. doi:10.1097/INF.0b013e31827687fc

Romagnani, S. (1999). Th1/Th2 cells. *Inflammatory Bowel Diseases*, 5(4), 285-294. doi:10.1097/00054725-199911000-00009

Romao, S., Memmi, G., Oggioni, M. R., & Trombe, M. C. (2006). LuxS impacts on LytA-dependent autolysis and on competence in *Streptococcus pneumoniae. Microbiology*, 152(Pt 2), 333-341. doi:10.1099/mic.0.28406-0

Rose, M. C., & Voynow, J. A. (2006). Respiratory tract mucin genes and mucin glycoproteins in health and disease. *Physiological Reviews*, 86(1), 245-278. doi:10.1152/physrev.00010.2005

Rosenow, C., Ryan, P., Weiser, J. N., Johnson, S., Fontan, P., Ortqvist, A., & Masure, H. R. (1997). Contribution of novel choline-binding proteins to adherence, colonization and immunogenicity of *Streptococcus pneumoniae. Molecular Microbiology*, 25(5), 819-829. doi:10.1111/j.1365-2958.1997.mmi494.x

Rosenow, C., Maniar, M., & Trias, J. (1999). Regulation of the alpha-galactosidase activity in *Streptococcus pneumoniae*: Characterization of the raffinose utilization system. *Genome Research*, 9(12), 1189-1197. doi:10.1101/gr.9.12.1189

Rubins, J. B., Charboneau, D., Fasching, C., Berry, A. M., Paton, J. C., Alexander, J. E., Andrew, P. W., Mitchell, T. J., & Janoff, E. N. (1996). Distinct roles for pneumolysin's cytotoxic and complement activities in the pathogenesis of pneumococcal pneumonia. *American Journal of Respiratory and Critical Care Medicine*, 153(4), 1339-1346. doi:10.1164/ajrccm.153.4.8616564

Rutherford, S. T., & Bassler, B. L. (2012). Bacterial quorum sensing: Its role in virulence and possibilities for its control. *Cold Spring Harbor Perspectives in Medicine*, 2(11). doi:10.1101/cshperspect.a012427

Saluja, S. K., & Weiser, J. N. (1995). The genetic basis of colony opacity in *Streptococcus pneumoniae*: Evidence for the effect of box elements on the frequency of phenotypic variation. *Molecular Microbiology*, 16(2), 215-227. doi:10.1111/j.1365-2958.1995.tb02294.x

Sampson, J. S., Furlow, Z., Whitney, A. M., Williams, D., Facklam, R., & Carlone, G. M. (1997). Limited diversity of *Streptococcus pneumoniae* PsaA among pneumococcal vaccine serotypes. *Infection and Immunity*, 65(5), 1967-1971. doi:10.1128/iai.65.5.1967-1971.1997

Sanchez, C. J., Kumar, N., Lizcano, A., Shivshankar, P., Dunning Hotopp, J. C., Jorgensen, J. H., Tettelin, H., & Orihuela, C. J. (2011). *Streptococcus pneumoniae* in biofilms are unable to cause invasive disease due to altered virulence determinant production. *PloS One*, 6(12), e28738. doi:10.1371/journal.pone.0028738

Schachern, P. A., Paparella, M. M., Hybertson, R., Sano, S., & Duvall, A. J., III. (1992). Bacterial tympanogenic labyrinthitis, meningitis, and sensorineural damage. *Archives of Otolaryngology–Head & Neck Surgery*, 118(1), 53-57. doi:10.1001/archotol.1992.01880010057016

Schauder, S., Shokat, K., Surette, M. G., & Bassler, B. L. (2001). The LuxS family of bacterial autoinducers: Biosynthesis of a novel quorum-sensing signal molecule. *Molecular Microbiology*, 41(2), 463-476. doi:10.1046/j.1365-2958.2001.02532.x

Serrano, I., Melo-Cristino, J., & Ramirez, M. (2006). Heterogeneity of pneumococcal phase variants in invasive human infections. *BMC Microbiology*, 6(1), 67-67. doi:10.1186/1471-2180-6-67

Shafeeq, S., Kloosterman, T. G., & Kuipers, O. P. (2011). CelR-mediated activation of the cellobiose-utilization gene cluster in *Streptococcus pneumoniae. Microbiology (Society for General Microbiology)*, 157(Pt 10), 2854-2861. doi:10.1099/mic.0.051359-0

Shak, J. R., Vidal, J. E., & Klugman, K. P. (2013). Influence of bacterial interactions on pneumococcal colonization of the nasopharynx. Trends in Microbiology, 21(3), 129-135. doi:10.1016/j.tim.2012.11.005

Shakhnovich, E. A., King, S. J., & Weiser, J. N. (2002). Neuraminidase expressed by *Streptococcus pneumoniae* desialylates the lipopolysaccharide of *Neisseria meningitidis* and *Haemophilus influenzae*: A paradigm for interbacterial competition among pathogens of the human respiratory tract. *Infection and Immunity*, 70(12), 7161-7164. doi:10.1128/IAI.70.12.7161-7164.2002

Shanker, E., & Federle, M. J. (2017). Quorum sensing regulation of competence and bacteriocins in *Streptococcus pneumoniae* and *mutans. Genes*, 8(1), 15. doi:10.3390/genes8010015

Shaper, M., Hollingshead, S. K., Benjamin, W. H., & Briles, D. E. (2004). PspA protects *Streptococcus pneumoniae* from killing by apolactoferrin, and antibody to PspA enhances killing of pneumococci by apolactoferrin. *Infection and Immunity*, 72(9), 5031-5040. doi:10.1128/IAI.72.9.5031-5040.2004

Shapiro, E. D., Berg, A. T., Austrian, R., Schroeder, D., Parcells, V., Margolis, A., Adair, R. K., & Clemens, J. D. (1991). The protective efficacy of polyvalent pneumococcal polysaccharide vaccine. *The New England Journal of Medicine*, 325(21), 1453-1460. doi:10.1056/NEJM199111213252101

Shiri, T., Nunes, M. C., Adrian, P. V., Van Niekerk, N., Klugman, K. P., & Madhi, S. A. (2013). Interrelationship of *Streptococcus pneumoniae*, *Haemophilus influenzae* and *Staphylococcus aureus* colonization within and between pneumococcal-vaccine naïve mother-child dyads. *BMC Infectious Diseases*, 13(1), 483-483. doi:10.1186/1471-2334-13-483

Shlla, B., Gazioglu, O., Shafeeq, S., Manzoor, I., Kuipers, O. P., Ulijasz, A., Hiller, N. L., Andrew, P. W., & Yesilkaya, H. (2021). The Rgg1518 transcriptional regulator is a necessary facet of sugar metabolism and virulence in *Streptococcus pneumoniae. Molecular Microbiology*, 116(3), 996-1008. doi:10.1111/mmi.14788

Sibold, C., Markiewicz, Z., Latorre, C., & Hakenbeck, R. (1991). Novel plasmids in clinical strains of *Streptococcus pneumoniae. FEMS Microbiology Letters*, 77(1), 91-96. doi:10.1111/j.1574-6968.1991.tb04327.x

Silva, N. A., McCluskey, J., Jefferies, J. M., Hinds, J., Smith, A., Clarke, S. C., Mitchell, T. J., & Paterson, G. K. (2006). Genomic diversity between strains of the same serotype and multilocus sequence type among pneumococcal clinical isolates. *Infection and Immunology*, 74(6), 3513-3518. doi:10.1128/iai.00079-06

Singh, J., Sundaresan, S., Manoharan, A., & Shet, A. (2017). Serotype distribution and antimicrobial susceptibility pattern in children ≤5 years with invasive pneumococcal disease in India - a systematic review. *Vaccine*, 35(35 Pt B), 4501-4509. doi:10.1016/j.vaccine.2017.06.079

Smit, P., Oberholzer, D., Hayden-Smith, S., Koornhof, H. J., & Hilleman, M. R. (1977). Protective efficacy of pneumococcal polysaccharide vaccines. *The Journal of the American Medical Association*, 238(24), 2613-2616. doi:10.1001/jama.1977.03280250039019

Smith, A. W., Roche, H., Trombe, M.-C., Briles, D. E., & Håkansson, A. (2002). Characterization of the dihydrolipoamide dehydrogenase from *Streptococcus pneumoniae* and its role in pneumococcal infection. *Molecular Microbiology*, 44(2), 431-448. doi:10.1046/j.1365-2958.2002.02883.x

Smith, M. D., & Guild, W. R. (1979). A plasmid in *Streptococcus pneumoniae. Journal of Bacteriology*, 137(2), 735-739. doi:10.1128/JB.137.2.735-739.1979

Soni, K. A., Jesudhasan, P., Cepeda, M., Widmer, K., Jayaprakasha, G. K., Patil, B. S., Hume, M. E., & Pillai, S. D. (2008). Identification of ground beef-derived fatty acid inhibitors of autoinducer-2-based cell signaling. *Journal of Food Protection*, 71(1), 134-138. doi:10.4315/0362-028X-71.1.134

Sørensen, U. B. S., Blom, J., Birch-Andersen, A., & Henrichsen, J. (1988). Ultrastructural localization of capsules, cell wall polysaccharide, cell wall proteins, and F antigen in pneumococci. *Infection and Immunity*, 56(8), 1890-1896. doi:10.1128/iai.56.8.1890-1896.1988

Sørensen, U. B. S., Henrichsen, J., Chen, H.-C., & Szu, S. C. (1990). Covalent linkage between the capsular polysaccharide and the cell wall peptidoglycan of *Streptococcus pneumoniae* revealed by immunochemical methods. *Microbial Pathogenesis*, 8(5), 325-334. doi:10.1016/0882-4010(90)90091-4

Sprent, J. (1994). T and B memory cells. *Cell*, 76(2), 315-322. doi:10.1016/0092-8674(94)90338-7

Srivastava, A., Henneke, P., Visintin, A., Morse, S. C., Martin, V., Watkins, C., Paton, J. C., Wessels, M. R., Golenbock, D. T., & Malley, R. (2005). Apoptotic response to pneumolysin is Toll-like receptor 4 dependent and protects against pneumococcal disease. *Infection and Immunity*, 73(10), 6479-6487. doi:10.1128/IAI.73.10.6479-6487.2005

Stacey, H. L., Rosen, J., Peterson, J. T., Williams-Diaz, A., Gakhar, V., Sterling, T. M., Acosta, C. J., Nolan, K. M., Li, J., Pedley, A., Benner, P., Abeygunawardana, C., Kosinski, M., Smith, W. J., Pujar, H., & Musey, L. K. (2019). Safety and immunogenicity of 15-valent pneumococcal conjugate vaccine (PCV-15) compared to PCV-13 in healthy older adults. *Human Vaccines and Immunotherapeutics*, 15(3), 530-539. doi:10.1080/21645515.2018.1532249

Stahl, W. L., & O'Toole, R. D. (1972). Pneumococcal neuraminidase: Purification and properties. *Biochimica et Biophysica Acta (BBA) - Enzymology*, 268(2), 480-487. doi:10.1016/0005-2744(72)90343-9

Stahlfeld, A., Glick, L. R., Ott, I. M., Craft, S. B., Yolda-Carr, D., Harden, C. A., Nakahata, M., Farhadian, S. F., Grant, L. R., Alexander-Parrish, R., Arguedas, A., Gessner, B. D., Weinberger, D. M., & Wyllie, A. L. (2022). Detection of pneumococcus during hospitalization for SARS-COV-2. *FEMS Microbes*, 3. doi:10.1093/femsmc/xtac026

Stanek, R. J. M. S., Norton, N. B. M. D., & Mufson, M. A. M. D. (2016). A 32-year study of the effect of pneumococcal vaccines on invasive *Streptococcus pneumoniae* disease. *The American Journal of the Medical Sciences*, 352(6), 563-573. doi:10.1016/j.amjms.2016.09.002

Steinmoen, H., Knutsen, E., & Håvarstein, L. S. (2002). Induction of natural competence in *Streptococcus pneumoniae* triggers lysis and DNA release from a subfraction of the cell population. *Proceedings of the National Academy of Sciences - PNAS*, 99(11), 7681-7686. doi:10.1073/pnas.112464599

Stevens, K. E., Chang, D., Zwack, E. E., & Sebert, M. E. (2011). Competence in *Streptococcus pneumoniae* is regulated by the rate of ribosomal decoding errors. *mBio*, 2(5). doi:10.1128/mBio.00071-11

Stock, A. M., Robinson, V. L., & Goudreau, P. N. (2000). Two-component signal transduction. *Annual Review of Biochemistry*, 69(1), 183-215. doi:10.1146/annurev.biochem.69.1.183

Stoodley, P., Hall-Stoodley, L., & Costerton, J. W. (2004). Bacterial biofilms: From the natural environment to infectious diseases. *Nature Reviews Microbiology*, 2(2), 95-108. doi:10.1038/nrmicro821

Stroeher, U. H., Paton, A. W., Ogunniyi, A. D., & Paton, J. C. (2003). Mutation of *luxS* of *Streptococcus pneumoniae* affects virulence in a mouse model. *Infection and Immunology*, 71(6), 3206-3212. doi:10.1128/iai.71.6.3206-3212.2003

Surette, M. G., Miller, M. B., & Bassler, B. L. (1999). Quorum sensing in *Escherichia coli, Salmonella typhimurium,* and *Vibrio harveyi*: A new family of genes responsible for autoinducer production. *Proceedings of the National Academy of Sciences - PNAS*, 96(4), 1639-1644. doi:10.1073/pnas.96.4.1639

Svendsen, L., Rasmussen, T., Nielsen, S., Hartling, P. E., & Trap-Jensen, O. (1979). Hemodynamic effects of acute and long-term treatment with labetalol. *Acta Medica Scandinavica*, 205(S625), 49-53. doi:10.1111/j.0954-6820.1979.tb00741.x

Swanson, J. (1982). Colony opacity and protein II compositions of gonococci. *Infection and Immunity*, 37(1), 359-368. doi:10.1128/IAI.37.1.359-368.1982

Swiatlo, E., Champlin, F. R., Holman, S. C., Wilson, W. W., & Watt, J. M. (2002). Contribution of choline-binding proteins to cell surface properties of *Streptococcus pneumoniae. Infection and Immunity*, 70(1), 412-415. doi:10.1128/IAI.70.1.412-415.2002

Talbot, U. M., Paton, A. W., & Paton, J. C. (1996). Uptake of *Streptococcus pneumoniae* by respiratory epithelial cells. *Infection and Immunology*, 64(9), 3772-3777. doi:10.1128/iai.64.9.3772-3777.1996

Teele, D. W., Klein, J. O., Chase, C., Menyuk, P., & Rosner, B. A. (1990). Otitis media in infancy and intellectual ability, school achievement, speech, and language at age 7 years. Greater Boston otitis media study group. *The Journal of Infectious Diseases*, 162(3), 685-694.

Tettelin, H., Nelson, K. E., Paulsen, I. T., Eisen, J. A., Read, T. D., Peterson, S., Heidelberg, J., DeBoy, R. T., Haft, D. H., Dodson, R. J., Durkin, A. S., Gwinn, M., Kolonay, J. F., Nelson, W. C.,

Peterson, J. D., Umayam, L. A., White, O., Salzberg, S. L., Lewis, M. R., Radune, D., Holtzapple, E., Khouri, H., Wolf, A. M., Utterback, T. R., Hansen, C. L., McDonald, L. A., Feldblyum, T. V., Angiuoli, S., Dickinson, T., Hickey, E. K., Holt, I. E., Loftus, B. J., Yang, F., Smith, H. O., Venter, J. C., Dougherty, B. A., Morrison, D. A., Hollingshead, S. K., & Fraser, C. M. (2001). Complete genome sequence of a virulent isolate of *Streptococcus pneumoniae. Science (American Association for the Advancement of Science)*, 293(5529), 498-506. doi:10.1126/science.1061217

Thigpen, M. C., Whitney, C. G., Messonnier, N. E., Zell, E. R., Lynfield, R., Hadler, J. L., Harrison, L. H., Farley, M. M., Reingold, A., & Bennett, N. M. (2011). Bacterial meningitis in the United States, 1998–2007. *New England Journal of Medicine*, 364(21), 2016-2025.

Tikhomirova, A., Brazel, E. B., McLean, K. T., Agnew, H. N., Paton, J. C., & Trappetti, C. (2022). The role of *luxS* in the middle ear *Streptococcus pneumoniae* isolate 947. *Pathogens*, 11(2), 216. doi:10.3390/pathogens11020216

Tilley, S. J., Orlova, E. V., Gilbert, R. J. C., Andrew, P. W., & Saibil, H. R. (2005). Structural basis of pore formation by the bacterial toxin pneumolysin. *Cell*, 121(2), 247-256. doi:10.1016/j.cell.2005.02.033

Tomczyk, S., Lynfield, R., Schaffner, W., Reingold, A., Miller, L., Petit, S., Holtzman, C., Zansky, S. M., Thomas, A., & Baumbach, J. (2016). Prevention of antibiotic-nonsusceptible invasive pneumococcal disease with the 13-valent pneumococcal conjugate vaccine. *Clinical Infectious Diseases*, 62(9), 1119-1125. doi:10.1093/cid/ciw067

Tomlinson, G., Chimalapati, S., Pollard, T., Lapp, T., Cohen, J., Camberlein, E., Stafford, S., Periselneris, J., Aldridge, C., Vollmer, W., Picard, C., Casanova, J.-L., Noursadeghi, M., & Brown, J. (2014). TLR-mediated inflammatory responses to *Streptococcus pneumoniae* are highly dependent on surface expression of bacterial lipoproteins. *The Journal of Immunology*, 193(7), 3736-3745. doi:10.4049/jimmunol.1401413

Tong, H. H., Blue, L. E., James, M. A., & Demaria, T. F. (2000). Evaluation of the virulence of a *Streptococcus pneumoniae* neuraminidase-deficient mutant in nasopharyngeal colonization and development of otitis media in the chinchilla model. *Infection and Immunity*, 68(2), 921-924. doi:10.1128/IAI.68.2.921-924.2000

Trappetti, C., Gualdi, L., Di Meola, L., Jain, P., Korir, C. C., Edmonds, P., Iannelli, F., Ricci, S., Pozzi, G., & Oggioni, M. R. (2011a). The impact of the competence quorum sensing system on *Streptococcus pneumoniae* biofilms varies depending on the experimental model. *BMC Microbiology*, 11(1), 75-75. doi:10.1186/1471-2180-11-75

Trappetti, C., Ogunniyi, A. D., Oggioni, M. R., & Paton, J. C. (2011b). Extracellular matrix formation enhances the ability of *Streptococcus pneumoniae* to cause invasive disease. *PloS One*, 6(5), e19844-e19844. doi:10.1371/journal.pone.0019844

Trappetti, C., Potter, A. J., Paton, A. W., Oggioni, M. R., & Paton, J. C. (2011c). LuxS mediates iron-dependent biofilm formation, competence, and fratricide in *Streptococcus pneumoniae. Infection and Immunity*, 79(11), 4550-4558. doi:10.1128/IAI.05644-11

Trappetti, C., van der Maten, E., Amin, Z., Potter, A. J., Chen, A. Y., van Mourik, P. M., Lawrence, A. J., Paton, A. W., & Paton, J. C. (2013). Site of isolation determines biofilm formation and

virulence phenotypes of *Streptococcus pneumoniae* serotype 3 clinical isolates. *Infection and Immunity*, 81(2), 505-513. doi:10.1128/IAI.01033-12

Trappetti, C., McAllister, L. J., Chen, A., Wang, H., Paton, A. W., Oggioni, M. R., McDevitt, C. A., & Paton, J. C. (2017). Autoinducer 2 signaling via the phosphotransferase FruA drives galactose utilization by *Streptococcus pneumoniae*, resulting in hypervirulence. *mBio*, 8(1), e02269-02216. doi:10.1128/mBio.02269-16

Trimble, A., Connor, V., Robinson, R. E., McLenaghan, D., Hancock, C. A., Wang, D., Gordon, S. B., Ferreira, D. M., Wright, A. D., & Collins, A. M. (2020). Pneumococcal colonisation is an asymptomatic event in healthy adults using an experimental human colonisation model. *PloS One*, 15(3). doi:10.1371/journal.pone.0229558

Tseng, H.-J., McEwan, A. G., Paton, J. C., & Jennings, M. P. (2002). Virulence of *Streptococcus pneumoniae: psaA* mutants are hypersensitive to oxidative stress. *Infection and Immunity*, 70(3), 1635-1639. doi:10.1128/IAI.70.3.1635-1639.2002

Tuomanen, E. I. (2000). Pathogenesis of pneumococcal inflammation: Otitis media. *Vaccine*, 19, S38-S40. doi:10.1016/S0264-410X(00)00276-0

Turovskiy, Y., & Chikindas, M. L. (2006). Autoinducer-2 bioassay is a qualitative, not quantitative method influenced by glucose. *Journal of Microbiological Methods*, 66(3), 497-503. doi:10.1016/j.mimet.2006.02.001

Tyx, R. E., Roche-Hakansson, H., & Hakansson, A. P. (2011). Role of dihydrolipoamide dehydrogenase in regulation of raffinose transport in *Streptococcus pneumoniae. Journal of Bacteriology*, 193(14), 3512-3524. doi:10.1128/jb.01410-10

van der Poll, T., & Opal, S. M. (2009). Pathogenesis, treatment, and prevention of pneumococcal pneumonia. *The Lancet*, 374(9700), 1543-1556. doi:10.1016/S0140-6736(09)61114-4

van Gils, E. J. M., Veenhoven, R. H., Hak, E., Rodenburg, G. D., Bogaert, D., Ijzerman, E. P. F., Bruin, J. P., van Alphen, L., & Sanders, E. A. M. (2009). Effect of reduced-dose schedules with 7-valent pneumococcal conjugate vaccine on nasopharyngeal pneumococcal carriage in children: A randomized controlled trial. *The Journal of the American Medical Association*, 302(2), 159-167. doi:10.1001/jama.2009.975

van Ginkel, F. W., McGhee, J. R., Watt, J. M., Campos-Torres, A., Parish, L. A., & Briles, D. E. (2003). Pneumococcal carriage results in ganglioside-mediated olfactory tissue infection. *Proceedings of the National Academy of Sciences - PNAS*, 100(24), 14363-14367. doi:10.1073/pnas.2235844100

Van Hoek, A. J., Andrews, N., Waight, P. A., George, R., & Miller, E. (2012). Effect of serotype on focus and mortality of invasive pneumococcal disease: Coverage of different vaccines and insight into non-vaccine serotypes. *PloS One*, 7(7), e39150. doi:10.1371/journal.pone.0039150

van Opijnen, T., & Camilli, A. (2012). A fine scale phenotype-genotype virulence map of a bacterial pathogen. *Genome Research*, 22(12), 2541-2551. doi:10.1101/gr.137430.112

van Pee, K., Neuhaus, A., D'Imprima, E, Mills, D. J., Kühlbrandt, W., & Yildiz , Ö. (2017). CryoEM structures of membrane pore and prepore complex reveal cytolytic mechanism of Pneumolysin. *eLife* 6, :23644. doi: org/10.7554/eLife.23644

van Selm, S., van Cann, L. M., Kolkman, M. A. B., van der Zeijst, B. A. M., & van Putten, J. P. M. (2003). Genetic basis for the structural difference between *Streptococcus pneumoniae* serotype 15B and 15C capsular polysaccharides. *Infection and Immunity*, 71(11), 6192-6198. doi:10.1128/IAI.71.11.6192-6198.2003

van Tonder, A. J., Bray, J. E., Jolley, K. A., Quirk, S. J., Haraldsson, G., Maiden, M. C. J., Bentley, S. D., Haraldsson, A., Erlendsdottir, H., Kristinsson, K. G., & Brueggemann, A. B. (2017). Heterogeneity among estimates of the core genome and pan-genome in different pneumococcal populations. In. *Cold Spring Harbor*: Cold Spring Harbor Laboratory Press.

Verhagen, L. M., de Jonge, M. I., Burghout, P., Schraa, K., Spagnuolo, L., Mennens, S., Eleveld, M. J., van der Gaast-de Jongh, C. E., Zomer, A., Hermans, P. W. M., & Bootsma, H. J. (2014). Genome-wide identification of genes essential for the survival of *Streptococcus pneumoniae* in human saliva. *PloS One*, 9(2), e89541. doi:10.1371/journal.pone.0089541

Vidal, J. E., Ludewick, H. P., Kunkel, R. M., Zähner, D., & Klugman, K. P. (2011). The LuxS-dependent quorum-sensing system regulates early biofilm formation by *Streptococcus pneumoniae* strain D39. *Infection and Immunology*, 79(10), 4050-4060. doi:10.1128/iai.05186-11

Vidal, J. E., Howery, K. E., Ludewick, H. P., Nava, P., & Klugman, K. P. (2013). Quorum-sensing systems LuxS/Autoinducer 2 and Com regulate *Streptococcus pneumoniae* biofilms in a bioreactor with living cultures of human respiratory cells. *Infection and Immunity*, 81(4), 1341-1353. doi:10.1128/IAI.01096-12

Vögele, M., Bhaskara, R. M., Mulvihill, E., van Pee, K., Yildiz, Ö., Kühlbrandt, W., Müller, D. J., & Hummer, G. (2019). Membrane perforation by the pore-forming toxin pneumolysin. *Proceedings of the National Academy of Sciences*, 116(27), 13352-13357. doi:10.1073/pnas.1904304116

von Bodman, S. B., Willey, J. M., & Diggle, S. P. (2008). Cell-cell communication in bacteria: United we stand. *Journal of Bacteriology*, 190(13), 4377-4391. doi:10.1128/JB.00486-08

von Gottberg, A., de Gouveia, L., Tempia, S., Quan, V., Meiring, S., von Mollendorf, C., Madhi, S. A., Zell, E. R., Verani, J. R., O'Brien, K. L., Whitney, C. G., Klugman, K. P., & Cohen, C. (2014). Effects of vaccination on invasive pneumococcal disease in South Africa. *The New England Journal of Medicine*, 371(20), 1889-1899. doi:10.1056/NEJMoa1401914

Voss, S., Hallström, T., Saleh, M., Burchhardt, G., Pribyl, T., Singh, B., Riesbeck, K., Zipfel, P. F., & Hammerschmidt, S. (2013). The choline-binding protein PspC of *Streptococcus pneumoniae* interacts with the C-terminal heparin-binding domain of vitronectin. *The Journal of Biological Chemistry*, 288(22), 15614–15627. doi: 10.1074/jbc.M112.443507

Walker, C. L. F., Rudan, I., Li, L. I. U., Nair, H., Theodoratou, E., Bhutta, Z. A., O'Brien, K. L., Campbell, H., & Black, R. E. (2013). Global burden of childhood pneumonia and diarrhoea. *The Lancet*, 381(9875), 1405-1416. doi:10.1016/S0140-6736(13)60222-6

Walsh, R. L., & Camilli, A. (2011). *Streptococcus pneumoniae* is desiccation tolerant and infectious upon rehydration. *mBio*, 2(3), e00092-e00011. doi:10.1128/mBio.00092-11

Wang, B.-Y., & Kuramitsu, H. K. (2005). Interactions between oral bacteria: Inhibition of *Streptococcus mutans* bacteriocin production by *Streptococcus gordonii. Applied and Environmental Microbiology*, 71(1), 354-362. doi:10.1128/AEM.71.1.354-362.2005

Wang, L., Fu, J., Liang, Z., & Chen, J. (2017). Prevalence and serotype distribution of nasopharyngeal carriage of *Streptococcus pneumoniae* in China: A meta-analysis. *BMC Infectious Diseases*, 17(1), 765-765. doi:10.1186/s12879-017-2816-8

Wang, Q., He, Z., Hu, Y., Jiang, Y., Ma, R., Tang, Z., Liang, J., Liu, Z., & Huang, Z. (2012). *luxS* mutant regulation: Quorum sensing impairment or methylation disorder? *Sensors*, 12(5), 6155-6185. doi:10.3390/s120506176

Weimer, K. E. D., Armbruster, C. E., Juneau, R. A., Hong, W., Pang, B., & Swords, W. E. (2010). Coinfection with *Haemophilus influenzae* promotes pneumococcal biofilm formation during experimental otitis media and impedes the progression of pneumococcal disease. *The Journal of Infectious Diseases*, 202(7), 1068-1075. doi:10.1086/656046

Weiser, J. N., Williams, A., & Moxon, E. R. (1990). Phase-variable lipopolysaccharide structures enhance the invasive capacity of *Haemophilus influenzae. Infection and Immunity*, 58(10), 3455-3457. doi:10.1128/IAI.58.10.3455-3457.1990

Weiser, J. N., Austrian, R., Sreenivasan, P. K., & Masure, H. R. (1994). Phase variation in pneumococcal opacity: Relationship between colonial morphology and nasopharyngeal colonization. *Infection and Immunity*, 62(6), 2582-2589. doi:10.1128/IAI.62.6.2582-2589.1994

Weiser, J. N., Markiewicz, Z., Tuomanen, E. I., Wani, J. H., & O'Brien, A. (1996). Relationship between phase variation in colony morphology, intrastrain variation in cell wall physiology, and nasopharyngeal colonization by *Streptococcus pneumoniae. Infection and Immunity*, 64(6), 2240-2245. doi:10.1128/iai.64.6.2240-2245.1996

Weiser, J. N. (2010). The pneumococcus: Why a commensal misbehaves. *Journal of Molecular Medicine*, 88(2), 97-102. doi:10.1007/s00109-009-0557-x

Weiser, J. N., Ferreira, D. M., & Paton, J. C. (2018). *Streptococcus pneumoniae*: Transmission, colonization and invasion. *Nature Reviews Microbiology*, 16(6), 355-367. doi:10.1038/s41579-018-0001-8

Wen, Z., Liu, Y., Qu, F., & Zhang, J.-R. (2016). Allelic variation of the capsule promoter diversifies encapsulation and virulence in *Streptococcus pneumoniae. Scientific Reports*, 6(1), 30176. doi:10.1038/srep30176

Whalan, R. H., Funnell, S. G. P., Bowler, L. D., Hudson, M. J., Robinson, A., & Dowson, C. G. (2005). PiuA and PiaA, iron uptake lipoproteins of *Streptococcus pneumoniae*, elicit serotype independent antibody responses following human pneumococcal septicaemia. *FEMS Immunology and Medical Microbiology*, 43(1), 73-80. doi:10.1016/j.femsim.2004.07.010

Whitchurch, C. B., Tolker-Nielsen, T., Ragas, P. C., & Mattick, J. S. (2002). Extracellular DNA required for bacterial biofilm formation. *Science*, 295(5559), 1487-1487. doi:10.1126/science.295.5559.1487

Whitney, C. G., Farley, M. M., Hadler, J., Harrison, L. H., Bennett, N. M., Lynfield, R., Reingold, A., Cieslak, P. R., Pilishvili, T., Jackson, D., Facklam, R. R., Jorgensen, J. H., & Schuchat, A. (2003). Decline in invasive pneumococcal disease after the introduction of protein–polysaccharide conjugate vaccine. *The New England Journal of Medicine*, 348(18), 1737-1746. doi:10.1056/NEJMoa022823

Whitsett, J. A., & Alenghat, T. (2015). Respiratory epithelial cells orchestrate pulmonary innate immunity. *Nature Immunology*, 16(1), 27-35. doi:10.1038/ni.3045

Wholey, W.-Y., Kochan, T. J., Storck, D. N., & Dawid, S. (2016). Coordinated bacteriocin expression and competence in *Streptococcus pneumoniae* contributes to genetic adaptation through neighbor predation. *PLoS Pathogens*, 12(2), e1005413-e1005413. doi:10.1371/journal.ppat.1005413

Wilson, R., Cohen, J. M., Jose, R. J., de Vogel, C., Baxendale, H., & Brown, J. S. (2015). Protection against *Streptococcus pneumoniae* lung infection after nasopharyngeal colonization requires both humoral and cellular immune responses. *Mucosal Immunology*, 8(3), 627-639. doi:10.1038/mi.2014.95

Wilson, R., Cohen, J. M., Reglinski, M., Jose, R. J., Chan, W. Y., Marshall, H., de Vogel, C., Gordon, S., Goldblatt, D., Petersen, F. C., Baxendale, H., & Brown, J. S. (2017). Naturally acquired human immunity to pneumococcus is dependent on antibody to protein antigens. *PLoS pathogens*, 13(1), e1006137-e1006137. doi:10.1371/journal.ppat.1006137

Winter, A. J., Comis, S. D., Osborne, M. P., Tarlow, M. J., Stephen, J., Andrew, P. W., Hill, J., & Mitchell, T. J. (1997). A role for pneumolysin but not neuraminidase in the hearing loss and cochlear damage induced by experimental pneumococcal meningitis in guinea pigs. *Infection and Immunity*, 65(11), 4411-4418. doi:10.1128/IAI.65.11.4411-4418.1997

Winzer, K., Hardie, K. R., & Williams, P. (2003). LuxS and Autoinducer-2: Their contribution to quorum sensing and metabolism in bacteria. *Advances in Applied Microbiology*, 53, 291-396. doi:10.1016/S0065-2164(03)53009-X

Wren, J. T., Blevins, L. K., Pang, B., Basu Roy, A., Oliver, M. B., Reimche, J. L., Wozniak, J. E., Alexander-Miller, M. A., & Swords, W. E. (2017). Pneumococcal neuraminidase A (NanA) promotes biofilm formation and synergizes with Influenza A Virus in nasal colonization and middle ear infection. *Infection and Immunology*, 85(4), e01044-01016. doi:10.1128/iai.01044-16

Xu, Q., & Pichichero, M. E. (2014). Co-colonization by *Haemophilus influenzae* with *Streptococcus pneumoniae* enhances pneumococcal-specific antibody response in young children. *Vaccine*, 32(6), 706-711. doi:10.1016/j.vaccine.2013.11.096

Yadav, M. K., Vidal, J. E., Go, Y. Y., Kim, S. H., Chae, S. W., & Song, J. J. (2018). The LuxS/AI-2 quorum-sensing system of *Streptococcus pneumoniae* is required to cause disease, and to regulate virulence- and metabolism-related genes in a rat model of middle ear infection. *Frontiers in Cellular and Infection Microbiology*, 8, 138. doi:10.3389/fcimb.2018.00138

Yao, J., & Rock, C. O. (2017). Exogenous fatty acid metabolism in bacteria. *Biochimie*, 141, 30-39. doi:10.1016/j.biochi.2017.06.015

Yesilkaya, H., Kadioglu, A., Gingles, N., Alexander, J. E., Mitchell, T. J., & Andrew, P. W. (2000). Role of manganese-containing superoxide dismutase in oxidative stress and virulence of *Streptococcus pneumoniae. Infection and Immunity*, 68(5), 2819-2826. doi:10.1128/IAI.68.5.2819-2826.2000

Yesilkaya, H., Manco, S., Kadioglu, A., Terra, V. S., & Andrew, P. W. (2008). The ability to utilize mucin affects the regulation of virulence gene expression in *Streptococcus pneumoniae. FEMS Microbiology Letters*, 278(2), 231-235. doi:10.1111/j.1574-6968.2007.01003.x

Yesilkaya, H., Spissu, F., Carvalho, S. M., Terra, V. S., Homer, K. A., Benisty, R., Porat, N., Neves, A. R., & Andrew, P. W. (2009). Pyruvate formate lyase is required for pneumococcal fermentative metabolism and virulence. *Infection and Immunity*, 77(12), 5418-5427. doi:10.1128/IAI.00178-09

Yun, K. W., Lee, H., Choi, E. H., & Lee, H. J. (2015). Diversity of pneumolysin and pneumococcal histidine triad protein D of *Streptococcus pneumoniae* isolated from invasive diseases in Korean children. *PloS One*, 10(8), e0134055-e0134055. doi:10.1371/journal.pone.0134055

Zafar, M. A., Hamaguchi, S., Zangari, T., Cammer, M., & Weiser, J. N. (2017). Capsule type and amount affect shedding and transmission of *Streptococcus pneumoniae. mBio*, 8(4), 10.1128/mbio.00989-00917. doi:10.1128/mbio.00989-17

Zafar, M. A., Wang, Y., Hamaguchi, S., & Weiser, J. N. (2017). Host-to-host transmission of *Streptococcus pneumoniae* is driven by its inflammatory toxin, pneumolysin. *Cell Host and Microbe*, 21(1), 73-83. doi:10.1016/j.chom.2016.12.005

Zhanel, G. G., Dueck, M., Hoban, D. J., Vercaigne, L. M., Embil, J. M., Gin, A. S., & Karlowsky, J. A. (2001). Review of macrolides and ketolides: Focus on respiratory tract infections. *Drugs*, 61(4), 443-498. doi:10.2165/00003495-200161040-00003

Zhanel, G. G., Wolter, K. D., Calciu, C., Hogan, P., Low, D. E., Weiss, K., & Karlowsky, J. A. (2014). Clinical cure rates in subjects treated with azithromycin for community-acquired respiratory tract infections caused by azithromycin-susceptible or azithromycin-resistant *Streptococcus pneumoniae*: Analysis of phase 3 clinical trial data. *Journal of Antimicrobial Chemotherapy*, 69(10), 2835-2840. doi:10.1093/jac/dku207

Zhang, J.-R., Mostov, K. E., Lamm, M. E., Nanno, M., Shimida, S.-i., Ohwaki, M., & Tuomanen, E. (2000). The polymeric immunoglobulin receptor translocates pneumococci across human nasopharyngeal epithelial cells. *Cell*, 102(6), 827-837. doi:10.1016/S0092-8674(00)00071-4

Zhang, Y.-M., & Rock, C. O. (2008). Membrane lipid homeostasis in bacteria. *Nature Reviews Microbiology*, 6(3), 222-233. doi:10.1038/nrmicro1839

Zheng, C. J., Yoo, J.-S., Lee, T.-G., Cho, H.-Y., Kim, Y.-H., & Kim, W.-G. (2005). Fatty acid synthesis is a target for antibacterial activity of unsaturated fatty acids. *FEBS Letters*, 579(23), 5157-5162. doi:10.1016/j.febslet.2005.08.028

Zhu, L., & Lau, G. W. (2011). Inhibition of competence development, horizontal gene transfer and virulence in *Streptococcus pneumoniae* by a modified competence stimulating peptide. *PLoS Pathogens*, 7(9), e1002241. doi:10.1371/journal.ppat.1002241